Bisphosphonate-based ionic liquids as potential pharmacological tools for breast cancer-induced bone osteolytic metastasis

Sónia Manuela Arantes Teixeira

2018

Sónia Manuela Arantes Teixeira

Bisphosphonate-based ionic liquids as potential pharmacological tools for breast cancer-induced bone osteolytic metastasis

Tese de Candidatura ao Grau de Doutor em Patologia e Genética Molecular submetida ao Instituto de Ciência Biomédicas Abel Salazar da Universidade do Porto.

Orientador:

Professor Doutor João Miguel Silva e Costa Rodrigues

Professor Auxiliar

Faculdade de Medicina Dentária da Universidade do Porto

Coorientador:

Professora Doutora Maria Helena Raposo Fernandes

Professora Catedrática

Faculdade de Medicina Dentária da Universidade do Porto

Coorientador:

Professor Doutor Luís Alexandre Almeida Fernandes Cobra Branco

Investigador Auxiliar

Faculdade de Ciências e Tecnologia da Universidade Nova Lisboa

Publications

In accordance with "Artigo 4º do Despacho nº 7982/2017", this thesis contains materials and results from the following papers, which were accepted or submitted for publication:

- S. Teixeira, L.C. Branco, M.H. Fernandes, J. Costa-Rodrigues. Bisphosphonates and cancer: a relationship beyond the antiresorptive effects. *Mini-Reviews in Medicina Chemistry* (aceppted - in press). 2017

- S. Teixeira, M.M. Santos, R. Ferraz, M.H, Fernandes, J. Costa-Rodrigues, L.C. Branco. Novel approach for bisphosphonates: ionic liquids and salts from zoledronic acid. *European Journal Medical Chemistry* (re-submitted). 2018

- S. Teixeira, M.M. Santos, M.H, Fernandes, J. Costa-Rodrigues, L.C. Branco. Alendronic acid as ionic liquid: new perspective on osteosarcoma. *International Journal of Pharmaceuticals* (submitted). 2018

- S. Teixeira, M.M. Santos, L.C. Branco, M.H, Fernandes, J. Costa-Rodrigues. Etidronate-based ionic liquids: in vitro effects on bone metabolism. Etidronate-based ionic liquids: in vitro effects on bone metabolism. *European Journal of Medicinal Chemistry* (submitted). 2018

Acknowledgments

List of Contents

List of Figures

List of Tables

List of Schemes

List of Abbreviations

ALN – Alendronic Acid

ALP - Alkaline phosphatase

ANT – Adenine Nucleotide Translocase

APIs – Active Pharmacological Ingredients

ApppI - Triphosphoric Acid 1-adenosin-5'-ylster 3-(3-methylbut 3-enyl) Ester

ATP – Adenosine triphosphate

BCS – Biopharmaceutics Drug Classification System

BMP2 - Bone Morphogenetic Proteins 2

BP – Bisphosphonate

BPs – Bisphosphonates

CA2 - Carbonic Anydrase 2

CATK - Cathepsin K

CH – Choline

COL1 - Collagen type 1 (COL1)

DBN - 1,5-diazabicyclo(4.3.0)non-5-ene

DMSO - Dimethyl sulfoxide

DSC - Differential scanning calorimetry

ECM - ExtraCellular Matrix

EMIM – 1-Ethyl-3-methylimidazolium

C_2OHMIM - 1-(2-hydroxyethyl)-3-methylimidazolium

C_3OMIM - 1-(2-methoxyethyl)-3-methylimidazolium

EDTA - Ethylenediamine tetraacetic acid

ERKs - Extracellular Signal-Regulated Kinase

ETI – Etidronic Acid

FDA - Food and Drug Administration

FTIR - Fourier-transform infrared spectroscopy

FPP - Farnesyl Diphosphate

FPPS - Farnesyl Diphosphate Synthase

GGPP - Geranylgeranyl Diphosphate

GUSB - Beta-glucuronidase

HMG-CoA - 3-hidroxi-3-methylglutaryl coenzyme A

HMSC - Human Mesenchymal Stem Cells

HPLC - High-performance liquid chromatography

IPP - Isopentenyl Diphosphate

IL – Ionic Liquid

ILs – Ionic Liquids

JNK - c-Jun N-terminal kinases

M-CSF - Macrophage colony-stimulating factor

MMPs – Matrix Metalloproteinases

MST-1 – Macrophage-Stimulating 1

NaOH - Sodium hydroxide

N-BPs – Non Nitrogen-Containing Bisphosphonates

Non-N-BPs - Nitrogen-Containing Bisphosphonates

NFKB - Factor Nuclear Kappa B

NMR - Nuclear magnetic resonance

ONJ – Osteonecrosis of the Jaw

PBMC - Human Peripheral Blood Mononuclear Cells

PBS - Phosphate Buffered Saline

PKC - Proteína quinase C

PPi - Inorganic Pyrophosphate

PTHrH - Parathyroid Hormone-Related Protein

RANKL - Receptor activator of nuclear factor kappa-   ligand

RTILs – Room Temperature Ionic Liquids

SREs - Skeletal-Related Events

Tc – Cristalization Temperature

Tg – Glass Transition Temperature

Tm – Melting Temperature

TMG - 1,1,3,3-tetramethylguanidine

TNF   - Tumor necrosis factor alpha

TRAP - Tartrate-resistant acid phosphatase

VEGF - Vascular Endothelial Growth Factors

Zol – Zoledronic Acid

Resumo

O osso é um dos sítios mais comuns para o desenvolvimento de metástases derivadas do cancro da mama. Geralmente, estas mestástases são de natureza osteolílita e podem ser caracterizadas por um enfraquecimento significativo da estrutura óssea, associada por dor intensa e um aumento do risco de fraturas patológicas.

Hoje em dia, existem alguns medicamentos anti-reabsortivos, como os Bisfosfonatos, que podem ser usados no contexto de metástases ósseas. No entanto, eles atuam principalmente na reabsorção óssea, sem um efeito significativo como agentes anticancerígenos. Portanto, o objetivo principal desta tese é a síntese de novos líquidos iónicos (ILs) e/ou sais fundidos com base em diferentes aniões de bisfosfonatos (zoledronato, alendronato e etidronato) combinados com catiões orgânicos biocompatíveis; e estudar as suas propriedades físico-químicas e biológicas.

No total, foram sintetizados 24 novos ILs ou sais fundidos (12 com base no Zoledronato, 8 com base no Alendronato e 4 com base no Etidronato) e estes foram caracterizados por métodos espectroscópicos e analíticos para confirmar sua estrutura e pureza. O estudo das propriedades biológicas dos ILs sintetizados demonstrou citotoxicidade média a alta contra linhas celulares cancerígenas conhecidas pela sua associação com metástases ósseas; comparativamente, alguns deles revelaram baixa citotoxicidade em relação aos fibroblastos. Além disso, alguns dos ILs desenvolvidos contendo [ETI] também pareciam modular diretamente o metabolismo ósseo. Mais precisamente, eles pareciam promover o anabolismo ósseo, inibindo a osteoclastogénese e promovendo a osteoblastogénese.

Isto prova que, com uma cuidadosa seleção do catião orgânico, é possível provocar importantes alterações fisicoquímicas e biológicas nas propriedades dos ILs-API, tendo em mente suas aplicações.

Palavras-Chave: Bisfosfonatos, Líquidos Iónicos (IL), Actividades anti-tumoral, Metástases osseas, Osteoclastos, Reabsorção óssea, Metabolismo ósseo, Citotoxicidade, Cancro da Mama

Abstract

The Bone is one of most common sites for the development of breast cancer metastasis. Usually, these metastases have an osteolytic nature, which can be characterized by a significant weakening of bone structure, associated with intense pain and an increase on the risk of pathological fractures.

Nowadays, there are some anti-reabsorptive drugs, such as the Bisphosphonates, that can be used in the bone metastasis context. However, these act mainly on bone resorption, lacking a significant effect as anti-cancer agents. Therefore, the main goal of this thesis is the synthesis of new ionic liquids, ILs (and molten salts) based on different bisphosphonate anions (zoledronate, alendronate and etidronate) combined with biocompatible organic cations; and study of the physicochemical and biological properties.

Overall a total of 24 new ILs or molten salts were synthesised (12 based on Zoledronate, 8 based on Alendronate and 4 based on Etidronate) and were characterized by spectroscopic and analytical methods in order to confirm their structure and purity. The study of the biological properties of the synthesised ILs demonstrated average-to-high cytotoxicity against cancer cells lines from cancers that are known for their association with bone metastasis; comparatively, some of them revealed low cytotoxicity toward fibroblasts. Furthermore, some of the developed ILs containing [ETI] also appeared to directly modulate bone metabolism. More precisely, they seemed to promote bone anabolism, by inhibiting osteoclastogenesis and promoting osteoblastogenesis.

This proves that with a careful selection of the organic cation, it is possible to provoke important physico-chemical and biological alteration in the properties of ILs-APIs with great impact, having in mind their applications.

Keywords: Bisphosphonates, Ionic Liquids (IL), Anti-tumoral Activity, Bone Metastatsis, Osteoclasts, Bone Resorption, Bone Metabolism, Cytotoxicity, Breast Cancer

Chapter 1 – Objectives and General Plan

1.1 – Introduction

The Bisphosphonate (BPs) have been used for various purposes since the middle of the 19th century, but the propriety that elicited more curiosity was their ability to regulate bone mineralization. This characteristic made this drug the elite choice for treatment of skeletal disorders like multiple forms of osteoporosis, Paget's disease, multiple myeloma and cancer-related conditions, such as bone metastasis and hypercalcaemia of malignancy (1-5).

Although, the preferential uptake of these drugs are localized in regions of active bone remodeling or accelerated bone turnover, the BPs have a big problem.Their bioavailability is very low, less than 5%, so one way to try to solve this problem is to deliver this drug though intravenous administration instead of oral administration, which increases the bioavailability but also increases acute phase reactions (1). Therefore with this work, we decided to change the BPs chemically, in order to make Ionic Liquids (ILs), so this way we could enhance the solubility and permeability of the drug parent avoiding problems related to polymorphism.

1.2 – Biopharmaceutics Drug Classification System (BCS)

The BPs, because of their low solubility and permeability, are classified in BCS system as a Class IV. The BCS is a scientific framework used for classifying drug substance based on physical and chemical properties of a biologically active compound as well as the formulation and physiology of the route of administration. (6, 7)

The BCS system classifies drugs in 4 classes (Table 1):

Table 1 - Classification of BCS System

BCS System		
Class I	Higher solubility and permeability	The absorption rate is usually higher than the excretion rate
Class II	Lower solubility and higher permeability	The absorption is slower than Class I drugs, resulting in a limited bioavailability by their solvation rates.
Class III	Higher solubility and lower permeability	The dissolution is rapid but the membrane permeability varies the absorption rate.
Class IV	Lower solubility and permeability	Their absorption and dissolution is poorly, resulting in a low bioavailability

So, with this work we are attempting to transform the BPs from a Class IV drug to a Class I or II drug in the BCS system.

1.3 Synthesis and Characterization of ILs

The ILs are non-aqueous solvents (cations and anions), with a melting point until 100 °C, which both ions influences their physicochemical properties. The anions are responsible for the water immiscibility while the cations have little influence on this matter; while the viscosity, in most cases, hinders the dissolution of solid compounds, which is related to the size of the side chains of the cation. The melting and boiling points are very important so that the ILs are liquid at room temperature, these proprieties are related to the emission of vapors, therefore in order to comply with the standards of Green Chemistry, it is necessary for the vapor pressure be practically zero, which is possible with a high boiling point (8). The ILs have gone through 3 generations: first generation include accessible physical properties such as vapor pressure density and high thermal stability; the second generation have a potential use as functional materials such as energetics, lubricants, and complexing agents of ionic metals; and the third generation are described as Active Pharmacological Ingredients (APIs) used to produce biologically active ILs. Some of the RTILs (Room temperature ILs) are used as a means to produce or improve the preparation of various APIs products (8). The idea of making BPs-based ILs was to develop different IL and/or molten salts, as cations or anions combined with appropriate biocompatible counter-ions, which can act on osteoclast and breast cancer cells. For this purpose, this study was conducted in two parts: first the synthesis, characterization of the BPs-based with Zoldronate, Alendronate and Etidronate was performed; then the assays with our new API-ILs and our cell lines (Fibroblasts, Breast cancer cells, Lung cancer cells and Osteosarcoma cells) was done.

1.4 Work Distribuition

The present work is composed by 6 chapters, including the current one that is describing the main context of the study and its objectives (Chapter 1). The Chapter 2 is related to the relationship between the BPs and Bone Tissue, which is reported in the review that was accepted in the journal "Mini-Reviews in Medicinal Chemistry". This

review focuses various mechanisms of action of the BPs that affect the cellular activity and survival, and especially their antitumoral effects. The Chapter 3 describes the synthesis and characterization of Zoledronic-based ILs and molten salts, reporting interesting results about solubility, thermal and cytotoxicity tests. This article was submitted to the "European Journal Medical Chemistry". The Chapter 4 is related to the synthesis of Alendronate based-ILs, the 2nd generation of BPs, and its perspective on osteosarcoma, which was submitted to "International Journal of Pharmaceuticals". And the Chapter 5 studied the relation between the bone metabolism and the Etidronate-based ILs. This article was submitted to "Translational Research".

For the last, the Chapter 6, we have our Discussion and Conclusion of our work.

Chapter 2 - Bisphosphonates and Bone Tissue

This chapter contains parts of a published review article:

"Bisphosphonates and cancer: a relationship beyond the antiresorptive effects"

S. Teixeira, L.C. Branco, M.H. Fernandes, J.Costa-Rodrigues

2.1 – Abstract

Bisphosphonates (BPs) are stable analogues of the Inorganic Pyrophosphate (PPi), an endogenous regulator of bone mineralization, which can resist the hydrolysis in the gastrointestinal tract. Their conformation allows targeting the bone as a result of their three-dimensional structure, which makes them primary agents against osteoclast-mediated bone loss. They are used in many bone pathological conditions, like bone metastasis, because of their ability to modulate bone metabolism into a less favorable place to cancer cell growth, through the inhibition of osteoclastogenesis and bone resorption. This review is focused in the mechanisms of action through which BPs affect the cellular activity and survival, mainly on their antitumoral effects. In conclusion, BPs are considered the primary therapy for skeletal disorders due to its high affinity for bone, but now they are also been considered as potential antitumor agents due to its ability to induce tumor cell apoptosis, inhibition of cell adhesion, invasion and proliferation, modulation of the immune system to target and eliminate cancer cells as well as affect the angiogenic mechanisms. Like any other drug, they also have some adverse effects, but the most common, the acute phase reaction, can be minimized with the intake of calcium and vitamin D.

2.2 - Introduction

Bisphosphonates (BPs) have been known since the middle of the 19th century because of their use in numerous industrial applications, such as preventers of scaling (9), water softening, glassware cleaning and synthetic detergents (10). Afterwards, they started to be used in other contexts because of their resemblance towards the Inorganic Pyrophosphate (PPi) (1).

PPi is an endogenous regulator of bone mineralization that is comprised of two phosphate groups linked by an oxygen linkage (P-O-P) (Figure 1) (1, 11). The first studies that reported its presence in human body were conducted in plasma and urine, and showed its ability to inhibit calcium phosphate precipitation *in vitro* (1, 9, 10), being proposed that PPi could prevent calcification of soft tissues and regulate bone mineralization (12), and, therefore, could prevent ectopic calcification *in vivo* (9, 10). This was exploited using PPi in animal models. According reported studies from literature, the successful results were only achieved for the cases where the compounds are injected, because after oral administration they were inactivated by hydrolysis in the

gastrointestinal tract (11, 12). This incited a search for a more stable analogue that could show the same activity but was not destroyed enzymatically, the BPs (9, 10, 12).
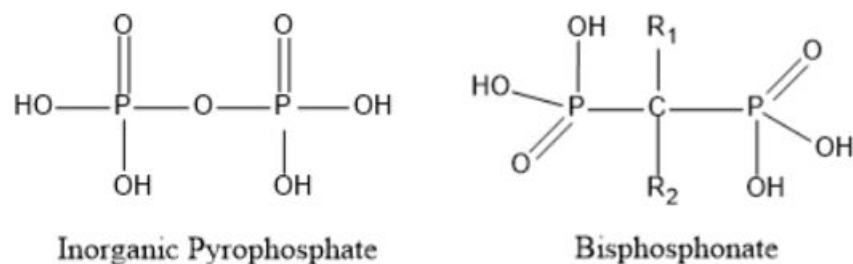
BPs possess a similar chemical structure to the PPi, but instead of an oxygen they have a carbon atom that binds the two phosphonate groups (P-C-P) (Figure 1) (1, 2, 9, 13). This structure provides more chemical and biological stability and resistance to degradation (10, 13) due to the phosphoester bonds that are resistant to hydrolysis (14). Their conformation allows targeting to the bone mineralized matrix as a result of their three-dimensional structure capable of binding divalent metal ions like calcium, magnesium and iron (14). Modifications on one or both phosphonate groups result in a dramatically reduced affinity for bone mineral (11, 14, 15), as well as a reduced biochemical activity (13).

Besides their conformation, BPs also have two additional groups, the R1 and R2, which are side chains attached to the central carbon (10, 13). These chains are responsible for a large range of activities: the R1 group is in charge for enhancing bone targeting and binding affinity; the R2 is the primarily determinant for the antiresorptive potency of the molecule (2, 13, 15). The presence of nitrogen, an amino group or nitrogen within a heterocyclic ring increases the antiresorptive potency from 10 to 10.000 fold (1, 2, 11, 13). This effect is mainly due the fact that unlike what happens with non-N-BPs, N-BPs are not metabolized to AppCp-type nucleotides (16). For example, risedronate and zoledronate have a nitrogen atom in an alkyl chain providing much less antiresorptive potency to the corresponding compounds (13, 15). The BPs that have a hydroxyl (OH) group sited in the R1 side chain, show remarkable specificity for hydroxyapatite because of the tertiary interaction created between them and the phosphate group (1, 12, 14). More recently, it became evident that the R2 group also has an influence on the affinity for bone mineral (4). This was observed on a study conducted by Nancollas *et. al* (15), showing that several BPs that shared the same P-C-P structure with a OH group at R1 exhibit differences in binding affinity and effects on mineral surface properties. This highlight that the nature of the R2 side chain also influences other surface proprieties is an important information for the affinity for bone mineral, including kinetic affinity, zeta potential and interfacial tension.

There is evidence that small chemical changes in the BPs side chains can significantly also affect their clinical outcomes, by modulating the strength of the interaction with bone matrix, their distribution through bone and the clearance of bone tissue after discontinuation of treatment (9, 13). Nevertheless, it is important to stress out that, in addition to the side chains, both phosphonate groups are required for their pharmacological activities. For example, methylation of one phosphonate group (to form a phosphonophosphinate) causes a sharp decrease in the affinity for bone matrix and also in the antiresorptive activity. If both phosphonate groups become methylated (to form a bisphosphinate), there is a total loss of bone affinity and antiresorptive effects (17). Currently, and despite all the chemical differences, the available BPs share some properties, like their uptake mainly by the skeleton, strong binding ability for hydroxyapatite crystals, ability to suppress osteoclast-mediated bone resorption, retention in the bone for a long period and excretion in the urine (10).

Being bone tissue the main target of BPs, it is important to highlight some relevant features about its metabolism. It consists in a continuous chain of breakdown by osteoclasts and new synthesis by osteoblasts, which act in equilibrium to ensure normal bone structure and function (18, 19). This process is regulated by the osteocytes that detect mechanical stress and respond to biochemical stimuli by recruiting osteoclasts to remove the old bone tissue that is no longer required. Then, osteoblasts to create an organic matrix, the osteoid, which becomes mineralized by the deposition of calcium phosphate crystals in the form of hydroxyapatite. During this process some of the osteoblasts become trapped and become located in the resulting lacuna as osteocytes (18-21). This remodeling process is essential for the maintenance of structural integrity of the skeleton and to its metabolic functions as a storehouse of many ions, particularly calcium and phosphate (18, 21).

Due to their biological activities, BPs are widely used in bone pathologic conditions, the majority characterized by extensive osteoclast activity, like multiple forms of osteoporosis (juvenile, postmenopausal or involutional/senil, glucocorticoid-induced, transplant-induced, immobility-induced and androgen-deprivation-related) (1), Paget's disease, multiple myeloma and cancer-related conditions, such as bone metastasis and hypercalcaemia of malignancy (2-5). Additionally, their affinity for bone mineral component allow its use as diagnostic tools, like scanning agents (9) in order to detect hotspots characteristic of bone metastases and Pagetic lesions (13).

The bioavailability of a drug is a complex characteristic that takes into account all the factors that influence the rate and extent to which a drug reaches the systemic circulation. In the case of BPs, mainly due to their high hydrophilicity, their oral bioavailability is very low and highly variable, which has been a problem when considering
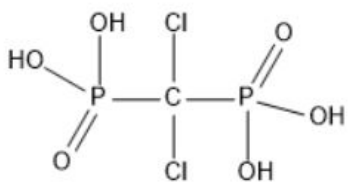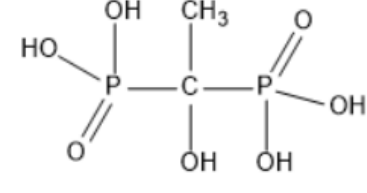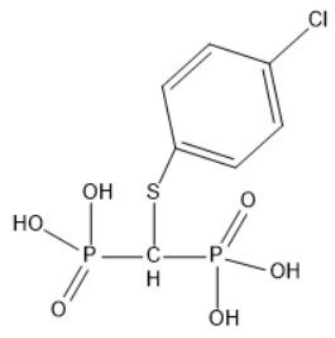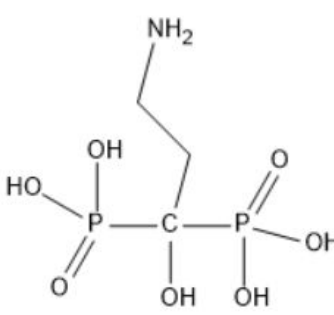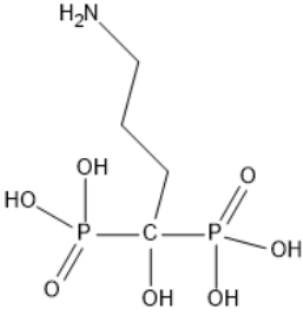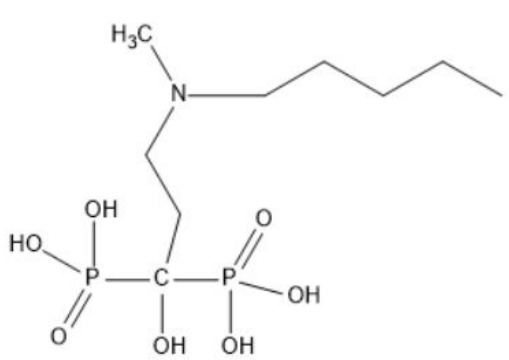
their oral doses and efficacy in the clinical context. Unfortunately, the chemical and biological improvements among the different BPs generation did not elicited significant improvements in their oral bioavailability, since, for example, for non-N-BPs it is around 2.3-2.5%, while for N-BPs it usually ranges between 0.1-4% (22). Moreover, there are several factors that may significantly compromise oral absorption of BPs, like, for example, the presence of food, since if the drug is taken during a meal, its absorption may become totally impaired (23), and the presence of drinks containing calcium, magnesium or aluminum (24). On the other hand, the presence of EDTA or an increased gastric pH seem to increase it (24, 25). In order to minimize such interferences, patients are required to remain upright for 30 minutes and the consumption of any food is restrained 2 hours before and 30 minutes after ingesting the BPs (1). A more successful way to increase the bioavailability is to change drug delivery from oral to intravenous administration (IV) (26). With this approach, the occurrence of gastrointestinal adverse effects is prevented, although the rate of acute phase reactions is increased (1). Once in the bloodstream, almost the entire dose is either absorbed by the bone or eliminated in the urine (1, 26).

In clinical terms, over the last decade the effect of the BPs are being translated in an increase and improvement of bone mass and strength with the decrease of the risk of pathological fracture (3, 13).

2.3 - Molecular Mechanism of Action

Over time, BPs structure has been modified to increase their efficacy (Table 2). The 1st generation of BPs have minimally modified side chains (1), and they are called Non-Nitrogen-containing Bisphosphonates (Non-N-BPs). As the name explicit says, these compounds do not contain a nitrogen group and due to that they are more similar to PPi, since they present a backbone containing two bounded phosphate groups, though in this case the bound is mediated by a carbon atom, not by an oxygen (26, 27). Some examples of molecules belonging to this group are clodronate, etidronate and tiludronate (13, 19). In order to increase the bioavailability of clodronate and etidronate (the two BPs with the smaller side chains), these drugs are usually used as prodrugs, which mean that their ionizable oxygen atoms from the bisphosphonate core are masked with biodegradable groups (28).

Table 2 - Classification of BPs

Non-N-BPs	1st Generation	 Clodronate Etidronate Tiludronate
N-BPs	2nd Generation	 Pamidronate Alendronate Ibandronate

| 3rd Generation | |

Risedronate   Zoledronate
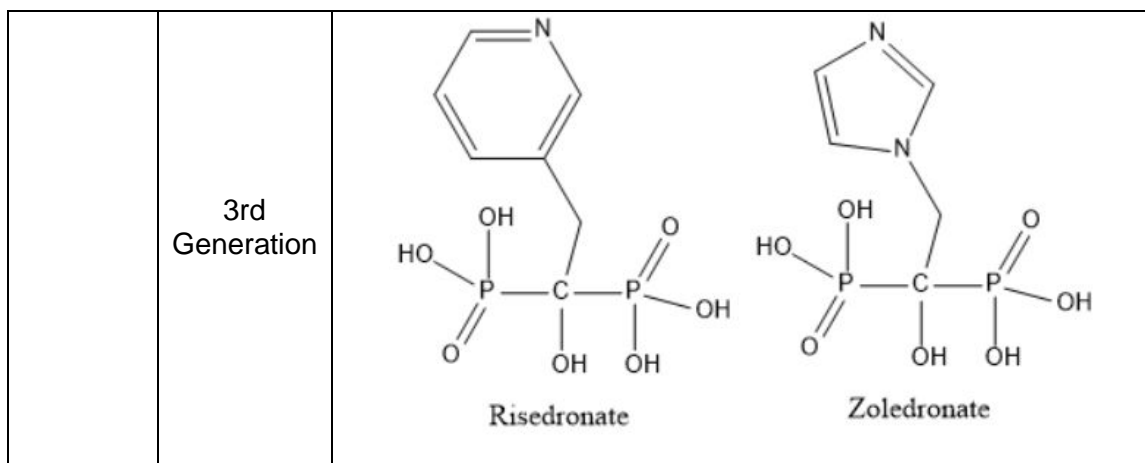
With the addition of a nitrogen group in the side chain, the Nitrogen-containing Bisphosphonates (N-BPs) were created (1). The 2nd generation includes a simple nitrogen group, which increases BP potency by 10- to a 100- fold, being examples of this group pamidronate, alendronate and ibandronate. The 3rd generation is the result of an insertion of a heterocyclic ring containing nitrogen which increases even more BP potency, up to 10,000 times, which is observed in risedronate and zoledronate (14, 26).

The Non-N-BPs are simple molecules that are metabolized into nonhydrolyzable analogues of adenosine triphosphate (ATP) (27, 29, 30) through reversing reactions of aminoacyl–tRNA synthetases, to induce osteoclast apoptosis (1, 2, 13, 31). This occurs because of its resemblance towards PPi, which enables them to be incorporated into the enzyme active site allowing a back-reaction (1, 31) to form methylene-containing analogues of ATP (AppCp-type) nucleotide (32). At high concentrations, their accumulation in the cytosol of osteoclasts, macrophages or other cell types, causes the inhibition of numerous intracellular metabolic enzymes that have damaging effects on cell function and can induce apoptosis (31, 32). More precisely, the induction of apoptosis response is due to the ability that the AppCp-type metabolites have to interfere with the Adenine Nucleotide Translocase (ANT) (13, 27, 29, 31, 33). In other words, the AppCp-type inhibits the ANT preventing the translocation of ATP across the inner mitochondrial membrane. This causes the opening of the mitochondrial permeability transition pore, a component of the ANT, that subsequently allows cytochrome c to be released into cytosol, leading to caspase-3 activation (2, 34) and the caspase-mediated cleavage and activation of Mst-1, an apoptosis-promoting kinase (31).

N-BPs affect cellular activity and survival by interfering with Farnesyl Diphosphate Synthase (FPPS), a key enzyme of the mevalonate pathway (1, 4, 9, 35). This pathway is responsible for the production of important isoprenoids, like cholesterol, which is a lipid essential to membrane formation (2, 13, 36), but also to several others processes that use isoprenoid diphosphates as a substrate (1), such as Isopentenyl Diphosphate (IPP),

Farnesyl Diphosphate (FPP) and Geranylgeranyl Diphosphate (GGPP), which are important for the synthesis of dolichol, ubiquinone, among others (13, 30, 31). N-BPs are internalized but not metabolized by osteoclasts (27, 32), where they subsequently inhibit the FPPS, leading to a reduction in the production of isoprenoids (13, 27). As a consequence, several metabolic pathways became inhibited, (32), as well as the post-translational modification (prenylation) of small GTPases (2, 13) such as Ras, Rab, Rho, and Rac (9, 14, 27, 33). Prenylation is the addition of a lipid residue to proteins, which is essential for the correct subcellular membrane localization and for their consequent activation by external signals (13, 37). These small GTPases are a large family of signaling proteins that regulate cell proliferation, invasive proprieties and pro-angiogenic activity in tumor cells (37), as well as a variety of cell processes important for osteoclastic bone resorption which includes cytoskeleton actin structure, integrin signalling, membrane ruffling, trafficking of endossomes, and signalling pathways that regulate apoptosis (1, 31, 37, 38). These processes are required for a proper osteoclastic function, survival, proliferation and cytoskeletal organization (2, 33, 35). It was also demonstrated that the potency for inhibiting the FPPS is correlated with the antiresorptive potency of the molecules *in vivo*, which suggests that this enzyme may be a major determinant of BPs potency (4). It is thought that the accumulation of unprenylated small GTPases in FPPS active site can cause inappropriate activation of downstream signaling pathways (13). Besides the reduction of FPP that is necessary for the production of GGPP, the inhibition of FPPS also elicit the accumulation of IPP, the metabolite immediately upstream of FPPS in the mevalonate pathway (13, 32). This leads to the production of another ATP analog, the triphosphoric acid 1-adenosin-5'-ylster 3-(3-methylbut 3-enyl) ester (ApppI) (33), which inhibits ANT and causes osteoclast apoptosis, like what happens with Non-N-BPs (27, 29, 31, 37). This was observed by Mönkkönen et al. that showed the ability of N-BPs to induce the production of ATP analogs, like AppI, and subsequent accumulation of IPP in the mevalonate pathway, promoting apoptosis.

Another way that evidenced the inhibition of the mevalonate pathway by N-BPs was achieved with statin drugs. These are inhibitors of the 3-hydroxy-3-methylglutaryl coenzyme A (HMG-CoA) reductase that is a key enzyme in the mevalonate pathway (5, 14, 36). It was demonstrated their ability to interfere with this pathway via allosteric modulation and epigenetic activation, resulting in the inhibition of DNA synthesis, repair, and methylation of some genes as well as associated microRNAs (5). They were also reported to be more potent than BPs at inhibiting osteoclast formation and bone resorption *in vitro*, but there was no substantial evidence of their effect on bone when used clinically, perhaps because of the preferential uptake of statins by the liver. Like most drugs, statins

don't have high affinity for bone hydroxyapatite, therefore they have ineffective therapeutic potential (15) on bone metabolic disorders context.

2.4 - Biochemical Mechanisms and Cellular Uptake

Although the main site for BPs uptake is the skeleton, they also appear to be distributed in extraskeletal tissues, like liver, kidney and spleen (13). This seems to be related to differences in plasma protein binding and renal excretion (39), and may explain, at least in part, some of the direct effects of BPs on tumor cells (40).

Regarding bone tissue, there are some important points that remain elusive. On one hand, it is difficult to quantify the amount of BP taken up by bone during the first passage. On the other hand, how BPs reach bone tissue from blood circulation is, at the present, not known (39, 41). Furthermore, the presence of BPs in the skeleton seems to be heterogeneous, as observed in studies with radiolabeled drugs in animals and humans (40, 41).

Nevertheless, the preferential uptake of BPs by the skeleton is localized in regions of active bone remodeling or accelerated bone turnover (1), and where new mineral is being deposited beneath the osteoblasts, like, for example, in the femur neck and spine (42, 43). Due to this, it was proposed that the differential skeletal distribution of BPs may be related to variations in bone mineral affinity (13), which may account for the different anti-fracture effects of BPs in different locations. This preferential affinity for highly dynamic bone metabolic locations brings BPs into close contact with osteoclasts, osteocytes and osteoblasts, but also prevents prolonged exposure to other cell types (31).

Because of their negative charge and chemical structure, BPs may remain embedded in bone tissue for long periods of time (26). Although their half-life tends to be high, it strongly depends on bone turnover rate (1, 44). BPs that do not bind to bone tissue, or are released from it and are not taken up again by the skeleton are excreted in urine in their free form. The dependence of BPs half-life on bone metabolic rate is a concern, for example, in the administration of BPs to females in fertility age before conception, because these molecules can be released from the maternal skeleton during pregnancy and affect the foetus (3). For this reason, BPs are contraindicated during pregnancy and all females in reproductive age should have a negative pregnancy test before each treatment cycle (3). Regarding bone uptake, it is also important to mention that age and gender may contribute to significant differences on it, since bone metabolism is strongly influenced by both factors (45). In addition to age and gender effects, when two

or more BPs are co-administered at high doses, a competition may occur (46), which can have important consequences on the efficacy of the treatment.

Taken together, the present knowledge about the factors governing uptake and distribution of BPs is far from being sufficient, and studies aiming to investigate the distribution of BPs in properly performed human studies are required.

To exert their effects in bone tissue, BPs must be released from bone and then internalized by the different bone cells. Their effects on osteocytes and osteoblasts consist mainly in the inhibition of the apoptosis (1, 13, 14) (Figure 2).
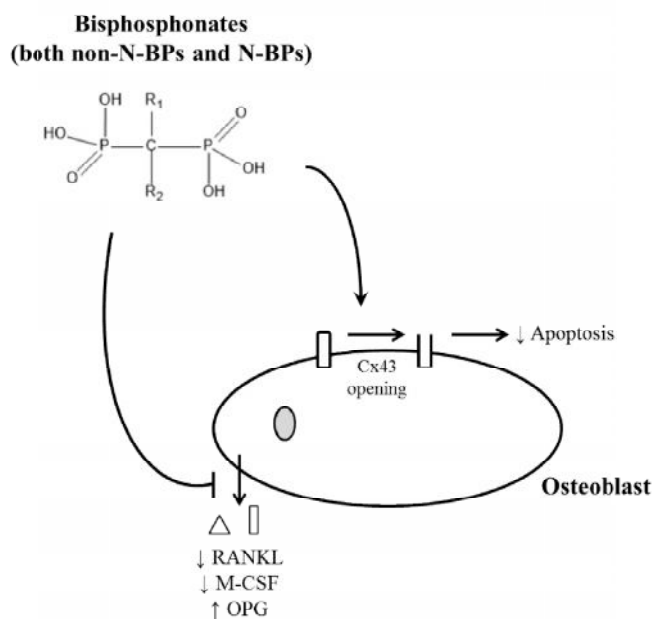
Figure 2 - Main effects of BPs on osteoblasts

The inhibition of apoptosis on osteocytes and osteoblasts appears to be mediated through the opening of connexin 43 (Cx43) hemichannels and subsequent activation of extracellular signal-regulated kinase (ERKs). This is a completely different pathway than the one used to induce apoptosis or inhibit bone resorption in osteoclasts (13), since there are some BPs that only inhibit apoptosis on osteoblasts and osteocytes while do not interefere with osteoclastic function (47-49). So, this characteristic can be exploited in order to increase the therapeutic potential of some BPs, particularly when it is important to avoid their antiresorptive effects. However, despite its relevance, Cx43 is not the binding site for BPs, as reported previously (49, 50). In addition to their antiapoptotic effects, BPs also affect the expression of several osteoclastogenic modulators (1, 13, 14). More precisely, they downregulate the production of RANKL and M-CSF (osteoclastogenesis activators), and upregulate the production of OPG (osteoclastogenesis inhibitor). Finally, BPs also stimulate the proliferation and differentiation rates of osteoblastic cells, when present at concentrations between 10^{-9} and 10^{-6}M, although at concentrations higher than 10^{-5}M they display inhibitory effects (49).

Regarding anti-resorbing effects of BPs, it is important to highlight that bone resorption occurs by the acidification of the subcellular space beneath the osteoclasts (30) by the action of vacuolar-type proton pumps (12), which causes the dissolution of the hydroxyapatite, and subsequently occurs the internalization of the products, which may comprise BPs, by fluid-phase endocytosis (14, 51). This was demonstrated by Thompson *et. al* (30), which confirmed that the internalization of BPs requires its transportation into membrane-bound vesicles by fluid-phase endocytosis, followed by acidification of endocytic vesicles, so that the BPs can enter the cytosol and presumably into other organelles, such as peroxisomes, to exert their actions.

After being internalized, BPs exert their biochemical function by causing partly inhibition of bone resorption, instigating the decrease in cell number, altering the osteoclastic recruitment and stimulating apoptosis (12, 51). In the case of N-BPs, their main mechanism of action comprises the inhibition of the mevalonate synthesis, which is crucial not only for the synthesis of cholesterol and other sterols, but also for the prenylation of essential small GTPases, a process that requires farnesyl pyrophosphate (31, 52). This latter effect appears to not only stimulate apoptosis, but also elicit important morphological changes, like loss of the ruffled border, disruption of actin rings and altered vesicular trafficking (53) (Figure 3). After apoptosis induction, the apoptotic bodies are phagocytized by the neighboring macrophages and monocytes in the bone marrow, a process that has been reported as the main reason beneath the associated acute phase response in many patients (51).
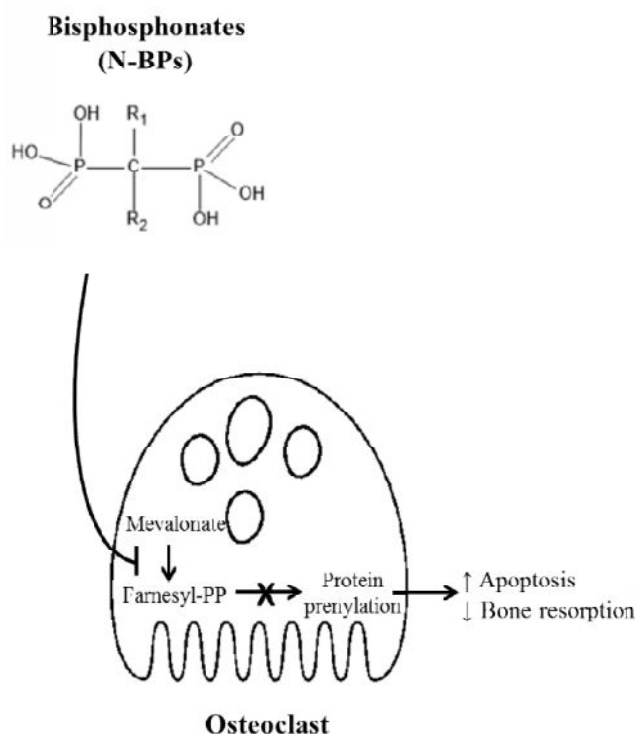
Figure 3 - Main effects of BPs on osteoclasts

Due to their ability to interfere with protein prenylation, bisphosphonates have been implicated in many different processes and, consequently, have been studied for different potential clinical applications, such as anti-tumor, anti-viral and anti-parasite agents (53-55). One major problem about the ability of BPs to inhibit farnesyl pyrophoshphate synthase (and, in some cases, also geranylgeranyl pyrophosphate synthase) is related with their very low bioavailability. In the case of bone tissue, this may not represent a relevant problem, since BPs tend to become concentration in bone matrix, but this situation can cause a sharp decrease on BPs concentration in other locations (56). In order to overcome this problem and, also, to increase their effectiveness, BPs have been serving as the basis of molecular modelling techniques, aiming to design new agents with improved properties (57). Nevertheless, from a mechanistic point of view there are still important issues to be addressed, namely at the level of farnesyl pyrophosphate synthase inhibition. Also, one cannot rule out the existence of other intracellular targets that may contribute to the global BPs effects on the different cell types. This may explain, for example, the need for different concentrations to achieve effects on the different bone cells. The formation of AppCp-type metabolites, which are analogs of ATP may be part of this equation and cause cytotoxicity, possibly by inhibiting ATP synthesis in mitochondria (13, 27, 29, 31, 33).

Finally, it is worthy to mention that although BPs and statins have inhibitory effects on mevalonate pathway, their molecular targets are different. Also, their selective uptake by different organs (liver in the case of statins and bone in the case of BPs) may also account for the different biological properties of both cases, which is a notable example of how tissue target may also account for drug specificity.

2.5 - Anti-tumoral effect

The skeleton is the most common site for metastasis in numerous types of solid neoplasms (1, 58, 59), like, for example, breast and prostate (65%-75%), thyroid gland (60%), lungs (40%), urinary bladder (30%-40%), and kidney cancers (19). Bone metastases appear in the last stages of those cancers and lead to multiple types of symptoms and complications like Skeletal-Related Events (SREs), such as severe pain, pathological fractures, spinal cord and nerve compression, hypercalcemia of malignancy and bone marrow aplasia (1, 13, 19, 27, 58). The development of bone metastases is a multistep process: first, the tumor grows and then some cancer cells begin to detach, which initially invade the tissue stroma. After that, neoangiogenesis occurs, and the

cancer cells that escaped from the tissue by intravasation, survive in the circulatory system. Latter succeeds the chemoattraction and arrest (docking and locking) in the bone marrow endothelial vessel wall, which is followed by extravasation. Finally, the metastatic microenvironment is created and developed via the cross-talks between the cancer and osseous cells (27, 60-62). Bone metastases can be classified as osteolytic, osteoblastic or mixed (19). As denoted by their names, osteolytic metastasis are characterized by significant bone disruption due to increased osteoclastic activity and are considerably more common; on the other side, osteoblastic metastases are characterized by overproduction of osseous tissue; and the mixed lesions presents a mixture of both types of metastases (27). The mechanisms underlying osteolytic bone metastases are complex and involve unique characteristics of both osseous and tumoral cells (63). Cancer cells within bone marrow interfere with normal bone cells through a local release of cytokines, such as interleukin-1 and -6, and growth factors like, Parathyroid Hormone-Related Protein (PTHrH), Tumor Necrosis Factor- or - and others. Those molecules can act directly on osteoclastic cells (or their precursors), or indirectly, *via* osteoblasts. Nevertheless, they increase bone turnover leading to osteolysis or osteosclerosis (20, 27, 60-62, 64, 65).

Since bone tissue is an active microenvironment for cancer cells, BPs appear as potential important players that can modulate it to create a less favorable place for cancer cell growth (66). This can be achieved through the inhibition of osteoclast-mediated bone resorption and osteoclastogenesis (19), leading to a reduced release of bone-derived growth factors (33, 59), and ultimately altering the bone microenvironment, avoiding this way bone metastases (66). Numerous studies have described the BPs ability to reduce the proliferation and viability of tumor cell lines, as well as the adhesion, migration, and invasion *in vitro* (32, 58, 59, 67); furthermore, the reduction of skeletal tumor burden was also shown, as well as a slower progression of bone lesions in animal models treated with BPs (33, 68). These effects can be caused directly or indirectly by the BPs. The main mechanisms responsible for the direct antitumor activity are the induction of tumor cell apoptosis, and the inhibition of tumor cell adhesion, invasion and proliferation (32, 33, 35, 59) (Figure 4).
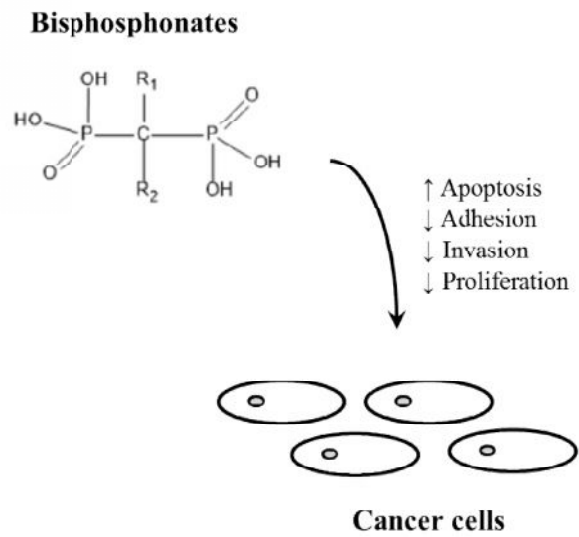
Figure 4 - Main direct effects of BPs on cancer cells

Cell adhesion and invasion are key events in the development of metastasis and are effectively inhibited by low doses of BPs (69-71). The main indirect and direct effects of BPs on cancer cells are summarized in Table 3.

Table 3 - Main effects of BPs on cancer cells

Indirect effects	Direct effects
release of bone-derived growth factors	cell proliferation
Changes in bone microenvironment	cell migration
Modulation of immune system	cell invasion
Angiogenesis	apoptosis

The apoptosis can be induced through the production of ATP analogues by the Non-N-BPs (31, 33), or through the disruption of the mevalonate pathway by the N-BPs. This provokes the reduction of isoprenoid lipids that are required for prenylation of small GTPases (33, 37), like Ras, that are essential to many cancers cells, as part of activating growth receptor pathways or for the acquisition of activating mutations during carcinogenesis (36). This makes Ras an attractive target for therapeutic interventions in breast cancer treatment, for example (68). In a study conducted by Senaratne *et al.* (68) about the effects of zoledronic acid on human breast cancer cells, it was reported a role for protein prenylation and impaired Ras membrane localization in apoptosis, being also demonstrated that the disruption of the mevalonate pathway was associated with cytochrome c release from the mitochondria into the cytosol and subsequent activation of

the caspase cascade, which resulted in the apoptosis of the breast cancer cells. It was shown that BPs could inhibit adhesion of tumor cells to extracellular matrix (ECM) (37), through the impairing of matrix metalloproteinases (MMPs) (33, 58). It was also demonstrated that the inhibition of tumor cell adhesion to ECM proteins was dependent on the prenylation of proteins. Therefore, the inhibition of the mevalonate pathway and induction of caspase activity are important for the impairment of tumor cell invasion and metastasis, being also reported that an activating Ras mutation enhanced the adhesion of a normal breast epithelial cell line to ECM proteins, which suggests that increased Ras activation may increase the metastatic potential of breast cancer cells. So, by inhibiting protein prenylation and Ras signalling, N-BPs could reduce the ability of tumor cells to expand once they colonise the bone (37) Besides their effects on mevalonate pathway, and, consequently, in the inhibition of protein prenylation, BPs also decrease cancer cell proliferation through the blockade of epidermal growth factor receptor (human EGFR or HER) tyrosine kinase (72).

Furthermore, BPs have also shown an indirect antitumor activity, such as, the ability to modulate the immune system to target and eliminate cancer cells, and through antiangiogenic mechanisms (35, 37). The former was attributed to N-BPs, which could induce a significant dose-dependent expansion of   T cells both *in vitro* and *in vivo*, mainly affecting the V 9V 2 subset. This subset is known to have an important role in immune system surveillance and defense. In fact,   T cells showed potent lytic activity against different tumor cells *in vitro*, suggesting their potential utility in anti-cancer therapy (19, 32, 37, 73). Gober *et al.* (73) showed that tumor cells treated with N-BPs (Zoledronate and Pamidronate) *in vitro* caused the accumulation of IPP, which provoked the activation and proliferation of the TCR   cells that are cells capable of recognize and kill tumor targets. Another potentially important target for BPs are the tumor-associated macrophages. In addition of being cells that belong to the same monocyte lineage as osteoclasts, it was previously demonstrated direct effects of BPs on these macrophages, namely, increased apoptosis, inhibition of pro-angiogenic behavior and phenotypic changes (74).

The inhibition of angiogenesis is another indirect mechanism, caused by the decrease of molecules that contribute to the development of the mature vascular system (75), such as, the released bone-derived growth factors, circulating levels of proangiogenic vascular endothelial growth factors (VEGF), platelet-derived growth factors, fibroblast growth factors, integrins and others (32, 65, 75, 76). It was demonstrated that zoledronate may block angiogenesis by acting on VEGF production and, consequently, on VEGF-dependent mechanisms, which is a process that also involved the mevalonate pathway (77).

Angiogenesis is a complex and tightly controlled physiological process in which new blood vessels are formed during normal growth and tissue repair. This event is relatively rare in normal healthy adults and the turnover of vascular endothelial cells is generally low. However, it is a prominent pathological feature of many nonmalignant diseases, such as rheumatoid arthritis, psoriasis and transplant rejection, and plays an essential role in tumor growth and metastasis (67).

Osteoclast-mediated bone resorption and angiogenesis are critically dependent on integrin-mediated cell adhesion and signaling. Integrins are heterodimeric cell surface complexes acting as the main receptors for ECM (75) with bidirectional signaling activity (76, 78). Ligand binding function is tightly regulated by cell signaling events, and once activated, integrins stimulate multiple signaling pathways essential for cell migration, proliferation, and survival (75, 76, 78). Interestingly, $_v$ $_3$ integrin is required for both osteoclasts and tumor cells. In osteoclasts, it is essential to adhere tightly to the bone surface and to form the sealing zones that line resorption lacunae during active bone resorption. In tumor cells, its expression confers a greater propensity to metastasize to bone (33, 78). Its binding to ECM proteins mediates signaling events consistent to stimulation of angiogenesis, through the promotion of endothelial cell proliferation, enhancing cell survival and stimulating endothelial cell mobility (75). In a study conducted by Bezzi *et al.* (76) it was demonstrated that Zoledronate inhibited cell adhesion on human umbilical vein endothelial cell cultures. This effect was mediated by integrin $_v$ $_3$, and zoledronate blocked migration and disrupted established focal adhesions without modifying cell surface integrin expression. It was also evidenced that zoledronate treatment slightly decreased cell viability and strongly enhanced tumor necrosis factor (TNF) induced cell death. On the other hand, clodronate was also tested and revealed no effects on cellular adhesion, migration, and survival, neither enhanced TNF cytotoxicity.

In conclusion, studies with BPs have demonstrated antitumoral effects that can be both direct and indirect. It was shown an impaired tumor cell adhesion to bone, inhibition of tumor migration, induction of tumor cell apoptosis, and inhibition of angiogenesis which mediate the antitumor effects in a complementary manner (58, 64). Evidences from *in vitro* and *in vivo* experiments indicated that N-BPs synergizes with a variety of anti-cancer agents including chemotherapeutic drugs, molecular targeted agents, and other biological agents (19). Based on their ability to inhibit crucial processes of protein isoprenylation, N-BPs have been combined with different biological agents (37). In this context, N-BPs and chemotherapy drugs have increasingly gained relevance in the treatment of metastatic hormone resistant prostate and breast cancer (37). So, combining BPs with a variety of standard anticancer and chemotherapy agents may result in synergistic antitumor effects against different tumor cells (11, 32, 33, 36). This was observed by Jagdev *et al.* (38),

where a combination of zoledronic acid and paclitaxel demonstrated an enhanced pro-apoptotic behavior on MCF-7 breast cancer cells. Similar results were reported with the combination of zoledronic acid and fluvastatin in breast and ovarian cancer (36).

Taken together, it was hypothesized that treatment with BPs in patients with bone metastatic disease would improve outcomes related to SREs, such as fractures, bone pain, and hypercalcemia of malignancy (12, 58). Several clinical trials confirmed that BPs revealed a bone-protective role in cancer (58). At the present, BPs are approved for use in the prevention of SREs in patients with bone metastatic disease (59), in the treatment of hypercalcemia of malignancy, and in the prevention of therapy-induced bone loss for patients being treated with aromatase inhibitors (64). In this context, to date, dozens of clinical trials using bisphosphonates in Oncology are being conducted, particularly in the breast and prostate cancers context. Accordingly, the European Myeloma Network recommends the utilization of zoledronic acid or pamidronate in patients with adequate renal function and bone disease (79). Also in patients with solid tumors, particularly in the case of skeletal involvement, BPs are part of the current clinical guidelines (80). Regarding osteoporosis management in patients with early breast, current EMAS recommendations include the use of BPs to prevent bone loss events, particularly in those with high risk of fracture (81).

2.6 - Adverse effects

There are some adverse effects associated with BPs therapies, the more common being acute phase reaction, gastrointestinal irritation and chemical oesophagitis, and severe musculoskeletal pain (1, 3).

The acute phase reaction is the most common side effect of BPs, which is responsible for the accumulation of IPP in the tissues, (31) causing fever, myalgias, arthralgias, headaches, and influenza-like symptoms that are transient (1). It occurs predominantly on the first intravenous (IV) administration (3, 13, 31), in about 10-30% of the patients (1). IPP is known to be a ligand for the receptor on the most common subset of , -T cells in humans (31), which causes the release of TNF , a proinflammatory cytokine, that subsequently initiates the pro-inflammatory acute phase reaction (1, 13). *In vitro*, it was observed that an administration of both N-BPs and statins prevented the activation of these cells, because it blocked the accumulation of IPP, raising the possibility that the administration of these two compounds could prevent the acute phase reaction (13). Also, a pretreatment with histamine receptor antagonists or antipyretics is

recommended, to reduce the incidence and severity of the symptoms among susceptible patients; occasionally, corticosteroids can also be beneficial (1).

Gastroesophageal irritation and chemical oesophagitis can occur during oral BPs therapy (3), particularly in patients with known gastroesophageal reflux disease or oesophageal stricture. A strict maintenance of an upright posture for 30 to 60 minutes after ingestion with a full glass of water, and the use of weekly rather than daily preparations, are both likely to limit the risk of adverse effects. For patients unable to tolerate oral BPs, the IV administrations are an alternative with no association with gastroesophageal irritation (1).

Urinary excretion is the main route of elimination of BPs. Depending on the dose and on the way of administration, BPs can cause transient renal toxicity. Due to that, BPs are counter indicated in patients with creatinine clearance lower than 35 mL/min (82).

Musculoskeletal pain is another potential adverse effect of BPs. Indeed, it has been issued an alert highlighting the possibility of severe, incapacitating musculoskeletal pain that can occur at any point after initiation of BPs therapy. This have been reported in late 2002 and mid 2003 in about 120 cases (1).

Besides these adverse reactions, there is another one that deserves attention, though it is not so common. The osteonecrosis of the jaw (ONJ) is a rare condition, that may appear spontaneously or after an oral surgical procedure, and it has been also associated with BPs therapy. ONJ involves necrosis of a section of the jaw, and it is primarily observed in oncology patients treated with high doses of IV BPs (1, 3). The incidence of this condition is estimated to be 1 to 10 per 100 oncology patients, and the risk of ONJ appears to be substantially lower among patients receiving oral BPs for osteoporosis. Also, it appears that along with the high doses, a poor oral hygiene, as well as a history of dental procedures or denture use, may be risk factors (1). Another bone-related complication, although rare, is atypical femoral fractures in the subtrochanteric and mid-diaphyseal portions (83).

When hypocalcemia occurs, usually following intravenous BP therapy, the treatment must be interrupted. If the hypocalcemia was mild after resuming the normal serum calcium levels, therapy can be resumed, but if hypocalcemia was severe, BPs usage must be discontinued (84).

Taken together, further studies are required to assess the long-term consequences associated with BPs consumption, and if and how it can be possible to avoid them. While these estimates do not have a high accuracy, it is important to balance the potential risks with the potential benefits, in order to adequate therapeutics to each individual characteristics.

Despite all these adverse effects, there are some complications that can be avoided. The hypovitaminosis D is common among elderly patients who frequently have limited sun exposure, reduced dietary intake, and some renal impairment; this limits dietary absorption of calcium, leading to secondary hyperparathyroidism and loss of skeletal calcium to maintain normocalcemia (1). This situation can be avoided by assuring the intake of vitamin D and calcium during the BPs therapy (64).

2.7 - Conclusion

BPs are a class of drugs that can be grouped in two major classes, according to their chemical structure and molecular mechanism of action: the Non-N-BPs and the N-BPs. The Non-N-BPs are considered the 1st generation of BPs and are the simplest. They don't have a nitrogen group and can be metabolically incorporated into nonhydrolyzable analogues of ATP, resulting in the induction of osteoclast apoptosis. In contrast, the N-BPs are more potent and complex, and can be considered as the 2nd or 3rd generation of BPs. The 2nd generation have a simple nitrogen group while the 3rd generation have a nitrogen group within a heterocyclic ring. Their mechanism of action involves the inhibition of the mevalonate pathway which prevents the prenylation of small GTPases necessary for osteoclast function, survival, proliferation and cytoskeletal organization.

BPs have a high affinity for bone mineral, so they achieve a high local concentration throughout the entire skeleton. Therefore, they become the primary therapy for skeletal disorders characterized by excessive or imbalanced skeletal remodelling, like for example, the prevention of SREs in patients with bone metastasis. In addition to their effects on bone tissue, several studies have shown that BPs also display some antitumoral activity. More precisely, BPs could induce tumor cell apoptosis, inhibition of cell adhesion, invasion and proliferation, modulation the immune system to target and eliminate cancer cells and affect the angiogenic mechanisms.

BPs also present some adverse effects, like acute phase reaction, gastrointestinal irritation, chemical oesophagitis, severe musculoskeletal pain and ONJ. The most common is the acute phase reaction which involves transient symptoms like the flu, and some complications that can be avoided with the intake of calcium and vitamin D.

Taken together, BPs are a class of drugs widely used in osteolytic bone disorders context. Their anti-osteoclastic effects account for several benefits for patients. In addition, in the last years BPs were also considered as potential antitumor agents. This can unravel

new clinical applications for BPs, which ultimately can lead to substantial improvements in the health condition of patients with bone osteolytic metastases.

Chapter 3 - Novel approach for bisphosphonates: ionic liquids and salts from zoledronic acid

3.1 – Introduction

The discovery of novel effective drugs is currently one of the greatest challenges for pharmaceutical industry (85). The convenient manipulation of solid active pharmaceutical ingredients (APIs) has been associated with several drawbacks such as polymorphic conversion, low bioavailability from crystalline solids, and spontaneous crystallization of amorphous forms (86-89). In addition, it is recognized that the bioavailability of pharmaceutical drugs is significantly dependent on their water solubility as well as high permeability. In fact, many phase II trials of new APIs fail because of their reduced bioavailability, a consequence of poor solubility in water and biological fluids. The most common approach followed by the pharmaceutical industry in order to increase the bioavailability of an API is to transform it into a salt, usually by combining it with metallic cations such as sodium or potassium, or with chloride anions, depending on the chemical structure of the API. Recently, the use of APIs as Ionic Liquids (API-ILs) as an alternative has been investigated by the academy (8, 90-92). The works involving the preparation of API-ILs from ampicillin, fluoroquinolones, ibuprofen, ranitidine and lidocaine, and also acetylsalicylic and salicylic acids, among others, have shown that the combination of an API, either as a cation or as an anion, with a suitable biocompatible counter-ion can increase the water solubility of the parent drug and even change its biological effect (93-102). In face of these results, it is suggested that the oral bioavailability of the formed API-ILs is particularly enhanced, or alternatively it may open new perspectives for their local administration/application. Therefore, the therapeutic dosage of the drug may be reduced, decreasing the side effects.

Bisphosphonates (BPs) are considered the primary therapy for skeletal disorders due to their high affinity for bone tissue. BPs are stable analogues of the Inorganic Pyro-phosphate, an endogenous regulator of bone mineralization, which can withstand hydrolysis in the gastrointestinal tract (20, 64, 66). Their conformation allows targeting the bone because of their three-dimensional structure, which makes them primary agents against osteoclast-mediated bone loss. In addition, recently they have been also considered as potential antitumor agents due to their ability to induce tumor cell apoptosis, inhibition of cell adhesion, invasion and proliferation, modulation of the immune system to target and eliminate cancer cells as well as affect the angiogenic mechanisms. However, zoledronic acid must be administered intravenously by lack of absorption in the GI tract. In addition, many debilitating side effects take place such as muscle, joint and bone pain, muscle spasms, numbness, among many others. In this context, there is a need to develop new ways to increase oral bioavailability of zoledronic acid, while the side effects are significantly reduced.

Thus, herein we report the preparation of twelve new Ionic Liquids and salts from zoledronic acid (Zol-ILs) in quantitative yields by following two distinct sustainable and straightforward methodologies, according to the type of cation. All prepared zoledronate-ILs were characterized by spectroscopic and thermal analysis and their solubility in water and biological fluids was determined. An additional evaluation of the toxicity towards human healthy cells was performed. Figure 5 depicts the structure of the cations used in the synthesis of the zoledronic acid-based ILs.
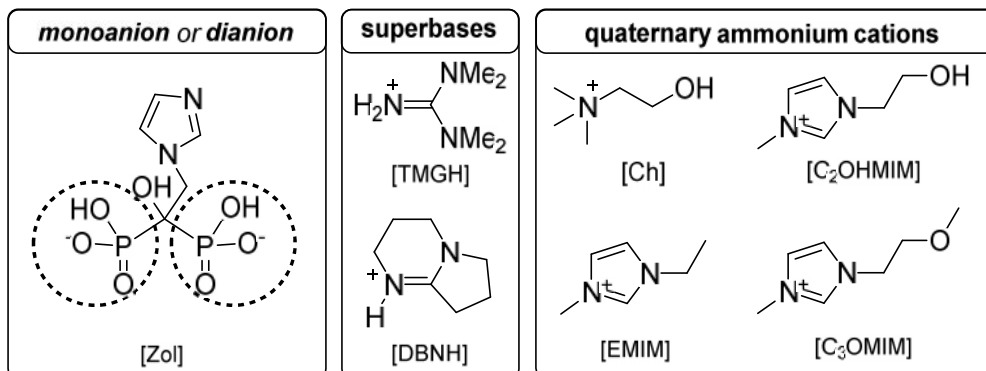
Figure 5 - Structure of mono- and dianionic zoledronic acid, protonated superbases and organic quaternary cations

3.2 – Synthesis and Characterization of Zol-ILs

The protic zoledronate-ILs were prepared by adding 1 or 2 equivalents of organic superbases, more specifically 1,1,3,3-tetramethylguanidine (TMG) and 1,5-diazabicyclo(4.3.0)non-5-ene (DBN), to a solution of zoledronic acid, whose phosphonate group(s) become(s) deprotonated (general procedure A from scheme 1). With this straightforward synthetic methodology two monoan-ionic and two dianionic zoledronic acid-based ionic salts were prepared. Room Temperature Ionic Liquids (RTIL) were obtained whenever two units of superbase were added, while the monoionic compounds were obtained as protic organic solid salts.
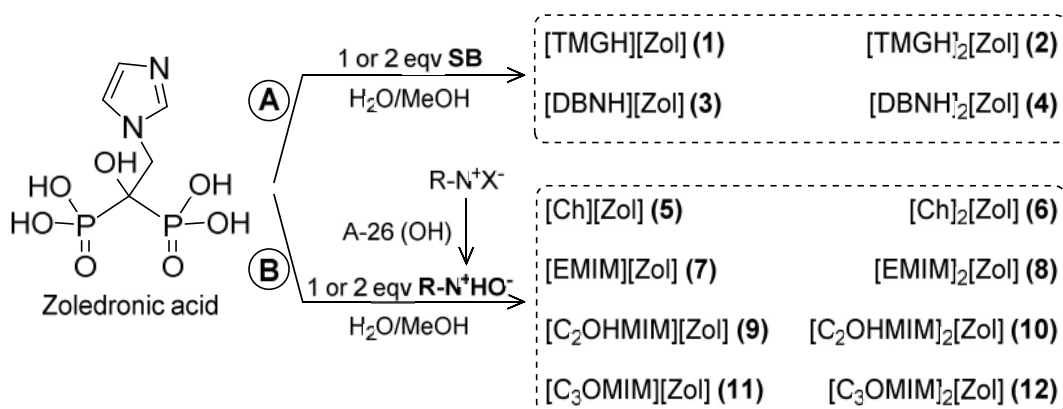
Scheme 1 - Synthetic methodologies A and B for the synthesis of Zol-ILs.

For the coupling of Zoledronate with quaternary ammonium salts a different methodology was employed (general procedure B from scheme 1) already described by our group for the previous preparation of Ampicillin-based Ionic Liquids and Salts (99, 102). In this case, quaternary ammonium hydroxide cations are previously prepared from the corresponding chloride or bromide salts by reaction with hydroxide exchange resins (e.g. Amberlyst A26-OH) in methanolic solution. The very basic solutions are then neutralized by addition to an aqueous solution of Zoledronic acid yielding the desired salts in quantitative yields. By using one or two molar equivalents of cation hydroxide salts we synthesized four monoionic compounds [5, 7, 9, 11], three ILs and one salt, and also four dianionic Zol-based RTILs [6, 8, 10, 12].

All products were characterized by NMR (^{1}H and ^{13}C) and FTIR spectroscopic techniques, as well as elemental analysis. The thermal properties were evaluated by DSC and the solubility in water and saline solution was determined for all compounds.

Additionally, the structure of [DBNH][Zol] (3) was definitively established by single crystal X-ray difraction analysis. Compound 3 crystallized from an asymmetric unit composed of one zwitterionic Zol unit where both phosphonate groups are deprotonated and one nitrogen atom of the imidazolium moiety is protonated. The DBN unit is protonated at the nitrogen atom from the 6-membered ring (Figure 6). The crystal structure is stabilized by several intra and intermolecular hydrogen bonds (see packing in Figure 58).
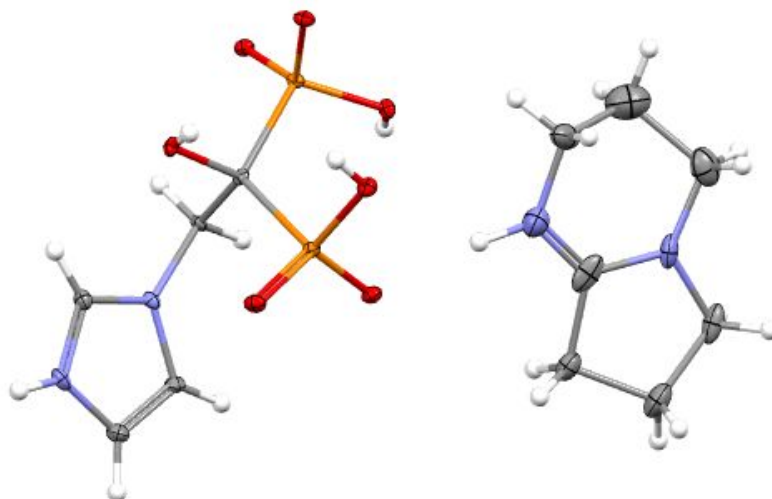
Figure 6 - ORTEP-3 diagram of [DBNH][Zol] (3) with thermal ellipsoids drawn at 30% probability level illus-trating one cationic DBN unit and one zwitterionic Zol entity bearing two anionic phosphonate groups and one cationic imidazolium moiety. The hydrogen, carbon, oxygen, nitrogen and phosphorous atoms are shown in white, grey, red, blue and orange, respectively.

3.3 – Thermal analysis of Zol-ILs

All prepared Zol-ILs were studied by DSC and the melting, crystallization and glass transition temperatures were determined (see Table 4) and compared to the parent drugs.

Depending on the hydration level, zoledronic acid displays a melting point between 214 and 230 °C, to which decomposition rapidly follows (103). Only two of the prepared Zol-ILs, namely have a melting point in the same range, which are [TMGH][Zol] (225.3 °C) and [Ch][Zol] (220.4 °C). These two compounds, in addition to the remaining four solid compounds obtained, are not considered ionic liquids, but organic salts because their melting temperatures are higher than 100 °C.

Table 4 - Physical state, melting (Tm), crystallization (Tc) and glass transition (Tg) temperatures of the prepared Zol-ILs

Salt	Physical state	T_m /°C	T_c /°C	T_g /°C
[TMGH][Zol]	White solid	225.3	-	n.d.
[TMGH]$_2$[Zol]	Colorless paste	-	-	12.4
[DBNH] [Zol]	White solid	208.7	-	45.7
[DBNH]$_2$[Zol]	Colorless paste	-	-	15.1
[Ch] [Zol]	White solid	220.4	-	78.4
[Ch]$_2$[Zol]	White paste	18.6	13.2	-
[EMIM] [Zol]	White solid	198.0	-	29.5
[EMIM]$_2$[Zol]	Colorless paste	-	-	31.7
[C$_2$OHMIM] [Zol]	White solid	143.8 195.9	170.1*	57.3
[C$_2$OHMIM]$_2$[Zol]	Colorless paste	-	-	10.8
[C$_3$OMIM] [Zol]	White solid	125.9 185.0	139.8*	45.7
[C$_3$OMIM]$_2$[Zol]	Colorless paste	-	-	3.4

* cold crystallization

[C$_3$OMIM][Zol] shows a first melt at 125.9 °C followed by a cold crystallization step at 139.8 °C, to which then follows a second melt that occurs at 185 °C. After this the compound remains in an amorphous state characterized by a glass transition temperature of 45.7 °C. [EMIM][Zol] also becomes amorphous after first melt (at 198 °C) with a glass transition temperature of 29.5 °C.

Even though [Ch]$_2$[Zol] is a thick white paste at room temperature, it was possible to determine its melting temperature and the corresponding crystallization peak by DSC,

which occur at 18.6 (exo) and 13.2 °C (endo), respectively. Except for this ionic liquid, all remaining Zol-RTILs are clearly amorphous compounds with defined glass transition temperatures.

3.4 – Solubility Studies

As expected, all ionic liquids and salts were more soluble in water and saline solution at 37 °C than neutral zoledronic acid. Figure 7 summarizes the data obtained from the solubility studies.
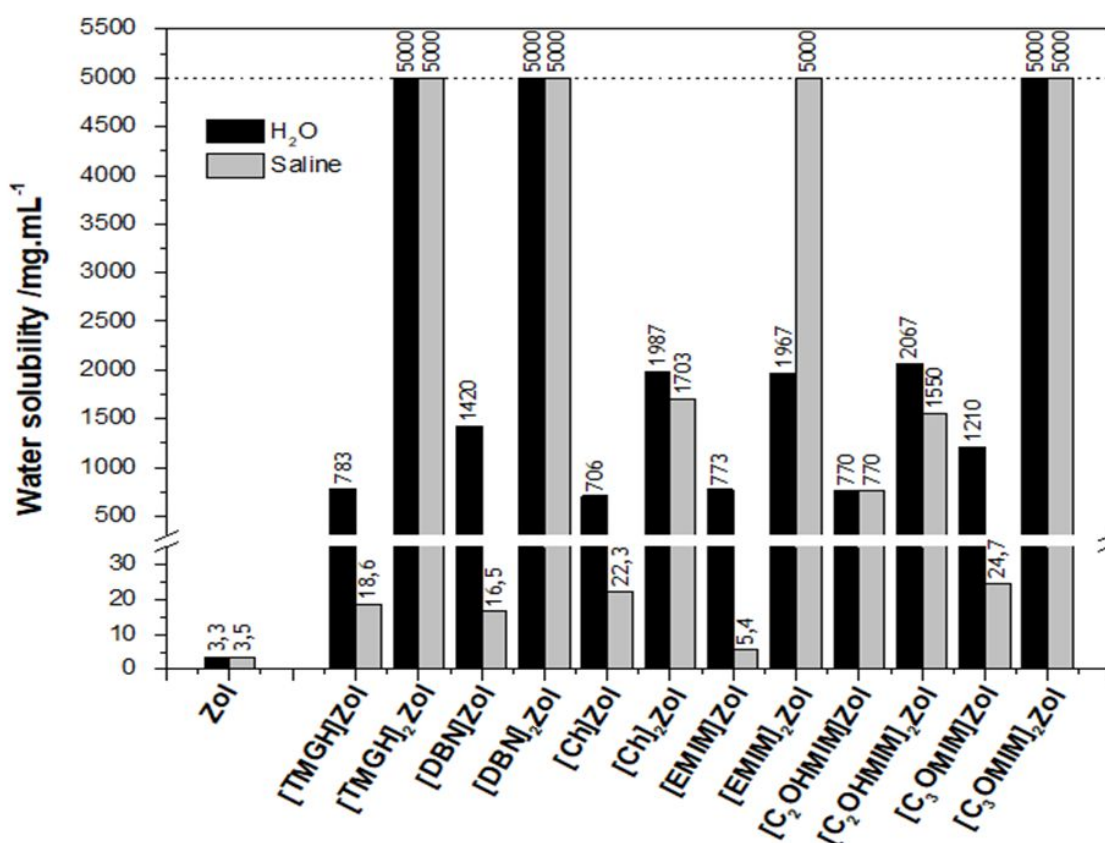
Figure 7- Solubility in water and saline solution at 37 °C of zoledronic acid and Zol-ILs (detection limit is 5g/mL, represented by the upper threshold).

All dianionic zoledronate ionic liquids were more soluble in the tested media than the monoanionic siblings, with three of them ([TMGH]$_2$[Zol], [DBNH]$_2$[Zol] and [C$_3$OMIM]$_2$[Zol]) being completely soluble in water and saline solution. For unknown reasons, [EMIM]$_2$[Zol] was the only ionic compound which was less soluble in water than in saline solution (in which, in fact, it was entirely soluble). Moreover, the monoionic compounds were found to be between 214 and 624-fold more soluble in water than the neutral parent drug. With the exception of [C$_2$OHMIM][Zol], the monoionic compounds had

solubility in saline solution lower than 25 mg/mL with a ratio between 1.5 and 7.0 times in comparison with zoledronic acid.

3.5 – Toxicity studies on normal and cancer cells

The cytotoxicity (IC_{50}) data of the studies with the prepared zoledronic-containing ILs in different human cell lines are presented in Table 5.

Table 5- Antitumor activity (IC50) of zoledronate ionic liquids.

IL	IC_{50} / M Skin fibroblasts	T47D	MG63
Zol	2.43×10^{-6}	a)	5.74×10^{-7}
[TMGH][Zol]	a)	a)	a)
[TMGH]$_2$[Zol]	1.02×10^{-6}	6.87×10^{-6}	6.97×10^{-3}
[DBNH][Zol]	2.50×10^{-3}	1.98×10^{-4}	1.65×10^{-6}
[DBNH]$_2$[Zol]	5.96×10^{-10}	1.25×10^{-10}	a)
[Ch][Zol]	3.98×10^{-6}	6.15×10^{-7}	1.51×10^{-10}
[Ch]$_2$[Zol]	1.46×10^{-10}	1.69×10^{-9}	2.10×10^{-5}
[EMIM][Zol]	4.97×10^{-5}	2.11×10^{-6}	a)
[EMIM]$_2$[Zol]	1.78×10^{-2}	3.82×10^{-5}	5.01×10^{-7}
[C$_2$OHMIM][Zol]	a)	1.84×10^{-5}	5.60×10^{-7}
[C$_2$OHMIM]$_2$[Zol]	1.58×10^{-10}	1.48×10^{-10}	5.58×10^{-8}
[C$_3$OMIM][Zol]	1.47×10^{-2}	2.01×10^{-3}	1.23×10^{-2}
[C$_3$OMIM]$_2$[Zol]	9.71×10^{-8}	8.02×10^{-6}	3.27×10^{-10}

a) Not detected in the tested concentration range.

In general, all monoanionic compounds present lower toxicity to the skin fibroblasts than the dianionic ones, with the seldom exception of the ILs with [EMIM] cation. More specifically, the ILs containing [TMGH], [DBNH], [EMIM]$_2$ and [C$_3$OMIM] were found to be the least toxic from the tested set towards the non-neoplastic cells, with IC_{50} 2.5 mM. These IC_{50} values are at least three orders of magnitude lower than the one found for Zol

(2.43 µM). Regarding the effects on breast cancer cells (T47D), all tested ILs, with the exception of [TMGH][Zol], showed cytotoxic activity whereas Zol was inactive. However, the profile was similar to the one found with skin fibroblasts, which means that they are not selective for any of these cells. In the case of the human osteosarcoma cell line MG63, [Ch][Zol] and [C_3OMIM]$_2$[Zol] showed IC_{50} values of 0.15 and 0.33 nM, which are three orders of magnitude lower than for zoledronic acid (57 mM). In addition, their toxicity towards normal cells was found to be, respectively, four and two orders of magnitude lower than for the osteosarcoma cells, while for Zol this ratio is only of one order of magnitude. Finally, [EMIM]$_2$[Zol] is also worth considering because, while it has comparable activity to Zol towards MG63 cell lines (*ca.* 5×10^{-7} M), it has very low toxicity towards skin fibroblasts (*ca.* 2×10^{-2} M).

The data retrieved from this study may be particularly relevant since osteosarcoma cells are known to induce disturbances in bone metabolism, with an increase in bone turnover rate (62, 104, 105). Thus, the synthesis of compounds with a simultaneous potential inhibitory effect on bone resorption and a selective cytotoxicity against osteosarcoma cells may represent an important strategy for the development of new drugs against osteosarcoma.

3.6 – Experimental Section

General procedure (A) for the synthesis of Zol-ILs with organic superbases as cations:

To a dispersion of zoledronic acid (500 mg, 1.84 mmol) in MeOH/H_2O (15 mL, 1:1) a methanolic solution of 1 or 2 molar equivalents of organic superbase (15 mg/mL) was added dropwise under magnetic stirring. After reacting for 1h the solvent was evaporated and the desired product was dried under vacuo for 24 h.

General procedure (B) for the preparation of Zol-ILs with ammonium cations:

The halide salts of the selected quaternary ammonium cations were dissolved in methanol and passed slowly through an anion-exchange column A-26(OH) (3 equivalents). The freshly formed methanolic solutions of the corresponding hydroxide salts (1 or 2 equivalents) were consequently added dropwise to zoledronic acid (500 mg, 1 equivalent) dispersed in H_2O under magnetic stirring. After 1 h, the solvent of the clear solution was evaporated and the desired product was dried under vacuo for 24 h.

Materials, experimental procedures, compound characterization data, NMR and FTIR spectra, and DSC thermograms. X-Ray diffraction data for compound 3. Cytotoxicity data for the cation halides and Zoledronate.

3.7 - Supplementary Information

3.7.1 - Experimental

Materials

All acquired reagents were used without further purification. Zoledronic acid (98.5%) was purchased from Molekula, 1,1,3,3-tetramethylguanidine (TMG, 99%), 1,5-diazabicyclo(4.3.0)non-5-ene (DBN, 99%), and choline chloride (ChCl, 99%), were supplied by Sigma-Aldrich. 1-Ethyl-3-methylimidazolium chloride ([EMIM]Cl, 99%), 1-(2-hydroxyethyl)-3-methylimidazolium chloride ([C_2OHMIM]Cl], 98%), 1-(2-methoxyethyl)-3-methylimidazolium chloride ([C_3OMIM]Cl], 98%) were purchased at Solchemar. Methanol HPLC grade was acquired from Honeywell and deionized water was processed by Diwer Technologies water max w2 equipment.

General procedure A for the synthesis of Zol-ILs with organic superbases as cations

To a dispersion of zoledronic acid (500 mg, 1.84 mmol) in MeOH/H_2O (15 mL, 1:1) a methanolic solution of 1 or 2 molar equivalents of organic superbase (15 mg/mL) was added dropwise under magnetic stirring. After reacting for 1h the solvent was evaporated and the desired product was dried under vacuo for 24 h.

General procedure (B) for the preparation of Zol-ILs with ammonium cations

The halide salts of the selected quaternary ammonium cations were dissolved in methanol and passed slowly through an anion-exchange column A-26 (OH) (3 equivalents). The freshly formed methanolic solutions of the corresponding hydroxide salts (1 or 2 equivalents) were consequently added dropwise to zoledronic acid (500 mg, 1 equivalent) dispersed in H_2O under magnetic stirring. After 1 h, the solvent of the clear solution was evaporated and the desired product was dried under vacuo for 24 h.

The prepared compounds were characterized by ^{1}H and ^{13}C NMR recorded on a Bruker AMX400 spectrometer. Chemical shifts are reported downfield in parts per million considering the solvent residual signal. ^{13}C NMR spectra in D_2O were referenced to added MeOH or MeCN. IR spectra were recorded on a FTIR Bruker Tensor 27 Spectrometer using KBr matrixes. DSC analysis was carried out using a TA Instruments Q-series TM Q2000 DSC with a refrigerated cooling system. Between 2 and 10 mg of salt were crimped into an aluminum standard sample pan with lid which was continuously purged with nitrogen gas at 50 mL/min. The employed procedure was dependent on the melting point of the sample. A typical experiment consisted on a heating step (20 ºC/min) to 80 or 120 ºC (15-20 minutes), cooling (20 ºC/min) to -90 ºC, heating (10 ºC/min) to 200 ºC, cooling (10 ºC/min) to -90 ºC, heating (10 ºC/min) to 200 ºC, cooling (10 ºC/min) to -90 ºC, heating (20 ºC/min) to 200 ºC and cooling (20 ºC/min) to -90 ºC. Glass transition (T_g), melting (T_m) cold crystallization (T_{cc}) and decomposition temperatures were determined in the heating steps, while crystallization temperatures (T_c) were acquired in the cooling steps. The solubility of the salts in water and saline solution was determined by adding 5 to 10 µL of solvent to an Eppendorf containing precisely weighed *ca.* 30 mg of sample until a homogeneous solution is obtained upon mixture in a vortex.

Experimental data of the synthesized compounds

Preparation of bis(dimethylaminomethaniminium) hydrogen (1-hydroxy-2-(1*H*-imidazol-1-yl)-1-phosphonoethyl)phosphonate, [TMGH][Zol]

Figure 8 - [TMGH][Zol]

Using tetramethylguanidine (212 mg, 1.84 mmol) [TMGH][ZolH] was obtained as a white solid in quantitative yield (712 mg). T_m = 225.3 ºC; ^{1}H NMR (400.13 MHz, D_2O) 8.69 (br s, 1H, c), 7.51 (br s, 1H, e), 7.34 (br s, 1H, d), 4.66 (d, J = 7.4 Hz, 1H, b$_1$), 4.64 (d, J = 8.5 Hz, 1H, b$_2$), 2.92 (s, 12H, f). ^{13}C NMR (100.62 MHz, D_2O) 161.4 (g), 135.7 (c), 123.9 (d), 118.2 (e), 72.9 (t, J = 132.0 Hz, a), 52.6 (b), 38.8 (f) ppm; FTIR (KBr) 3456, 3180, 3114, 2815, 2708, 2363, 1648, 1609, 1579, 1414, 1209, 1173, 1034, 1014, 915,

889 cm^{-1}. Anal. calcd for $C_{10}H_{23}N_5O_7P_2.H_2O$: C, 29.71; H, 5.98; N, 17.32; found: C, 29.77; H, 6.14; N, 17.36.

Preparation of bis(bis(dimethylamino)methaniminium) (1-hydroxy-2-(1*H*-imidazol-1-yl)ethane-1,1-diyl)bis(hydrogenphosphonate), [TMGH]$_2$[Zol]
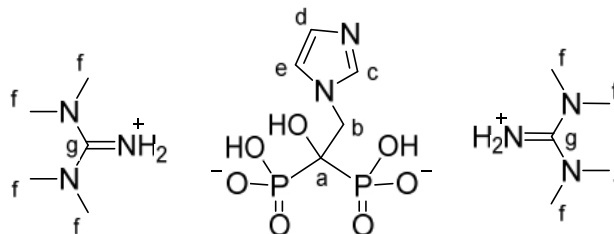
Figure 9 - [TMGH]2[Zol]

Using tetramethylguanidine (423 mg, 3.68 mmol) [TMGH]$_2$[Zol] was obtained as a colorless paste in quantitative yield (922 mg). T_g = 43.8 °C; ^{1}H NMR (400.13 MHz, DMSO-d^6) 7.54 (br s, 1H, c), 7.17 (br s, 1H, e), 6.65 (br s, 1H, d), 4.29 (d, J = 10.9 Hz, 1H, b$_1$), 4.27 (d, J = 9.2 Hz, 1H, b$_2$), 2.86 (s, 24H, f). ^{13}C NMR (100.62 MHz, DMSO-d^6) 161.4 (g), 138.9 (c), 125.9 (d), 121.9 (e), 72.3 (t, J = 120.6 Hz, a), 48.6 (b), 39.3 (f) ppm; FTIR (KBr) 3410, 3167, 2961, 2817, 2708, 2449, 2358, 1612, 1565, 1351, 1167, 1118, 1044, 973, 879 cm^{-1}. Anal. calcd for $C_{15}H_{36}N_8O_7P_2.(H_2O)_{2.5}$: C, 32.91; H, 7.55; N, 20.47; found: C, 32.93; H, 6.71; N, 20.83.

Preparation of (2,3,4,6,7,8-hexahydropyrrolo[1,2-a]pyrimidin-1-ium) hydrogen (1-hydroxy-2-(1*H*-imidazol-1-yl)-1-phosphonoethyl)phosphonate, [DBNH][Zol]
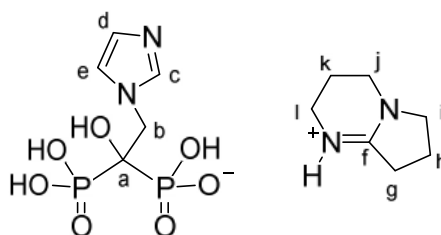
Figure 10 - [DBNH][Zol]

Using 1,5-diazabicyclo(4.3.0)non-5-ene (227 mg, 1.84 mmol) [DBNH][Zol] was obtained as a white solid in quantitative yield (729 mg). This compound crystallized from slow evaporation of water at room temperature. T_m = 208.7 °C, T_g = 45.7 °C; ^{1}H NMR (400.13 MHz, D$_2$O) 8.69 (br s, 1H, c), 7.51 (br s, 1H, e), 7.35 (br s, 1H, d), 4.67 (d, J = 12.1 Hz, 1H, b$_1$), 4.65 (d, J = 11.1 Hz, 1H, b$_2$), 3.65 (t, J = 7.2 Hz, 2H, l), 3.40 (t, J = 5.6 Hz, 2H, i), 3.35 (t, J = 5.6 Hz, 2H, j), 2.82 (t, J = 7.8 Hz, 2H, g), 2.10 (quint, J = 7.6 Hz, 2H, h), 1.98 (quint, J = 5.6 Hz, 2H, k). ^{13}C NMR (100.62 MHz, D$_2$O) 165.9 (f), 137.3 (c), 125.4 (d), 119.7 (e), 74.4 (t, J = 124.3 Hz, a), 54.9 (i), 54.1 (b), 43.7 (j), 39.5 (l), 31.4 (g),

19.7, 19.7 (h, k) ppm; FTIR (KBr) 3418, 3231, 3133, 2959, 2781, 2360, 1680, 1606, 1309, 1146, 1040, 909 cm^{-1}. Anal. calcd for $C_{12}H_{22}N_4O_7P_2 \cdot H_2O$: C, 34.79; H, 5.84; N, 13.52; found: C, 34.67; H, 6.04; N, 13.32.

Preparation of bis(2,3,4,6,7,8-hexahydropyrrolo[1,2-a]pyrimidin-1-ium) (1-hydroxy-2-(1*H*-imidazol-1-yl)ethane-1,1-diyl)bis(hydrogenphosphonate), [DBNH]$_2$[Zol]
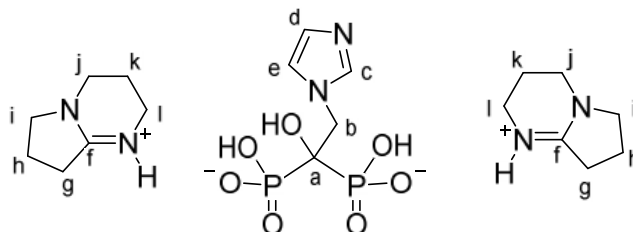
Figure 11 - [DBNH]2[Zol]

Using 1,5-diazabicyclo(4.3.0)non-5-ene (457 mg, 3.68 mmol) [DBNH]$_2$[Zol] was obtained as a colorless paste in quantitative yield (956 mg). T_g = 15.1 °C; ^{1}H NMR (400.13 MHz, D$_2$O) 8.55 (br s, 1H, c), 7.48 (br s, 1H, e), 7.26 (br s, 1H, d), 4.60 (d, J = 13.4 Hz, 1H, b$_1$), 4.58 (d, J = 12.4 Hz, 1H, b$_2$), 3.64 (t, J = 7.2 Hz, 4H, l), 3.39 (t, J = 5.7 Hz, 4H, i), 3.34 (t, J = 5.6 Hz, 4H, j), 2.82 (t, J = 7.6 Hz, 4H, g), 2.10 (quint, J = 7.6 Hz, 4H, h), 1.98 (quint, J = 5.6 Hz, 4H, k). ^{13}C NMR (100.62 MHz, D$_2$O) 165.9 (f), 137.6 (c), 125.1 (d), 120.7 (e), 74.1 (t, J = 124.6 Hz, a), 54.9 (i), 54.5 (b), 43.7 (j), 39.5 (l), 31.4 (g), 19.7, 19.7 (h, k) ppm; FTIR (KBr) 3415, 3273, 3126, 2961, 2888, 2786, 2671, 2448, 2358, 2103, 1680, 1309, 1118, 1045, 973, 888 cm^{-1}. Anal. calcd for $C_{19}H_{34}N_6O_7P_2 \cdot (H_2O)_3$: C, 39.72; H, 7.02; N, 14.63; found: C, 39.74; H, 7.17; N, 14.55.

Preparation of 2-hydroxy-*N,N,N*-trimethylethan-1-aminium hydrogen (1-hydroxy-2-(1*H*-imidazol-1-yl)-1-phosphonoethyl)phosphonate, [Ch][Zol]
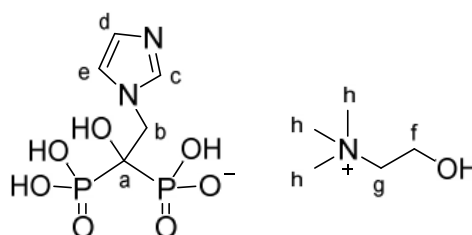
Figure 12 - [Ch][Zol]

Using choline chloride (257 mg, 1.84 mmol) [Ch][Zol] was obtained as a white solid in quantitative yield (690 mg). T_m = 220.4 °C; T_g = 78.4 °C; ^{1}H NMR (400.13 MHz, D$_2$O) 8.71 (br s, 1H, c), 7.53 (br s, 1H, e), 7.36 (br s, 1H, d), 4.68 (d, J = 11.7 Hz, 1H, b$_1$), 4.66 (d, J = 12.1 Hz, 1H, b$_2$), 4.10 – 3.99 (m, 2H, f), 3.56 – 3.46 (m, 2H, g), 3.18 (s, 9H, h). ^{13}C NMR (100.62 MHz, D$_2$O) 136.4 (c), 124.5 (d), 118.8 (e), 73.5 (t, J = 131.8 Hz, a), 68.0 (t, J = 3.1 Hz, g), 56.2 (f), 54.5 (t, J = 3.9 Hz, h), 53.2 (t, J = 2.3 Hz, b) ppm; FTIR (KBr) 3251,

3138, 3062, 2735, 2361, 1642, 1480, 1401, 1165, 1081, 953, 895 cm^{-1}. Anal. calcd for C$_{10}$H$_{23}$N$_3$O$_8$P$_2$: C, 32.01; H, 6.18; N, 11.20; found: C, 32.22; H, 6.20; N, 11.07.

Preparation of bis(2-hydroxy-*N,N,N*-trimethylethan-1-aminium) (1-hydroxy-2-(1*H*-imidazol-1-yl)ethane-1,1-diyl)bis(hydrogen phosphonate), [Ch]$_2$[Zol]
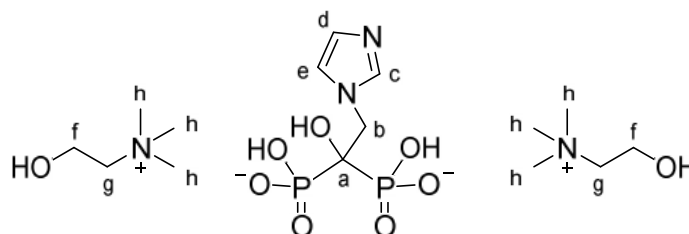
Figure 13 - [Ch]2[Zol]

Using choline chloride (514 mg, 3.68 mmol) [Ch]$_2$[Zol] was obtained as a white paste in quantitative yield (1014 mg). T$_m$ = 18.6 °C, T$_c$ = 13.2 °C; ^{1}H NMR (400.13 MHz, D$_2$O) 8.67 (br s, 1H, c), 7.52 (br s, 1H, e), 7.33 (br s, 1H, d), 4.64 (d, J = 12.1 Hz, 1H, b$_1$), 4.62 (d, J = 12.9 Hz, 1H, b$_2$), 4.09 – 4.01 (m, 4H, f), 3.54 – 3.47 (m, 4H, g), 3.18 (s, 18H, h). ^{13}C NMR (100.62 MHz, D$_2$O) 136.4 (c), 124.4 (d), 119.1 (e), 73.2 (t, J = 131.8 Hz, a), 68.0 (t, J = 3.1 Hz, g), 56.2 (f), 54.5 (t, J = 3.9 Hz, h), 53.7 (t, J = 2.3 Hz, b) ppm; FTIR (KBr) 3379, 3260, 3018, 2958, 2908, 2742, 2355, 1643, 1478, 1405, 1175, 1090, 949, 869 cm^{-1}. Anal. calcd for C$_{15}$H$_{36}$N$_4$O$_9$P$_2$.(H$_2$O)$_3$: C, 33.84; H, 7.95; N, 10.52; found: C, 33.72; H, 7.39; N, 10.89.

Preparation of (1-ethyl-3-methyl-1*H*-imidazol-3-ium) hydrogen (1-hydroxy-2-(1*H*-imidazol-1-yl)-1-phosphonoethyl)phosphonate, [EMIM][Zol]
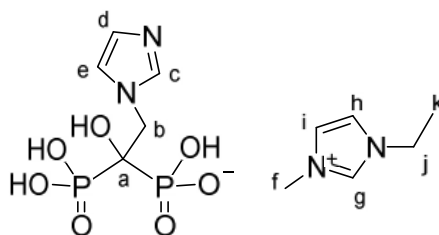
Figure 14 - [EMIM][Zol]

Using ethylmethylimidazolium bromide (352 mg, 1.84 mmol) [EMIM][Zol] was obtained as a white solid in quantitative yield (702 mg). T$_m$ = 198.0 °C, T$_g$ = 29.5 °C; ^{1}H NMR (400.13 MHz, D$_2$O) 8.72 (br s, 1H, g), 8.69 (br s, 1H, c), 7.54 (br s, 1H, e), 7.47 (br s, 1H, i), 7.41 (br s, 1H, h), 7.37 (br s, 1H, d), 4.69 (d, J = 12.4 Hz, 1H, b$_1$), 4.67 (d, J = 12.1 Hz, 1H, b$_2$), 4.21 (q, J = 7.3 Hz, 2H, j), 3.88 (s, 3H, f), 1.48 (t, J = 7.3Hz, 3H, k). ^{13}C NMR (100.62 MHz, D$_2$O) 136.4 (c), 124.5 (d), 124.0 (i), 122.5 (h), 119.8 (e), 73.5 (t, J = 135.0 Hz, a), 53.2 (b), 45.3 (j), 36.2 (f), 15.1 (k) ppm; FTIR (KBr) 3378, 3262, 3099, 2772,

2320, 1969, 1711, 1565, 1452, 1208, 1162, 1032, 947, 873 cm^{-1}. Anal. calcd for C$_{11}$H$_{20}$N$_4$O$_7$P$_2$.H$_2$O: C, 33.01; H, 5.54; N, 14.00; found: C, 32.87; H, 5.64; N, 13.74.

Preparation of bis(1-ethyl-3-methyl-1*H*-imidazol-3-ium) (1-hydroxy-2-(1*H*-imidazol-1-yl)ethane-1,1-diyl)bis(hydrogen phosphonate), [EMIM]$_2$[Zol]
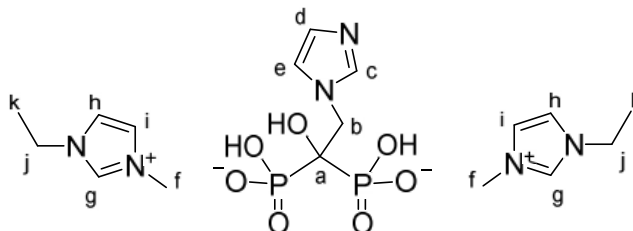
Figure 15 - [EMIM]2[Zol]

Using ethylmethylimidazolium chloride (703 mg, 3.68 mmol) [EMIM]$_2$[Zol] was obtained as a colorless paste in quantitative yield (905 mg). T_g = 31.7 ºC; ^{1}H NMR (400.13 MHz, D$_2$O) 8.70 (br s, 2H, g), 8.62 (br s, 1H, c), 7.52 (br s, 1H, e), 7.47 (br s, 2H, i), 7.41 (br s, 2H, h), 7.31 (br s, 1H, d), 4.64 (d, J = 12.7 Hz, 1H, b$_1$), 4.62 (d, J = 13.2 Hz, 1H, b$_2$), 4.21 (q, J = 7.4 Hz, 4H, j), 3.88 (s, 6H, f), 1.48 (t, J = 7.4Hz, 6H, k). ^{13}C NMR (100.62 MHz, D$_2$O) 136.5 (c), 124.3 (d), 124.0 (i), 122.5 (h), 119.4 (e), 73.2 (t, J = 124.6 Hz, a), 53.7 (b), 45.4 (j), 36.2 (f), 15.1 (k) ppm; FTIR (KBr) 3417, 3152, 3113, 2961, 2679, 2453, 2359, 2314, 2094, 1654, 1570, 1399, 1169, 1118, 1046, 974, 888 cm^{-1}. Anal. calcd for C$_{17}$H$_{30}$N$_6$O$_7$P$_2$.(H$_2$O)$_2$: C, 38.47; H, 6.80; N, 15.68; found: C, 38.64; H, 6.49; N, 15.90.

Preparation of (1-(2-hydroxyethyl)-3-methyl-1*H*-imidazol-3-ium) hydrogen (1-hydroxy-2-(1*H*-imidazol-1-yl)-1-phosphonoethyl)phosphonate, [C$_2$OHMIM][Zol]
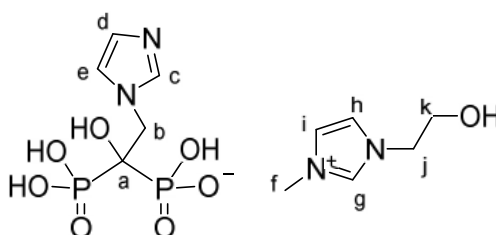
Figure 16 - [C2OHMIM][Zol]

Using hydroxyethylmethylimidazolium chloride (299 mg, 1.84 mmol) [C$_2$OHMIM][Zol] was obtained as a white solid in quantitative yield (732 mg). T_m = 143.8, 195.9 ºC, T_{cc} = 170.1 ºC; T_g = 57.3 ºC; ^{1}H NMR (400.13 MHz, D$_2$O) 8.74 (br s, 1H, g), 8.70 (br s, 1H, c), 7.53 (br s, 1H, e), 7.50 (br s, 1H, i), 7.44 (br s, 1H, h), 7.36 (br s, 1H, d), 4.68 (d, J = 11.4 Hz, 1H, b$_1$), 4.66 (d, J = 12.2 Hz, 1H, b$_2$), 4.31 (t, J = 4.7 Hz, 2H, j), 3.99 – 3.85 (m, 5H, f, k). ^{13}C NMR (100.62 MHz, D$_2$O) 136.4 (c), 124.5 (d), 124.2 (i), 123.0 (h), 118.8 (e), 73.5 (t, J = 130.9 Hz, a), 60.4 (k), 53.2 (b), 52.1 (j), 36.3 (f) ppm; FTIR (KBr) 3404, 3142, 3112, 2850, 2309, 1962, 1668, 1549, 1410, 1294, 1223, 1146, 1084, 1031,

949, 902 cm^{-1}. Anal. calcd for $C_{11}H_{20}N_4O_8P_2 \cdot (H_2O)_{0.5}$: C, 32.44; H, 5.20; N, 13.76; found: C, 32.26; H, 5.41; N, 13.49.

Preparation of bis(1-(2-hydroxyethyl)-3-methyl-1*H*-imidazol-3-ium) (1-hydroxy-2-(1*H*-imidazol-1-yl)ethane-1,1-diyl)bis(hydrogen phosphonate), [C$_2$OHMIM]$_2$[Zol]
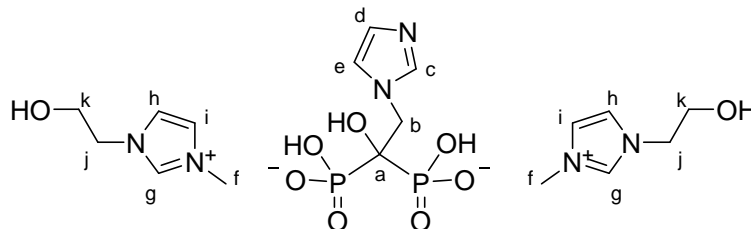
Figure 17 - [C2OHMIM]2[Zol]

Using hydroxyethylmethylimidazolium chloride (598 mg, 3.68 mmol) [C$_2$OHMIM]$_2$[Zol] was obtained as a colorless paste in quantitative yield (965 mg). T$_g$ = 10.8 ºC; ^{1}H NMR (400.13 MHz, D$_2$O) 8.75 (br s, 2H, g), 8.56 (br s, 1H, c), 7.54 – 7.48 (m, 3H, e, i), 7.45 (br s, 2H, h), 7.27 (br s, 1H, d), 4.62 (d, J = 13.1 Hz, 1H, b$_1$), 4.60 (d, J = 13.1 Hz, 1H, b$_2$), 4.31 (t, J = 4.8 Hz, 4H, j), 3.92 (t, J = 4.8 Hz, 4H, k), 3.90 (s, 6H, f). ^{13}C NMR (100.62 MHz, D$_2$O) 136.7 (c), 124.2 (d, i), 123.0 (h), 119.9 (e), 73.2 (t, J = 124.3 Hz, a), 60.4 (k), 53.5 (b), 52.1 (j), 36.3 (f) ppm; FTIR (KBr) 3417, 3152, 3113, 2960, 2362, 1636, 1566, 1400, 1167, 1118, 1090, 1064, 974, 879, 828 cm^{-1}. Anal. calcd for $C_{17}H_{30}N_6O_9P_2 \cdot (H_2O)_3$: C, 35.30; H, 6.27; N, 14.53; found: C, 34.94; H, 6.64; N, 14.08.

Preparation of 1-(2-methoxyethyl)-3-methyl-1*H*-imidazol-3-ium hydrogen (1-hydroxy-2-(1*H*-imidazol-1-yl)-1-phosphonoethyl)phosphonate, [C$_3$OMIM][Zol]
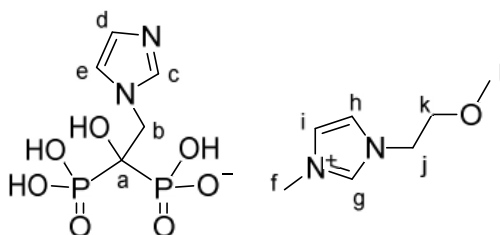

Figure 18 - [C3OMIM][Zol]

Using methoxyethylmethylimidazolium chloride (325 mg, 1.84 mmol) [C$_3$OMIM][Zol] was obtained as a white solid in quantitative yield (758 mg). T$_m$ = 125.9, 185 ºC; T$_{cc}$ = 139.8 ºC; T$_g$ = 45.7 ºC; ^{1}H NMR (400.13 MHz, D$_2$O) 8.73 (br s, 1H, g), 8.71 (br s, 1H, c), 7.53 (br s, 1H, e), 7.49 (br s, 1H, i), 7.44 (br s, 1H, h), 7.37 (br s, 1H, d), 4.69 (d, J = 12.1 Hz, 1H, b$_1$), 4.67 (d, J = 11.8 Hz, 1H, b$_2$), 4.38 (t, J = 4.8 Hz, 2H, j), 3.89 (s, 3H, f), 3.82 (t, J = 4.8 Hz, 2H, k), 3.37 (s, 3H, l). ^{13}C NMR (100.62 MHz, D$_2$O) 136.3 (c), 124.5 (d), 124.1 (i), 123.0 (h), 118.7 (e), 73.4 (t, J = 132.2 Hz, a), 70.3 (l), 58.7 (k), 53.2 (b), 49.4 (j), 36.2 (f) ppm; FTIR (KBr) 3424, 3146, 3105, 2836, 2360, 1964, 1647, 1577,

1401, 1265, 1173, 1084, 890, 850, 771 cm^{-1}. Anal. calcd for $C_{12}H_{22}N_4O_8P_2 \cdot H_2O$: C, 33.50; H, 5.62; N, 13.02; found: C, 33.44; H, 5.86; N, 12.80.

Preparation of bis(1-(2-methoxyethyl)-3-methyl-1*H*-imidazol-3-ium) (1-hydroxy-2-(1*H*-imidazol-1-yl)ethane-1,1-diyl)bis(hydrogen phosphonate), [C$_3$OMIM]$_2$[Zol]
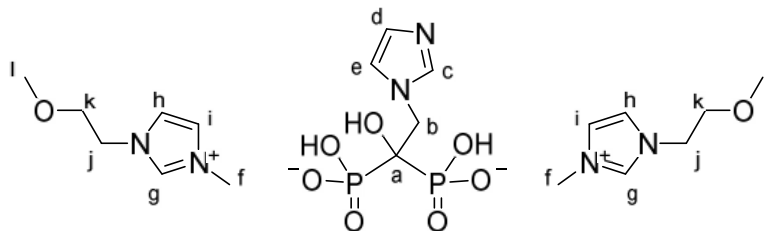

Figure 19 - [C3OMIM]2[Zol]

Using methoxyethylmethylimidazolium chloride (650 mg, 3.68 mmol) [C$_3$OMIM][Zol] was obtained as a white solid in quantitative yield (1016 mg). T_g = 3.4 ºC; ^{1}H NMR (400.13 MHz, D$_2$O)   8.73 (br s, 2H, g), 8.57 (br s, 1H, c), 7.55 – 7.46 (m, 3H, e, i), 7.44 (br s, 2H, h), 7.28 (br s, 1H, d), 4.63 (d, J = 12.2 Hz, 1H, b$_1$), 4.61 (d, J = 13.0 Hz, 1H, b$_2$), 4.38 (t, J = 4.7 Hz, 4H, j), 3.89 (s, 6H, f), 3.82 (t, J = 4.7 Hz, 4H, k), 3.37 (s, 6H, l). ^{13}C NMR (100.62 MHz, D$_2$O)   136.0 (c), 123.6 (d), 123.5 (i), 122.4 (h), 119.1 (e), 72.5 (t, J = 124.5 Hz, a), 69.8 (l), 58.1 (k), 53.0 (b), 48.8 (j), 35.6 (f) ppm; FTIR (KBr) 3425, 3150, 3113, 2960, 2900, 2830, 2459, 2360, 1635, 1567, 1400, 1169, 1118, 1090, 1044, 973, 829 cm^{-1}. Anal. calcd for $C_{19}H_{34}N_6O_9P_2 \cdot (H_2O)_6$: C, 34.55; H, 7.02; N, 12.72; found: C, 34.83; H, 5.99; N, 13.02.
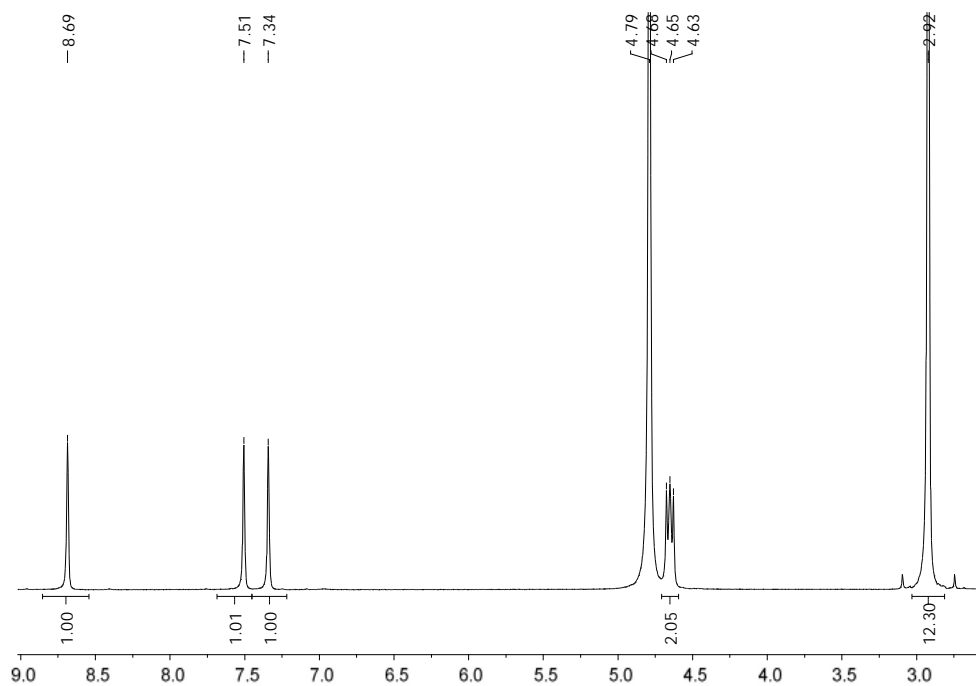
Figure 20 - ¹H NMR spectra of [TMGH][Zol]
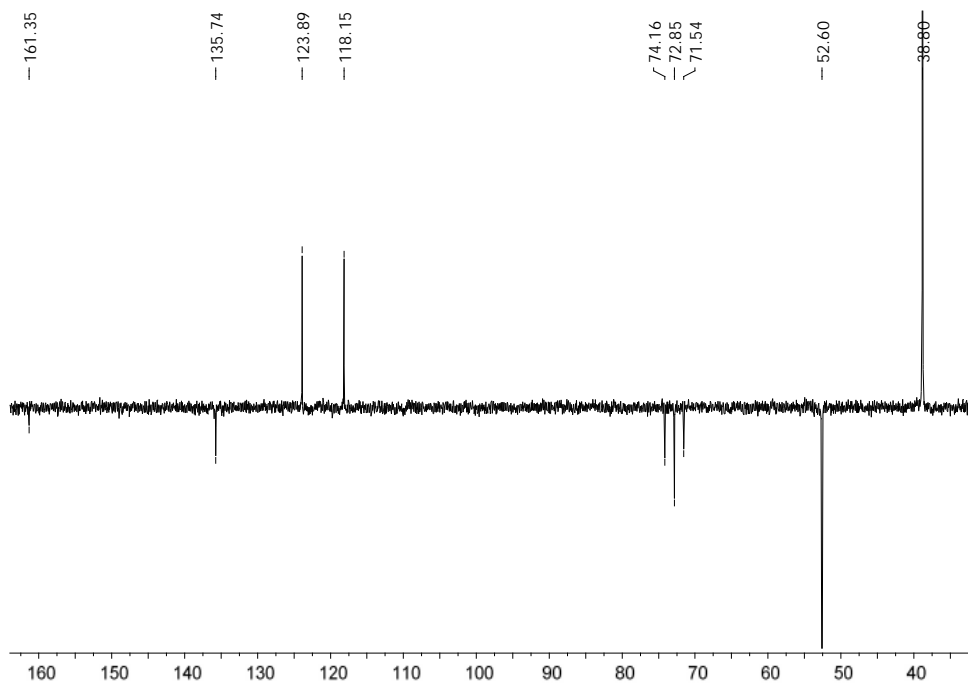
Figure 21 - ¹³C NMR spectra of [TMGH][Zol]
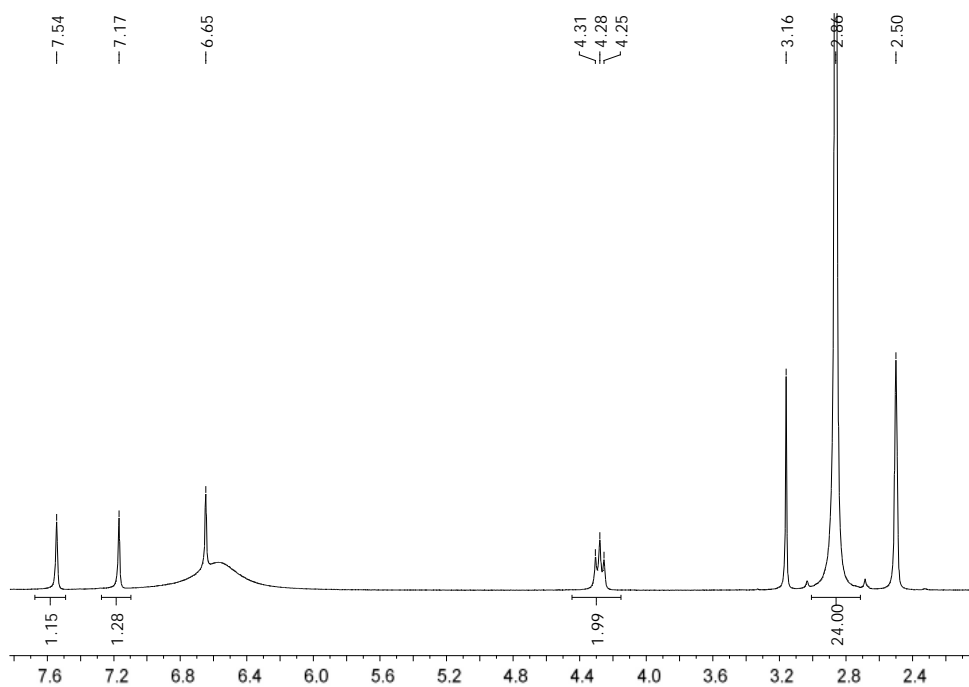
Figure 22 - ¹H NMR spectra of [TMGH]2[Zol]
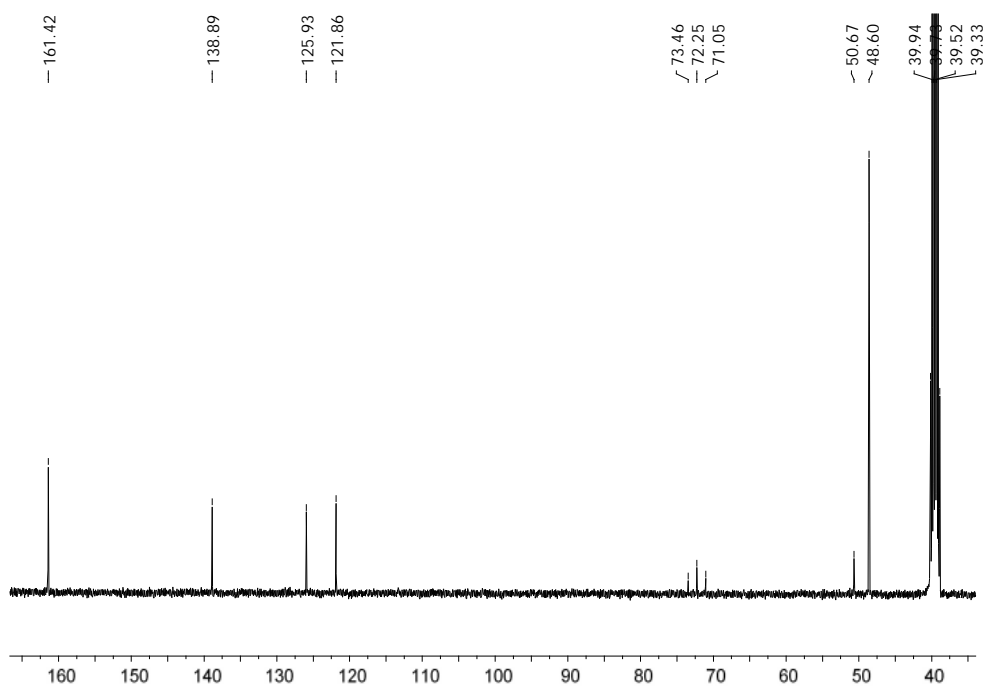
Figure 23 - ¹³C NMR spectra of [TMGH]2[Zol]
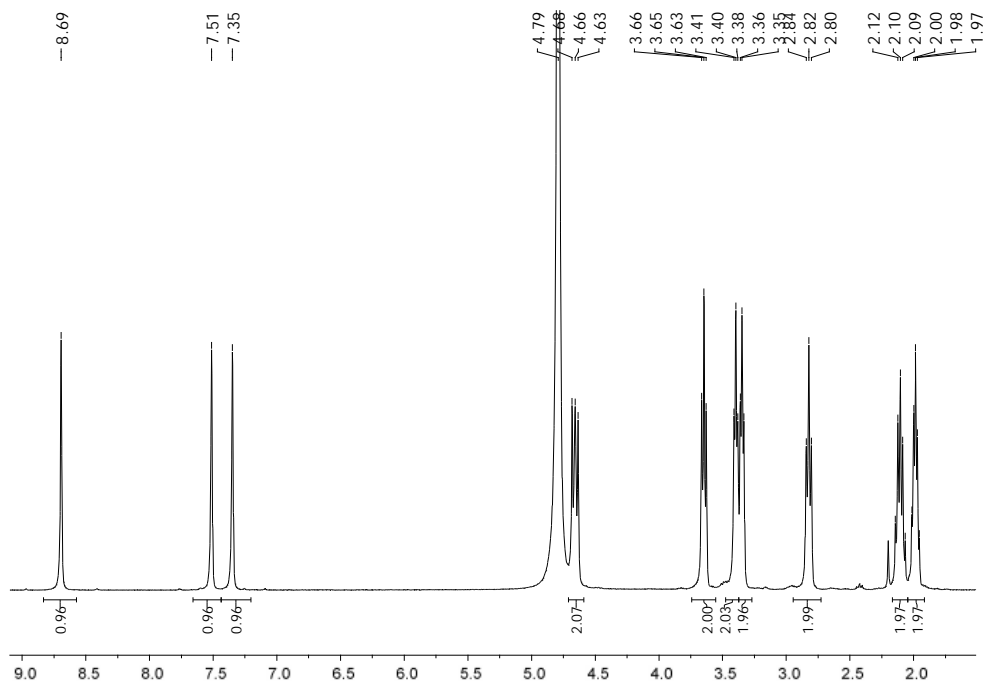
Figure 24 - ¹H NMR spectra of [DBNH][Zol]
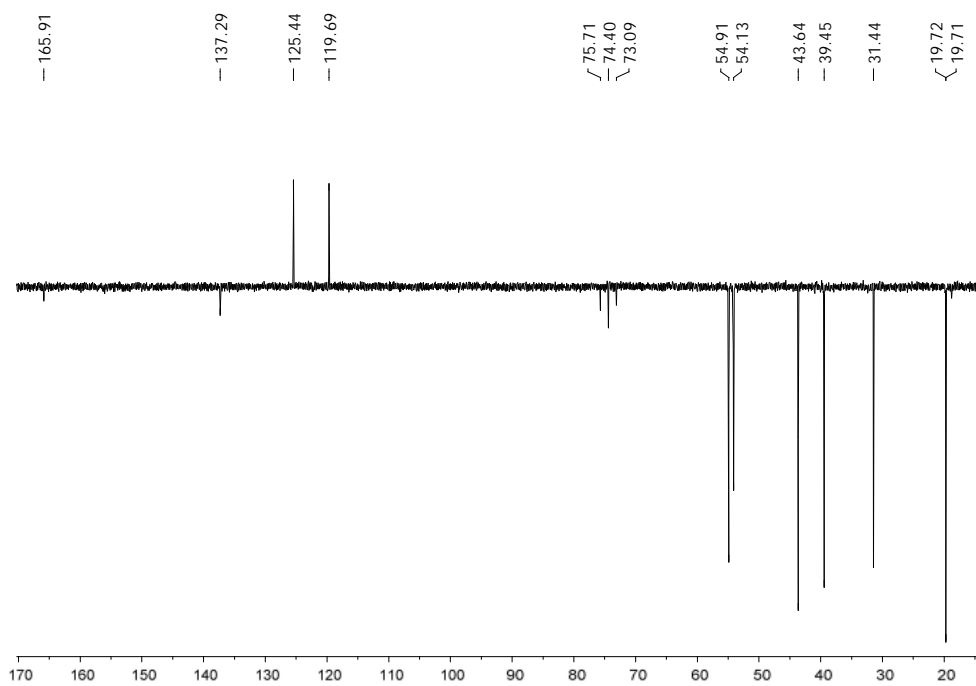
Figure 25 - ¹³C NMR spectra of [DBNH][Zol]
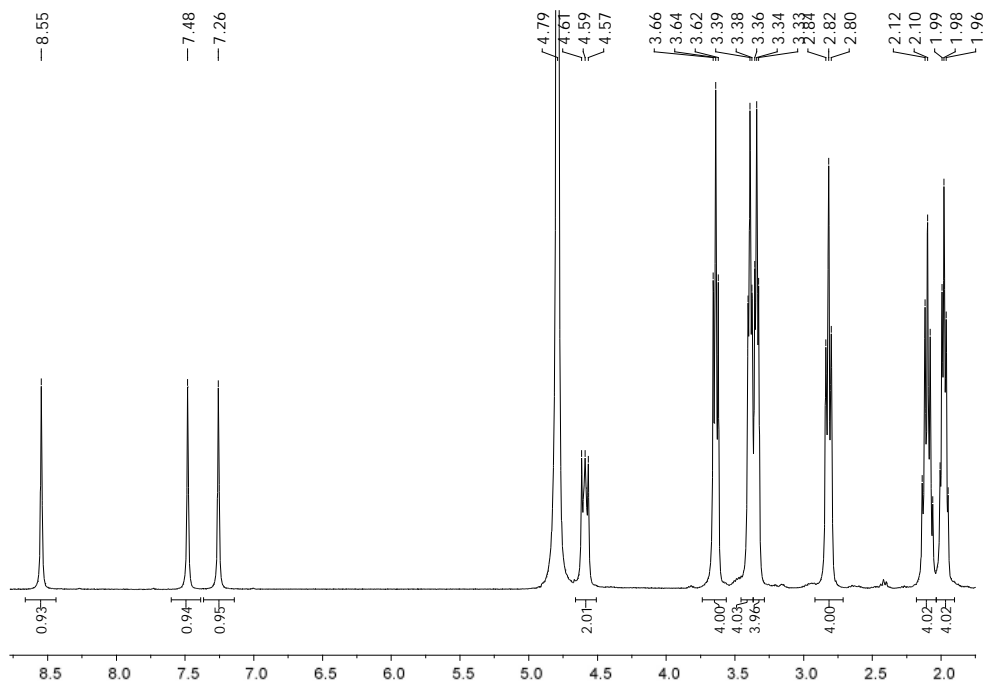
Figure 26 - ^{1}H NMR spectra of [DBNH]2[Zol]
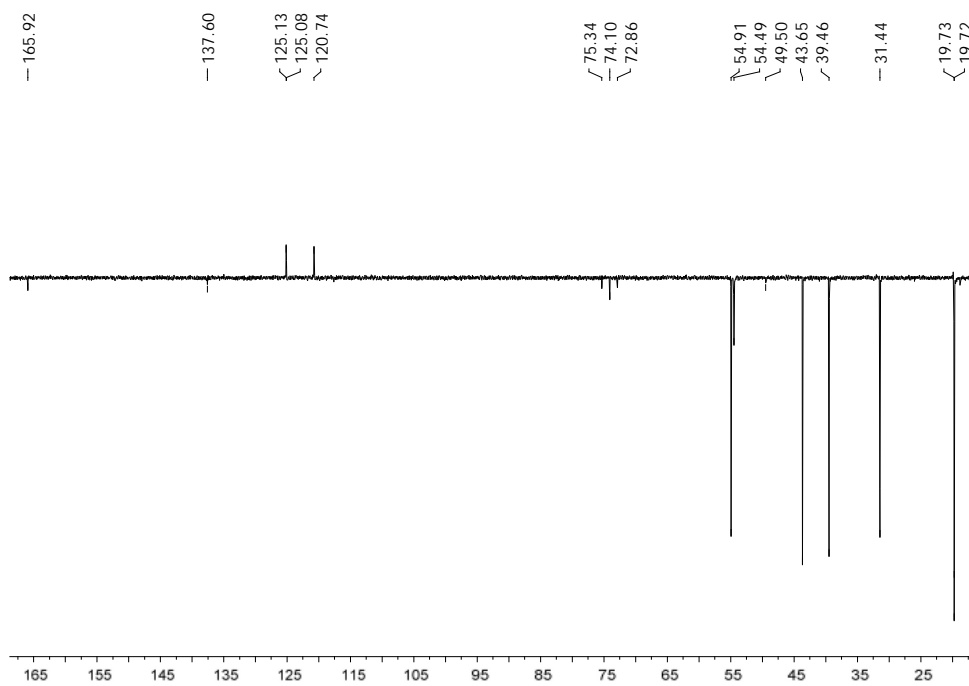
Figure 27 - ^{13}C NMR spectra of [DBNH]2[Zol]
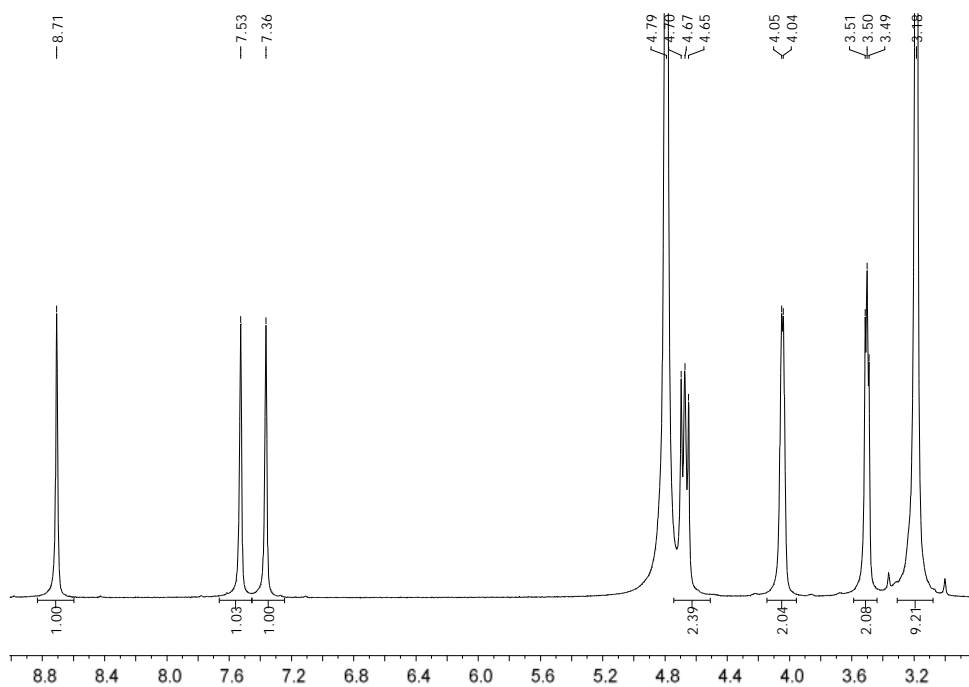
Figure 28 - ^{1}**H NMR spectra of [Ch][Zol]**
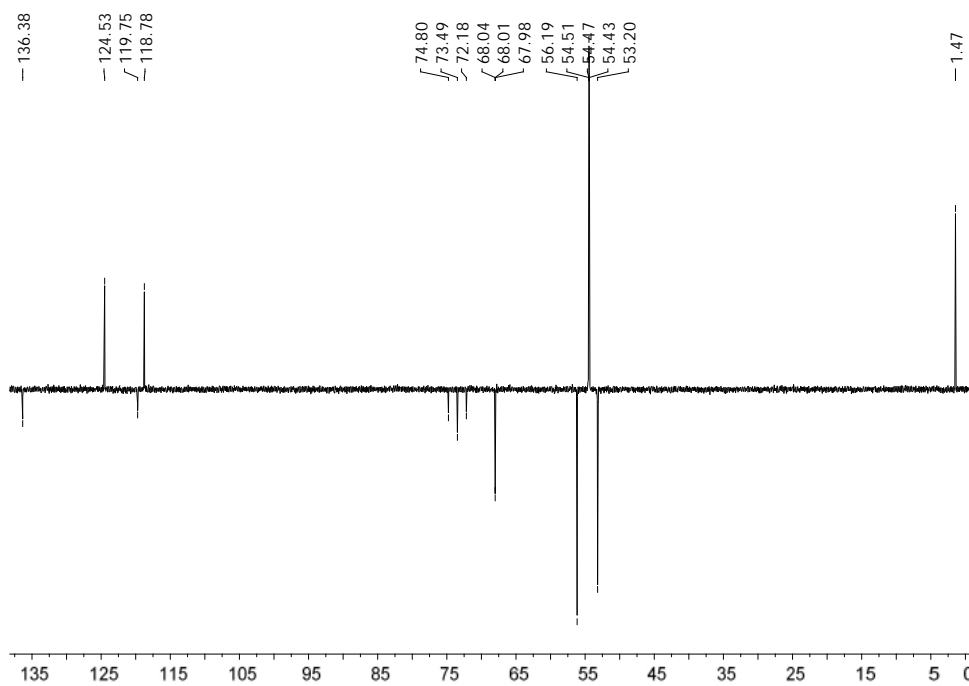
Figure 29 - ^{13}**C NMR spectra of [Ch][Zol]**
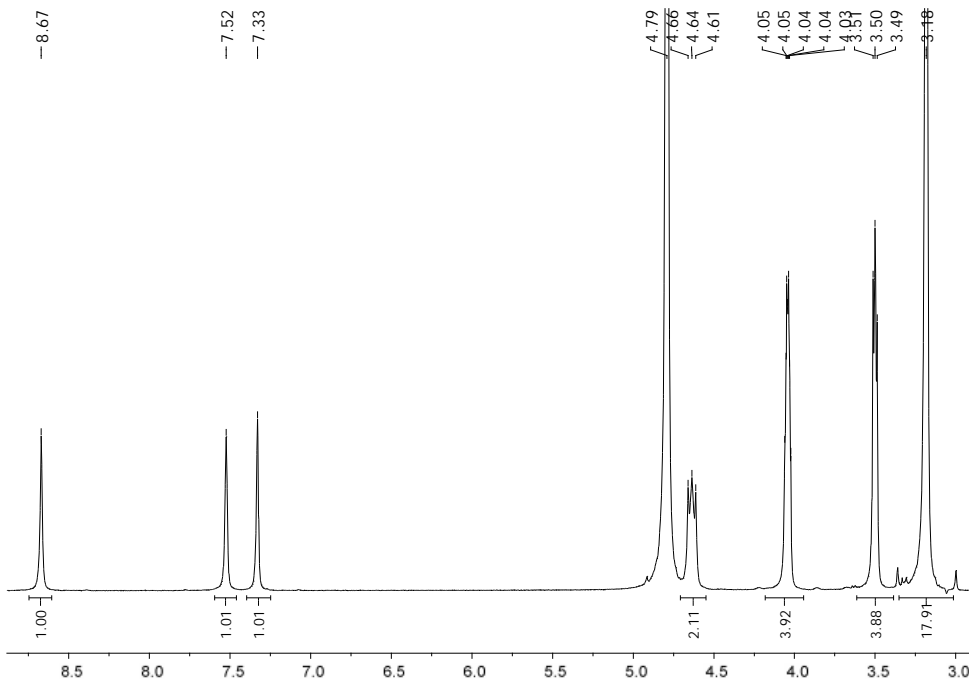
Figure 30 - ^{1}H NMR spectra of [Ch]2[Zol]
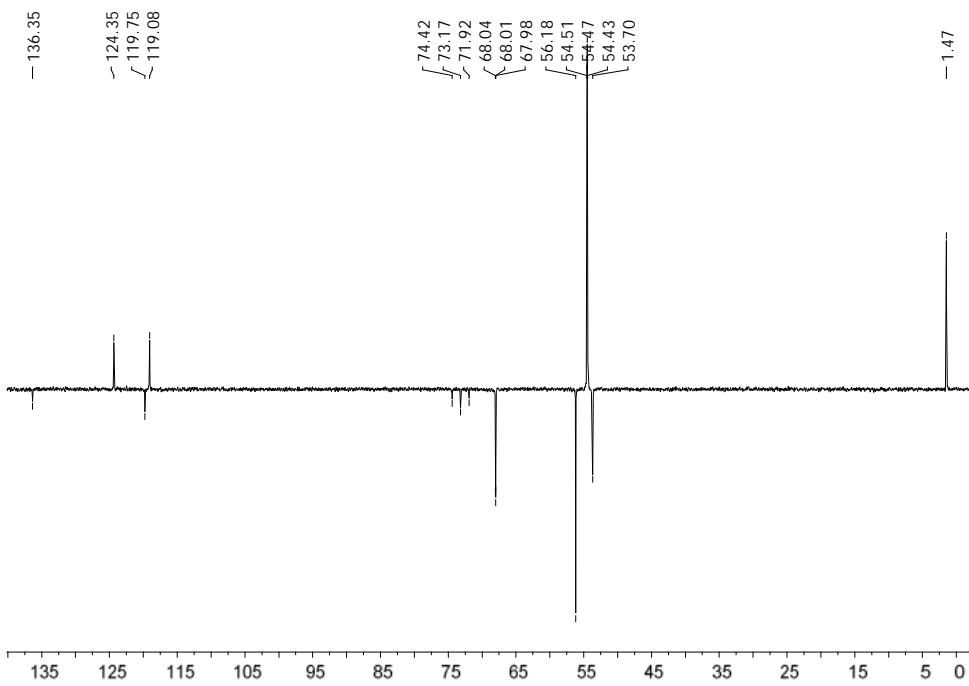
Figure 31 - ^{13}C NMR spectra of [Ch]2[Zol]
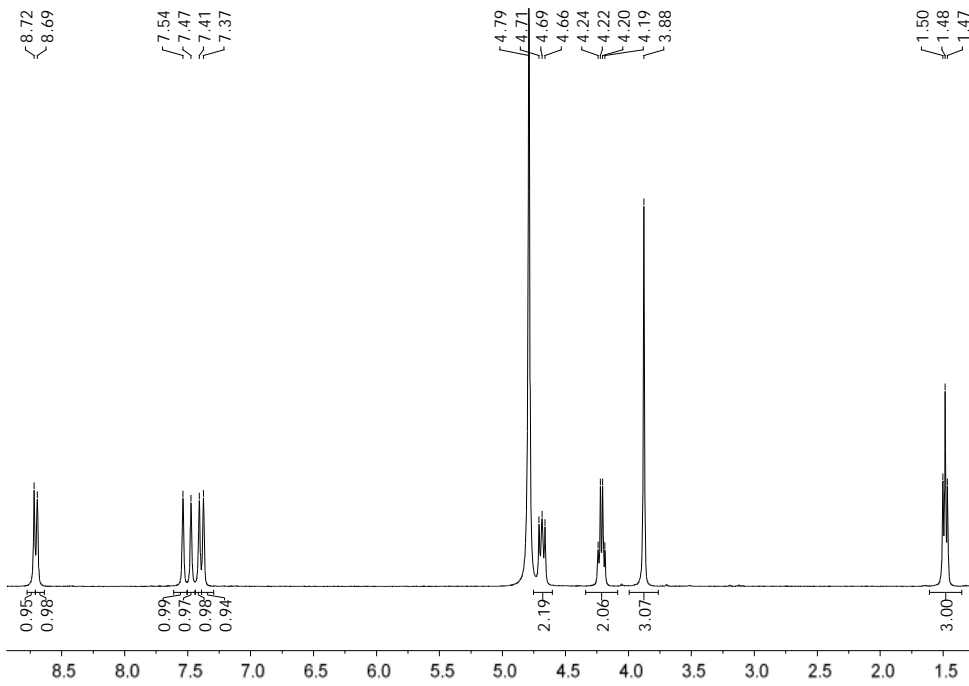
Figure 32 - ¹H NMR spectra of [EMIM][Zol]
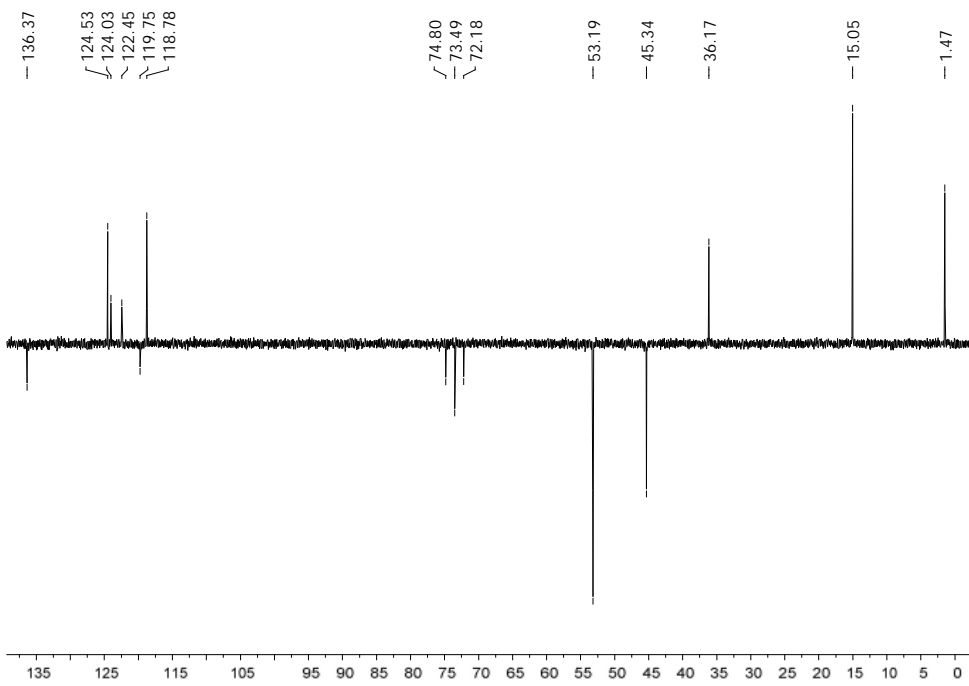
Figure 33 - ¹H NMR spectra of [EMIM][Zol]
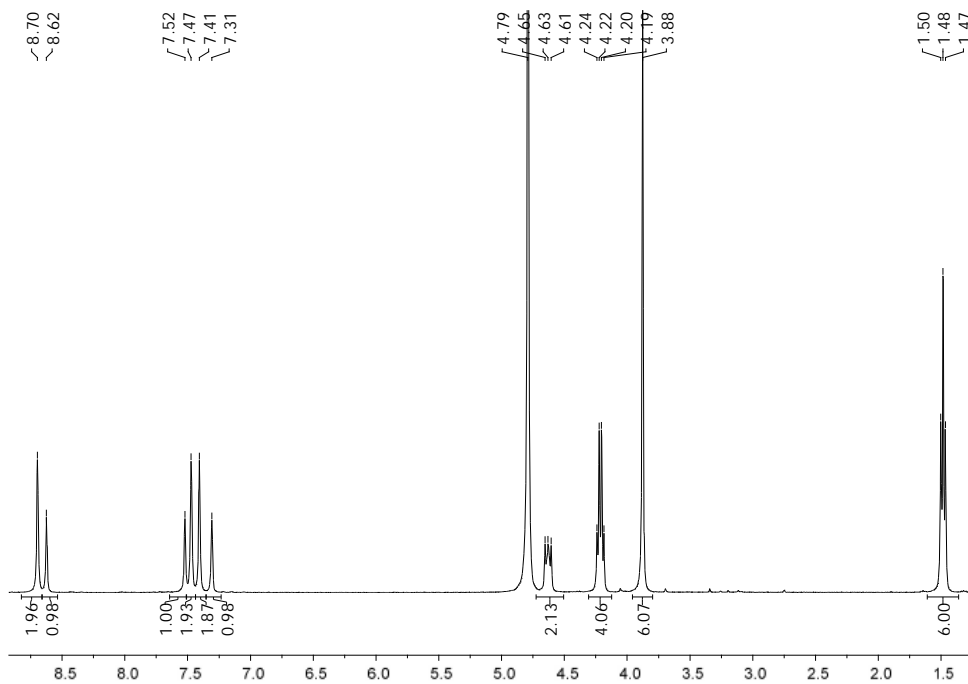
Figure 34 - ¹H NMR spectra of [EMIM]2[Zol]
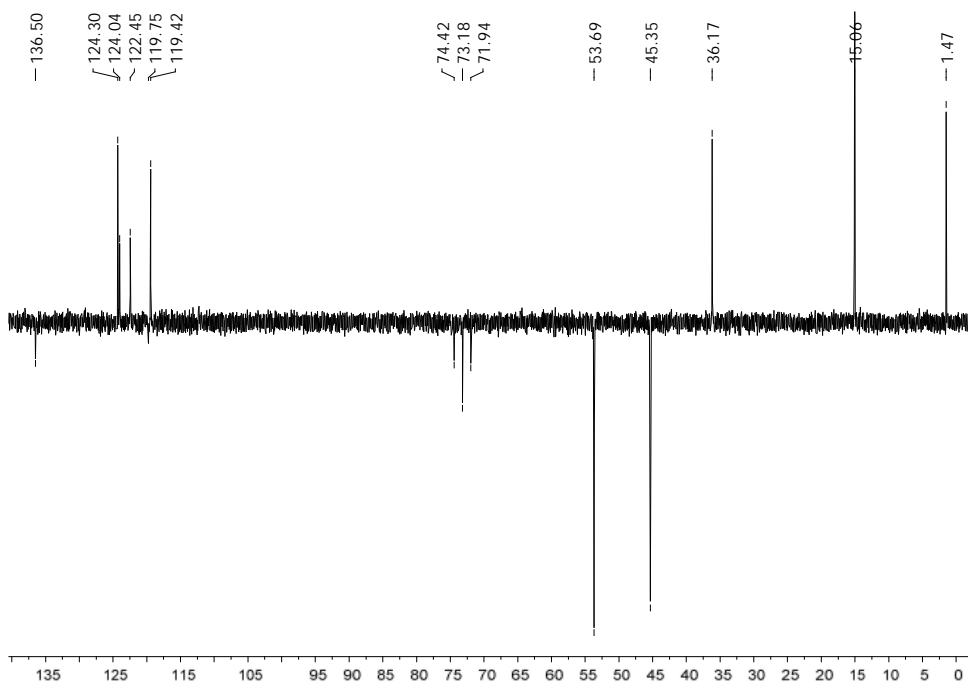
Figure 35 - ¹³C NMR spectra of [EMIM]2[Zol]
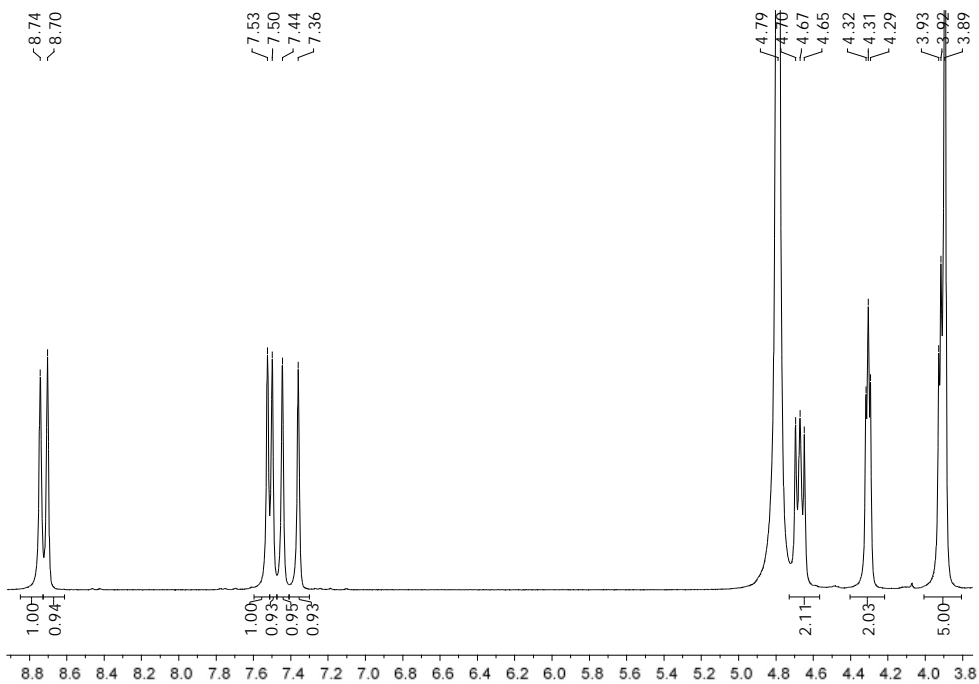
Figure 36 - ^{13}C NMR spectra of [EMIM]2[Zol]
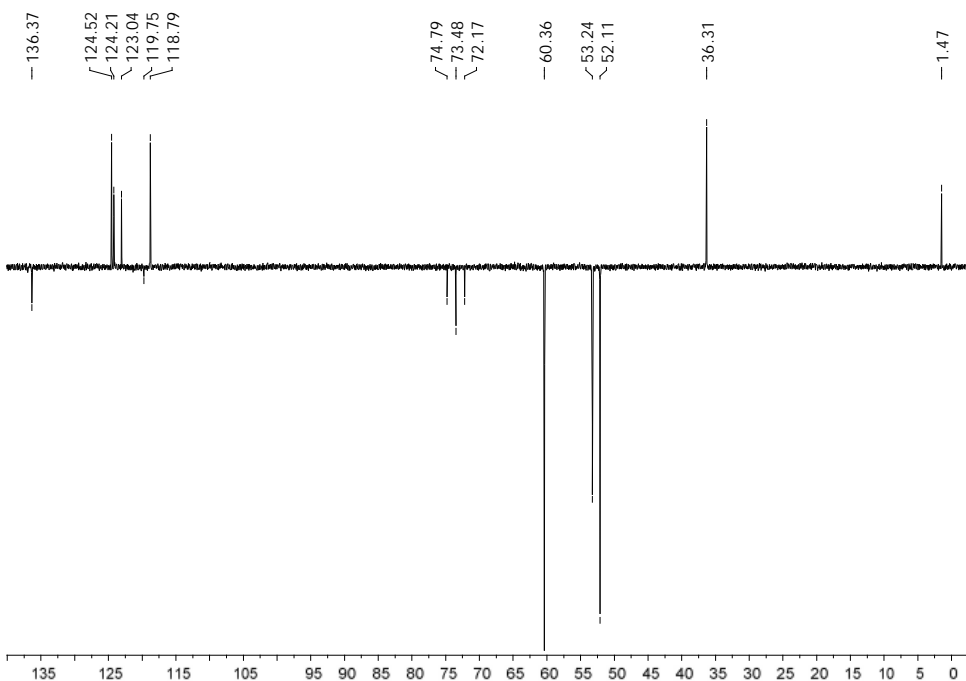
Figure 37 - ^{13}C NMR spectra of [C2OHMIM][Zol]
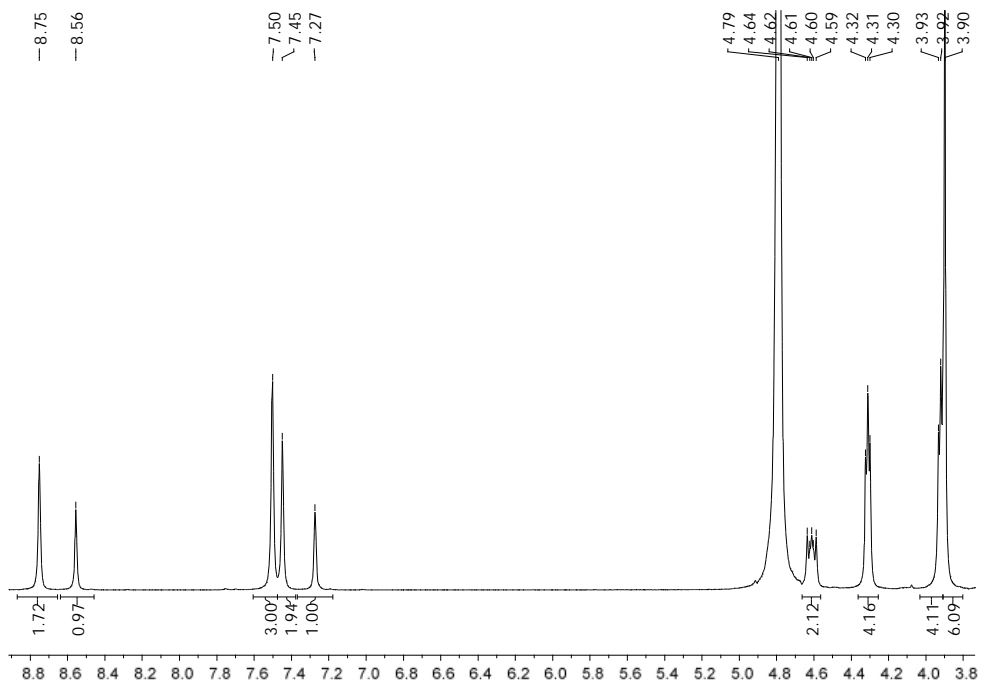
Figure 38 - ¹H NMR spectra of [C2OHMIM]2[Zol]
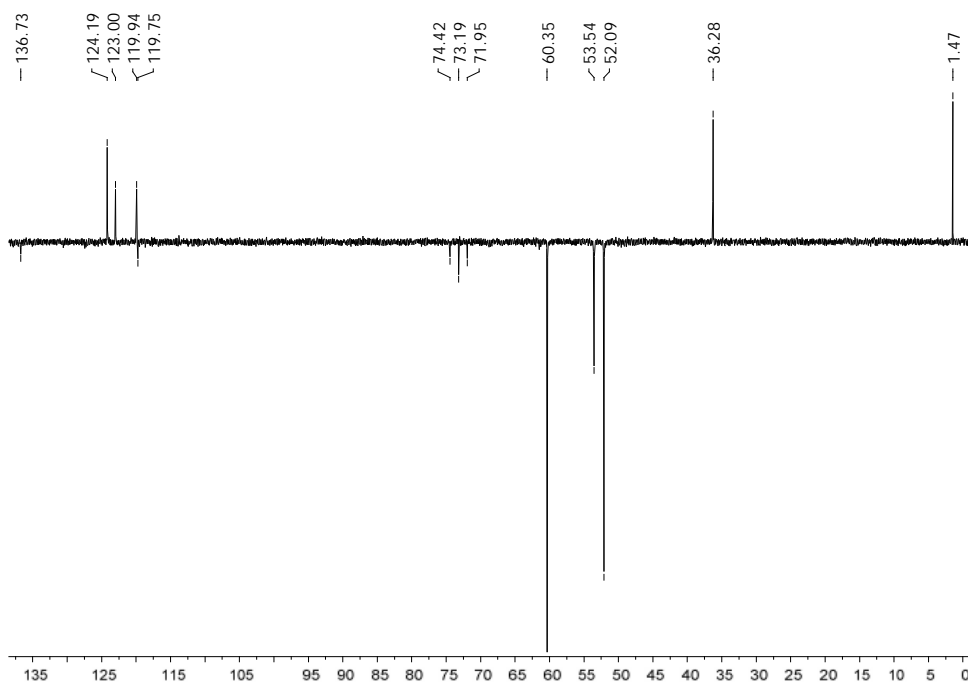
Figure 39 - ¹³C NMR spectra of [C2OHMIM]2[Zol]
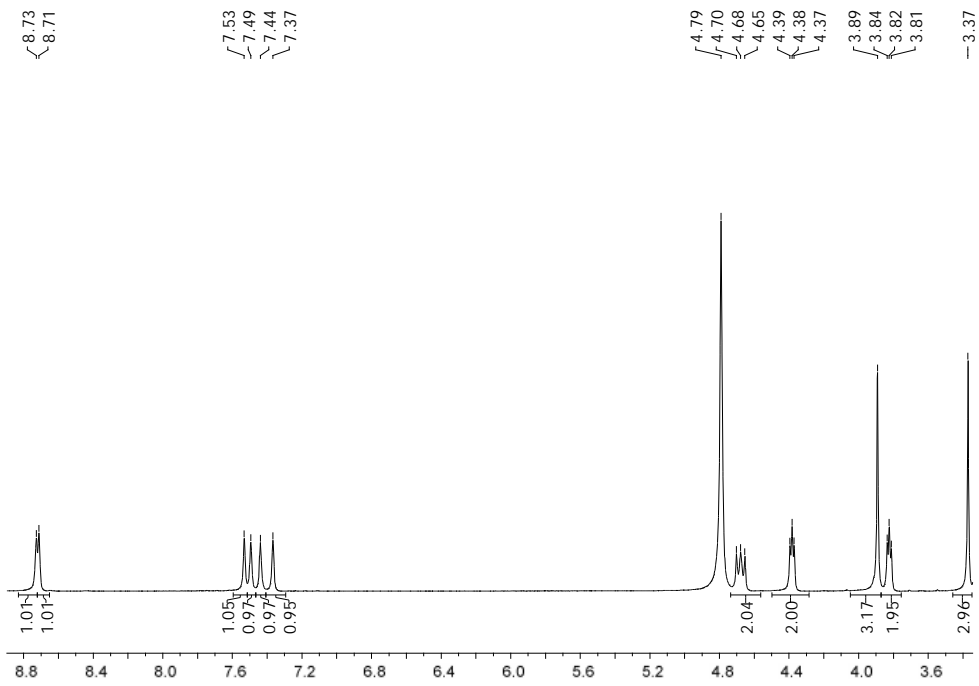
Figure 40 - ^{1}H NMR spectra of [C3OMIM][Zol]
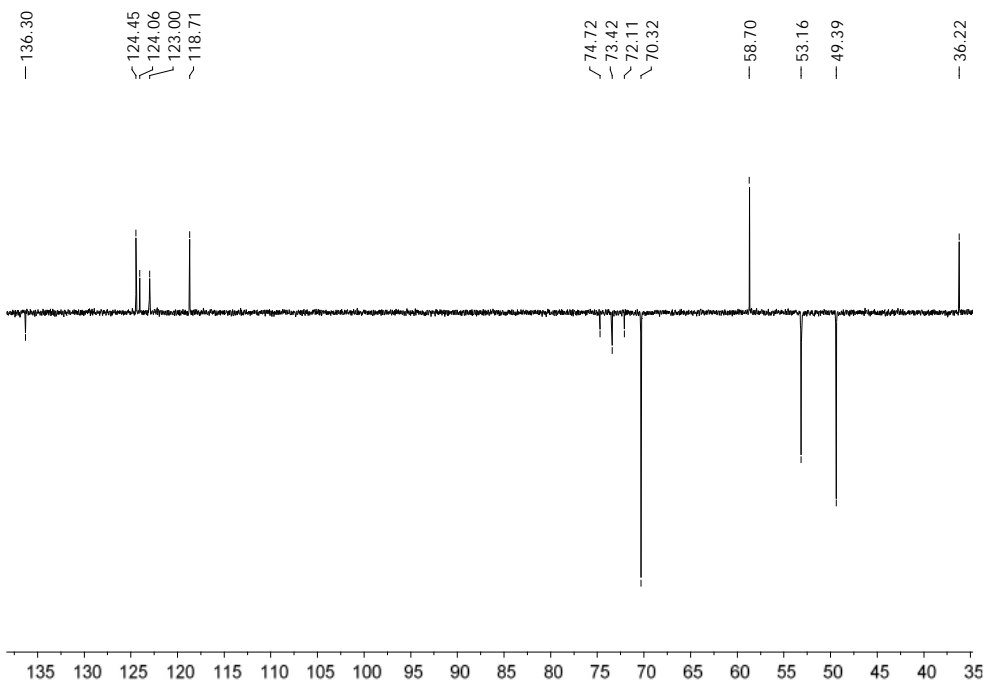
Figure 41 - ^{13}C NMR spectra of [C3OMIM][Zol]
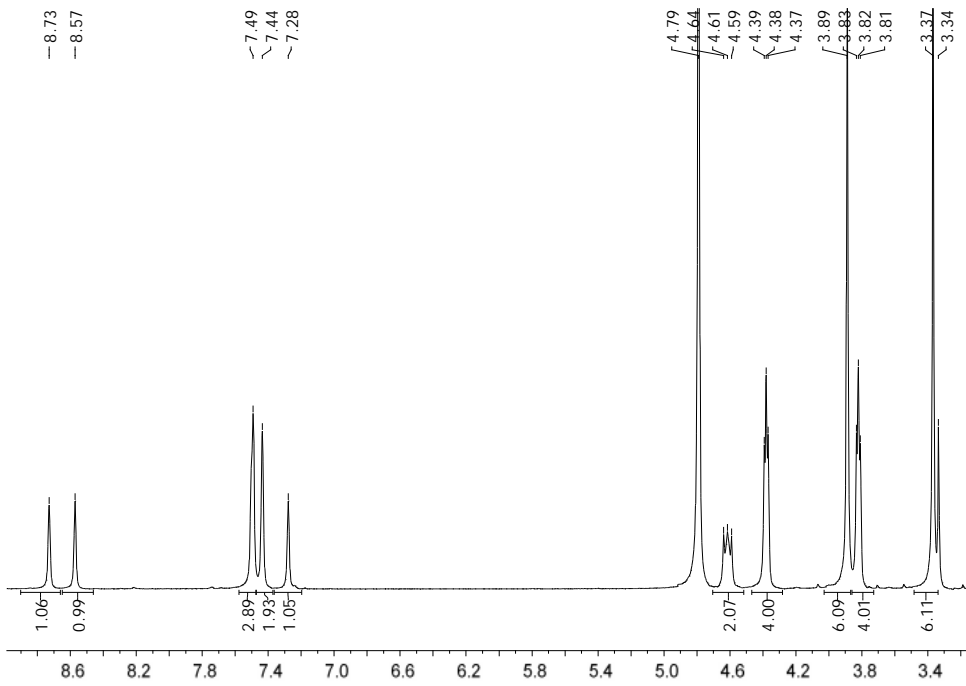
Figure 42 - ^{1}**H NMR spectra of [C3OMIM]2[Zol]**
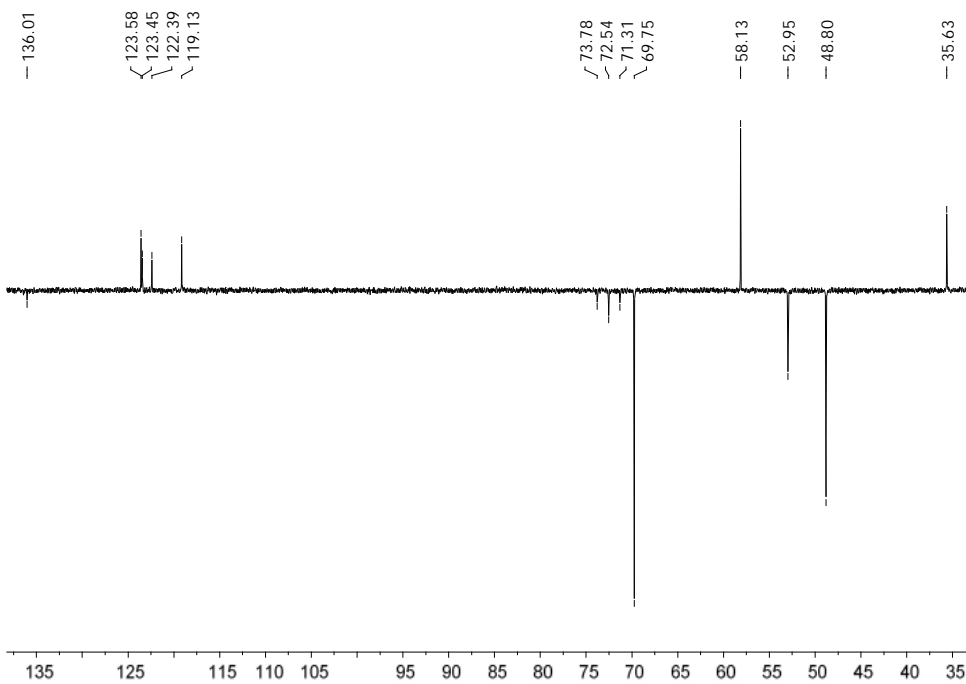
Figure 43 - ^{13}**C NMR spectra of [C3OMIM]2[Zol]**
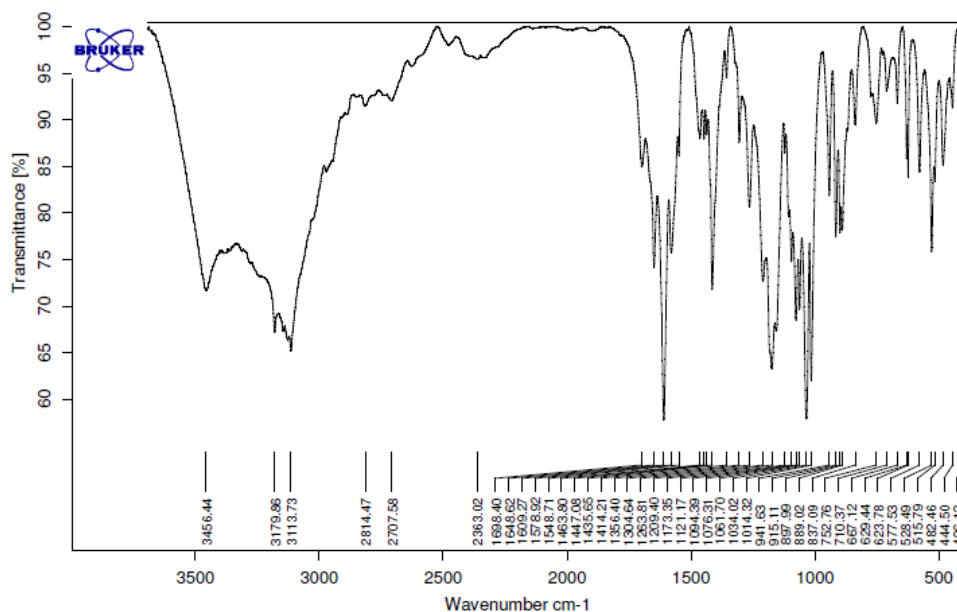
Figure 44 - FTIR spectra of [TMGH][Zol]
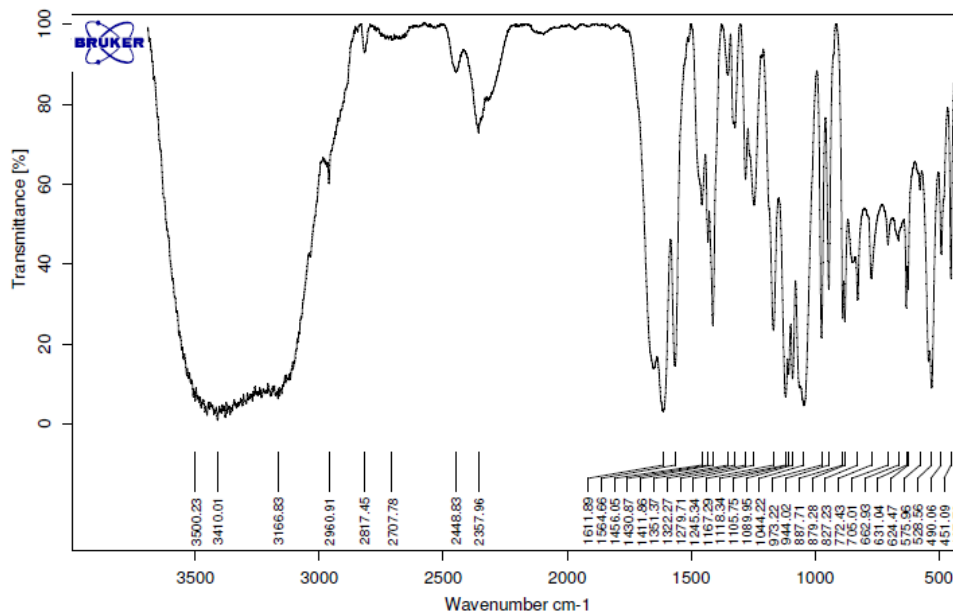
Figure 45 - FTIR spectra of [TMGH]2[Zol]
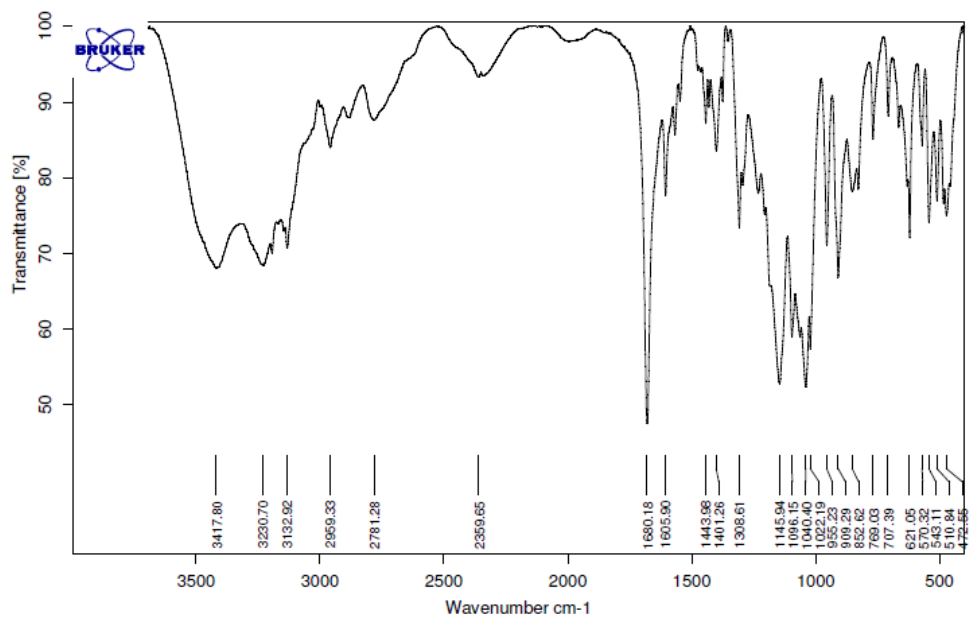
Figure 46 - FTIR spectra of [DBNH][Zol]
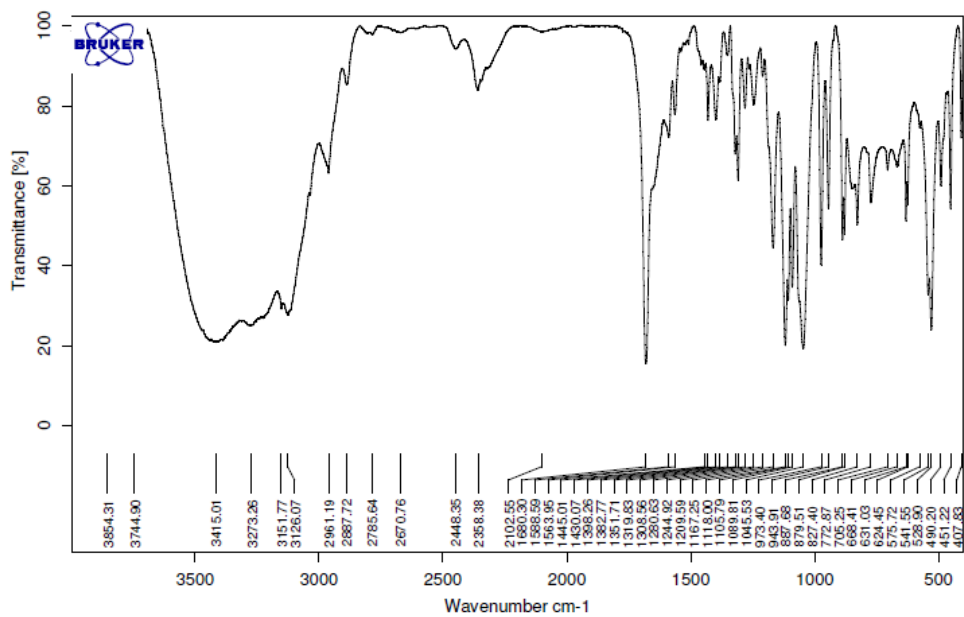
Figure 47 - FTIR spectra of [DBNH]2[Zol]
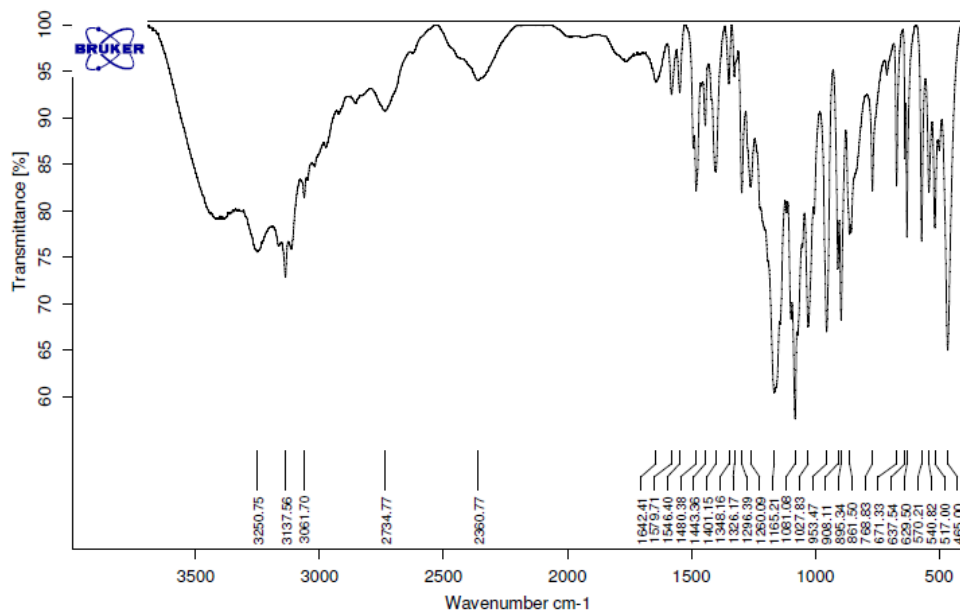
Figure 48 - FTIR spectra of [Ch][Zol]
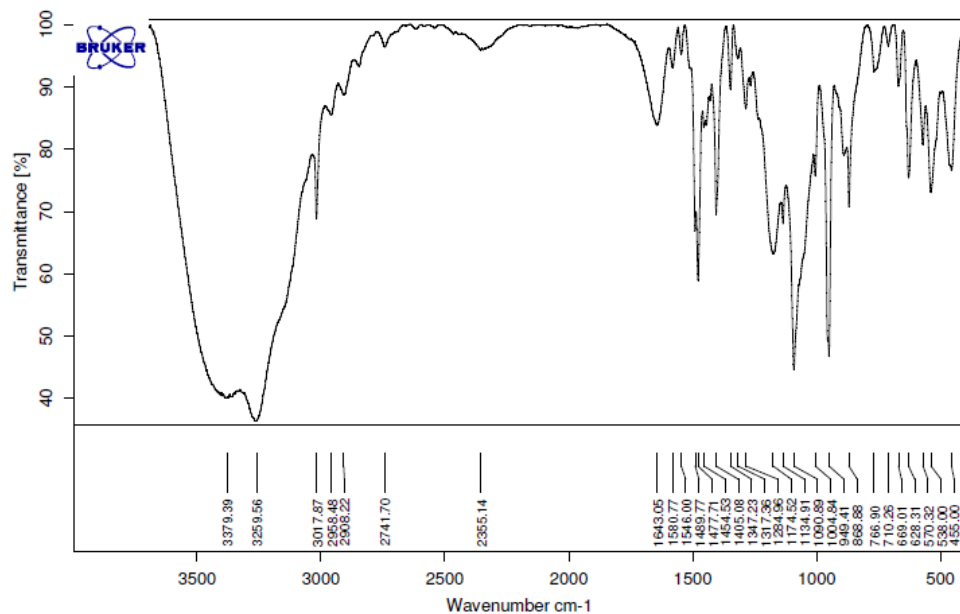
Figure 49 - FTIR spectra of [Ch]2[Zol]
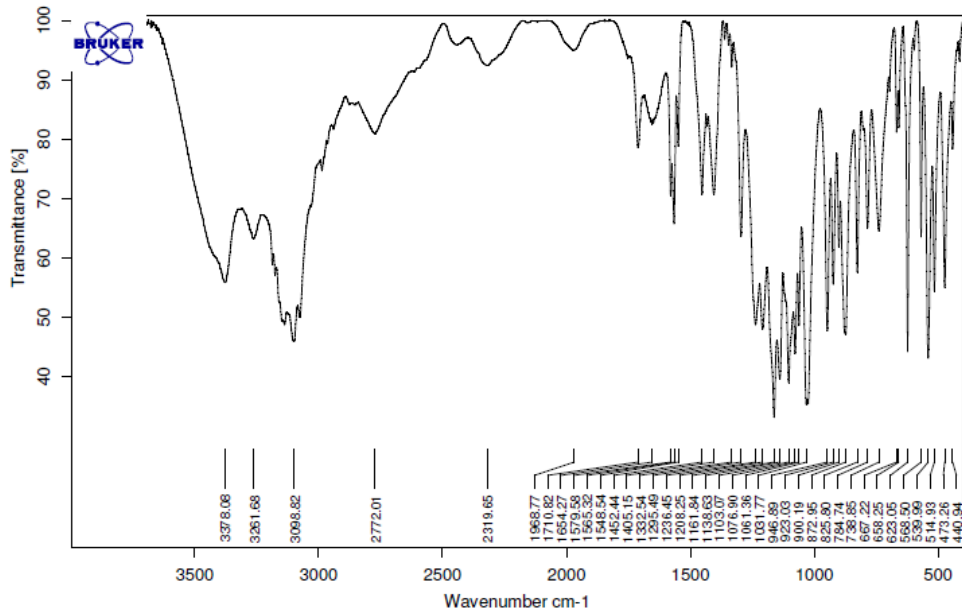
Figure 50 - FTIR spectra of [EMIM][Zol]
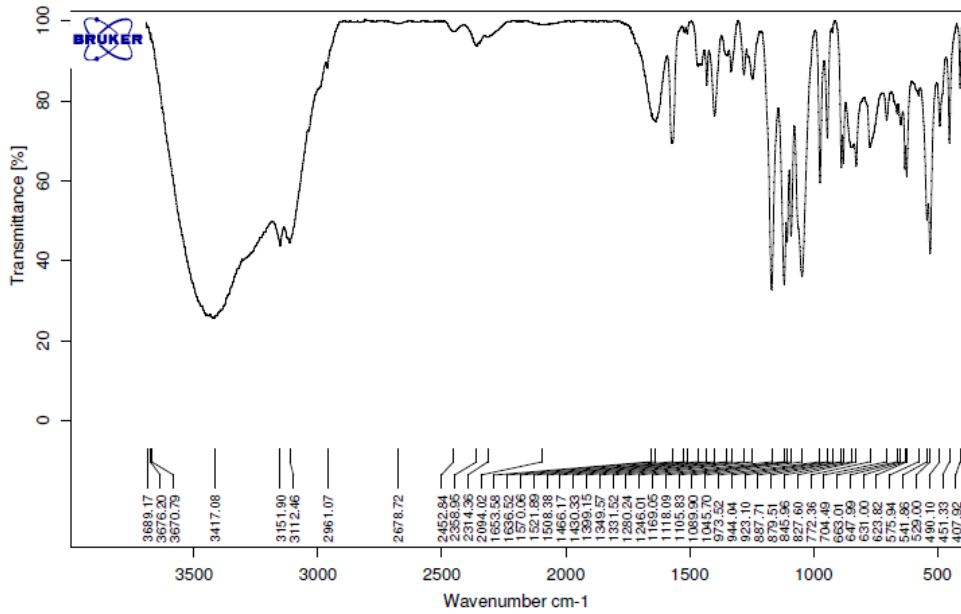
Figure 51 - FTIR spectra of [EMIM]2[Zol]
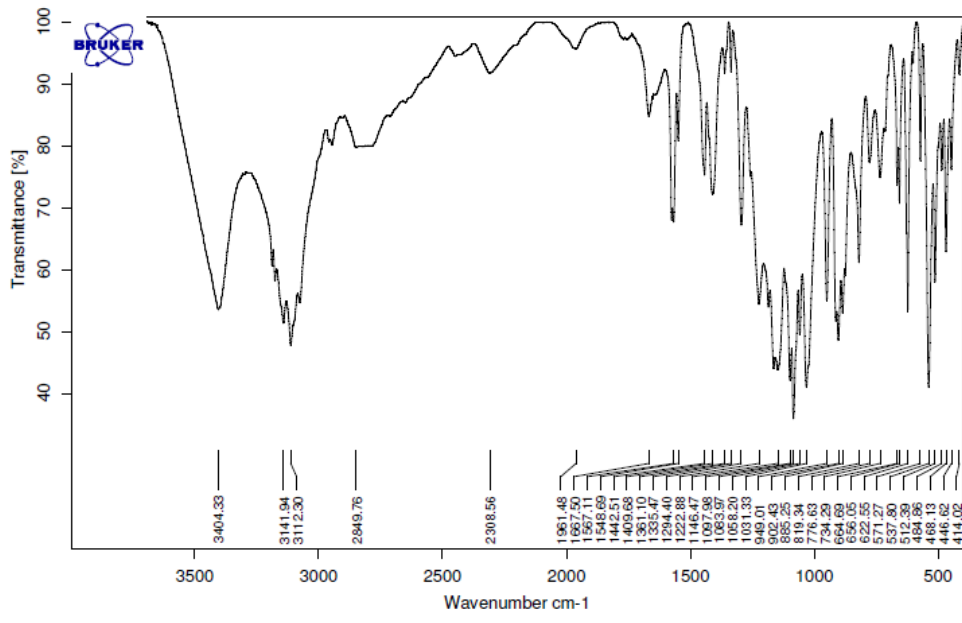
Figure 52 - FTIR spectra of [C2OHMIM][Zol]
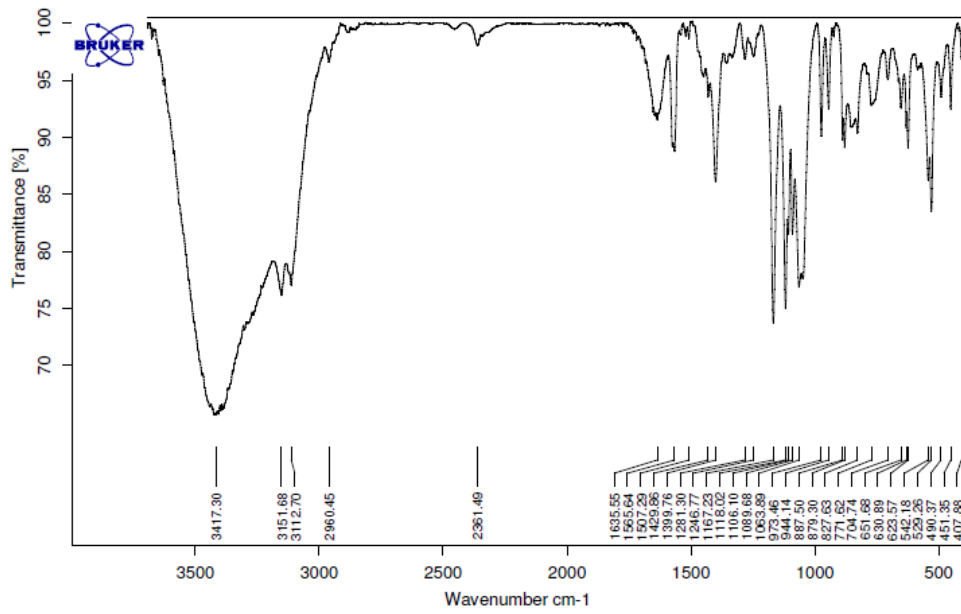
Figure 53 - FTIR spectra of [C2OHMIM]2[Zol]
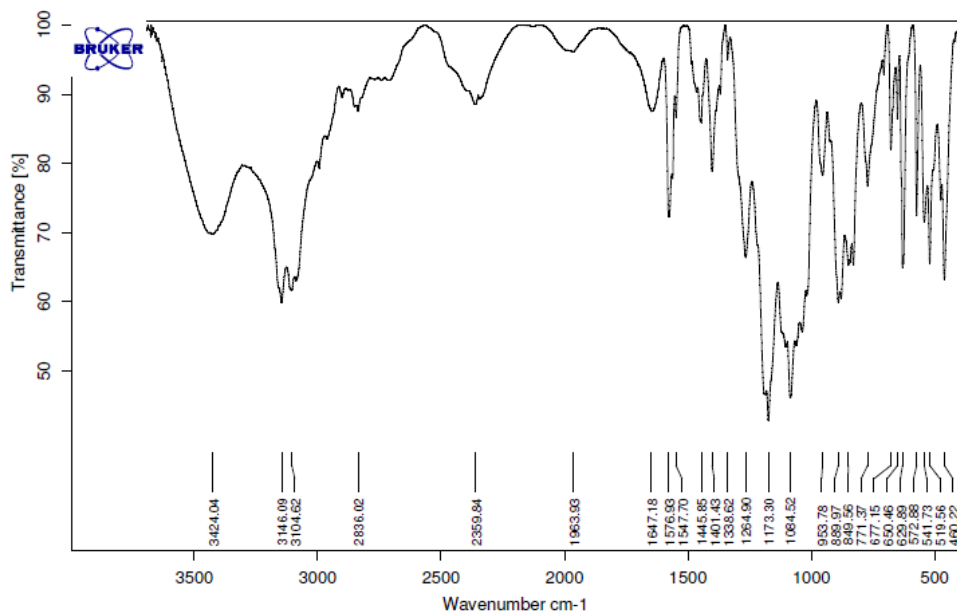
Figure 54 - FTIR spectra of [C3OMIM][Zol]
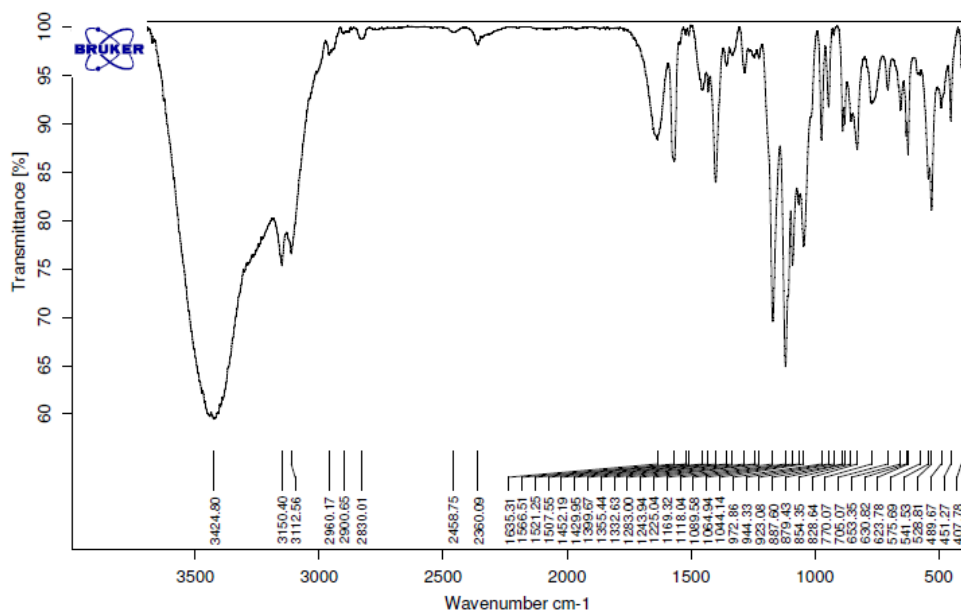
Figure 55 - FTIR spectra of [C3OMIM]2[Zol]
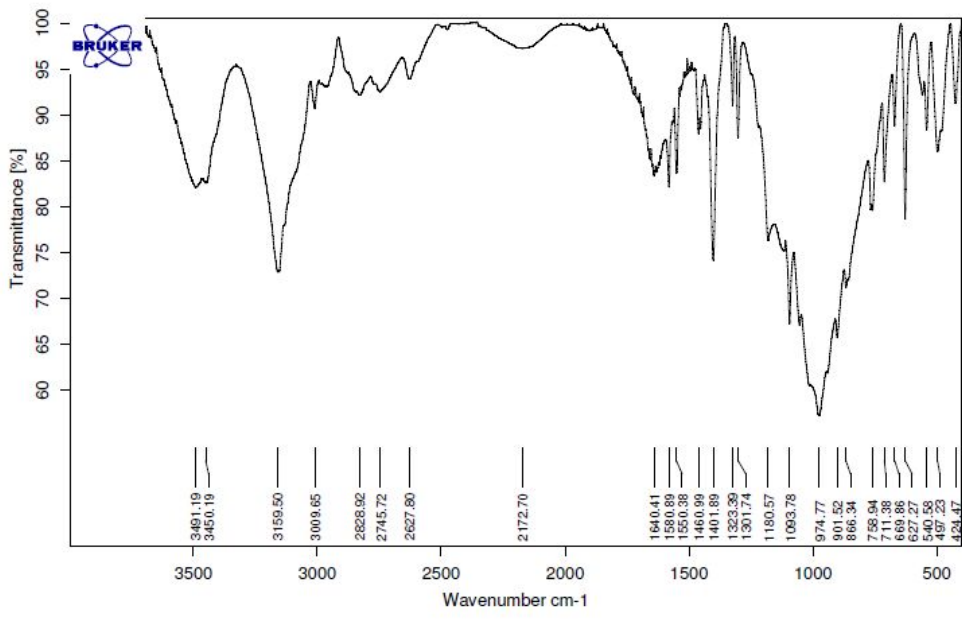
Figure 56 - FTIR spectra of zoledronic acid

Crystallographic data for [DBNH][Zol] (3)

Crystals of 3 suitable for single-crystal X-ray analysis were grown as described in the synthetic procedures. Selected crystals were covered with Fomblin (polyfluoroether oil) and mounted on a nylon loop. The data were collected at 110(2) K on a Bruker D8 Venture diffractometer equipped with a Photon 100 CMOS detector and an Oxford Cryosystems gaseous nitrogen stream Cooler, using graphite monochromated Mo-K radiation (λ = 0.71073 Å). Data were processed using APEX2 suite software package, which includes integration and scaling (SAINT), absorption corrections (SADABS) and space group determination (XPREP). Structure solution and refinement were done using direct methods with the programs SHELXS-16 inbuilt in APEX and WinGX-Version 2014.1[1] software packages. All non-hydrogen atoms were refined anisotropically and all the hydrogen atoms were inserted in idealized positions and allowed to refine riding on the parent carbon atom, except for the hydrogen atoms attached to O8, O9 and O10 (H_2O molecules) and those attached to N1 and N3 that were deduced by inspection of electron density maps. The molecular diagrams were drawn with ORTEP-3 for windows[2] and Mercury,[3] included in the software package. Table 3 contains crystallographic experimental data and structure refinement parameters. CCDC 1587530 contains the supplementary crystallographic data for this paper. The data can be obtained free of charge from The Cambridge Crystallographic Data Centre via www.ccdc.cam.ac.uk/structures.

Table 6- Crystal data and structure refinement for the title compound

Empirical formula	$C_{12} H_{28} N_4 O_{10} P_2$	
Formula weight	450.32	
Temperature	296(2) K	
Wavelength	0.71073 Å	
Crystal system	Triclinic	
Space group	P -1	
Unit cell dimensions	a = 9.2649(7) Å	= 84.852(4)°.
	b = 9.8500(8) Å	= 9.8500(8)°.
	c = 11.5844(9) Å	= 89.663(3)°.

[1] L. J. Farrugia, *J. Appl. Cryst.*, **2012**, 45, 849-854.

[2] L. J. Farrugia, *J. Appl. Cryst.*, **1997**, 30, 565.

[3] C. F. Macrae, P. R. Edgington, P. McCabe, E. Pidcock, G. P. Shields, R. Taylor, Towler and van der Streek, *J. Appl. Crystallogr.*, **2006**, 39, 453-457.

Volume	1022.25(14) Å^3
Z	2
Density (calculated)	1.463 Mg/m^3
1.463 Mg/m^3	1.463 Mg/m^3
F(000)	476
Crystal size	0.180 x 0.040 x 0.040 mm^3
Theta range for data collection	2.542 to 25.069°.
Index ranges	-11<=h<=11, -11<=k<=11, -13<=l<=13
Reflections collected	20969
Independent reflections	3587 [R(int) = 0.0521]
Completeness to theta = 25.069°	99.2 %
Refinement method	Full-matrix least-squares on F^2
Data / restraints / parameters	3587 / 8 / 288
Goodness-of-fit on F^2	1.046
Final R indices [I>2sigma(I)]	R1 = 0.0511, wR2 = 0.1240
R indices (all data)	R1 = 0.0663, wR2 = 0.1308
Largest diff. peak and hole	1.351 and -0.437 e.Å^{-3}
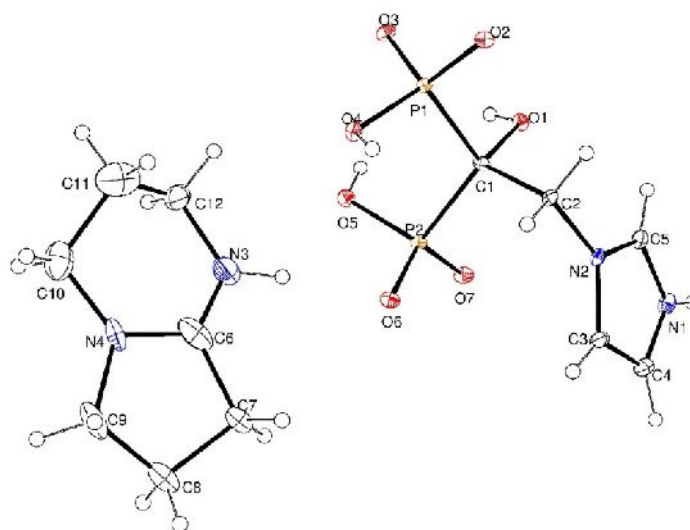
Figure 57 - ORTEP-3 diagram of [DBNH][Zol] (3), using 30% probability level ellipsoids.
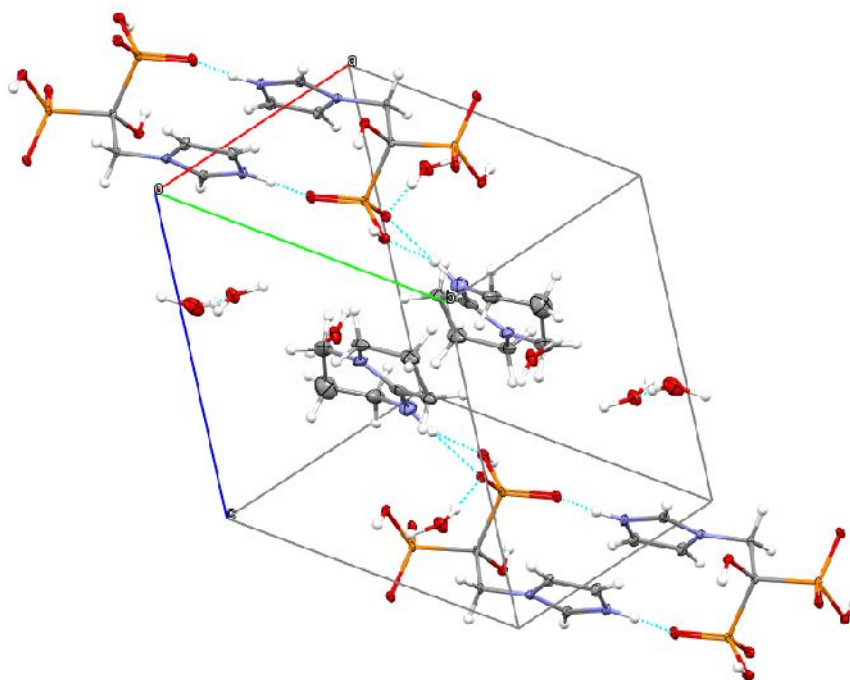
Figure 58 - MERCURY packing diagram of [DBNH][Zol] (3) showing hydrogen bonds (represented by dashed light-blue lines) and co-crystallized H$_2$O molecules.

Table 7 - Atomic coordinates (x 104) and equivalent isotropic displacement parameters (Å2x 103) for [DBNH][Zol] (3). U(eq) is defined as one third of the trace of the orthogonalized Uij tensor.

	x	y	z	U(eq)
P(2)	5951(1)	2834(1)	1651(1)	11(1)
P(1)	7796(1)	5130(1)	-95(1)	10(1)
O(2)	9147(2)	5237(2)	-1133(2)	13(1)
O(1)	6268(2)	3202(2)	-758(2)	12(1)
O(3)	6533(2)	6022(2)	-270(2)	13(1)
O(7)	5037(2)	1616(2)	1566(2)	16(1)
O(5)	4921(2)	4102(2)	1966(2)	15(1)
O(6)	6913(2)	2695(2)	2523(2)	15(1)
O(4)	8226(2)	5449(2)	1084(2)	13(1)
O(8)	9868(3)	2165(3)	2389(2)	26(1)
N(2)	7982(3)	957(3)	-81(2)	12(1)
O(9)	3750(3)	-381(3)	3307(2)	31(1)
N(1)	6893(3)	-876(3)	-335(3)	18(1)
O(10)	677(3)	-51(3)	3790(3)	45(1)
N(4)	7722(3)	5614(3)	5420(3)	30(1)
C(2)	8431(3)	2406(3)	-205(3)	11(1)
C(1)	7104(3)	3343(3)	125(3)	10(1)
C(3)	8200(4)	-29(3)	781(3)	17(1)
C(5)	7175(3)	412(3)	-738(3)	16(1)
C(4)	7522(4)	-1175(3)	612(3)	21(1)
N(3)	6819(4)	4969(4)	3836(3)	40(1)
C(6)	7414(4)	4670(5)	4718(3)	39(1)
C(9)	8348(4)	4960(5)	6366(3)	36(1)
C(7)	7860(4)	3235(4)	5134(3)	29(1)
C(8)	8029(5)	3454(5)	6374(4)	43(1)
C(12)	6454(6)	6378(4)	3577(4)	45(1)
C(10)	7514(5)	7066(5)	5221(4)	48(1)
C(11)	7384(7)	7373(6)	3877(6)	71(2)

Table 8 - Bond lengths [Å] and angles [°] for [DBNH][Zol] (3).

P(2)-O(7)	1.496(2)	O(4)-H(4B)	0.8200
P(2)-O(6)	1.496(2)	O(8)-H(8C)	0.94(2)
P(2)-O(5)	1.583(2)	O(8)-H(8D)	0.941(19)
P(2)-C(1)	1.860(3)	N(2)-C(5)	1.333(4)
P(1)-O(3)	1.500(2)	N(2)-C(3)	1.379(4)
P(1)-O(2)	1.511(2)	N(2)-C(2)	1.474(4)
P(1)-O(4)	1.569(2)	O(9)-H(9C)	0.94(2)
P(1)-C(1)	1.852(3)	O(9)-H(9D)	0.96(2)
O(1)-C(1)	1.439(3)	N(1)-C(5)	1.317(4)
O(1)-H(1)	0.8200	N(1)-C(4)	1.370(4)
O(5)-H(5B)	0.8200	N(1)-H(1B)	0.88(4)
C(2)-H(2A)	0.9700	O(10)-H(10D)	0.94(2)
C(2)-H(2B)	0.9700	O(10)-H(10C)	0.96(2)
C(3)-C(4)	1.346(5)	N(4)-C(6)	1.363(6)
C(3)-H(3)	0.9300	N(4)-C(10)	1.447(6)
C(5)-H(5)	0.9300	N(4)-C(9)	1.459(5)
C(2)-H(2A)	0.9700	C(2)-C(1)	1.527(4)
C(4)-H(4)	0.9300	N(3)-C(6)	1.284(5)
N(3)-C(6)	1.284(5)	C(12)-C(11)	1.428(8)
N(3)-C(12)	1.448(5)	C(12)-H(12A)	0.9700
N(3)-H(3B)	0.946(19)	C(12)-H(12B)	0.9700
C(6)-C(7)	1.539(6)	C(10)-C(11)	1.593(8)
C(9)-C(8)	1.512(6)	C(10)-H(10A)	0.9700
C(9)-H(9A)	0.9700	C(10)-H(10B)	0.9700
C(9)-H(9B)	0.9700	C(11)-H(11A)	0.9700
C(7)-C(8)	1.516(5)	C(11)-H(11B)	0.9700
C(7)-H(7A)	0.9700	C(12)-C(11)	1.428(8)
C(7)-H(7B)	0.9700	O(7)-P(2)-O(6)	117.33(12)
C(8)-H(8A)	0.9700	O(7)-P(2)-O(5)	110.46(12)
C(8)-H(8B)	0.9700	O(6)-P(2)-O(5)	106.91(12)
O(7)-P(2)-C(1)	107.23(13)	O(1)-C(1)-C(2)	105.1(2)
O(6)-P(2)-C(1)	110.00(13)	O(1)-C(1)-P(1)	106.51(18)
O(5)-P(2)-C(1)	104.15(13)	P(1)-O(4)-H(4B)	109.5
O(3)-P(1)-O(2)	114.57(12)	H(8C)-O(8)-H(8D)	104(4)
O(3)-P(1)-O(4)	109.03(12)	C(5)-N(2)-C(3)	108.5(3)
O(2)-P(1)-O(4)	110.59(12)	C(5)-N(2)-C(2)	124.6(3)
O(3)-P(1)-C(1)	107.35(12)	C(3)-N(2)-C(2)	126.7(3)
O(2)-P(1)-C(1)	107.77(13)	H(9C)-O(9)-H(9D)	106(9)
O(4)-P(1)-C(1)	107.24(12)	C(5)-N(1)-C(4)	109.0(3)
C(1)-O(1)-H(1)	109.5	C(5)-N(1)-H(1B)	121(3)
P(2)-O(5)-H(5B)	109.5	C(4)-N(1)-H(1B)	130(3)
H(10D)-O(10)-H(10C)	112(10)	C(1)-C(2)-H(2B)	109.1
C(6)-N(4)-C(10)	124.7(4)	H(2A)-C(2)-H(2B)	107.8
C(6)-N(4)-C(9)	110.3(3)	C(2)-C(1)-P(1)	108.62(19)
C(10)-N(4)-C(9)	124.9(3)	O(1)-C(1)-P(2)	110.75(19)
N(2)-C(2)-C(1)	112.5(2)	C(2)-C(1)-P(2)	111.4(2)
H(10D)-O(10)-H(10C)	112(10)	C(4)-C(3)-N(2)	106.7(3)
N(2)-C(2)-H(2A)	109.1	C(4)-C(3)-H(3)	126.6
C(1)-C(2)-H(2A)	109.1	N(2)-C(3)-H(3)	126.6
N(2)-C(2)-H(2B)	109.1	N(1)-C(5)-N(2)	108.5(3)
N(1)-C(5)-H(5)	125.8	C(6)-N(3)-C(12)	118.4(4)
N(2)-C(5)-H(5)	125.8	C(6)-N(3)-H(3B)	114(3)
C(3)-C(4)-N(1)	107.3(3)	C(12)-N(3)-H(3B)	127(3)
C(3)-C(4)-H(4)	126.3	N(3)-C(6)-N(4)	123.1(4)
N(1)-C(4)-H(4)	126.3	N(3)-C(6)-C(7)	125.7(4)
N(1)-C(5)-H(5)	125.8	C(6)-N(3)-C(12)	118.4(4)
N(4)-C(9)-C(8)	104.9(3)	C(6)-C(7)-H(7B)	111.6
N(4)-C(9)-H(9A)	110.8	H(7A)-C(7)-H(7B)	109.4
C(8)-C(9)-H(9A)	110.8	C(9)-C(8)-C(7)	106.4(3)

N(4)-C(9)-H(9B)	110.8	C(9)-C(8)-H(8A)	110.4
C(8)-C(9)-H(9B)	110.8	C(7)-C(8)-H(8A)	110.4
H(9A)-C(9)-H(9B)	108.8	C(9)-C(8)-H(8B)	110.4
C(8)-C(7)-C(6)	100.8(3)	C(7)-C(8)-H(8B)	110.4
C(8)-C(7)-H(7A)	111.6	H(8A)-C(8)-H(8B)	108.6
C(6)-C(7)-H(7A)	111.6	C(11)-C(12)-N(3)	115.7(5)
C(8)-C(7)-H(7B)	111.6	C(11)-C(12)-H(12A)	108.4
N(4)-C(9)-C(8)	104.9(3)	C(6)-C(7)-H(7B)	111.6
N(3)-C(12)-H(12A)	108.4	H(12A)-C(12)-H(12B)	107.4
C(11)-C(12)-H(12B)	108.4	N(4)-C(10)-C(11)	107.3(4)
N(3)-C(12)-H(12B)	108.4	N(4)-C(10)-H(10A)	110.3
N(4)-C(6)-C(7)	111.1(3)	N(4)-C(6)-C(7)	111.1(3)
C(11)-C(10)-H(10A)	110.3	C(11)-C(10)-H(10B)	110.3
N(4)-C(10)-H(10B)	110.3	H(10A)-C(10)-H(10B)	108.5
C(12)-C(11)-C(10)	110.7(4)	C(12)-C(11)-H(11B)	109.5
C(12)-C(11)-H(11A)	109.5	C(10)-C(11)-H(11B)	109.5
C(10)-C(11)-H(11A)	109.5	H(11A)-C(11)-H(11B)	108.1

Table 9 - Torsion angles [°] for [DBNH][Zol] (3).

C(5)-N(2)-C(2)-C(1)	65.2(4)
C(3)-N(2)-C(2)-C(1)	-108.7(3)
N(2)-C(2)-C(1)-O(1)	-65.2(3)
N(2)-C(2)-C(1)-P(1)	-178.81(19)
N(2)-C(2)-C(1)-P(2)	54.8(3)
O(3)-P(1)-C(1)-O(1)	44.2(2)
O(2)-P(1)-C(1)-O(1)	-79.7(2)
O(4)-P(1)-C(1)-O(1)	161.19(17)
O(3)-P(1)-C(1)-C(2)	156.85(19)
O(2)-P(1)-C(1)-C(2)	33.0(2)
O(4)-P(1)-C(1)-C(2)	-86.1(2)
O(3)-P(1)-C(1)-P(2)	-78.30(17)
O(2)-P(1)-C(1)-P(2)	157.82(14)
O(4)-P(1)-C(1)-P(2)	38.73(18)
O(7)-P(2)-C(1)-O(1)	39.2(2)
O(3)-P(1)-C(1)-O(1)	44.2(2)
O(6)-P(2)-C(1)-O(1)	167.79(18)
O(5)-P(2)-C(1)-O(1)	-77.9(2)
O(7)-P(2)-C(1)-C(2)	-77.4(2)
O(6)-P(2)-C(1)-C(2)	51.3(2)
O(5)-P(2)-C(1)-C(2)	165.52(19)
O(7)-P(2)-C(1)-P(1)	159.26(14)
O(6)-P(2)-C(1)-P(1)	-72.10(18)
O(5)-P(2)-C(1)-P(1)	42.16(18)
C(5)-N(2)-C(3)-C(4)	0.8(4)
C(2)-N(2)-C(3)-C(4)	175.5(3)
O(6)-P(2)-C(1)-O(1)	167.79(18)
C(4)-N(1)-C(5)-N(2)	0.5(4)
C(3)-N(2)-C(5)-N(1)	-0.8(3)
C(2)-N(2)-C(5)-N(1)	-175.6(3)
N(2)-C(3)-C(4)-N(1)	-0.5(4)
C(5)-N(1)-C(4)-C(3)	0.0(4)
C(12)-N(3)-C(6)-N(4)	-0.2(6)
C(12)-N(3)-C(6)-C(7)	179.3(4)
C(10)-N(4)-C(6)-N(3)	-4.2(6)
C(9)-N(4)-C(6)-N(3)	178.2(4)
C(10)-N(4)-C(6)-C(7)	176.3(3)
C(9)-N(4)-C(6)-C(7)	-1.3(4)

C(6)-N(4)-C(9)-C(8)	-14.4(4)
C(10)-N(4)-C(9)-C(8)	168.0(4)
N(3)-C(6)-C(7)-C(8)	-163.4(4)
N(4)-C(6)-C(7)-C(8)	16.1(4)
N(4)-C(9)-C(8)-C(7)	24.5(4)
C(6)-C(7)-C(8)-C(9)	-24.1(4)
C(6)-N(3)-C(12)-C(11)	30.1(6)
C(6)-N(4)-C(10)-C(11)	-17.7(6)
C(9)-N(4)-C(10)-C(11)	159.5(4)
N(3)-C(12)-C(11)-C(10)	-51.4(6)
N(4)-C(10)-C(11)-C(12)	43.4(6)

Table 10 - Hydrogen bonds for platon_sq [Å and °] for [DBNH][Zol] (3).

D-H...A	d(D-H)	d(H...A)	d(D...A)	<(DHA)
O1-H1...O3	0.82	1.91	2.7208(2)	169
N1-H1B...O3	0.88	2.57	3.0674(2)	117
N1-H1B...O7	0.88	1.87	2.6800(2)	152
N3-H3B...O6	0.95	1.87	2.8074(2)	173
O4-H4B…O2	0.82	1.72	2.5346(2)	174
O5-H5B...O3	0.82	1.85	2.6456(2)	162
O8-H8C…O6	0.94	1.81	2.7547(2)	177
O8-H8D...O2	0.94	1.95	2.8678(2)	165
O9-H9C…O7	0.94	1.80	2.7429(2)	177
O9-H9D...O10	0.96	1.85	2.7902(2)	165
O10-H10D...O8	0.94	1.92	2.8075(2)	155

O8, O9 and O10 belong to co-crystallized H_2O molecules.

DSC thermograms of Zol-ILs
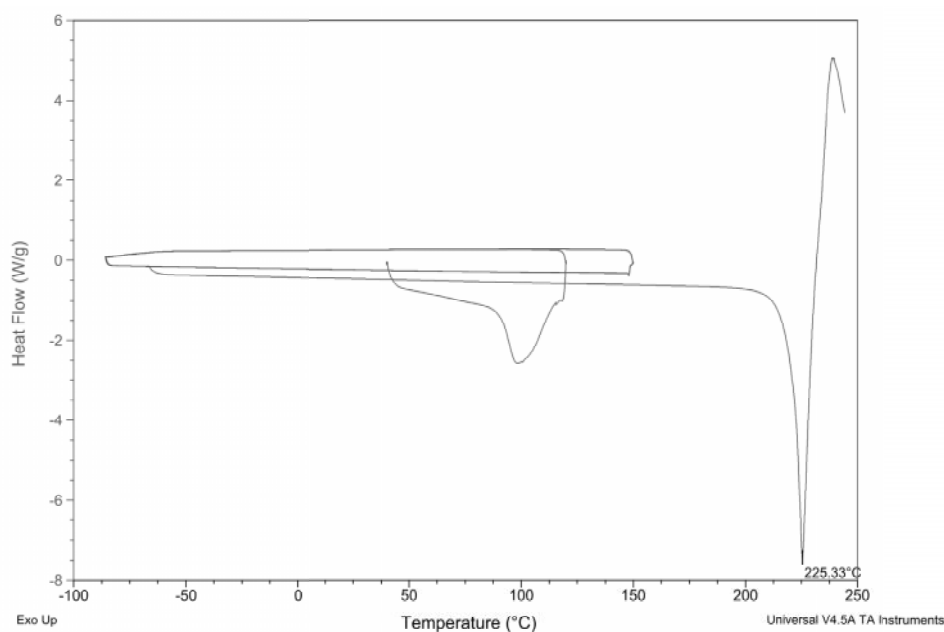
Figure 59 - DSC thermogram of [TMGH][Zol]
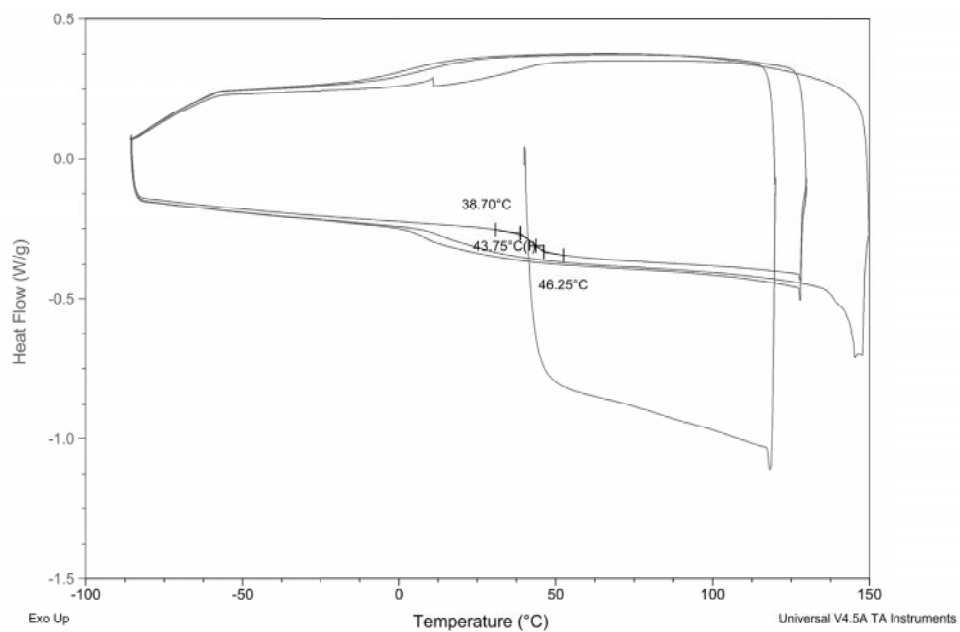
Figure 60 - DSC thermogram of [TMGH]2[Zol]
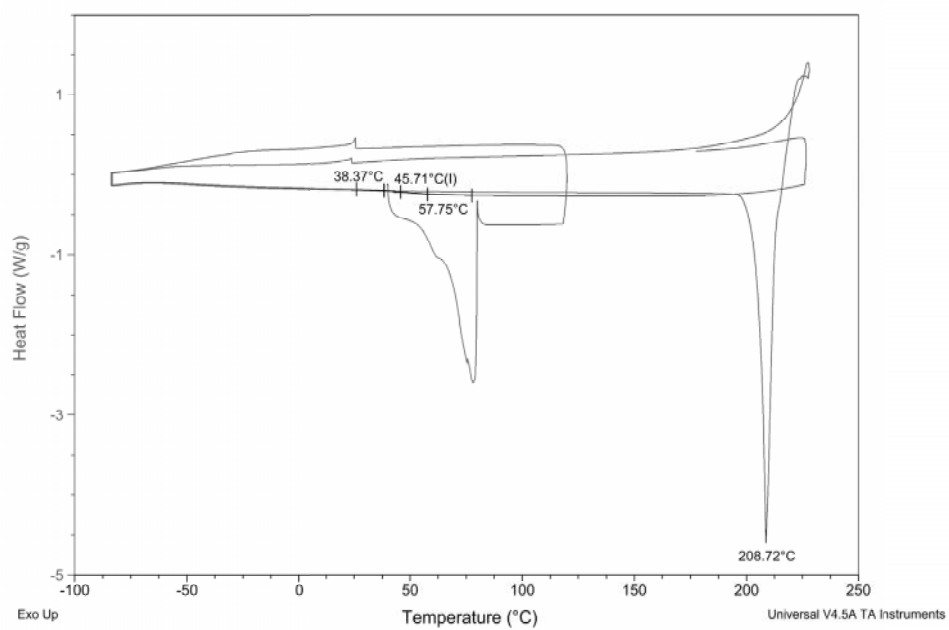
Figure 61 - DSC thermogram of [DBNH][Zol]
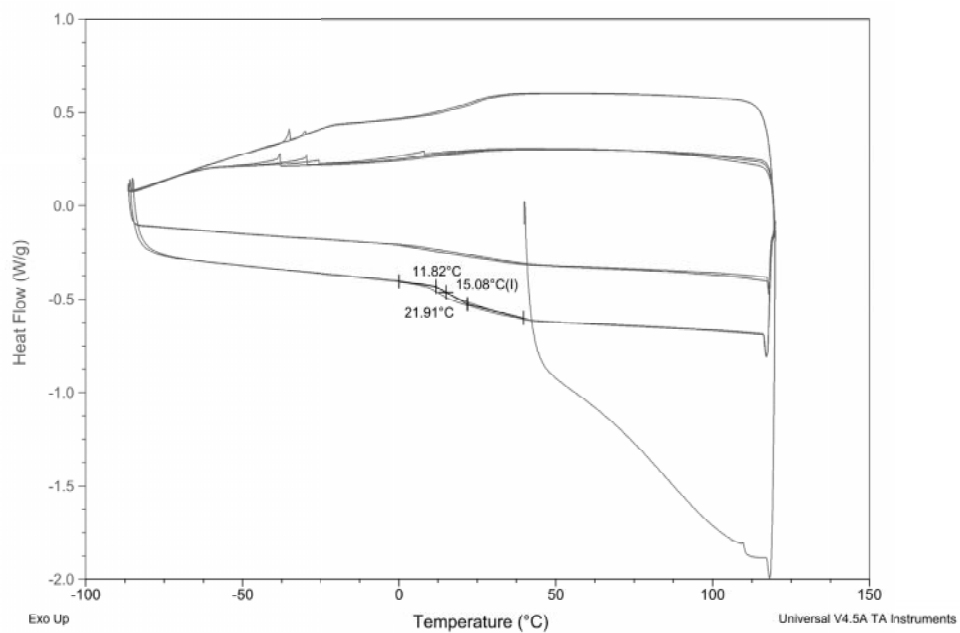
Figure 62 - DSC thermogram of [DBNH]2[Zol]
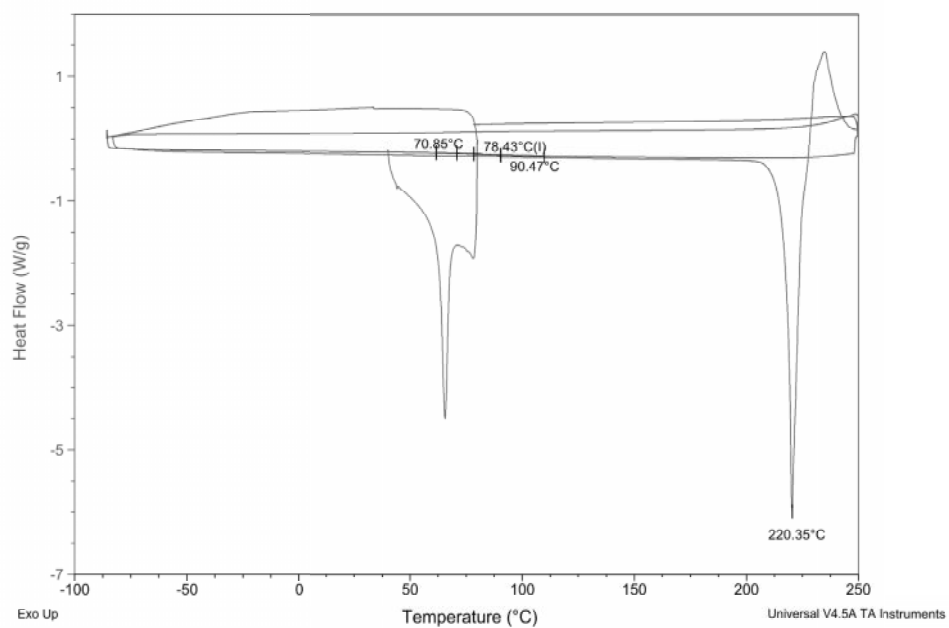
Figure 63 - DSC thermogram of [Ch][Zol]
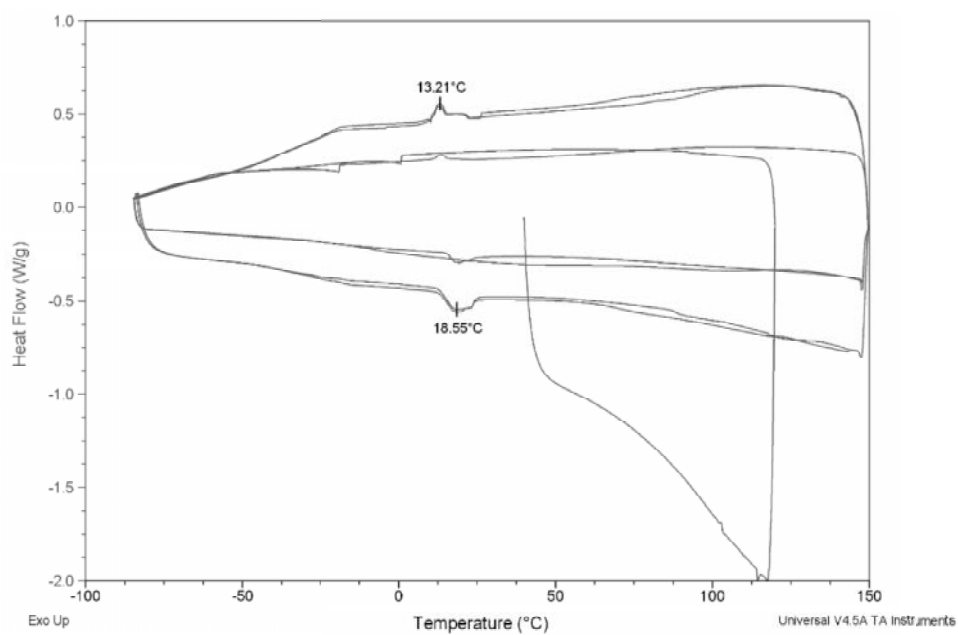
Figure 64 - DSC thermogram of [Ch]2[Zol]
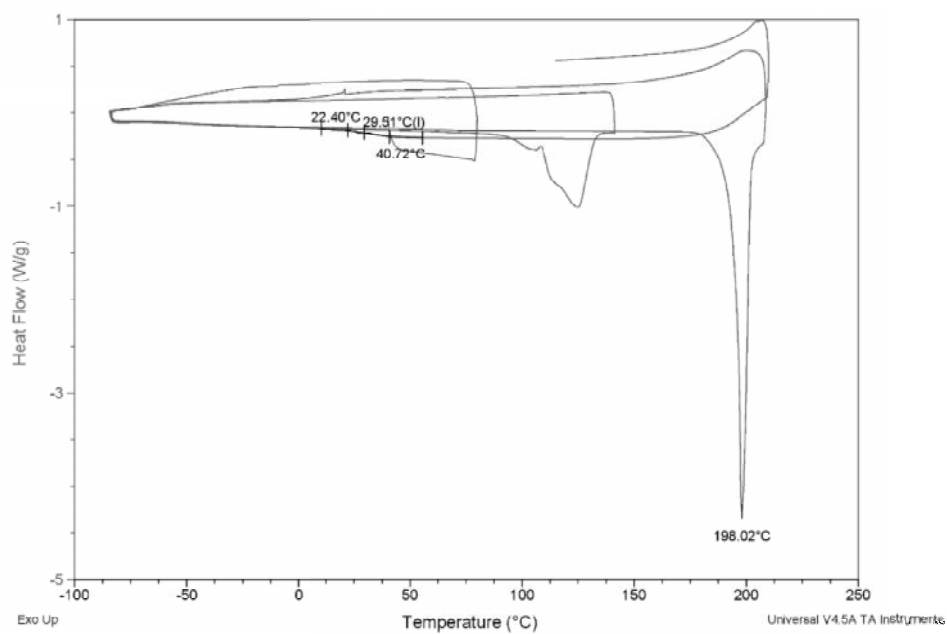
Figure 65 - DSC thermogram of [EMIM][Zol]
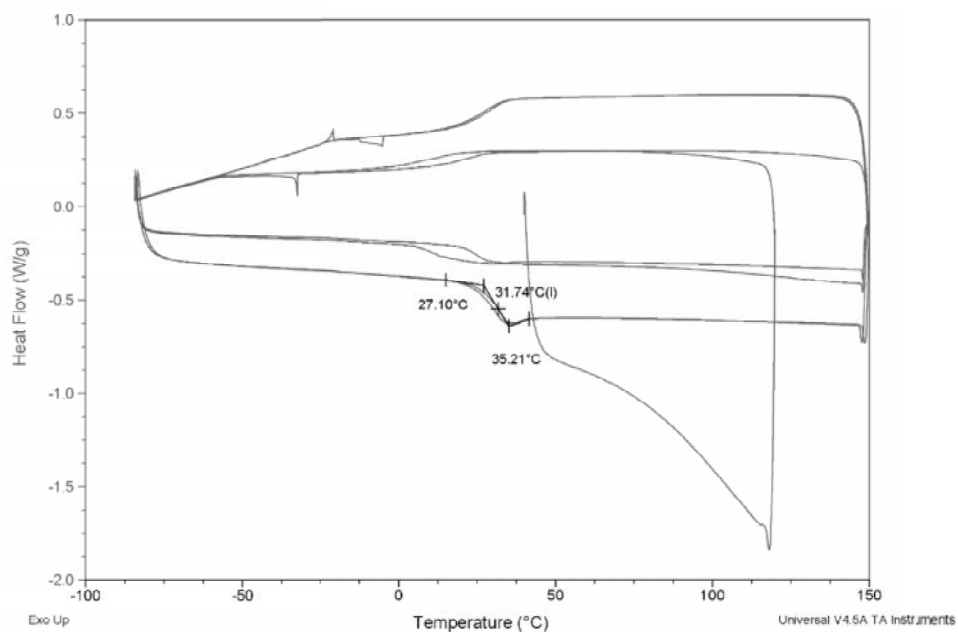
Figure 66 - DSC thermogram of [EMIM]2[Zol]
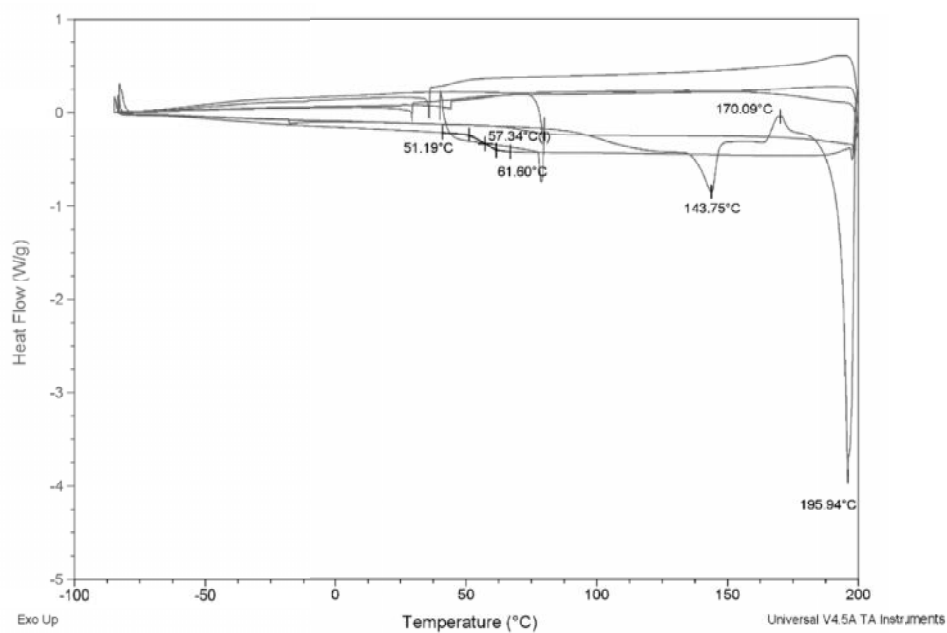
Figure 67 - DSC thermogram of [C2OHMIM][Zol]
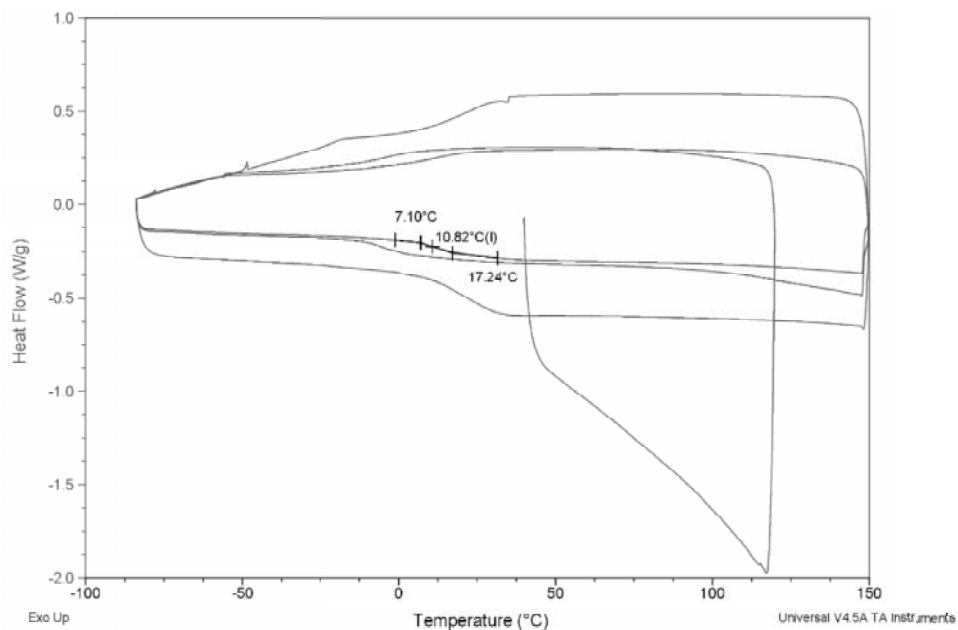
Figure 68 - DSC thermogram of [C2OHMIM]2[Zol]
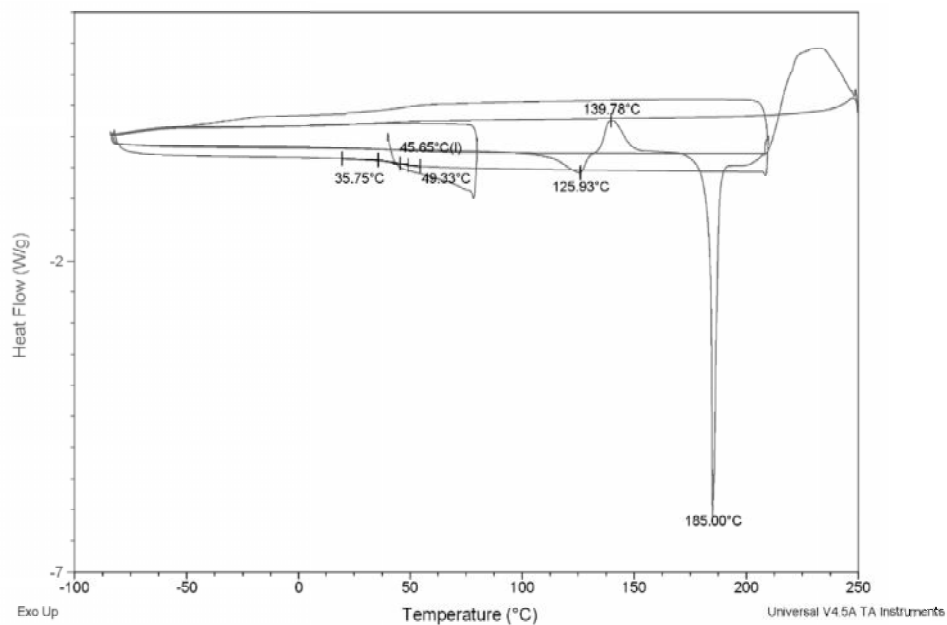
Figure 69 - DSC thermogram of [C3OMIM][Zol]
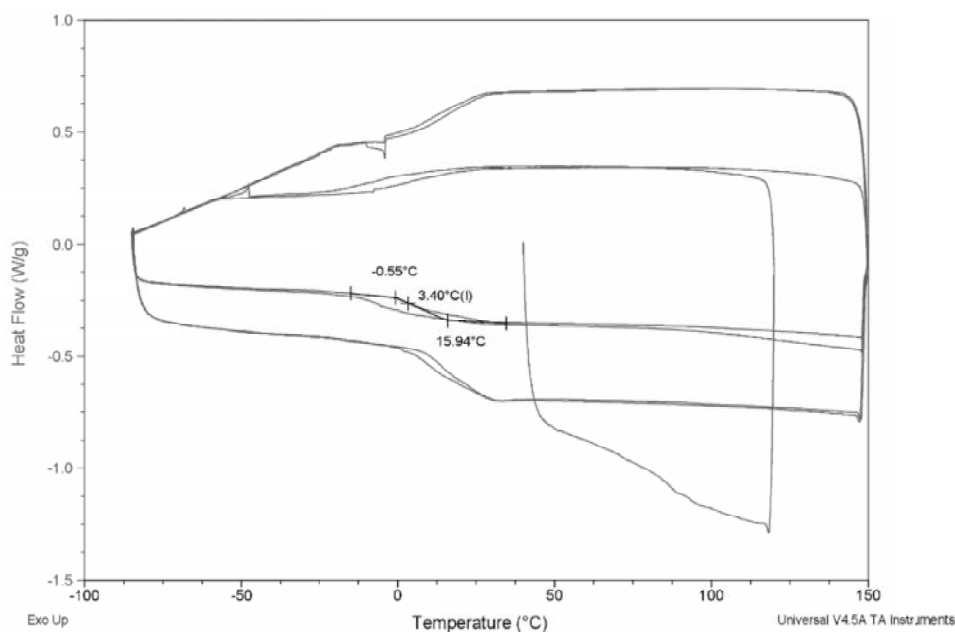
Figure 70 - DSC thermogram of [C3OMIM]2[Zol]

Cytotoxicity studies

The synthesized Zol-ILs were evaluated for their antiproliferative activity against the human cancer cell lines T47D (ductal breast epithelial tumor) and MG63 (osteosarcoma). Human primary skin fibroblasts were used as a non-neoplastic control. Cells were maintained in -minimal essential medium (a-MEM) containing 10% fetal bovine serum, 100 IU/mL penicillin, 2.5 µg/mL streptomycin, 2.5 µg/mL amphotericin B, and 50 µg/mL ascorbic acid. Cells were seeded at 10^4 cells/cm^2. After 24 h of cell attachment, the culture medium was renewed and supplemented with the Zol-containing ILs. Cell cultures were maintained in a 5% CO_2 humidified atmosphere at 37ºC. Cellular viability/proliferation was assessed by MTT assay. This assay is based on the reduction of 3-(4,5-dimethylthiazol-2-yl)-2,5-diphenyltetrazolium bromide to a purple formazan product by viable cells. Half-maximal inhibitory concentration (IC_{50}) values were obtained by nonlinear regression analysis of concentration-effect curves, using GraphPad Prism software (version 2012).

Table 11- Cytotoxicity results for isolated Zol and halide cations used to synthesize the ILs

Ions	IC$_{50}$ / M		
	Skin fibroblast	T47D	MG63
[Zol]	2.43×10^{-6}	a)	5.74×10^{-7}
[TMGH]Cl	1.47×10^{-6}	1.94×10^{-7}	2.46×10^{-7}
[DBNH]Cl	3.80×10^{-8}	2.78×10^{-7}	9.79×10^{-11}
[Ch]Cl	a)	a)	1.07×10^{-12}
[EMIM]Br	3.58×10^{-3}	4.30×10^{-6}	a)
[C$_2$OHMIM]Cl	5.61×10^{-7}	2.22×10^{-6}	1.91×10^{-10}
[C$_3$OMIM]Cl	1.47×10^{-6}	1.37×10^{-6}	1.40×10^{-5}

a) Not detected in the tested concentration range.

Chapter 4 - Alendronic acid as ionic liquid: new perspective on osteosarcoma

This chapter contains parts of a submitted article in:

S. Teixeira, M.M. Santos, M.H. Fernandes, J. Costa-Rodrigues, L.C. Branco

4.1 – Introduction

Alendronic acid is an aminobisphosphonate derivative which has shown efficacy in postmenopausal osteoporosis, malignant hypercalcemia and Paget's disease (106). Alendronate localizes preferentially at active sites of bone resportion, and bone resorption has been inhibited at doses that have no effect on bone mineralization (107).

Bisphosphonates bind at the bone mineral surface, where they potently inhibit osteoclast mediated bone resorption and subsequently embed in the bone, being released only during subsequent resorption (108). In contrast to other antiresorptive agents, Bisphosphonates with the greatest binding affinity to bone (zoledronic acid > alendronate > ibandronate > risedronate) may persist in bone, and patients continue to be exposed to the pharmacologic effects of these drugs several years after discontinuation.

All bisphosphonates rapidly reduce bone resorption, which leads to decreased bone formation because resorption and formation are coupled. Within three to six months equilibrium is reached at a lower rate of bone turnover (66).

It is described that alendronate in rats exhibited 200 to 1000 times more potency than etidronate and approximately 100 times comparing to clodronate or tiludronate (64). It is recognized that the presence of amino group side-chain from alendronate chemical structure contributes for greater potency and specificity. (64, 66, 108)

The introduction of specific functional groups in the BPs structure can lead to modifications in their physicochemical, biological, therapeutic and toxicological proprieties. In recent studies in the literature, it is reported the use of Alendronate as FDA drug already approved for the prevention and treatment of postmenopausal osteoporosis, treatment of osteoporosis in men, and treatment of glucocorticoid induced osteoporosis in men and women. (103)

The combination of Ionic Liquids (defined as organic salts with melting point below 100 ºC) as an attractive class of materials with some peculiar properties such as negligible vapor pressure, high thermal and chemical stability and the possibility to tune their physical-chemical properties according the adequate combination of organic cations and anions; or molten salts with active pharmaceutical ingredients (APIs) can offer novel and distinctive properties compared to the solid neutral original APIs (8, 90, 91). This novel API-ILs can improve the drug performance in terms of its stability, solubility, permeability and delivery (92, 93, 95, 97, 99, 100).

Recent achievements showed the suitable combination between pharmaceutical drugs such as anti-inflammatory (e.g. ibuprofen and naproxen) and antibiotics (e.g. ampicillin, amoxicillin, penicillin derivatives; ciprofloxacin, moxifloxacin and norfloxacin derivatives) and biocompatible counter-ions. According with these approaches, novel

pharmaceutical drugs based on ionic liquids or molten salts have been synthetized (101, 102). Elimination of original polymorphism drug behavior, significant improvement into water, biological fluids solubility and permeability as well as therapeutic efficiency were observed for these innovative salts (109).

Hence, in this paper we report the synthesis of eight new Ionic Liquids and salts from the BP alendronic acid in quantitative yields by following two distinct sustainable and straightforward methodologies, according to the type of cation. All prepared bisphosphonate-based ILs were characterized by spectroscopic techniques and their solubility in water and biological fluids was determined. An additional evaluation of the toxicity towards human healthy cells was performed. Figure 71 depicts the structure of the cations used in the synthesis of the bisphosphonate-ILs.
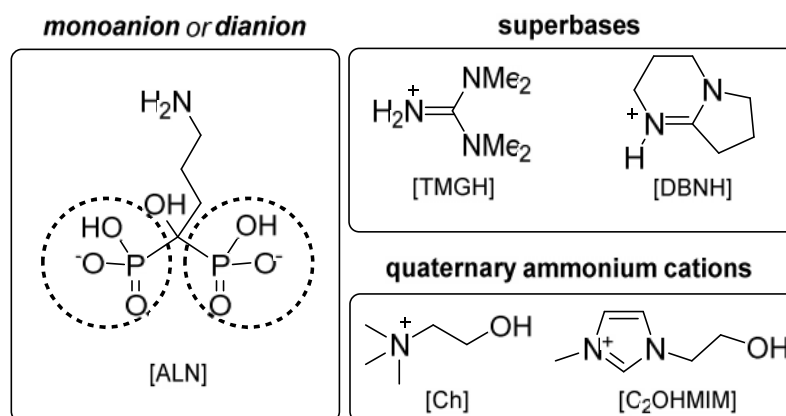
Figure 71- Structure of mono- and dianionic alendronate, protonated superbases and organic quaternary cations used to prepare the ALN-ILs.

4.2 – Synthesis and Characterization of ALN-ILs

In this work we synthesized four new Ionic Liquids and salts from alendronic acid (ALN) by combination with the organic superbases 1,1,3,3-tetramethylguanidine (TMG) and 1,5-diazabicyclo(4.3.0)non-5-ene (DBN) in 1:1 or 1:2 stoichiometry so that only one or the two bisphosphonate groups are deprotonated (general procedure A from scheme 2).
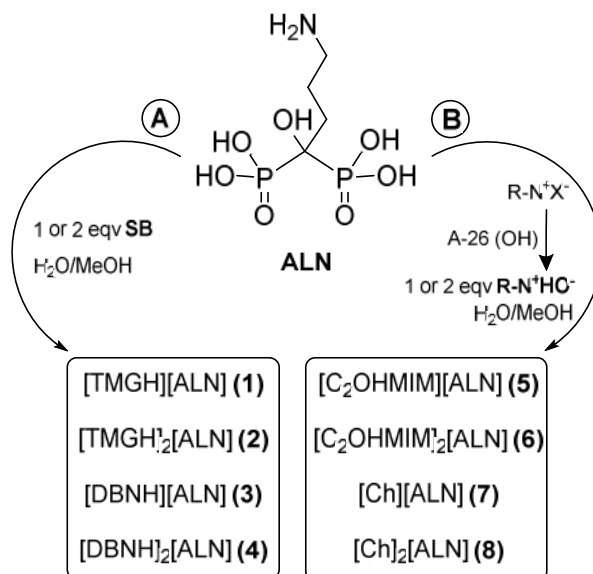
Scheme 2 - Methodologies A and B for the preparation of ALN-ILs.

With the exception of [TMGH][ALN] (**1**), all compounds were obtained as Room Temperature Ionic Liquids (RTILs).

On the other hand, quaternary ammonium and imidazolium cations were used to yield four more ALN-based ILs by combination with 1 and 2 equivalents of [C$_2$OHMIM] and [Ch] through a methodology already described by our group for the preparation of Ampicillin-based Ionic Liquids and Salts (general procedure B from scheme 1) (102). In this case, quaternary ammonium hydroxide cations are previously prepared by the corresponding halide exchange with hydroxide exchange resins (e.g. Amberlyst A26-OH) in methanolic solution. The very basic solutions were then neutralized by addition to an aqueous solution of bisphosphonate yielding the desired salts in quantitative yields. From the four synthesized compounds, one - [Ch]$_2$[ALN] (**8**) – is a RTIL and the remaining **5-7** were obtained as foams.

All products were characterized by NMR (^{1}H and ^{13}C) and FTIR spectroscopic techniques, as well as elemental analysis. The thermal properties were evaluated by DSC and the solubility in water and saline solution was determined for all compounds.

The NMR spectra of the ALN-ILs were acquired in D$_2$O taking advantage of their high solubility in water (see below). In all cases the ^{1}H NMR spectra showed that the cation/anion proportion is strictly 1.0:1.0 or 2.0:1.0, in agreement with the intended stoichiometry. In addition, only one set of signals was found meaning that the reactions were complete and only one product was formed. No comparison with alendronic acid is achievable because of its lack of solubility in the same solvents as the ALN-ILs. In the ^{13}C NMR spectra, the resonance of the quaternary carbon atom of Ale appears at *ca.* 74 ppm, with no particular difference if only one or the two neighboring phosphonate groups are

deprotonated. Similarly, the ^{1}H NMR data is also irreflective of the ionic state of the bisphosphonates and also of the cations. On the other hand, the collected FTIR spectra show pristine variations between the neutral bisphosphonates and the ALN-ILs, as well as between mono- and dianions. The FTIR spectra of Ale show two characteristic regions, namely a weak and undefined structure at 2400-2000 cm^{-1} with maximum intensity at 2256 cm^{-1}, and also very intense multiple peaks at 1250-900 cm^{-1}. While the first one accounts for O–H stretches from the O=P–OH groups, the second region contains peaks attributable to the stretch of both P=O and P–OH bonds (110). In the spectra of the synthesized ALN-ILs, the peaks in the first region become sharper and much weaker, and two other sets of peaks appear in the vicinity (at *ca.* 2600-2500 cm^{-1} and 2200-2100 cm^{-1}) which are more intense for the dianionic ALN-ILs than for the monoanionic. This is in complete agreement with changes in the vibrational modes of the OH groups from the phosphonate moieties that are particularly enhanced when both groups are deprotonated. This corollary is also sustained by the changes observed in the second region of peaks, which in general display two very intense broad peaks at *ca.* 1160 cm^{-1} and 1060 cm^{-1}, and one or two of medium intensity between 960-900 cm^{-1}.

4.3 – Thermal analysis of ALN-ILs

All prepared ILs from alendronic acid were studied by Differential Scanning Calorimetry (DSC) techniques. Table 12 contains the data obtained, namely melting, crystallization and glass transition temperatures, as well as the physical state of the analyzed compounds.

In general, the dianionic ALN-ILs are foam-like solids while the monoanionic ones were obtained as thick colorless pastes at room temperature, thus being considered Room Temperature Ionic Liquids (RTILs). The exceptions to this rule are the compounds with the [C${}_2$OHMIM] cation, where the mono- and dianionic are respectively a paste and a foam. This inversion of the trend is probably related with specific interactions of ALN with the electron-rich imidazolium ring.

In comparison with sodium alendronate, which presents a melting temperature of 259.3 ${}^{\circ}$C (111), all solid compounds melt at lower temperatures, more specifically between 48.1 and 162.7 ${}^{\circ}$C. Curiously, both these limits belong to [TMGH][ALN], in whose DSC thermogram (Figure 101) a first melt (48.1 ${}^{\circ}$C) and cold crystallization (107.1 ${}^{\circ}$C) were observed in the first cycle. This cycle consists on heating to 120 ${}^{\circ}$C and isotherm for 10 minutes in order to evaporate the residual water that exists in these hygroscopic

compounds. After cooling to -90 ⁰C and subsequent heating to 175 ⁰C, another endothermic signal was observed at 162.7 ⁰C consistent with a melting temperature from the differently organized solid formed after the cold crystallization. No glass transition was observed in the following cooling/heating cycles.

In its turn, the first heating cycle to 175 ⁰C in the DSC experiment with the dianionic [TMGH]-based ALN-IL (**2**) showed an endothermic signal at *ca* 150 ⁰C that could be assigned to a melting process. However, it is preceded by a glass transition at *ca* 40 ⁰C in the same cycle, meaning that the compound is in an amorphous state. So, the referred endothermic signal is most likely due to evaporation, in consistency with the irregular shape of the curve caused by the formation of bubbles in the thick pasty compound. A similar observation can also be performed to [C$_2$OHMIM][ALN] (Figure 110).

From the set of eight compounds, [DBNH][ALN] is the only one that possesses a polymorphic structure, given by the two melting temperatures at 130.3 and 133.2 ⁰C recorded in the DSC thermogram. The remaining RTILs, more precisely [DBNH]$_2$[ALN] and [Ch]$_2$[ALN] show well defined glass transitions confirming their amorphous nature at room temperature. Finally, the solid compounds [C$_2$OHMIM]$_2$[ALN] and [Ch][ALN] become supercooled products, i.e. amorphous after melting.

Table 12 - Physical state, melting (Tm), cold crystallization (Tcc) and glass transition (Tg) temperatures of the prepared ALN-ILs

Salt	Physical state	T_m/°C	T_{cc}/°C	T_g/°C
[TMGH][ALN]	White solid	48.1 162.7	107.1*	
[TMGH]$_2$[ALN]	Colorless paste	-	-	97.5
[DBNH][ALN]	White solid	130.3 133.2	-	-
[DBNH]$_2$[ALN]	Colorless paste	-	-	45.7
[C$_2$OHMIM][ALN]	Colorless paste	-	-	64.5
[C$_2$OHMIM]$_2$[ALN]	White solid	153.0	-	46.3
[Ch][ALN]	White solid	141.2	-	74.9
[Ch]$_2$[ALN]	Colorless paste	-	-	63.8

* cold crystallization

4.4 – Solubility Studies

As expected, all ionic liquids and salts were more soluble in water and saline solution at 37 °C than neutral alendronic acid. Figure 72 contains the data obtained from the solubility studies.
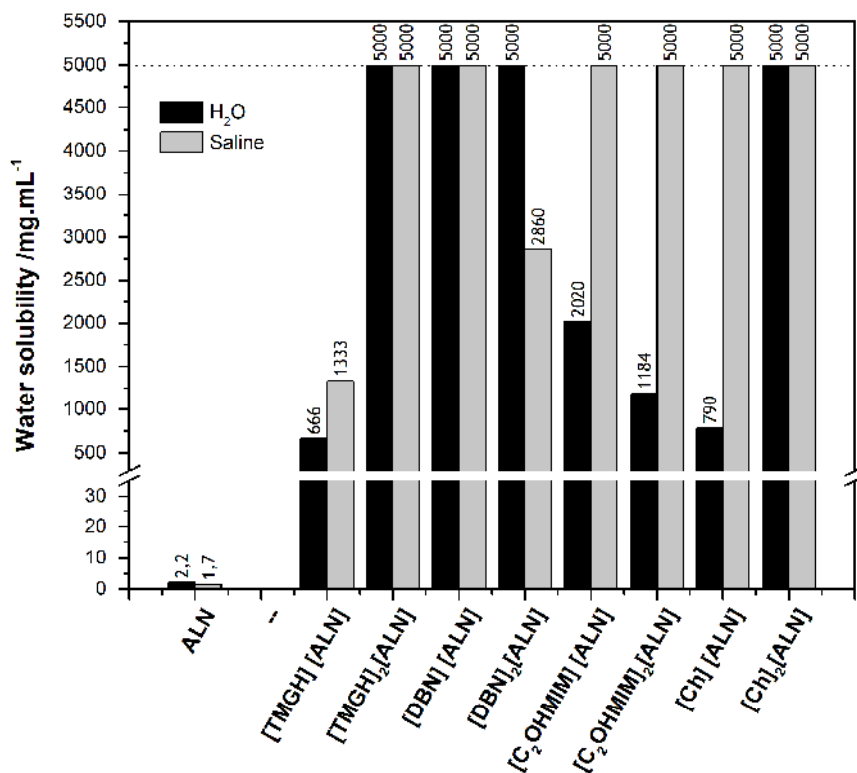
Figure 72 - Solubility in water and saline solution at 37 °C of ALN and corresponding ALN-ILs (detection limit is 5 g/mL, represented by the upper threshold).

With the exception of the [DBN]- and [C_2OHMIM]-containing ILs, the dianionic ALN-ILs are equally or more soluble than the monoanionic siblings in the tested media. In further detail it is noteworthy that [TMGH]$_2$[ALN], [DBN][ALN] and [Ch]$_2$[ALN] are completely soluble in both water and saline solution in the tested conditions. Moreover, the [C_2OHMIM]-, [C_2OHMIM]$_2$- and [Ch]-based ALN-ILs are also fully soluble in saline solution while the solubility in water was found to be between 392 and 918 times higher in comparison with the parent drug. In addition, [DBN]$_2$[ALN] presents full water solubility and a 1682-fold increase in solubility in saline solution. Finally, [TMGH][ALN] shows the lowest solubility in both media from the set of eight compounds.

4.5 – Cytotoxicity on human cells

The cytotoxicity of the different ALN-ILs was determined on human cells, by means of IC_{50} calculation. The analysis was performed on human gingival fibroblasts and on different cancer cell lines, namely T47D, A549 and MG63. The results are presented in Table 13.

Table 13 - Cytotoxicity of the ALN-ILs on different human cell types.

IC_{50} / mM IL	Gingival fibroblasts	T47D	A549	MG63
ALN	3.17×10^{-2}	4.09×10^{-3}	8.10×10^{-3}	5.55×10^{-4}
[TMGH][ALN]	7.19×10^{-3}	8.23×10^{-3}	2.54×10^{-3}	9.23×10^{-3}
[TMGH]$_2$[ALN]	1.11×10^{-3}	3.16×10^{-5}	5.14×10^{-4}	7.11×10^{-5}
[DBNH][ALN]	7.20×10^{-2}	a)	6.14	a)
[DBNH]$_2$[ALN]	6.01×10^{-5}	a)	3.12×10^{-2}	1.02
[C$_2$OHMIM][ALN]	2.19	5.92×10^{-3}	2.10×10^{-6}	5.16×10^{-5}
[C$_2$OHMIM]$_2$[ALN]	4.07×10^{-4}	3.28×10^{-6}	a)	7.84×10^{-5}
[Ch][ALN]	1.87×10^{-1}	3.14	6.66×10^{-2}	4.10×10^{-1}
[Ch]$_2$[ALN]	4.92×10^{-3}	2.64×10^{-3}	5.41×10^{-3}	1.01×10^{-2}

a) Not determined in the tested concentration range.

Globally, it was observed that the monoanionic ILs elicited a lower cytotoxicity than the corresponding dianionic versions. Regarding gingival fibroblast cell cultures, the ILs containing [TMGH], [TMGH]$_2$, [DBNH]$_2$, [C$_2$OHMIM]$_2$ and [Ch]$_2$ appeared to be more deleterious than alendronic acid. Comparatively, ILs containing [TMGH]$_2$, [C$_2$OHMIM] and [C$_2$OHMIM]$_2$ seemed to be more cytotoxic to breast cancer T47D cells. In the case of lung cancer A549 cell line, a high cytotoxic activity was observed in cell cultures supplemented with ILs containing [TMGH]$_2$, [C$_2$OHMIM]. Finally, osteosarcoma MG63 cell line seemed to be particularly sensitive to ILs containing [TMGH]$_2$, [C$_2$OHMIM] and [C$_2$OHMIM]$_2$.

Taken together, among the tested set of ALN-ILs, [TMGH]$_2$[ALN], [C$_2$OHMIM][ALN] and [C$_2$OHMIM]$_2$[ALN] displayed IC_{50} values selectively lower, and, thus, a higher cytotoxicity, in the case of the neoplastic cells, compared to the control (gingival fibroblasts). The highest effect was observed in ILs containing [C$_2$OHMIM], with a decrease in IC_{50} of at least 3 orders of magnitude.

Breast and lung cancers are often associated to bone osteolytic metastases (60, 112, 113) and also osteosarcoma is usually a cause of disturbances in bone metabolism and increases in bone turnover rates. (62, 103) Thus, the development of ILs with a high cytotoxicity towards the tested cancer cell types, and containing an anti-resorbing molecule (alendronate) may represent a promising strategy for the development of new pharmacological tools to be used in those pathological conditions.

4.6 - Experimental Section

General procedure (A) for the synthesis of ALN-ILs with organic superbases as cations:

To a dispersion of alendronic acid (400 mg, 1.61 mmol) in MeOH/H_2O (15 mL, 1:1) a methanolic solution of 1 or 2 molar equivalents of organic superbase (15 mg/mL) was added dropwise under magnetic stirring. After reacting for 1h the solvent was evaporated and the desired product was dried under vacuo for 24 h.

General procedure (B) for the preparation of ALN-ILs with ammonium cations:

The halide salts of the selected ammonium cations were dissolved in methanol and passed slowly through an anion-exchange column A-26(OH) (3 equivalents). The freshly formed methanolic solutions of the corresponding hydroxide salts (1 or 2 equivalents) were consequently added dropwise to alendronic acid (400 mg, 1.61 mmol) dispersed in H_2O under magnetic stirring. After 1 h, the solvent of the clear solution was evaporated and the desired product was dried under vacuo for 24 h.

Toxicity studies are described as supporting information.

4.7 - Supplementary Information
4.7.1 - Experimental

Materials

All acquired reagents were used without further purification. Alendronic acid (ALN, 98.5%) was purchased from Molekula, 1,1,3,3-tetramethylguanidine (TMG, 99%), 1,5-diazabicyclo(4.3.0)non-5-ene (DBN, 99%), and choline chloride (ChCl, 99%), were

supplied by Sigma-Aldrich, and 1-(2-hydroxyethyl)-3-methylimidazolium chloride ([C$_2$OHMIM]Cl], 98%), was purchased at Solchemar. Methanol HPLC grade was acquired from Honeywell and deionized water was processed by Diwer Technologies water max w2 equipment.

General procedure (A) for the synthesis of ALN-ILs with organic superbases as cations:

To a dispersion of alendronic acid (400 mg, 1.61 mmol) in MeOH/H$_2$O (15 mL, 1:1) a methanolic solution of 1 or 2 molar equivalents of organic superbase (15 mg/mL) was added dropwise under magnetic stirring. After reacting for 1h the solvent was evaporated and the desired product was dried under vacuo for 24 h.

General procedure (B) for the preparation of ALN-ILs with ammonium cations:

The halide salts of the selected ammonium cations were dissolved in methanol and passed slowly through an anion-exchange column A-26(OH) (3 equivalents). The freshly formed methanolic solutions of the corresponding hydroxide salts (1 or 2 equivalents) were consequently added dropwise to alendronic acid (400 mg, 1.61 mmol) dispersed in H$_2$O under magnetic stirring. After 1 h, the solvent of the clear solution was evaporated and the desired product was dried under vacuo for 24 h.

Characterization

The prepared compounds were characterized by ^{1}H and ^{13}C NMR recorded on a Bruker AMX400 spectrometer. Chemical shifts are reported downfield in parts per million considering the solvent residual signal. ^{13}C NMR spectra in D$_2$O were referenced to added MeOH or MeCN. IR spectra were recorded on a FTIR Bruker Tensor 27 Spectrometer using KBr matrixes. DSC analysis was carried out using a TA Instruments Q-series TM Q2000 DSC with a refrigerated cooling system. Between 2 and 10 mg of salt were crimped into an aluminum standard sample pan with lid which was continuously purged with nitrogen gas at 50 mL/min. The employed procedure was dependent on the melting point of the sample. A typical experiment consisted on a heating step (20 ºC/min) to 80 or 120 ºC (15-20 minutes), cooling (20 ºC/min) to -90 ºC, heating (10 ºC/min) to 200 ºC, cooling (10 ºC/min) to -90 ºC, heating (10 ºC/min) to 200 ºC, cooling (10 ºC/min) to -90 ºC, heating (20 ºC/min) to 200 ºC and cooling (20 ºC/min) to -90 ºC. Glass transition (T$_g$), melting (T$_m$) cold crystallization (T$_{cc}$) and decomposition temperatures were determined in the heating steps, while crystallization temperatures (T$_c$) were acquired in the cooling steps. The solubility of the salts in water and saline solution was determined by adding 5

to 10 µL of solvent to an Eppendorf containing precisely weighed *ca.* 30 mg of sample until a homogeneous solution is obtained upon mixture in a vortex.

Experimental data of the synthesized compounds

Preparation of bis(dimethylamino)methaniminium hydrogen (4-amino-1-hydroxy-1-phosphonobutyl)phosphonate, [TMGH][ALN] (**1**)
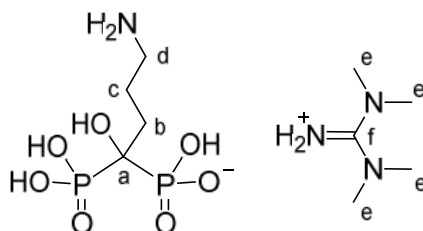
Figure 73 - [TMGH][ALN]

Using tetramethylguanidine (185 mg, 1.61 mmol) [TMGH][ALN] was obtained as a white solid in quantitative yield (585 mg). T_m = 48.1, 162.7 °C, T_{cc} = 107.1 °C; ^{1}H NMR (400.13 MHz, D_2O)   3.07 – 2.99 (m, 2H, d), 2.93 (s, 12H, e), 2.06 – 1.92 (m, 4H, b, c). ^{13}C NMR (100.62 MHz, D_2O)   162.0 (f), 74.1 (t, J = 135.3 Hz, a), 40.6 (d), 39.5 (e), 31.2 (c), 22.8 (t, J = 6.8 Hz, b) ppm; FTIR (KBr) 3407, 3112, 2966, 2818, 2337, 2137, 1649, 1610, 1566, 1412, 1164, 1064, 1039, 955, 916 cm^{-1}. Anal. calcd for $C_9H_{26}N_4O_7P_2.2H_2O$: C, 27.00; H, 7.55; N, 14.00; found: C, 27.60; H, 8.02; N, 14.25.

Preparation of bis(bis(dimethylamino)methaniminium) (4-amino-1-hydroxybutane-1,1-diyl)bis(hydrogen phosphonate), [TMGH]$_2$[ALN] (**2**)
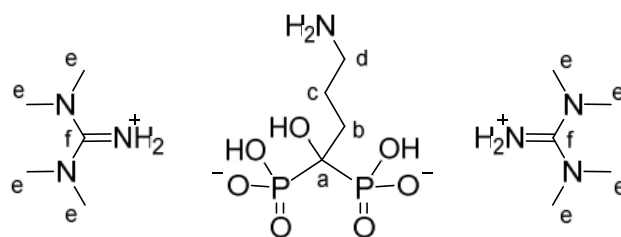
Figure 74 - [TMGH]2[ALN]

Using tetramethylguanidine (370 mg, 3.22 mmol) [TMGH]$_2$[ALN] was obtained as a colorless paste in quantitative yield (770 mg). T_m = 148.8 °C, T_g = 97.5 °C; ^{1}H NMR (400.13 MHz, D_2O)   3.07 – 2.98 (m, 2H, d), 2.93 (s, 24H, e), 2.02 – 1.88 (m, 4H, b, c); ^{13}C NMR (100.62 MHz, DMSO-d^6)   162.1 (f), 74.2 (t, J = 135.1 Hz, a), 40.7 (d), 39.5 (e), 31.7 (c), 23.1 (t, J = 7.1 Hz, b) ppm; FTIR (KBr) 3282, 3109, 2955, 2908, 2808, 2658, 2520, 2330, 2136, 1956, 1648, 1609, 1561, 1413, 1318, 1168, 1086, 1039, 970, 927 cm^{-1}.

Anal. calcd for $C_{14}H51N_7O_{13}P_2.6H_2O$: C, 28.62; H, 8.75; N, 16.69; found: C, 28.58; H, 8.86; N, 16.69.

Preparation of 2,3,4,6,7,8-hexahydropyrrolo[1,2-a]pyrimidin-1-ium hydrogen (4-amino-1-hydroxy-1-phosphonobutyl)phosphonate, [DBNH][ALN] (**3**)
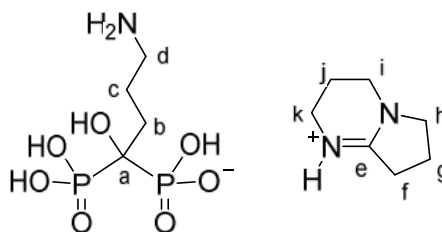
Figure 75 - [TMGH]2[ALN]

Using 1,5-diazabicyclo(4.3.0)non-5-ene (199 mg, 1.61 mmol) [DBNH][ALN] was obtained as a white solid in quantitative yield (598 mg). T_m = 130.3, 133.2 ºC; ^{1}H NMR (400.13 MHz, D_2O) 3.64 (t, J = 7.3 Hz, 2H, k), 3.39 (t, J = 5.6 Hz, 2H, h), 3.34 (t, J = 5.6 Hz, 2H, i), 3.07 – 2.98 (m, 2H, d), 2.82 (t, J = 8.0 Hz, 2H, f), 2.10 (quint, J = 7.6 Hz, 2H, g), 2.04 – 1.92 (m, 6H, b, c, j). ^{13}C NMR (100.62 MHz, D_2O) 165.1 (e), 74.2 (t, J = 134.0 Hz, a), 54.1 (h), 42.9 (i), 40.7 (d), 38.7 (k), 31.3 (c), 30.7 (f), 22.8 (t, J = 5.5 Hz, b), 18.9, 18.9 (g, j) ppm; FTIR (KBr) 3423, 3125, 2965, 2885, 2804, 2580, 2360, 1680, 1648, 1588, 1399, 1310, 1146, 1068, 926, 877 cm^{-1}. Anal. calcd for $C_{11}H_{25}N_3O_7P_2.2H_2O$: C, 35.39; H, 6.75; N, 11.26; found: C, 35.58; H, 6.09; N, 11.39.

Preparation of bis(2,3,4,6,7,8-hexahydropyrrolo[1,2-a]pyrimidin-1-ium) (4-amino-1-hydroxybutane-1,1-diyl)bis(hydrogen phosphonate), [DBNH]$_2$[ALN] (**4**)
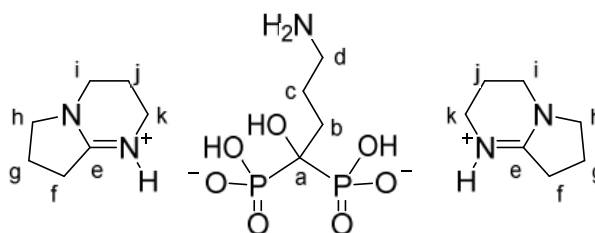
Figure 76 - [DBNH]2[ALN]

Using 1,5-diazabicyclo(4.3.0)non-5-ene (399 mg, 3.22 mmol) [DBNH]$_2$[ALN] was obtained as a colorless paste in quantitative yield (800 mg). T_g = 45.7 ºC; ^{1}H NMR (400.13 MHz, D_2O) 3.64 (t, J = 7.2 Hz, 4H, k), 3.39 (t, J = 5.7 Hz, 4H, h), 3.34 (t, J = 5.7 Hz, 4H, i), 3.06 – 2.97 (m, 2H, d), 2.82 (t, J = 8.0 Hz, 4H, f), 2.09 (quint, J = 7.6 Hz, 4H, g), 2.02 – 1.90 (m, 8H, b, c, j). ^{13}C NMR (100.62 MHz, D_2O) 165.0 (e), 74.2 (t, J = 127.4 Hz, a), 54.0 (h), 42.8 (i), 40.7 (d), 38.6 (k), 31.6 (c), 30.6 (f), 23.1 (t, J = 7.0 Hz, b), 18.8, 18.8 (g, j) ppm; FTIR (KBr) 3425, 3224, 3127, 2966, 2887, 2785, 2652, 2555, 2360, 2342, 1681,

1648, 1590, 1401, 1309, 1166, 1069, 979 cm^{-1}. Anal. calcd for $C_{18}H_{37}N_5O_7P_2.5H_2O$: C, 36.80; H, 8.06; N, 11.92; found: C, 36.88; H, 7.97; N, 12.01.

Preparation of (1-(2-hydroxyethyl)-3-methyl-1*H*-imidazol-3-ium) hydrogen (4-amino-1-hydroxy-1-phosphonobutyl)phosphonate, [C$_2$OHMIM][ALN] (**5**)
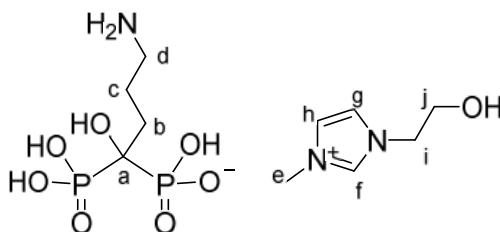
Figure 77 - [C2OHMIM][ALN]

Using hydroxyethylmethylimidazolium chloride (261 mg, 1.61 mmol) [C$_2$OHMIM][ALN] was obtained as a colorless paste in quantitative yield (660 mg). T$_g$ = 64.5 ºC; ^{1}H NMR (400.13 MHz, D$_2$O) 8.73 (br s, 1H, f), 7.49 (br s, 1H, h), 7.43 (br s, 1H, g), 4.29 (t, J = 4.9 Hz, 2H, i), 3.98 – 3.84 (m, 5H, e, j), 3.09 – 2.97 (m, 2H, d), 2.08 – 1.91 (m, 4H, b, c) ppm. ^{13}C NMR (100.62 MHz, D$_2$O) 124.2 (h), 123.1 (g), 74.1 (t, J = 134.5 Hz, a), 60.4 (j), 52.1 (i), 40.6 (d), 36.3 (e), 31.2 (c), 22.8 (t, J = 6.7 Hz, b) ppm; FTIR (KBr) 3418, 3156, 3112, 2960, 2785, 2552, 2359, 2341, 1640, 1575, 1339, 1167, 1066, 917 cm^{-1}. Anal. calcd for $C_{10}H_{23}N_3O_8P_2.2H_2O$: C, 29.20; H, 6.62; N, 10.22; found: C, 29.13; H, 6.71; N, 10.01.

Preparation of bis(1-(2-hydroxyethyl)-3-methyl-1*H*-imidazol-3-ium) (4-amino-1-hydroxybutane-1,1-diyl)bis(hydrogen phosphonate), [C$_2$OHMIM]$_2$[ALN]
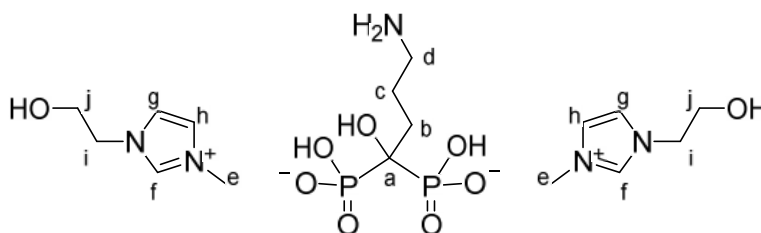
Figure 78 - [C2OHMIM]2[ALN]

Using hydroxyethylmethylimidazolium chloride (522 mg, 3.22 mmol) [C$_2$OHMIM]$_2$[ALN] was obtained as a white solid in quantitative yield (921 mg). T$_m$ = 153.0 ºC, T$_g$ = 46.3 ºC; ^{1}H NMR (400.13 MHz, D$_2$O) 7.49 (br s, 2H, h), 7.43 (br s, 2H, g), 4.30 (t, J = 4.9 Hz, 4H, i), 3.96 – 3.84 (m, 10H, e, j), 3.09 – 2.97 (m, 2H, d), 2.05 – 1.87 (m, 4H, b, c) ppm. ^{13}C NMR (100.62 MHz, D$_2$O) 124.2 (h), 123.0 (g), 74.2 (t, J = 127.1 Hz, a), 60.3 (j), 52.1 (i), 40.7 (d), 36.3 (e), 31.6 (c), 23.1 (t, J = 7.1 Hz, b) ppm; FTIR (KBr) 3388, 3149, 3107, 2961, 2881, 2658, 2543, 2360, 2340, 2128, 1645, 1575, 1451, 1398, 1340,

1169, 1072, 976 cm^{-1}. Anal. calcd for $C_{16}H_{33}N_5O_9P_2 \cdot H_2O$: C, 37.00; H, 6.79; N, 13.48; found: C, 36.65; H, 7.09; N, 12.87.

Preparation of 2-hydroxy-*N,N,N*-trimethylethan-1-aminium hydrogen (4-amino-1-hydroxy-1-phosphonobutyl)phosphonate, [Ch][ALN] (**7**)
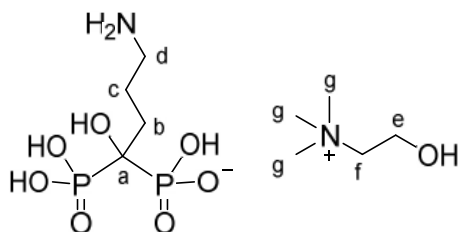
Figure 79 - [Ch][ALN]

Using choline chloride (224 mg, 1.61 mmol) [Ch][ALN] was obtained as a white solid in quantitative yield (623 mg). T_m = 141.2 °C; T_g = 74.9 °C; ^{1}H NMR (400.13 MHz, D$_2$O)   4.08 – 4.00 (m, 2H, e), 3.53 – 3.46 (m, 2H, f), 3.18 (s, 9H, g), 3.06 – 2.98 (m, 2H, d), 2.05 – 1.93 (m, 4H, b, c). ^{13}C NMR (100.62 MHz, D$_2$O)   74.1 (t, J = 133.1 Hz, a), 68.0 (t, J = 3.1 Hz, f), 56.2 (e), 54.5 (t, J = 4.0 Hz, g), 40.6 (d), 31.2 (c), 22.8 (t, J = 6.8 Hz, b) ppm; FTIR (KBr) 3423, 3253, 3019, 2967, 2923, 2857, 2785, 2550, 2359, 2341, 2101, 1646, 1489, 1478, 1400, 1163, 1059, 956, 919 cm^{-1}. Anal. calcd for $C_9H_{26}N_2O_8P_2 \cdot 2H_2O$: C, 27.84; H, 7.79; N, 7.21; found: C, 27.43; H, 7.74; N, 6.91.

Preparation of bis(2-hydroxy-*N,N,N*-trimethylethan-1-aminium) (4-amino-1-hydroxybutane-1,1-diyl)bis(hydrogen phosphonate), [Ch]$_2$[ALN] (**8**)
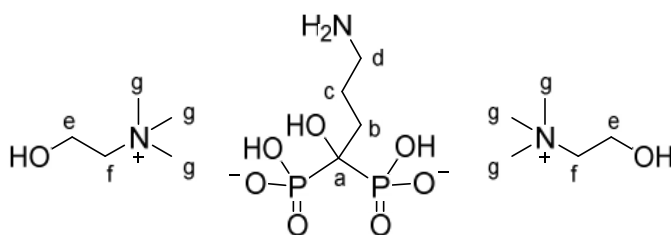
Figure 80 - [Ch]2[ALN]

Using choline chloride (447 mg, 3.22 mmol) [Ch]$_2$[ALN] was obtained as a colorless paste in quantitative yield (848 mg). T_g = 63.8 °C; ^{1}H NMR (400.13 MHz, D$_2$O) 4.10 – 4.02 (m, 4H, e), 3.55 – 3.48 (m, 4H, f), 3.19 (s, 18H, g), 3.08 – 3.00 (m, 2H, d), 2.03 – 1.93 (m, 4H, b, c). ^{13}C NMR (100.62 MHz, D$_2$O)   74.2 (t, J = 127.0 Hz, a), 68.1 (t, J = 3.8 Hz, f), 56.2 (e), 54.5 (t, J = 4.0 Hz, g), 40.7 (d), 31.6 (c), 23.1 (t, J = 7.0 Hz, b) ppm; FTIR (KBr) 3266, 3018, 2959, 2901, 2785, 2663, 2528, 2357, 2342, 2137, 1646, 1478, 1346, 1267, 1167, 1090, 1057, 1006, 970, 949 cm^{-1}. Anal. calcd for $C_{14}H_{39}N_3O_9P_2 \cdot 7H_2O$: C, 28.92; H, 9.19; N, 7.23; found: C, 28.48; H, 9.02; N, 6.90.
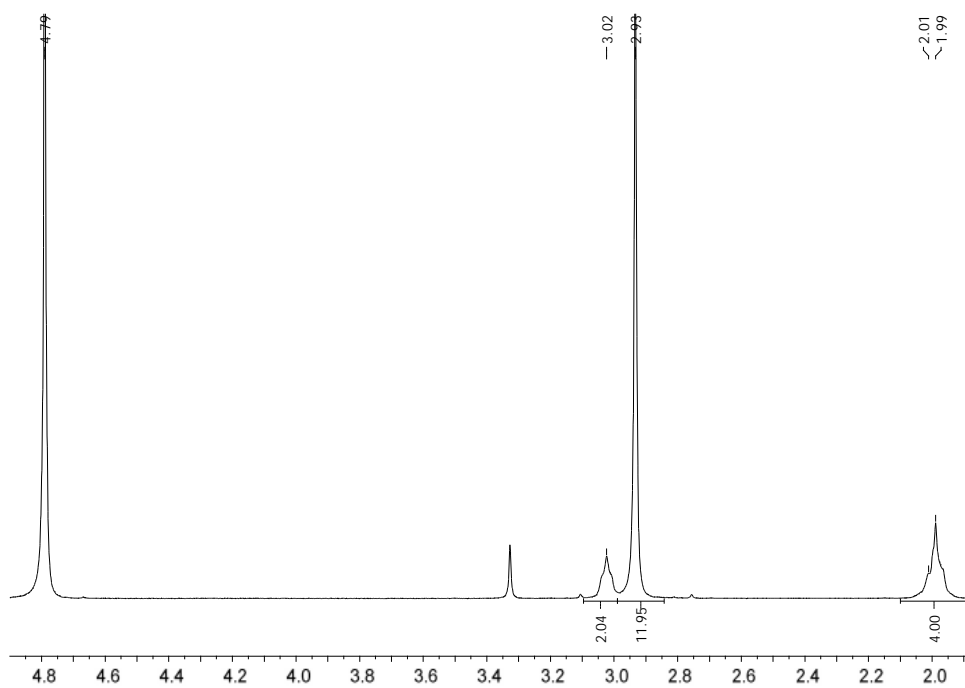
Figure 81 - ¹H NMR spectra of [TMGH][ALN]
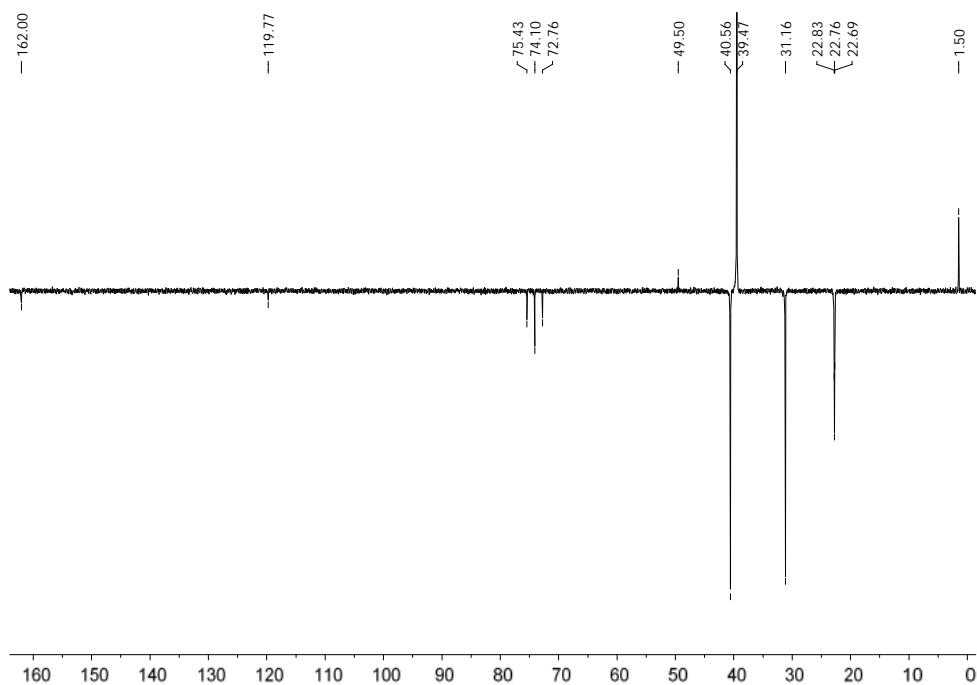
Figure 82 - ¹³C NMR spectra of [TMGH][ALN]
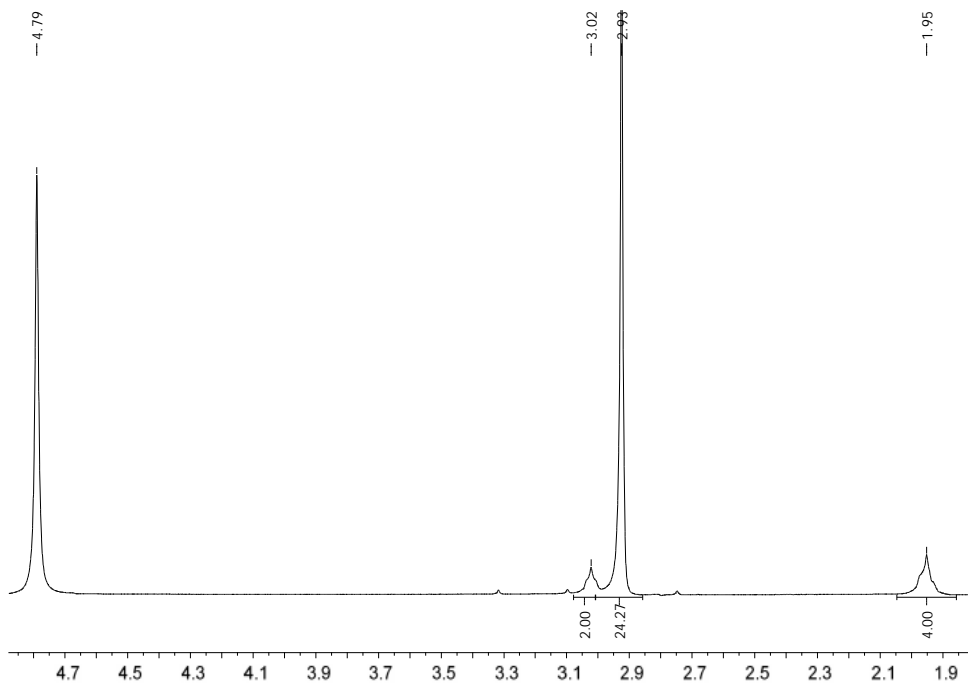
Figure 83 - ^{1}H NMR spectra of [TMGH]2[ALN]
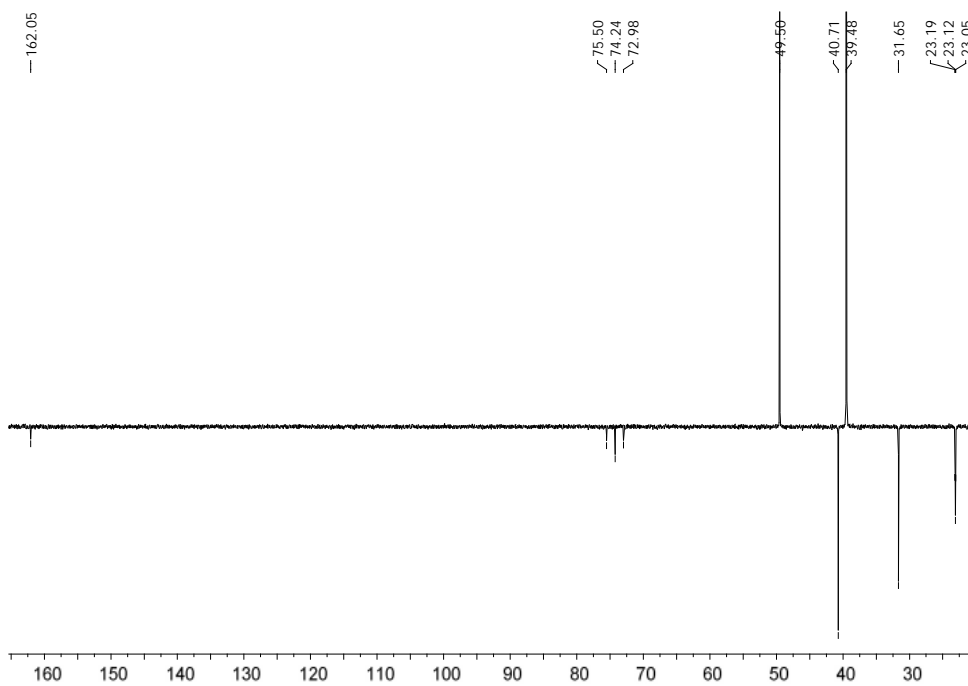
Figure 84 - ^{13}C NMR spectra of [TMGH]2[ALN]
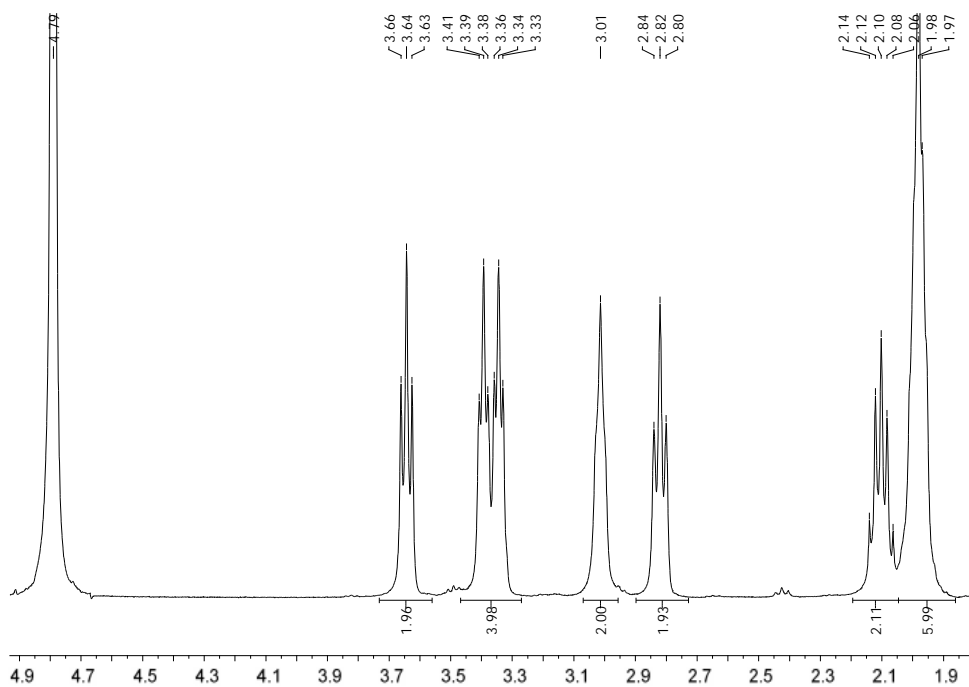
Figure 85 - ^{1}H NMR spectra of [DBNH][ALN]
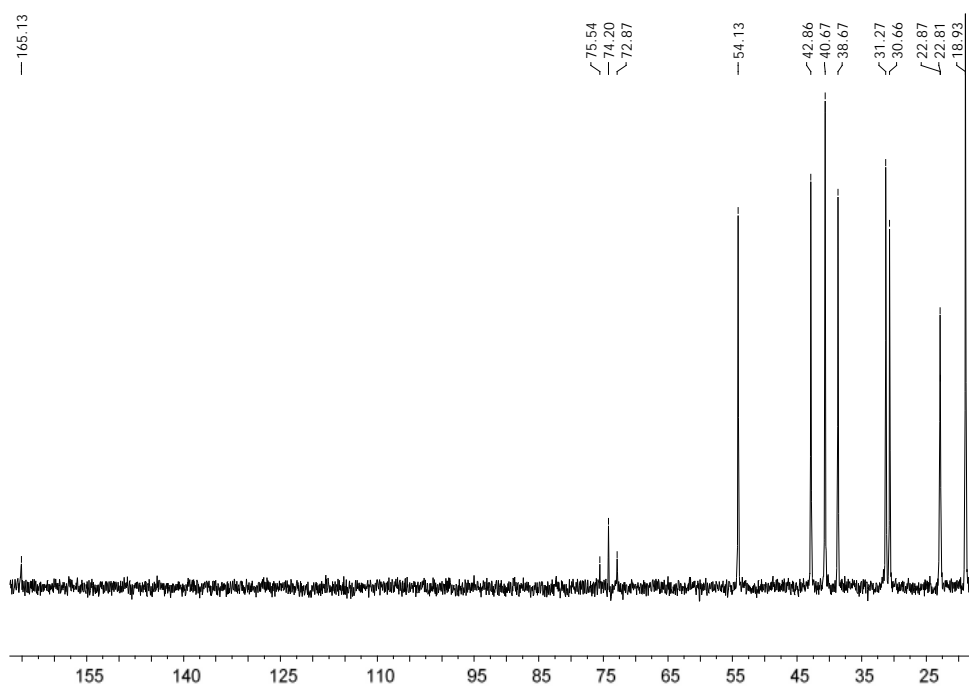
Figure 86 - ^{13}C NMR spectra of [DBNH][ALN]
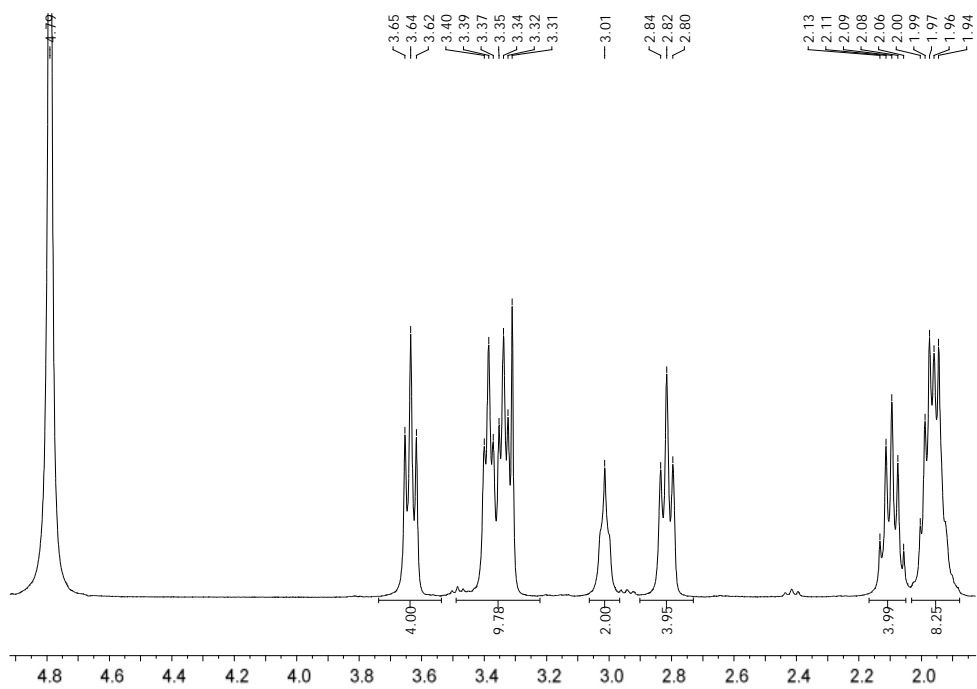
Figure 87 - ¹H NMR spectra of [DBNH]2[ALN]
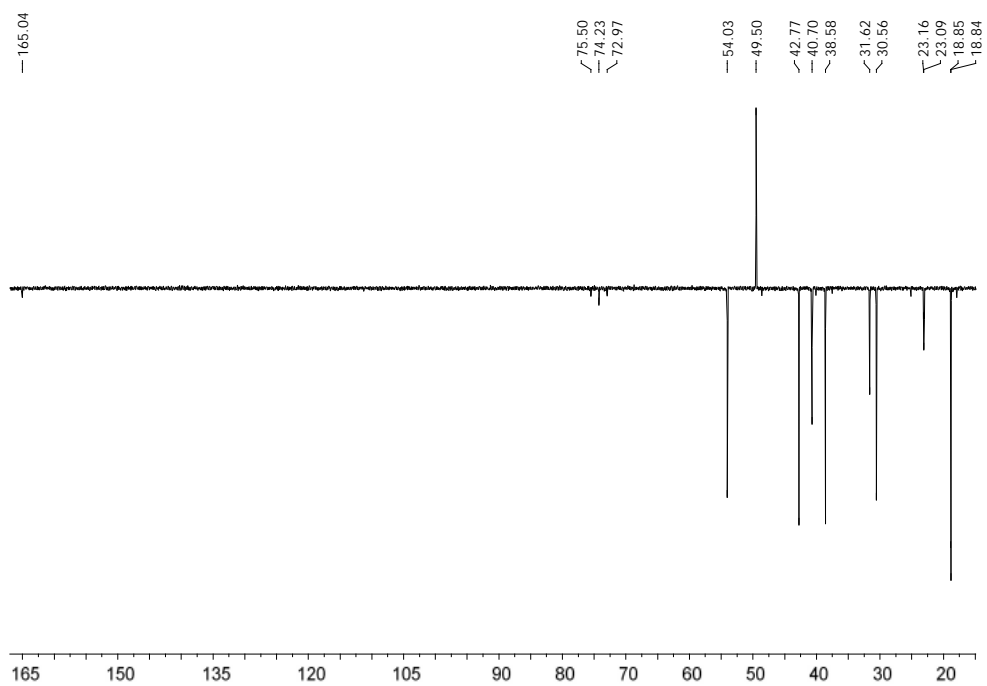
Figure 88 - ¹³C NMR spectra of [DBNH]2[ALN]
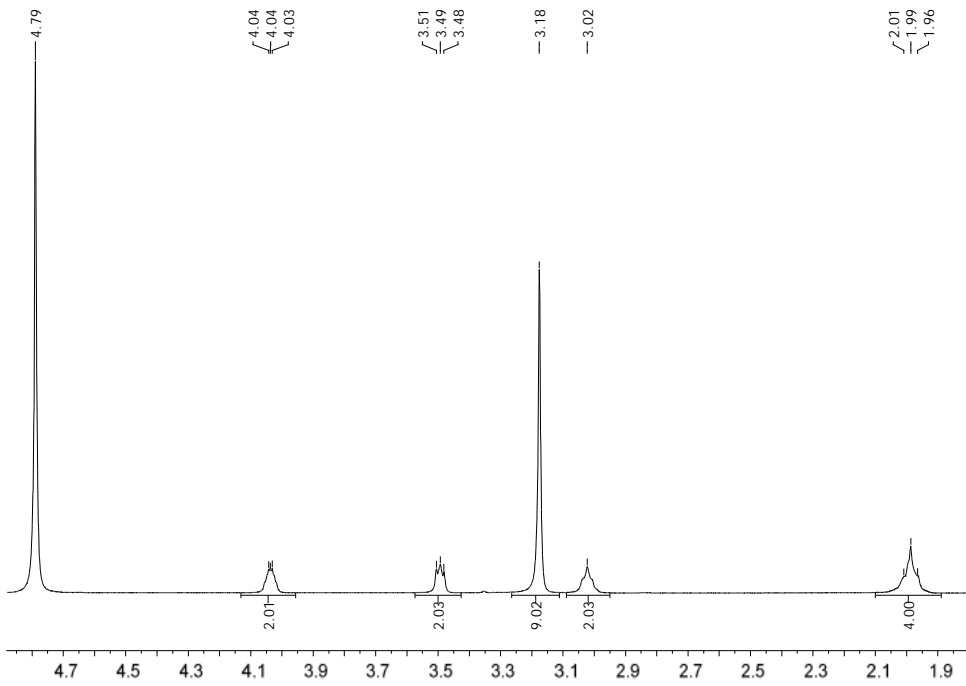
Figure 89 - ^{1}H NMR spectra of [Ch][ALN]
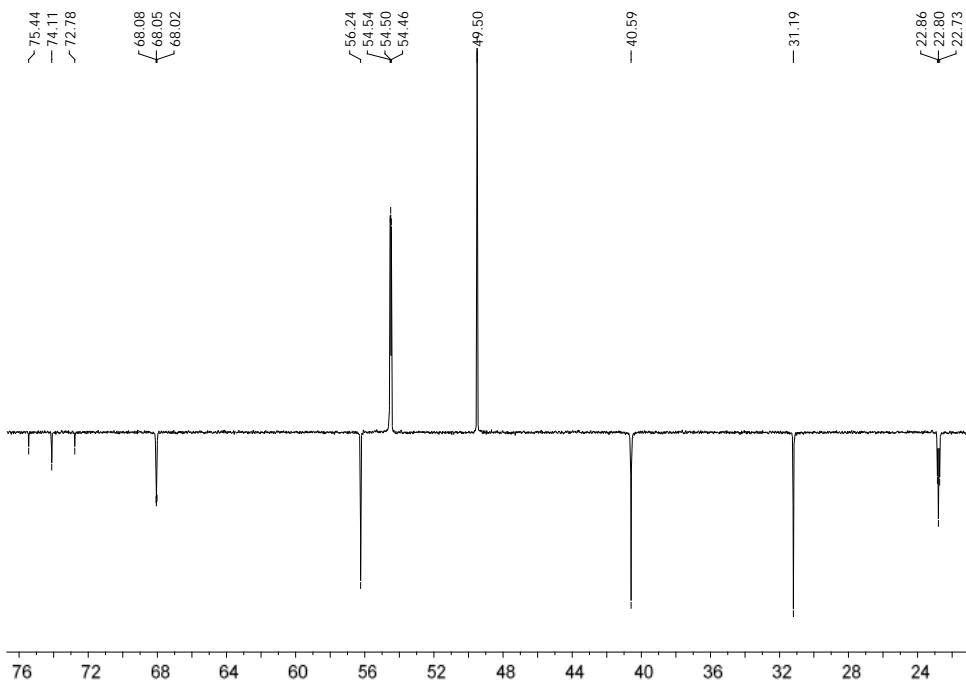
Figure 90 - ^{13}C NMR spectra of [Ch][ALN]
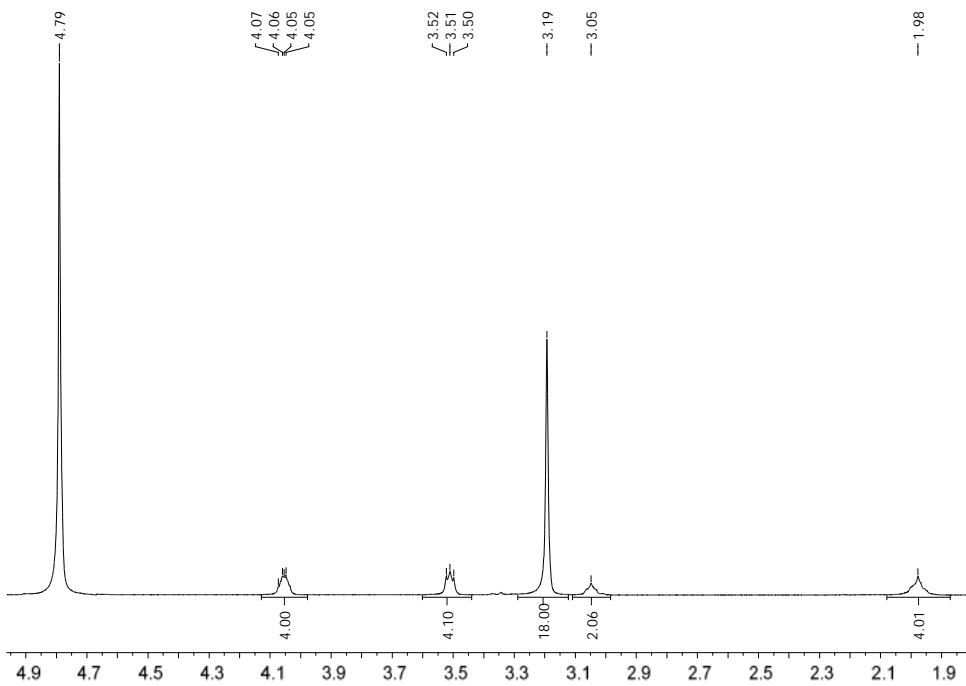
Figure 91 - ¹H NMR spectra of [Ch]2[ALN]
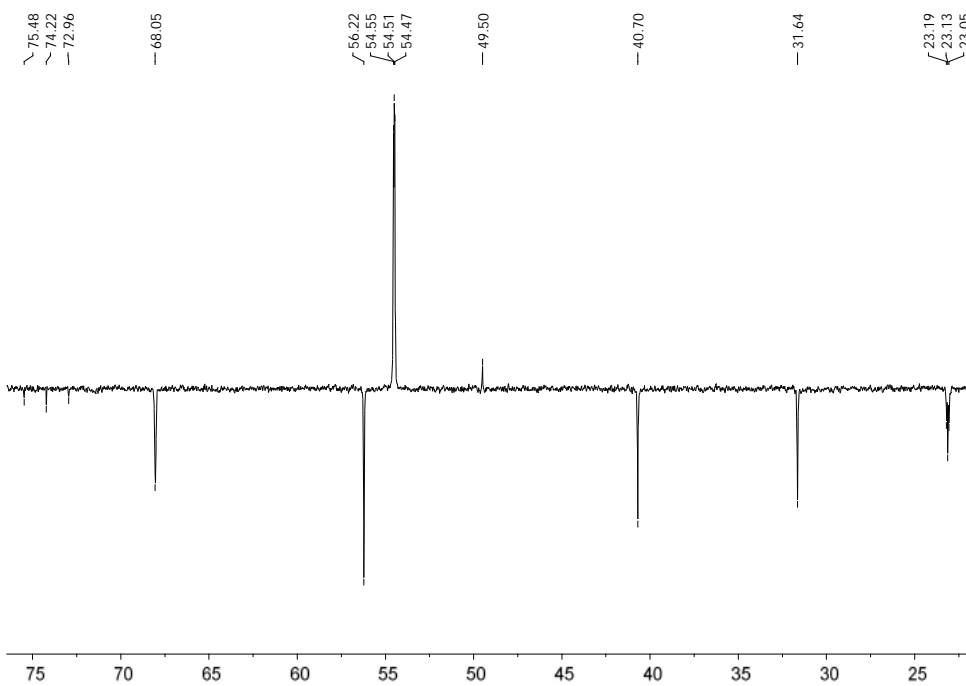
Figure 92 - ¹³C NMR spectra of [Ch]2[ALN]
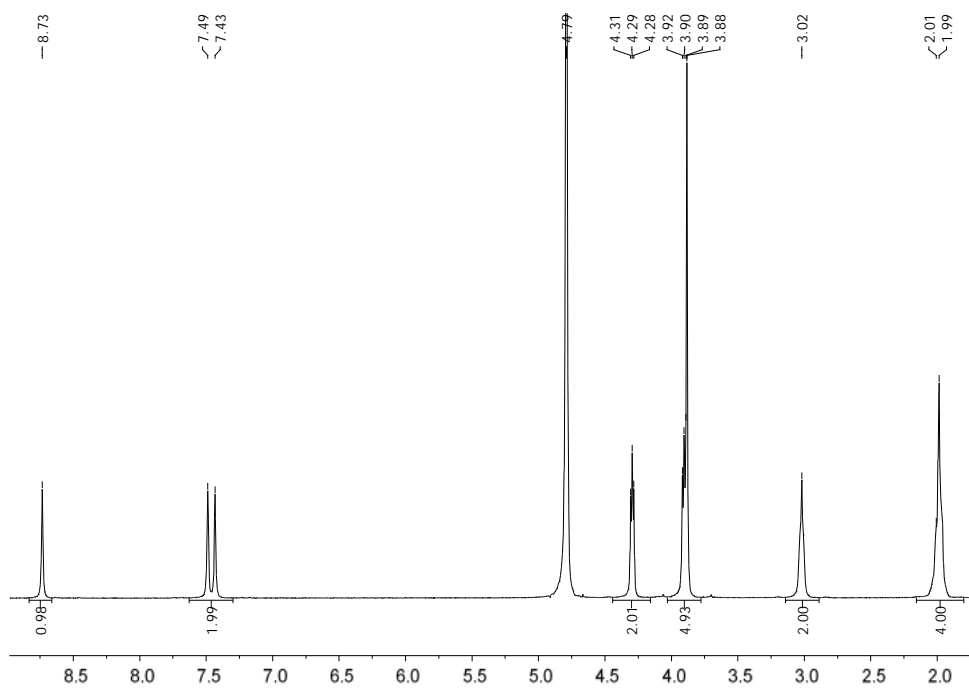
Figure 93 - ¹H NMR spectra of [C2OHMIM][ALN]
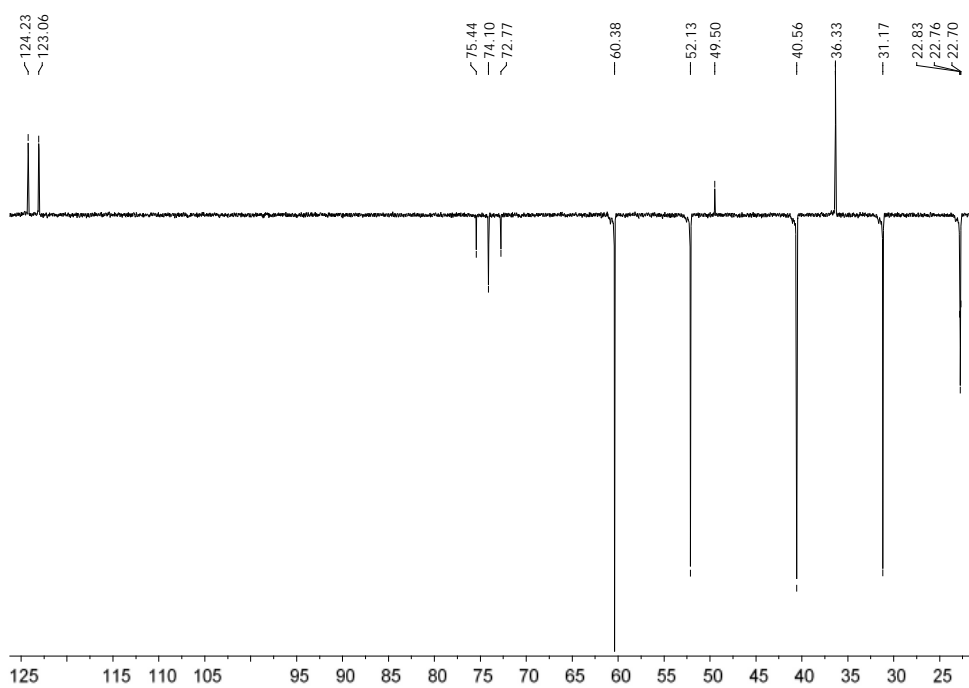
Figure 94 - ¹³C NMR spectra of [C2OHMIM][ALN]
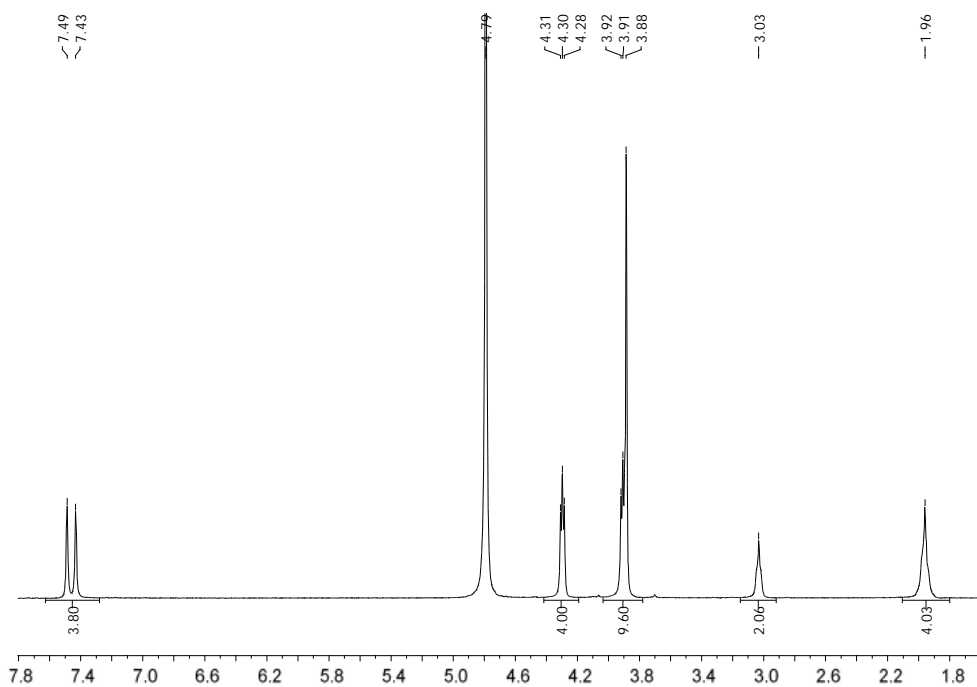
Figure 95 - ¹H NMR spectra of [C2OHMIM]2[ALN]
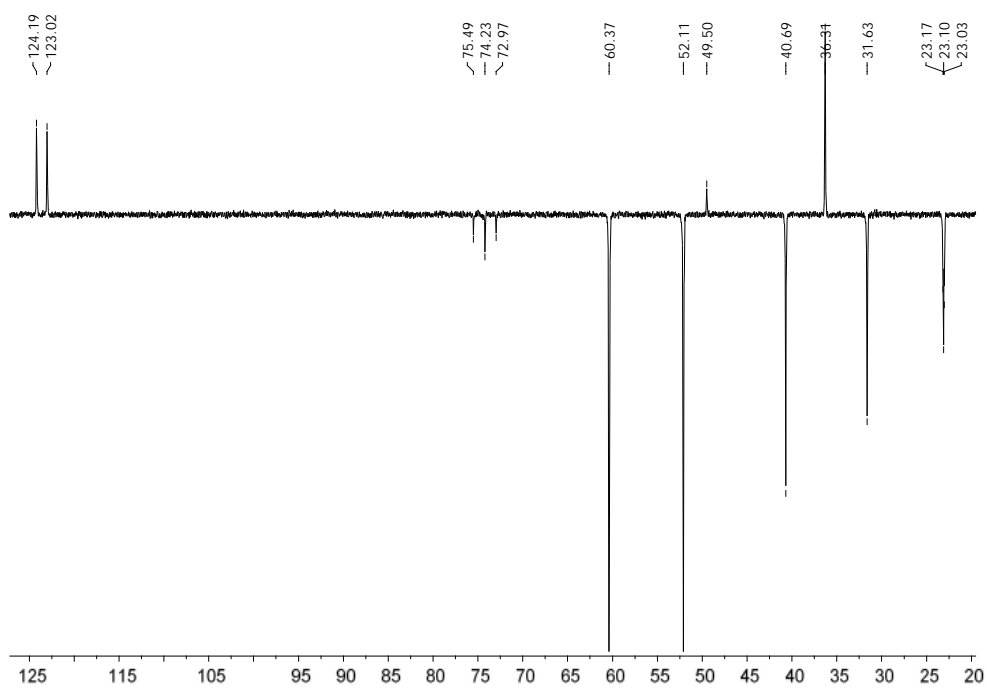
Figure 96 - ¹³C NMR spectra of [C2OHMIM]2[ALN]

FTIR spectra of ALN-ILs
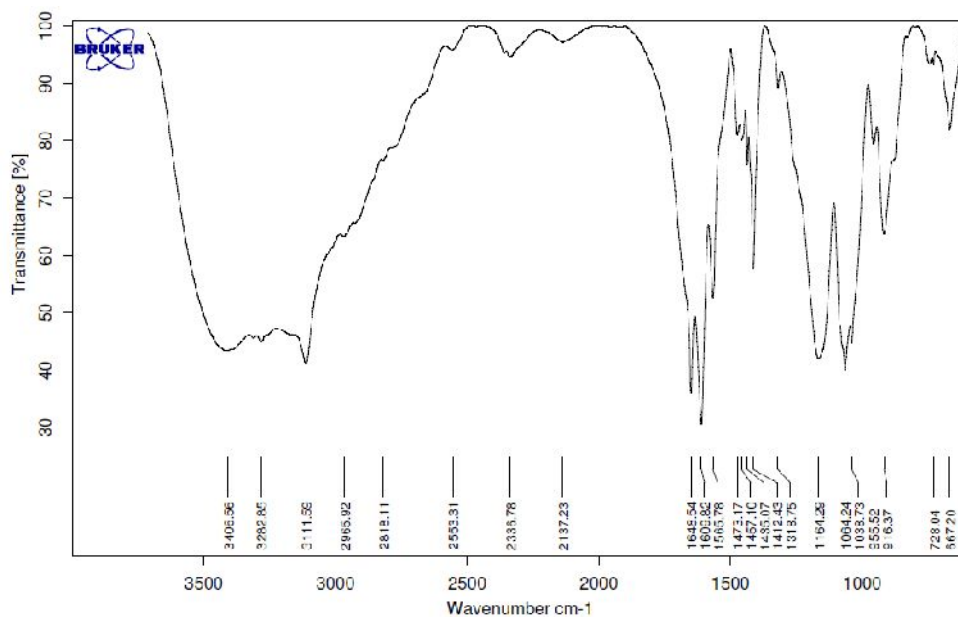
Figure 97 - FTIR spectra of [TMGH][ALN]
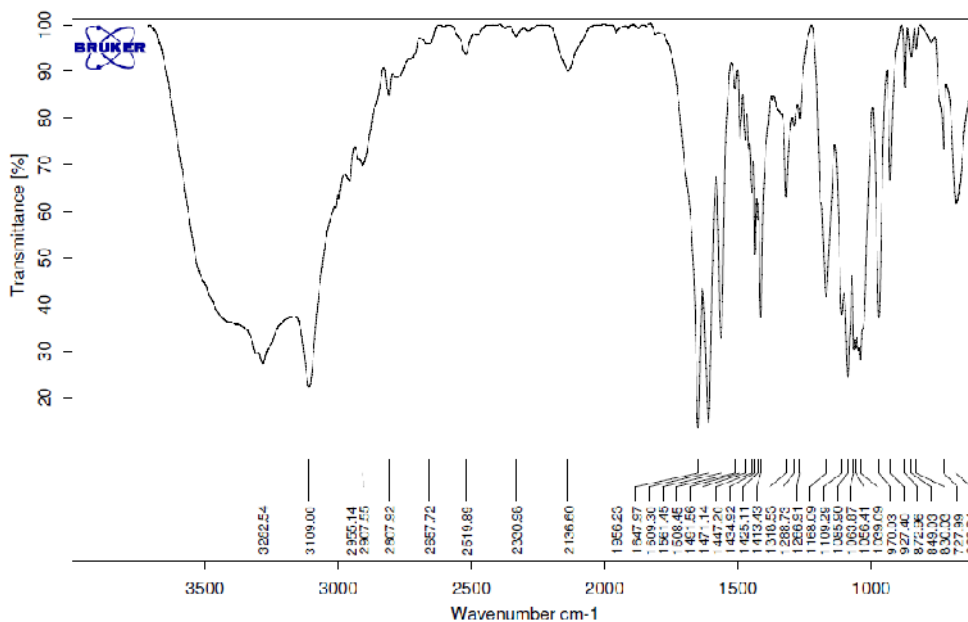
Figure 98 - FTIR spectra of [TMGH]2[ALN]
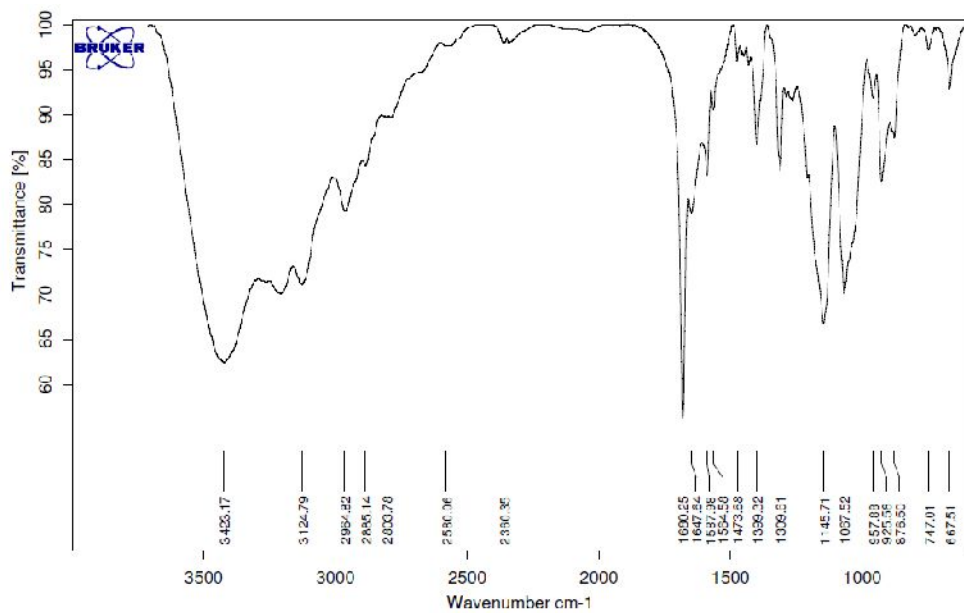
Figure 99 - FTIR spectra of [DBNH][ALN]
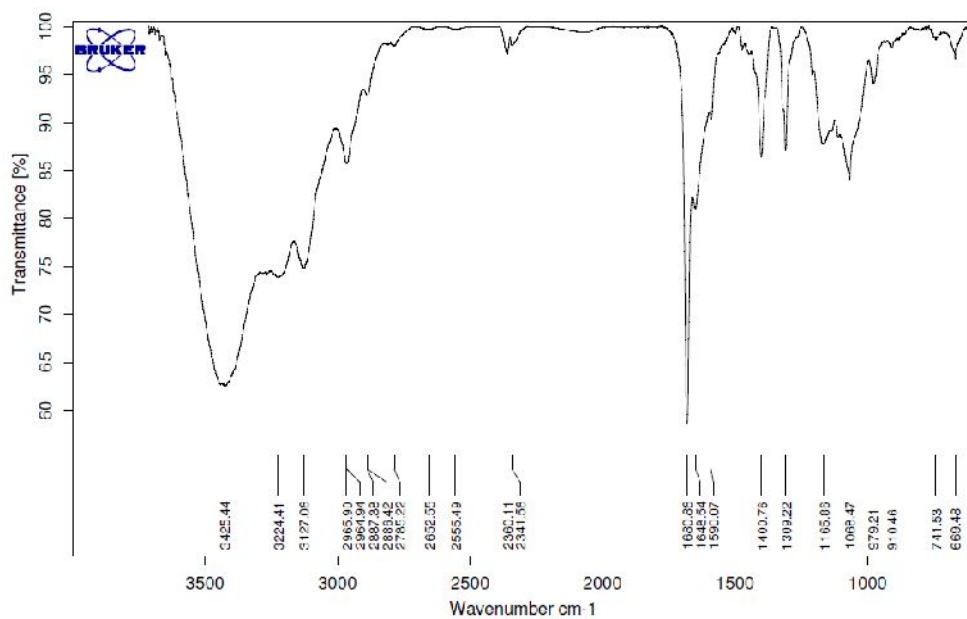
Figure 100 - FTIR spectra of [DBNH]2[ALN]
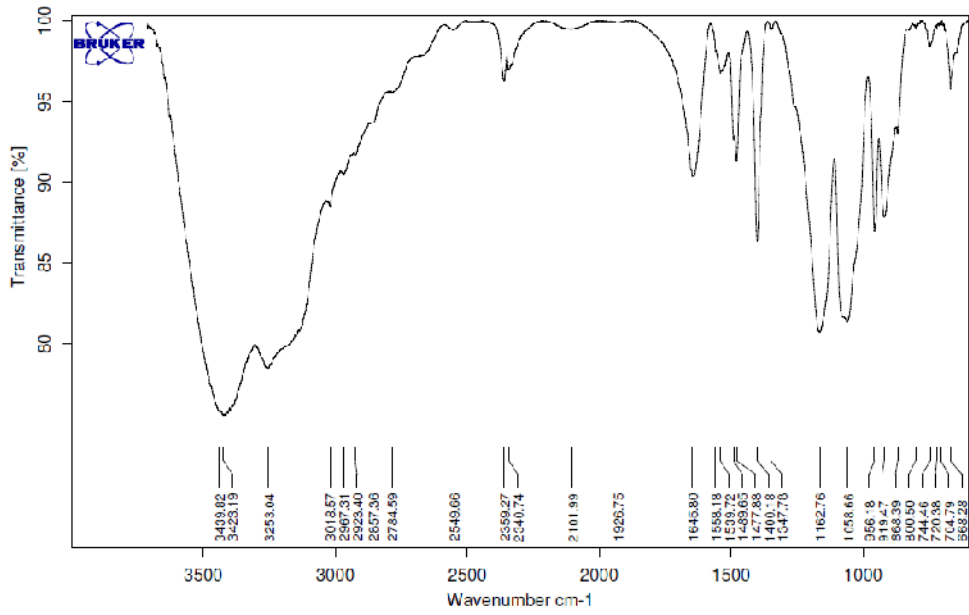
Figure 101 - FTIR spectra of [Ch][ALN]
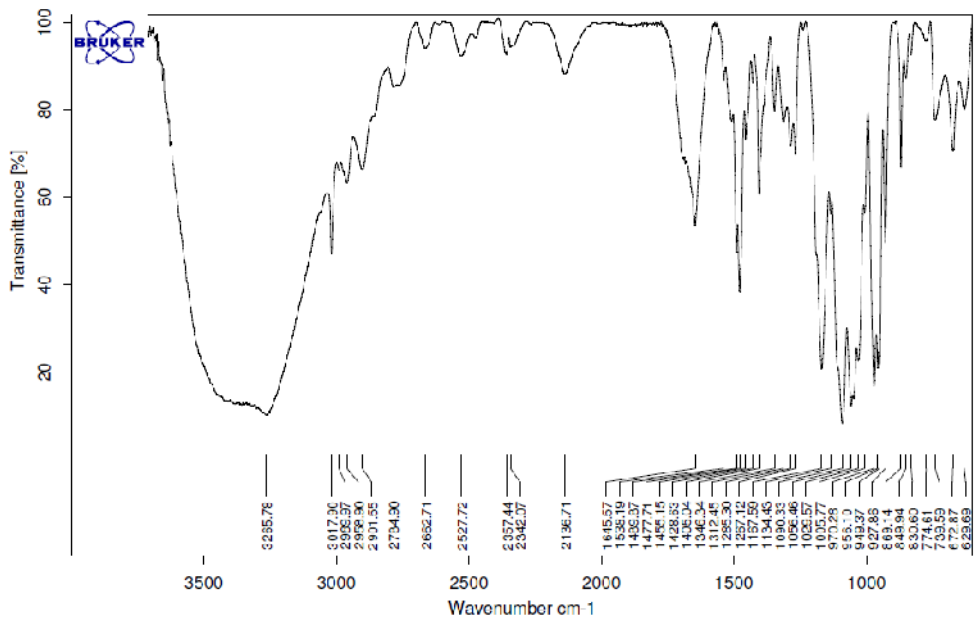
Figure 102 - FTIR spectra of [Ch]2[ALN]
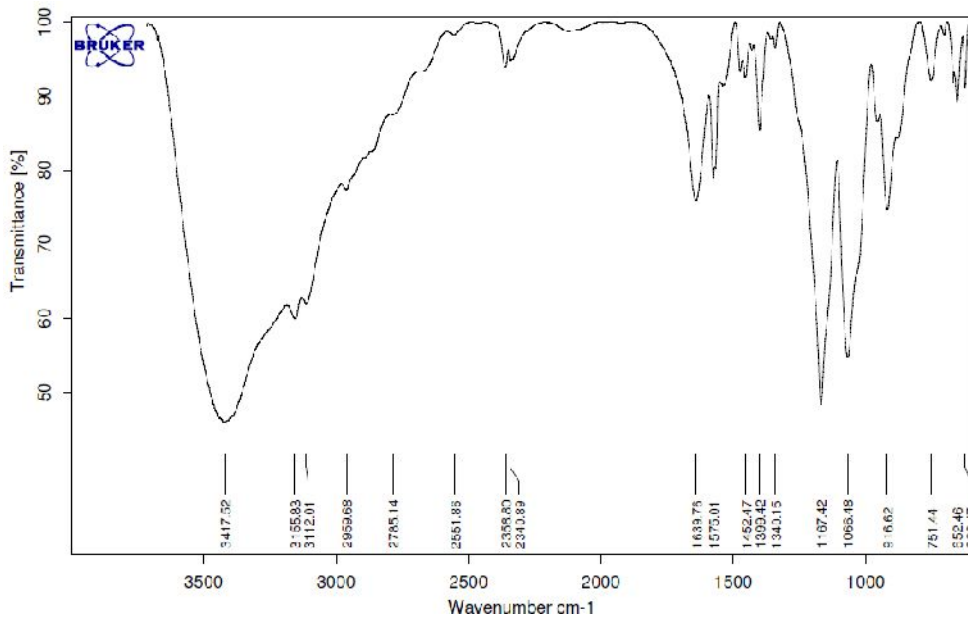
Figure 103 - FTIR spectra of [C2OHMIM][ALN]
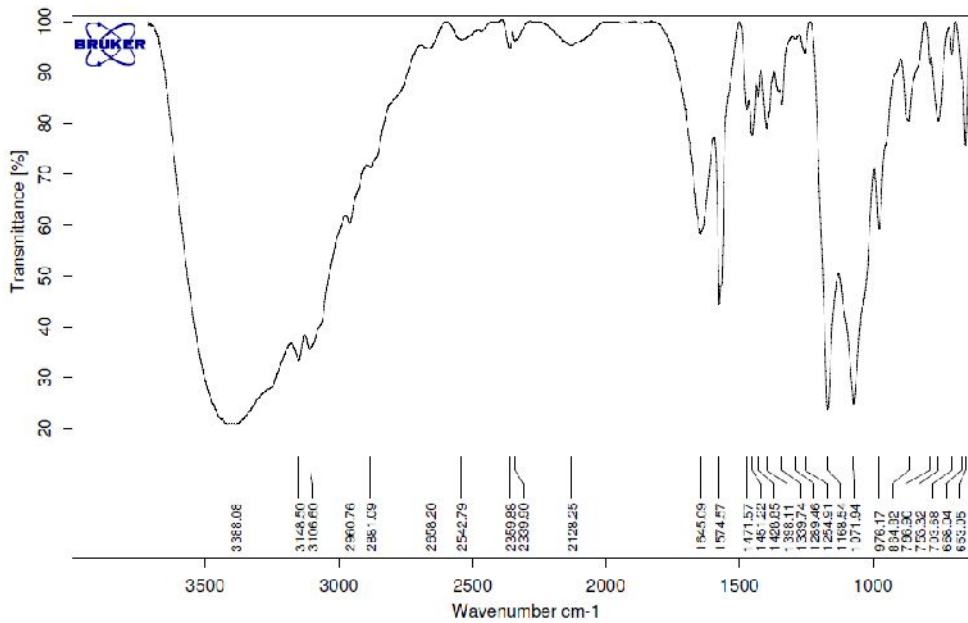
Figure 104 - FTIR spectra of [C2OHMIM]2[ALN]
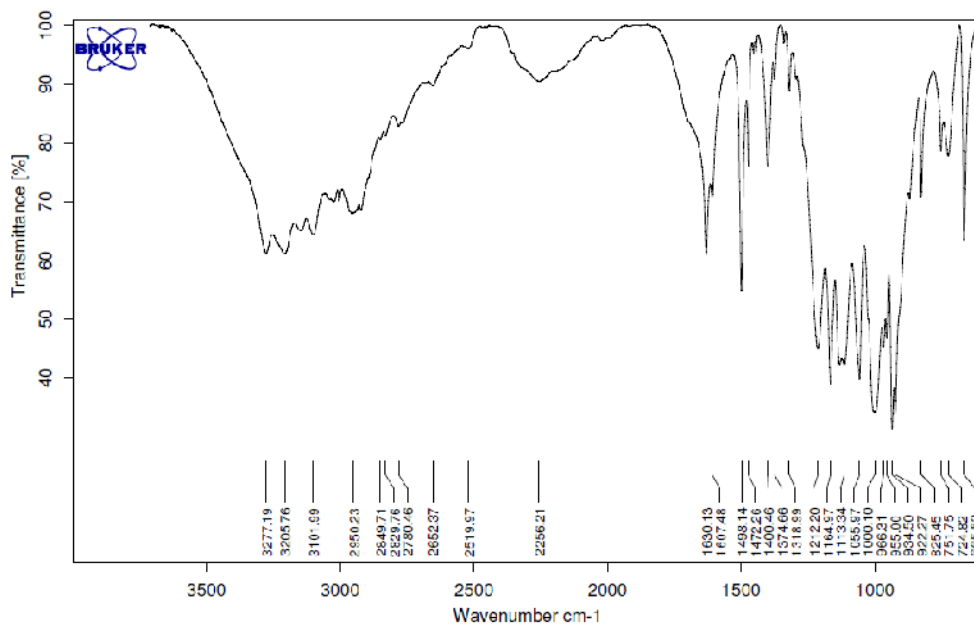
Figure 105 - FTIR spectra of alendronic acid

DSC thermograms of ALN-ILs
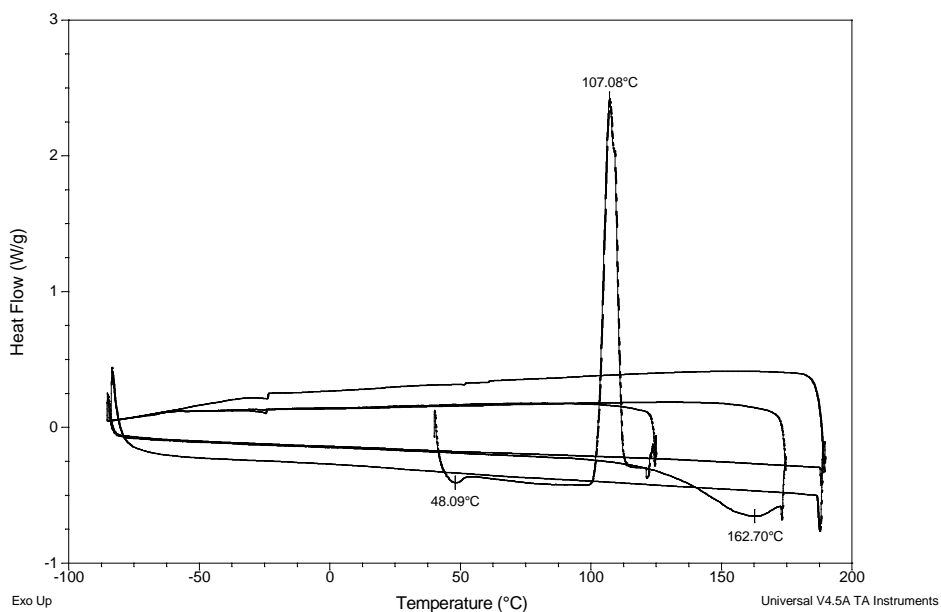
Figure 106 - DSC thermogram of [TMGH][ALN]
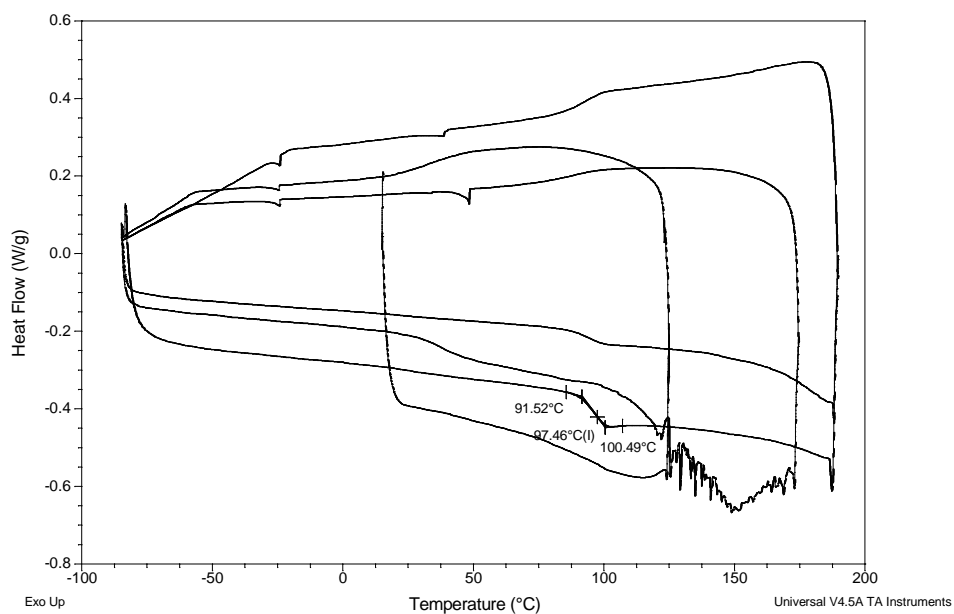
Figure 107 - DSC thermogram of [TMGH]2[ALN]
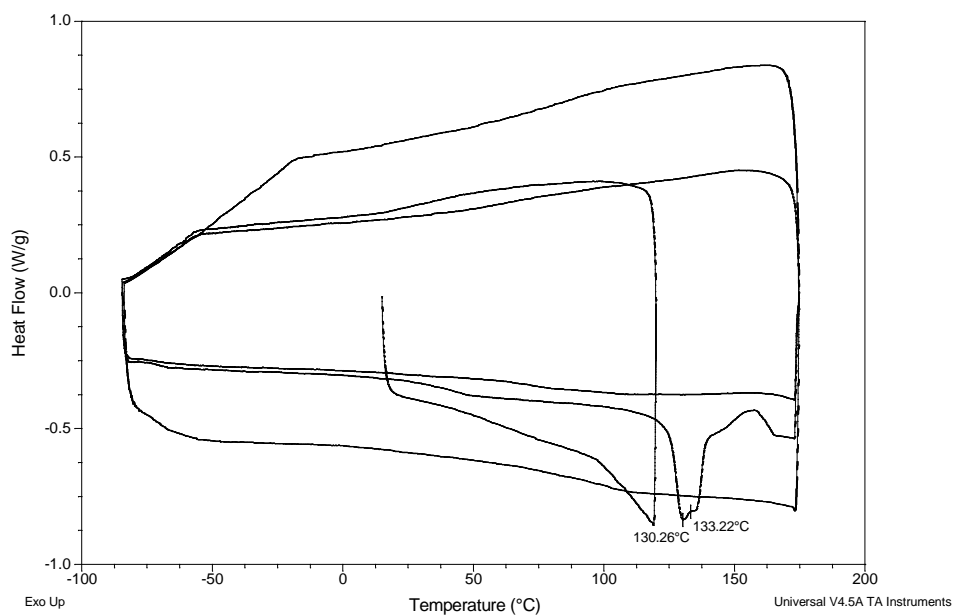
Figure 108 - DSC thermogram of [DBNH][ALN]

117
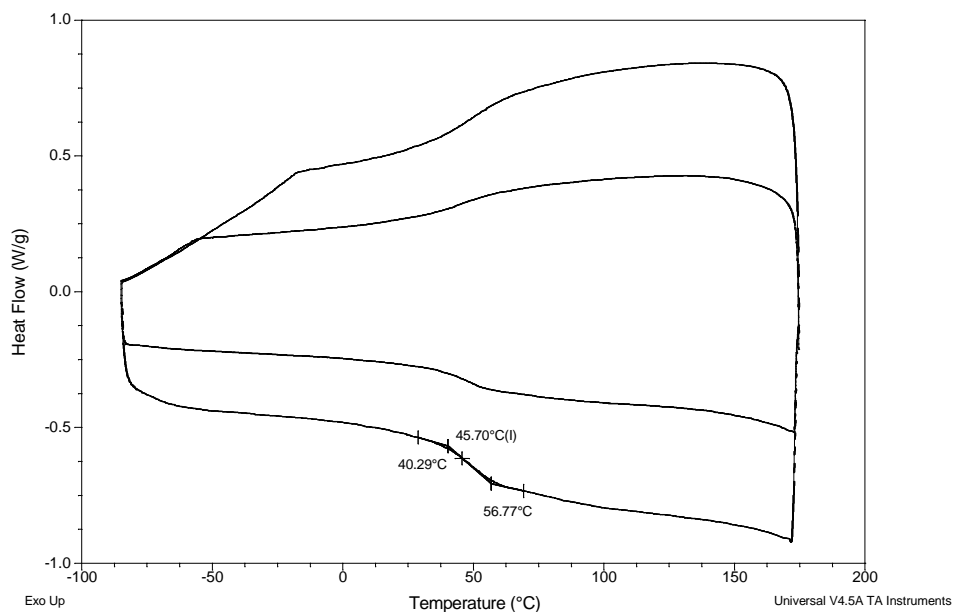
Figure 109 - DSC thermogram of [DBNH]2[ALN]
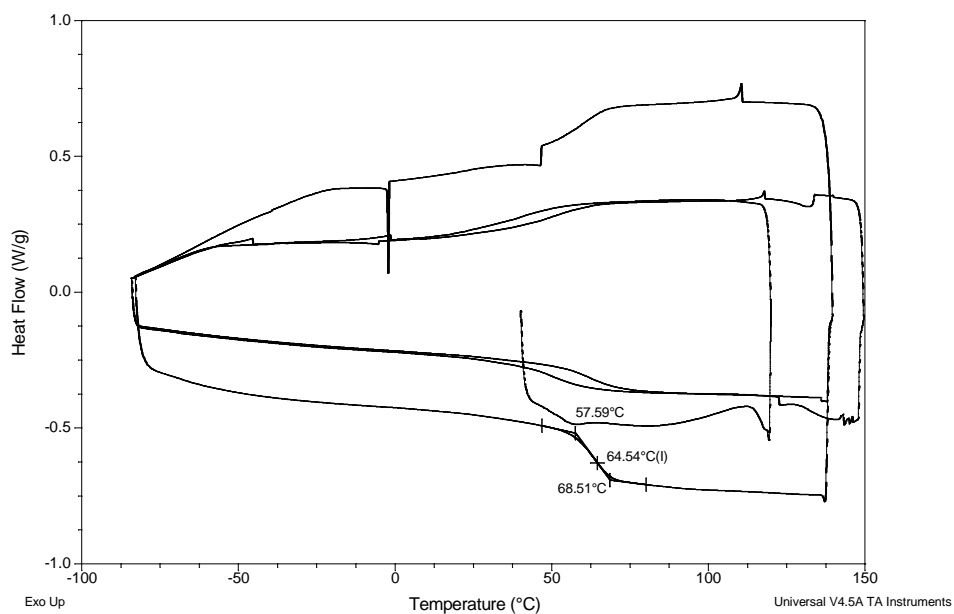
Figure 110 - DSC thermogram of [C2OHMIM][ALN]
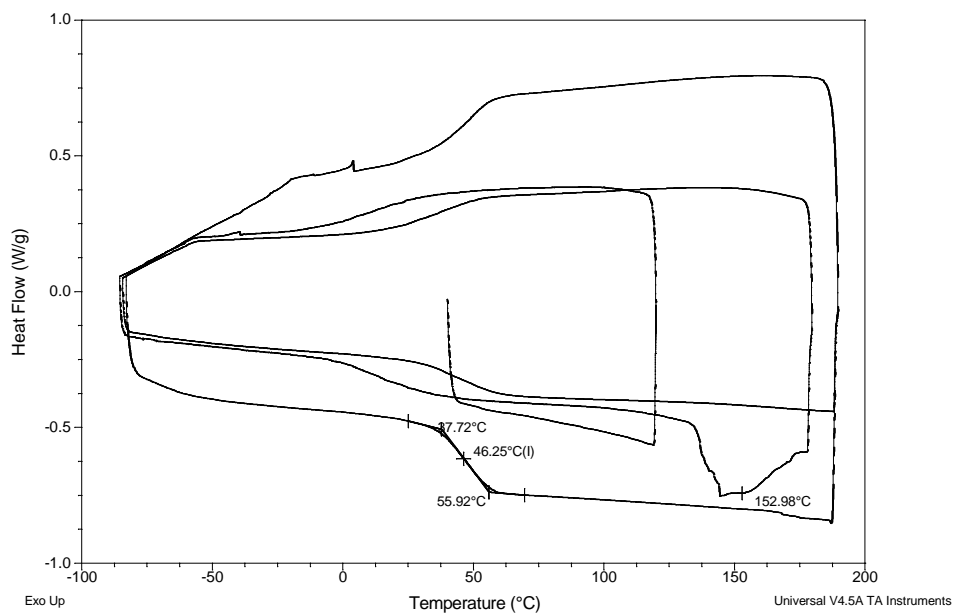
Figure 111 - DSC thermogram of [C2OHMIM]2[ALN]
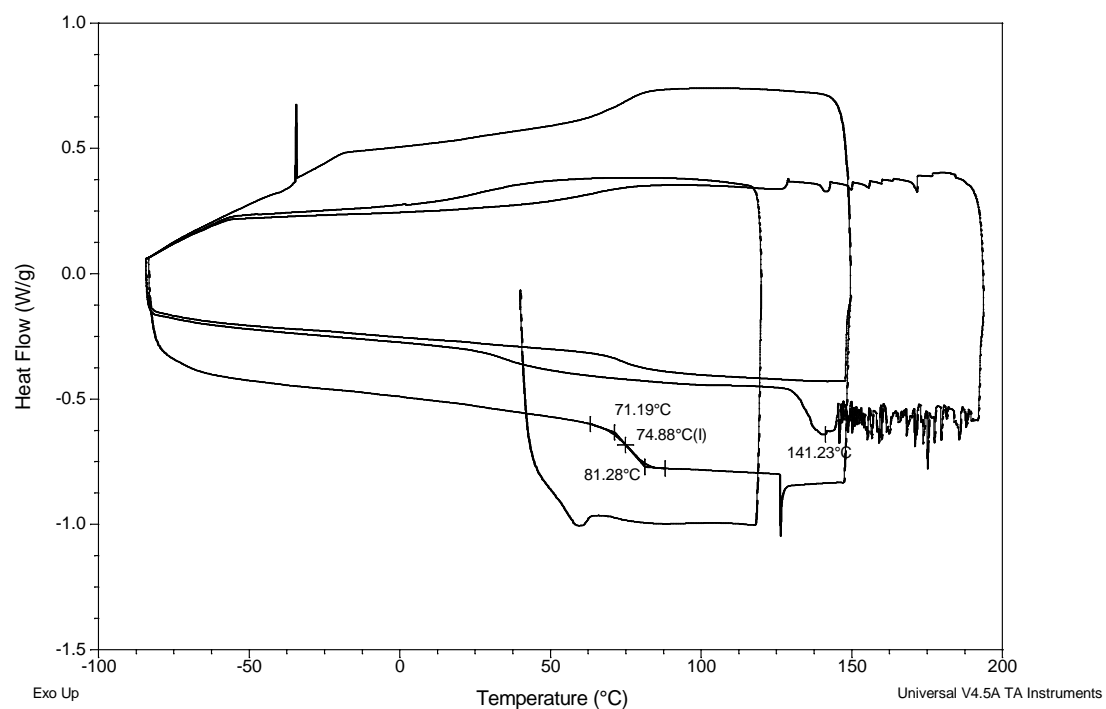
Figure 112 - DSC thermogram of [Ch][ALN]

119
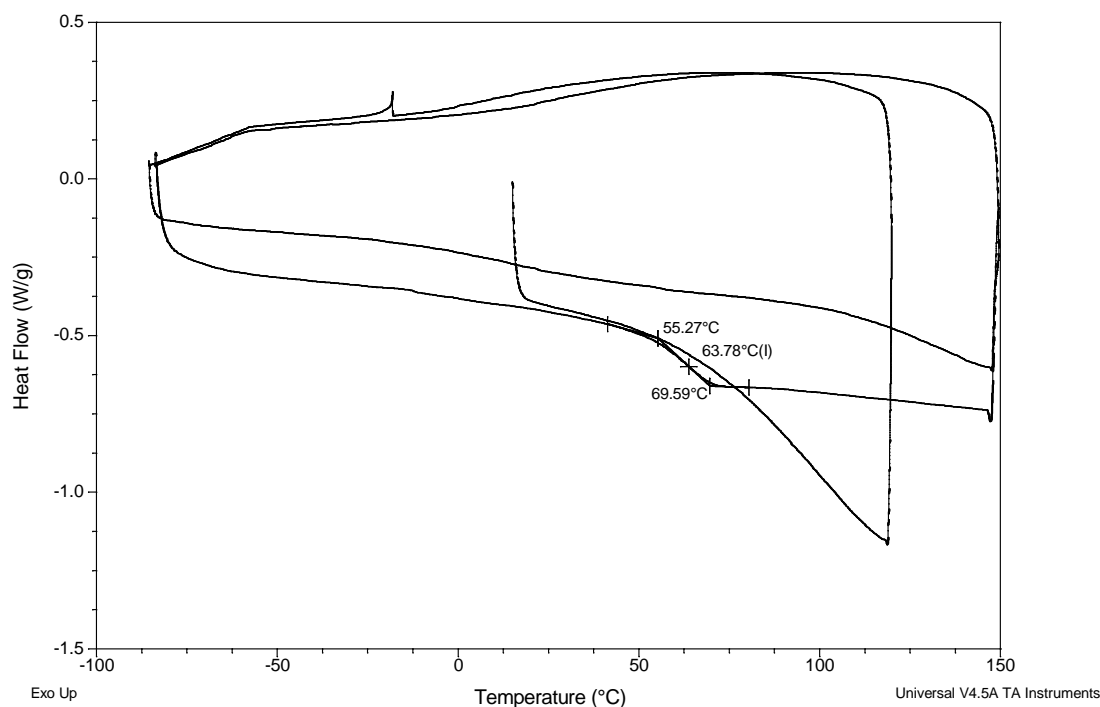
Figure 113 - DSC thermogram of [Ch]2[ALN]

Cytotoxicity studies

The antiproliferative effects of the developed ILs was assessed on different cell types: human gingival fibroblasts (non-neoplastic control), ductal breast epithelial cancer cells (T47D cell line), lung carcinoma cells (A549 cell line) and osteosarcoma cells (MG63 cell line). Cells were seeded at 10^4 cells/cm^2, and maintained in -minimal essential medium (a-MEM) supplemented with 10% fetal bovine serum, 100 IU/mL penicillin, 2.5 μg/mL streptomycin, 2.5 μg/mL amphotericin B, and 50 μg/mL ascorbic acid. After 24 h of incubation, culture medium was renewed and supplemented with the different ALN-containing ILs. Cell cultures were maintained in a 5% CO_2 humidified atmosphere at 37ºC.

Cellular viability/proliferation was evaluated by MTT assay, which relies in the reduction of 3-(4,5-dimethylthiazol-2-yl)-2,5-diphenyltetrazolium bromide to a purple formazan product by viable cells. Half-maximal inhibitory concentration (IC_{50}) values were calculated by means of a nonlinear regression analysis of concentration-effect curves, using GraphPad Prism software (version 2012).

Table 14- Cytotoxicity data for isolated ALN and halide cations used to synthesize the ILs.

| | IC_{50} / mM | | | |
Ions	Skin fibroblast	T47D	A549	MG63
[ALN]	3.17×10^{-2}	4.09×10^{-3}	8.10×10^{-3}	5.55×10^{-4}
[TMGH]Cl	1.47×10^{-3}	1.94×10^{-4}	4.98×10^{-4}	2.46×10^{-4}
[DBNH]Cl	3.80×10^{-5}	2.78×10^{-4}	9.13×10^{-3}	9.79×10^{-8}
[Ch]Cl	a)	a)	5.99×10^{-3}	1.07×10^{-9}
[C$_2$OHMIM]Cl	5.61×10^{-4}	2.22×10^{-3}	7.19×10^{-5}	1.91×10^{-7}

a) Not detected in the tested concentration range.

Chapter 5 - Etidronate-based ionic liquids: in vitro effects on bone metabolism

This chapter contains parts of a submitted article in:

"Etidronate-based ionic liquids: in vitro effects on bone metabolism"

S. Teixeira, M.M. Santos, L.C. Branco, M.H. Fernandes, J. Costa-Rodrigues

5.1 – Introduction

Bone metabolism requires an intricate and well-controlled balance between bone-resorbing activity, mediated by osteoclasts, and bone-synthesizing activity, mediated by osteoblasts (114-116). Osteoclasts promote bone resorption by secreting to bone surface H^+ cations, which erode the mineral component of bone matrix, mainly hydroxyapatite, and also cathepsin K and other proteases to digest organic molecules (117). Bone anabolism starts with the synthesis of extracellular organic matrix, mainly composed by collagen type. After that, hydroxyapatite nanocrystals start to be layed down over collagen fibers (118).

Bisphosphonates are a class of drugs widely used in bone metabolic pathologies with a marked osteolytic activity, like osteoporosis, Paget's disease and bone osteolytic metastasis (13). They were firstly described 40 years ago, being etidronate (Eti) one of the first developed compounds. Bisphosphonates are molecules that display a central carbon atom linked to two phosphate groups (P-C-P) that are responsible for one of their most important properties, their high affinity to bone tissue (119, 120). The accumulation in bone is particularly relevant since bisphosphonates present a low bioavailability. Mainly due to their low bioavailability, a lot of effort has been conducted since mid-90's, to improve their biological properties, giving rise to second- and third-generation Bisphosphonates (119-121). These changes focused on the remaining two positions of the central carbon, which can be occupied by different chemical groups (119, 120).

Ionic Liquids as organic salts with melting point below 100 ºC possess some peculiar properties such as negligible vapor pressure, high thermal and chemical stability and the possibility to tune their physical-chemical properties according the adequate combination of organic cations and anions (62). The third generation of ILs, API-ILs (active pharmaceutical drugs based ionic liquids) have attracted several studies including the drug performance in terms of its stability, solubility, permeability and delivery (122-127).

The present work aimed to develop several Eti-containing ILs, in order to improve not only its chemical properties but also its biological effects. The developed ILs were characterized by ^1H and ^{13}C NMR, and FTIR spectroscopic techniques, as well as elemental analysis. The thermal properties of the synthesized Eti-ILs were determined by Differential Scanning Calorimetry (DSC) techniques. Their cytotoxicity was evaluated on different human cell types; furthermore, their specific effects on bone metabolism were assessed on human osteoclast and osteoblast cells.

5.2 – Materials and methods

5.2.1 – Synthesis

Materials

All acquired reagents were used without further purification. Etidronic acid (ETI, 98.5%) was purchased from Molekula, 1,1,3,3-tetramethylguanidine (TMG, 99%) and 1,5-diazabicyclo(4.3.0)non-5-ene (DBN, 99%). Methanol HPLC grade was acquired from Honeywell and deionized water was processed by Diwer Technologies water max w2 equipment.

General procedure (A) for the synthesis of Eti-ILs:

To a dispersion of etidronic acid (500 mg, 2.43 mmol) in MeOH (15 mL) a methanolic solution of 1.0 or 2.0 molar equivalents of organic superbase (0.5 mmol/mL) was added dropwise under magnetic stirring. After reacting for 1h the solvent was evaporated and the desired product was dried under vacuo for 24 h.

Characterization

The prepared compounds were characterized by ^{1}H and ^{13}C NMR recorded on a Bruker AMX400 spectrometer. Chemical shifts are reported downfield in parts per million considering the solvent residual signal. ^{13}C NMR spectra in D_2O were referenced to added MeOH or MeCN. IR spectra were recorded on a FTIR Bruker Tensor 27 Spectrometer using KBr matrixes. DSC analysis was carried out using a TA Instruments Q-series TM Q2000 DSC with a refrigerated cooling system. Between 2 and 10 mg of salt were crimped into an aluminum standard sample pan with lid which was continuously purged with nitrogen gas at 50 mL/min. The employed procedure was dependent on the melting point of the sample. A typical experiment consisted on a heating step (20 ºC/min) to 80 or 120 ºC (15-20 minutes), cooling (20 ºC/min) to -90 ºC, heating (10 ºC/min) to 200 ºC, cooling (10 ºC/min) to -90 ºC, heating (10 ºC/min) to 200 ºC, cooling (10 ºC/min) to -90 ºC, heating (20 ºC/min) to 200 ºC and cooling (20 ºC/min) to -90 ºC. Glass transition (T_g) and melting (T_m) temperatures were determined in the heating steps.

Experimental data of the synthesized compounds

Preparation of bis(dimethylamino)methaniminium hydrogen (1-hydroxy-1-phosphonoethyl)phosphonate, [TMGH][Eti] (**1**)
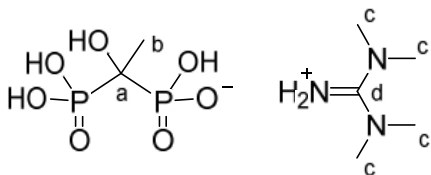
Figure 114 - [TMGH][Eti]

Using tetramethylguanidine (280 mg, 2.43 mmol) [TMGH][ETI] was obtained as a white solid in quantitative yield (779 mg). T_m = 166.6, 189.9 °C, T_g = 38.5 °C; ^{1}H NMR (400.13 MHz, D_2O) 2.93 (s, 12H, c), 1,56 (t, J = 15.6 Hz, 3H, b). ^{13}C NMR (100.62 MHz, D_2O) 162.0 (d), 71.2 (t, J = 144.3 Hz, a), 39.5 (c), 20.0 (b) ppm; FTIR (KBr) 3404, 3357, 3112, 2965, 2817, 2360, 1671, 1649, 1612, 1573, 1408, 1228, 1076, 921 cm^{-1}. Anal. calcd for $C_7H_{21}N_3O_7P_2$: C, 26.17; H, 6.59; N, 13.08; found: C, 27.20; H, 6.94; N, 13.86.

Preparation of bis(bis(dimethylamino)methaniminium) (1-hydroxyethane-1,1-diyl)bis(hydrogen phosphonate), [TMGH]$_2$[Eti] (**2**)
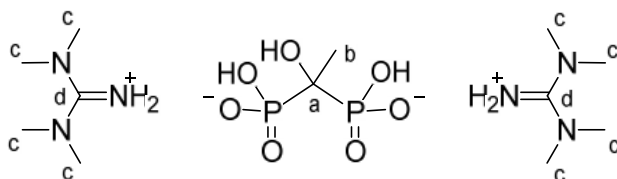
Figure 115 - [TMGH]2[Eti]

Using tetramethylguanidine (559 mg, 4.85 mmol) [TMGH]$_2$[ETI] was obtained as a colorless paste in quantitative yield (1060 mg). ^{1}H NMR (400.13 MHz, D_2O) 2.95 (s, 24H, c), 1.52 (t, J = 15.1 Hz, 3H, b).; ^{13}C NMR (100.62 MHz, DMSO-d^6) 162.0 (d), 71.8 (t, J = 136.0 Hz, a), 39.5 (c), 20.3 (b) ppm; FTIR (KBr) 3282, 3108, 2952, 2910, 2808, 2719, 2360, 2341, 1648, 1609, 1563, 1413, 1169, 1064, 1039, 894 cm^{-1}. Anal. calcd for $C_{14}H51N_7O_{13}P_2 \cdot 6H_2O$: C, 33.03; H, 7.85; N, 19.26; found: C, 33.15; H, 8.14; N, 19.91.

Preparation of 2,3,4,6,7,8-hexahydropyrrolo[1,2-a]pyrimidin-1-ium hydrogen (1-hydroxy-1-phosphonoethyl)phosphonate, [DBNH][Eti] (**3**)
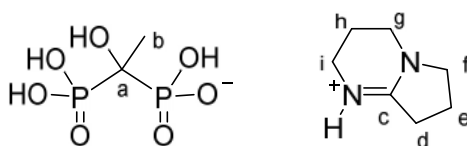
Figure 116 - [DBNH][Eti]

Using 1,5-diazabicyclo(4.3.0)non-5-ene (301 mg, 2.43 mmol) [DBNH][ETI] was obtained as a white solid in quantitative yield (800 mg). T_m = 195.2 °C; T_g = 27.7 °C. ^{1}H NMR (400.13 MHz, D$_2$O)   3.65 (t, J = 7.2 Hz, 2H, i), 3.40 (t, J = 5.6 Hz, 2H, f), 3.35 (t, J = 5.6 Hz, 2H, g), 2.83 (t, J = 8.0 Hz, 2H, d), 2.11 (quint, J = 7.6 Hz, 2H, e), 1.99 (quint, J = 5.8 Hz, 2H, h), 1.57 (t, J = 15.7 Hz, 3H, b). ^{13}C NMR (100.62 MHz, D$_2$O)   165.0 (c), 71.2 (t, J = 143.8 Hz, a), 54.0 (f), 42.8 (g), 38.6 (i), 30.6 (d), 20.0 (b), 18.8, 18.8 (e, h) ppm; FTIR (KBr) 3394, 3238, 3134, 2985, 2894, 2812, 2385, 1680, 1600, 1400, 1311, 1154, 1069, 926 cm^{-1}. Anal. calcd for C$_9$H$_{20}$N$_2$O$_7$P$_2$.2H$_2$O: C, 32.74; H, 6.10; N, 8.48; found: C, 33.63; H, 6.31; N, 8.73.

Preparation of bis(2,3,4,6,7,8-hexahydropyrrolo[1,2-a]pyrimidin-1-ium) (1-hydroxyethane-1,1-diyl)bis(hydrogen phosphonate), [DBNH]$_2$[Eti] (**4**)
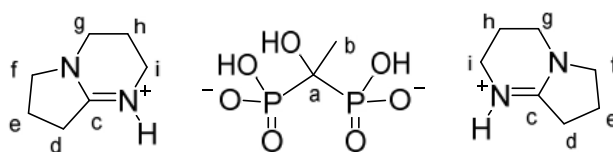
Figure 117 - [DBNH]2[Eti]

Using 1,5-diazabicyclo(4.3.0)non-5-ene (603 mg, 4.85 mmol) [DBNH]$_2$[ETI] was obtained as a colorless paste in quantitative yield (1102 mg). T_g = 0.68 °C; ^{1}H NMR (400.13 MHz, D$_2$O)   3.67 (t, J = 7.2 Hz, 4H, i), 3.42 (t, J = 5.6 Hz, 4H, f), 3.37 (t, J = 5.6 Hz, 4H, g), 2.85 (t, J = 8.0 Hz, 4H, d), 2.13 (quint, J = 7.6 Hz, 4H, e), 2.01 (quint, J = 5.6 Hz, 4H, h), 1.53 (t, J = 15.0 Hz, 3H, b). ^{13}C NMR (100.62 MHz, D$_2$O)   165.0 (c), 71.8 (t, J = 136.3 Hz, a), 54.0 (f), 42.8 (g), 38.6 (i), 30.6 (d), 20.2 (b), 18.8, 18.8 (e, h) ppm; FTIR (KBr) 3419, 3326, 3125, 2961, 2884, 2786, 2355, 2339, 1679, 1588, 1423, 1308, 1174, 1066, 893 cm^{-1}. Anal. calcd for C$_{16}$H$_{32}$N$_4$O$_7$P$_2$.H$_2$O: C, 40.68; H, 7.25; N, 11.86; found: C, 40.06; H, 7.74; N, 11.38.

5.2.2 – Cell cultures

Human gingival fibroblasts (Fibro), used as a non-neoplasic control, human ductal breast epithelial cancer cells (T47D cell line) and human osteosarcoma cells (MG63 cell line) were obtained from ATCC. Cells were cultured in □-MEM supplemented with 10% fetal bovine serum, 100 IU/mL penicillin, 2.5 μg/mL streptomycin, 2.5 μg/mL amphotericin B, and 50 μg/mL ascorbic acid. When reached a confluence of about 70%, cells were detached with 0.05% trypsin + 0.5 mM EDTA and seeded at 10^4 cells/cm^2 in the same

culture medium described before. In the following day, culture medium was renewed and supplemented with Eti, TMGH, DBNH and the different Eti-containing ILs at concentrations of 0.15-15mM. Cell cultures were maintained in a 5% CO_2 humidified atmosphere at 37ºC.

Cell viability/proliferation was evaluated at day 1, and the half-maximal inhibitory concentration (IC50) values were calculated by means of a nonlinear regression analysis of concentration-effect curves, using GraphPad Prism software (version 2012).

Osteoclastic cells

Human peripheral blood mononuclear cells (PBMC), used as osteoclastic precursors, were isolated from the blood of healthy donors with 25–35 years old, as described previously [128]. Briefly, blood was diluted with PBS + 2mM EDTA (1:1), and applied on top of Ficoll-Paque^{TM} PREMIUM (GE Healthcare Bio-Sciences). After centrifugation at 400g for 30 min, PBMC were collected, washed twice with PBS + 2mM EDTA and counted with a cytometer (Celltac MEK-5103).

Cells were seeded at $1.5x10^6$ cells/cm^2 in -MEM supplemented with 30% autologous human serum, 100 IU/ml penicillin, 2.5 µg/ml streptomycin, 2.5 µg/ml amphotericin B and 2 mM L-glutamine. Cell cultures were maintained for 21 days in a 5% CO_2 humidified atmosphere at 37 ºC, and culture medium was replaced once a week.

After overnight cell attachment, PBMC were treated with different concentrations (10^{-5}-10^{-1}mM) of Eti and the Eti-containing ILs. The tested concentration range was selected in order to include the plasma levels normally achieved following the therapeutic usage of etidronate [129]. In parallel, the isolated compounds used to synthesize the ILs (TMGH and DBNH) were also included in the experimental procedure. Cell cultures were also supplemented with the osteoclastogenic enhancers M-CSF (25 ng/mL) and RANKL (40 ng/mL) [123]. The ILs and the pro-osteoclastogenic growth factors were renewed at each medium change.

Cultures were assessed at days 7, 14 and 21 for total protein content and TRAP activity. Cultures treated with the minimum tested concentration of each IL that caused a significant effect in osteoclastic response (Eti(TMGH)$_2$, Eti(DBNH) and Eti(DBNH)$_2$: 10^{-3}mM; Eti and Eti(TMGH): 10^{-2}mM; TMGH and DBNH: 10^{-1}mM), were characterized for apoptosis, the expression of osteoclastic genes and for the involvement of several intracellular pathways on cell behavior.

Osteoblastic cells

Human mesenchymal stem cells derived from bone marrow (HMSC, Innoprot, Bizkaia, Spain), were used as osteoblastic precursors. Cells were cultured in -MEM

supplemented with 10% foetal bovine serum, 100 IU/ml penicillin, 2.5 µg/ml streptomycin, 2.5 µg/ml amphotericin B and 50 µg/mL ascorbic acid. Cells were detached with 0.05% trypsin + 0.5 mM EDTA after reaching ~70% confluence. HMSC were seeded at 3.3×10^3 cells/cm^2 and maintained for 21 days in the same culture medium, in a 5% CO_2 humidified atmosphere at 37 ºC. Culture medium was replaced once a week.

After cell attachment of 24h, cell cultures were exposed to different concentrations of the Eti-ILs (10^{-5}-10^{-1}mM), as well as the pro-osteogenic molecule dexamethasone (10 nM) (130). Both the ILs and the dexamethasone were renewed at each medium change. Cultures were assessed at days 7, 14 and 21 for total protein content and ALP activity.

Furthermore, HMSC were treated with the minimum tested concentration of each IL that elicited a significant effect in osteoblastogenesis (10^{-3}mM for all the tested compounds, except for Eti(TMGH)$_2$ and Eti(DBNH)$_2$, which were used at 10^{-4}mM), and were characterized for apoptosis, the expression of osteoblastic genes and for the involvement of several intracellular pathways on cell behavior.

5.2.3 – Characterization of cellular responses

Cell viability/proliferation

Cell viability/proliferation was assessed by MTT method. Shortly, cells were incubated for 3h at 37 ºC with tetrazolium salt MTT [3-(4,5-dimethylthiazol-2-yl)-2,5-diphenyltetrazolium bromide]. Following, the product of the reaction was solubilized with DMSO and the absorbance was measured at 550 nm on a microplate reader (Synergy HT, Biotek).

Total protein content

Protein quantification was performed by Bradford's method (131), using bovine serum albumin as a standard. Briefly, cells were washed twice with PBS and solubilized with 0.1M NaOH. Then, Coomassie Protein Assay Reagent was added and the samples were incubated for 2 min at room temperature. The absorbance was quantified at 695nm in an ELISA plate reader (Synergy HT, Biotek).

Tartrate-resistant acid phosphatase (TRAP) and alkaline phosphatase (ALP) activities

TRAP and ALP activities were evaluated by the *para*-nitrophenilphosphate (*p*NPP) hydrolysis assay. Cells were washed twice with PBS, and solubilized with 0.1% (V/V) Triton X-100. For TRAP activity measurement, cellular extracts were incubated at 37ºC

(30 min) with 12.5 mM *p*NPP prepared in 0.04 M tartaric acid and 0.09 M citrate (pH 4.8); for ALP activity quantification, cellular extracts were incubated at 37ºC (30 min) with 12.5 mM *p*NPP in bicarbonate buffer solution, pH 10.3. After incubation, the reaction was stopped with 5 M NaOH and the absorbance of the samples was measured at 400 nm in an ELISA plate reader (Synergy HT, Biotek). TRAP and ALP activities were normalized with total protein and results are expressed as $nmol/min.\mu g_{protein}^{-1}$.

Apoptosis quantification.

Cells were washed twice with PBS and caspase-3 activity was quantified with EnzCheck® Caspase-3 Assay Kit #2 (Molecular Probes, Eugene, USA), according to manufacturer's instructions. Fluorescence was measured at 496/520 nm (excitation/emission) in an ELISA plate reader (Synergy HT, Biotek). Results obtained in each experimental condition were normalized with the value obtained in the corresponding control (absence of any IL). Results are expressed as a % of response compared to the control.

Osteoclast and osteoblast gene expression.

Gene expression was analyzed by quantitative real-time PCR (qPCR). The tested housekeeping genes were beta-glucuronidase (GUSB) and proteasome subunit beta type-6 (PSMB6). The osteoclast-related genes were TRAP, cathepsin K (CATK) and carbonic anhydrase 2 (CA2) (126) and the osteoblast-related genes were collagen type 1 (COL1), ALP and bone morphogenetic protein 2 (BMP2) (118). RNA was isolated with RNeasy® Mini Kit (QIAGEN) according to manufacturer's instructions. cDNA synthesis was performed by reverse transcription with DyNAmo cDNA synthesis kit (Finnzymes, Finland) and random hexamers according to the manufacturer's instructions. Two ng of each cDNA sample was amplified with a DyNAmo Flash SYBR green qPCR kit (Finnzymes) on a Rotor-Gene thermocycler (Qiagen). The annealing temperature was 55 ºC and the extension time was 15 seconds. The primers used are listed in Table 1. The values obtained were normalized with the results obtained for the two tested housekeeping genes.

Intracellular signalling pathways.

The ability of Eti-ILs to interfere with several signalling pathways involved either in osteoclastogenesis (127, 132) and osteoblastogenesis (118, 133) was determined. PBMC and HMSC cultures were supplemented with the minimum concentration of each IL that elicited a significant response on each cell type. In addition, cells were further treated with commercial signalling pathway inhibitors (which were renewed at each medium change).

The tested pathways were: MEK (inhibitor U0126, 1 µM), NFkB (inhibitor PDTC, 10 µM), PKC (inhibitor GO6983, 5 µM) and JNK (inhibitor SP600125, 10 µM). Cultures were assessed for TRAP (PBMC cultures) and ALP (HMSC cultures) activities.

5.2.4 – Statistical analysis

Data presented in this work are the means of three independent experiments. Statistical differences were assessed using an unpaired Student's t-test with Bonferroni correction for multiple comparisons. All data are presented as the mean ± standard deviation\error. For values of $p \leq 0.05$, differences were considered statistically significant.

5.3 – Results
5.3.1 – Synthesis and characterization of Etidronate-containing ILs

Four novel etidronate-containing ionic liquids (Eti-ILs) were prepared by mixing 1 or 2 equivalents of organic superbases, more specifically 1,1,3,3-tetramethylguanidine (TMG) and 1,5-diazabicyclo(4.3.0)non-5-ene (DBN), with etidronic acid in methanol (Scheme 3).
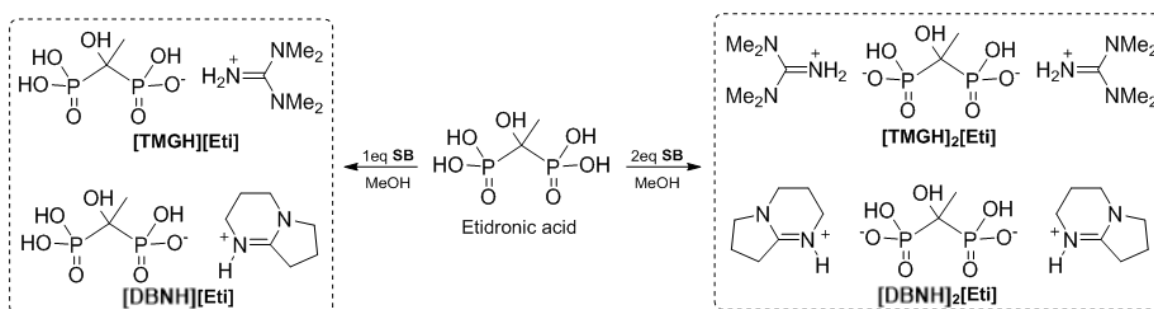
Scheme 3 - Synthetic methodology for the synthesis of Eti-ILs using organic superbases (SB).

This straightforward synthetic methodology produced two monoanionic and two dianionic Eti-ILs by proton transfer from one or the two phosphonate groups to the imine functional group of the superbases. The ^{1}H and ^{13}C NMR spectra obtained upon drying of the samples revealed that the reactions reached completion, as only one set of signals was present, and the cation-anion stoichiometry was stricktly in agreement with the intended. On the other hand, the presence of anionic phosphonate groups was observed

in the collected FTIR spectra, more specifically by changes in the 2500-2100 cm^{-1} (O–H bond stretch) and 1200-900 cm^{-1} (P=O and P–OH bonds stretch) regions.

Both dianionic compounds are Room Temperature Ionic Liquids (RTIL), while the monoanionic compounds were obtained as protic organic solid salts. Differential Scanning Calorimetry techniques were employed to determine the thermal properties of the synthesized Eti-ILs, and the data obtained is presented in Table 15.

Table 15 - Physical state, melting (Tm) and glass transition (Tg) temperatures of the Eti-ILs

Salt	Physical state	T_m/°C	T_g/°C
[TMGH][Eti]	White solid	166.6 189.9	38.5
[TMGH]$_2$[Eti]	Colorless paste	-	-
[DBNH][Eti]	White solid	195.2	27.7
[DBNH]$_2$[Eti]	Colorless paste	-	0.68

Through DSC it was possible to determine the melting temperatures of both monoanionic compounds. Curiously, [TMGH][Eti] showed two distinct endothermic peaks at 166.6 °C and 189.9 °C in the first heating cycle suggesting that this salt was obtained in different crystalline states. However, in the following heating/cooling cycles no crystallization peaks were observed and, in addition, glass transitions were determined, meaning that they become amorphous upon first melt. One glass transition temperature was also determined for [DBNH]$_2$[Eti], in agreement with the amorphous state of RTILs.

5.3.2 – Cytotoxicity of Eti-ILs

The cytotoxic potential of Eti-containing ILs was evaluated in one non-neoplastic cell type (human gingival fibroblasts) and two neoplastic cell lines (T47D and MG63). Cell viability/proliferation was determined and the observed cell response was used to calculate the IC50 values of each of the tested compound (Table 16).

Table 16 - Cytotoxic of Eti-containing ILs

Added molecule	IC50 / mM		
	Fibroblasts	**T47D**	**MG63**
Eti	15.6	48.9	61.1
TMGH	1.5×10^{-3}	1.9×10^{-4}	2.5×10^{-4}
DBNH	3.8×10^{-5}	2.8×10^{-4}	9.8×10^{-5}
Eti(TMGH)	a)	2.7×10^{-7}	1.6
Eti(TMGH)$_2$	1.4×10^{-3}	9.1×10^{-4}	12.0
Eti(DBNH)	11.4	9.3×10^{-4}	2.0×10^{-3}
Eti(DBNH)$_2$	18.6	a)	2.0×10^{-3}

a)   Not determined in the tested concentration range.

It was observed that etidronate appeared to be more cytotoxic to fibroblasts than to T47D and A549 cells. Comparatively, [TMGH]Cl and [DBNH]Cl displayed a significantly higher cytotoxicity for all the tested cell types. T47D cell line appeared to be particularly sensitive to [TMGH][Eti] and [TMGH]$_2$[Eti], while MG63 revealed the opposite behavior (even less sensitive than fibroblasts). Regarding [DBNH][Eti] and [DBNH]$_2$[Eti] their cytotoxicity was similar to Eti in fibroblastic cell cultures, but it was higher in T47D and MG63 cell lines.

5.3.3 – Modulation of osteoclastogenesis by Eti-ILs

PBMC cultures were supplemented with a wide range of concentrations of the different ILs, and total protein content (Fig. 118A) and TRAP activity (Fig. 118B) was assessed at days 7, 14 and 21.
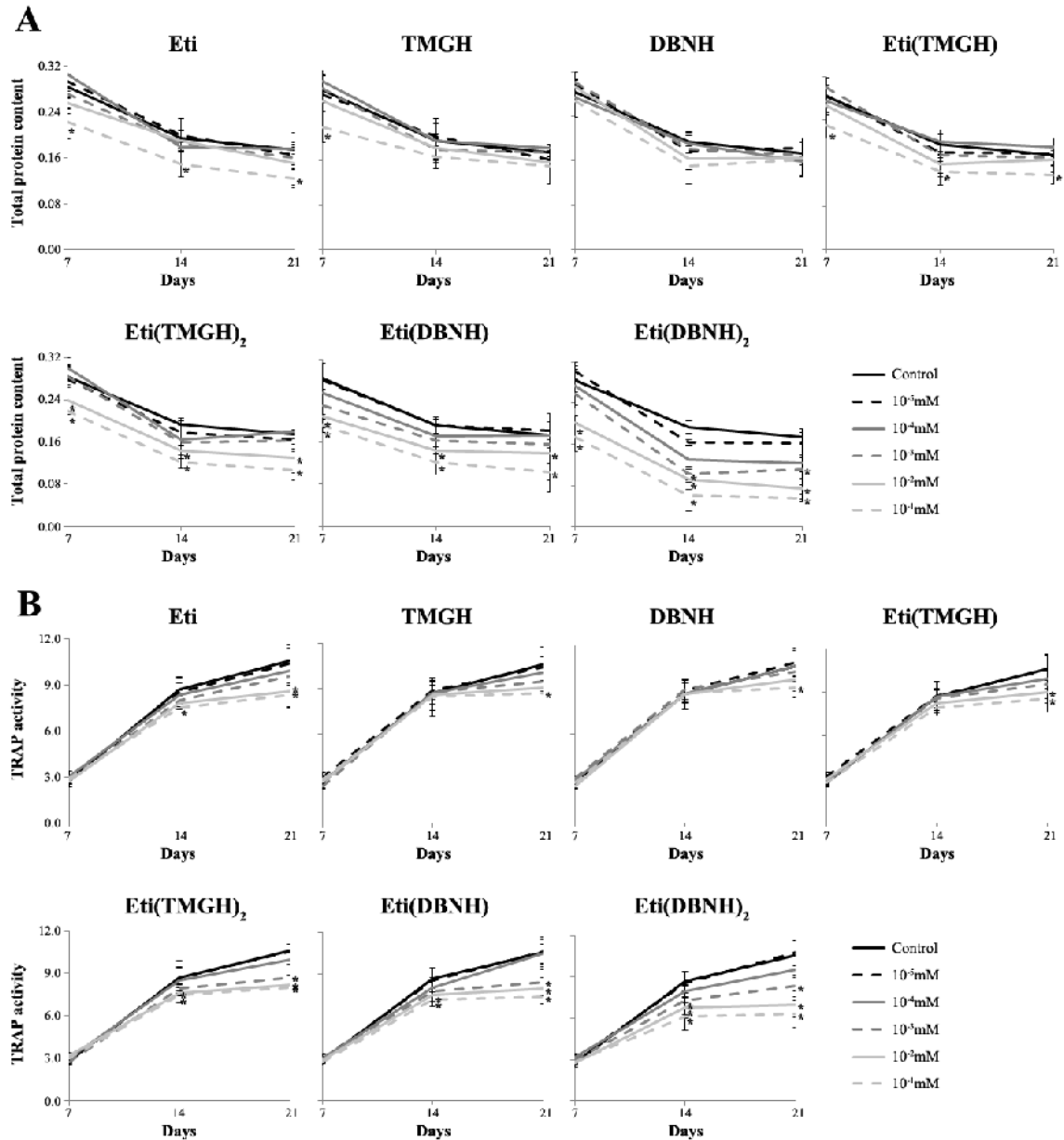
Figure 118 – Dose-response curves of PBMC cultures treated with Eti-ILs. A – Total protein content. B – TRAP activity. *Significantly different from the control

Globally, total protein content decreased with the increase in the culture period. The presence of [TMGH]Cl and [DBNH]Cl did not affect cell response. On the other hand, Eti and [TMGH][Eti] caused a significant decrease in protein content of cell cultures, when present at 10^{-1}mM (~21-29%). A similar behavior was observed in the presence of the remaining ILs, although in these cases the decrease (~20-36%) was observed even at lower concentrations (10^{-2}mM for [TMGH]$_2$[Eti] and [DBNH][Eti]; 10^{-3}mM for [DBNH]$_2$[Eti]. Considering TRAP activity, cell response increased during the 21 days of culture. [TMGH]Cl and [DBNH]Cl elicited a significant decrease (~14-18%) only when present at 10^{-1}mM, while Eti and [TMGH][Eti] appeared to inhibit TRAP activity (~15-19%) since 10^{-}

^{2}mM. Finally, cultures supplemented with [TMGH]$_2$[Eti], [DBNH][Eti] and [DBNH]$_2$[Eti] revealed lower enzyme activity values (~19-22%) for concentrations 10^{-3}mM.

Having established the dose-response curves for the Eti-ILs, their effects on apoptosis (Fig. 119A) and on gene expression (Fig. 119B) were evaluated. The tested concentrations were: [TMGH]$_2$[Eti], [DBNH][Eti] and [DBNH]$_2$[Eti] – 10^{-3}mM; Eti and [TMGH][Eti] – 10^{-2}mM; [TMGH]Cl and [DBNH]Cl – 10^{-1}mM. Furthermore, the modulation of several intracellular signaling pathways was also investigated (Fig. 119C).
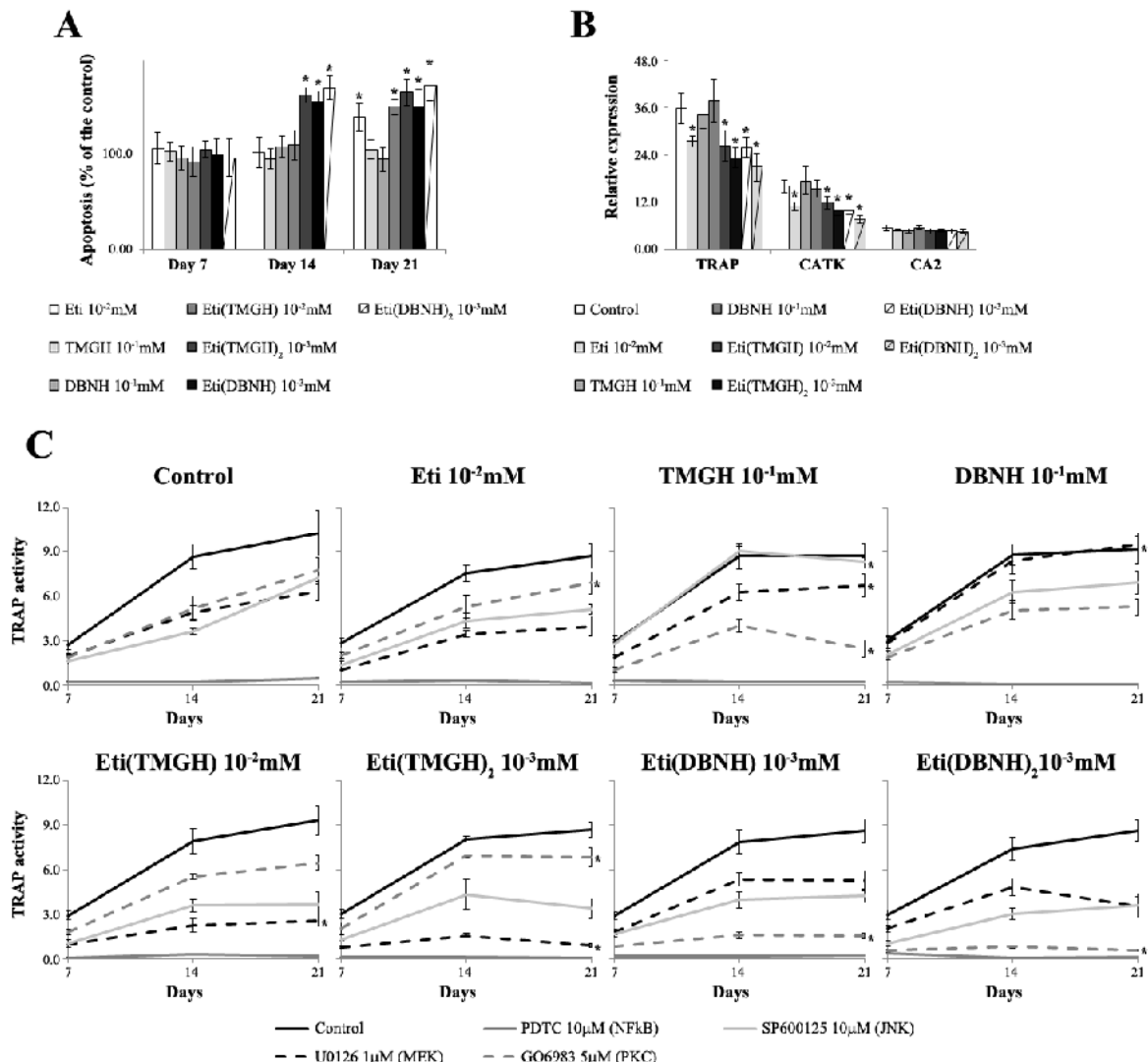
Figure 119 - Effects of Eti-ILs on PBMC cultures. A – Apoptosis. B – Expression of osteoclast-related genes. C – Modulation of MEK, NFkB, PKC and JNK signalling pathways. Cell response was evaluated by TRAP activity. *Significantly different from the control.

[TMGH]Cl and [DBNH]Cl did not promote any significant effect on caspase-3 activity. However, the remaining tested compounds caused an increase on apoptosis, particularly [TMGH]$_2$[Eti] and [DBNH]$_2$[Eti], with an increase of about 65% and 72% at day

21, respectively. Regarding gene expression, TRAP and CATK were less expressed in the presence of [TMGH]$_2$[Eti] and [DBNH]$_2$[Eti] (~35-41% for TRAP and ~48-51% for CATK), followed by Eti, [TMGH][Eti] and [DBNH][Eti] (~14-28% for TRAP and ~25-38% for CATK); isolated [TMGH]Cl and [DBNH]Cl did not affect cell response. CA2 expression was similar in all experimental conditions. Considering the intracellular mechanisms, it was observed that in the control condition all the tested inhibitors promoted a significant decrease in TRAP activity, being almost total in the presence of PDTC. The inhibition associated with U0126 was lower in the presence of [TMGH]Cl and [DBNH]Cl (in this case it did not cause any significant inhibition), and higher in the presence of [TMGH][Eti] and [TMGH]$_2$[Eti]. GO6983 inhibitory effect was decreased in cell cultures supplemented with Eti and [TMGH]$_2$[Eti], while an opposite situation was observed with [DBNH][Eti] and [DBNH]$_2$[Eti]. Finally, SP600125 did not affect TRAP activity in [TMGH]Cl-treated cell cultures.

5.3.4 – Modulation of osteoblastogenesis by Eti-ILs

The effects of Eti-containing ILs on osteoblastogenesis were evaluated using HMSC as precursor cells. Dose response curves for total protein content (Fig. 120) and ALP activity (Fig. 121) were established.
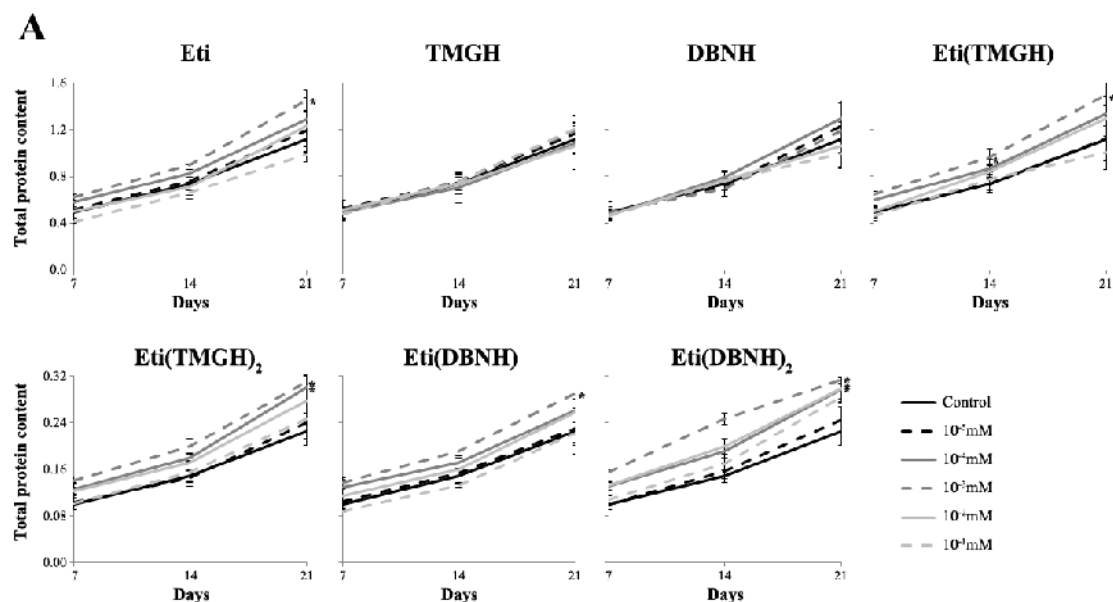
Figure 120 - Dose-response curves of HMSC cultures treated with Eti-ILs. A – Total protein content.
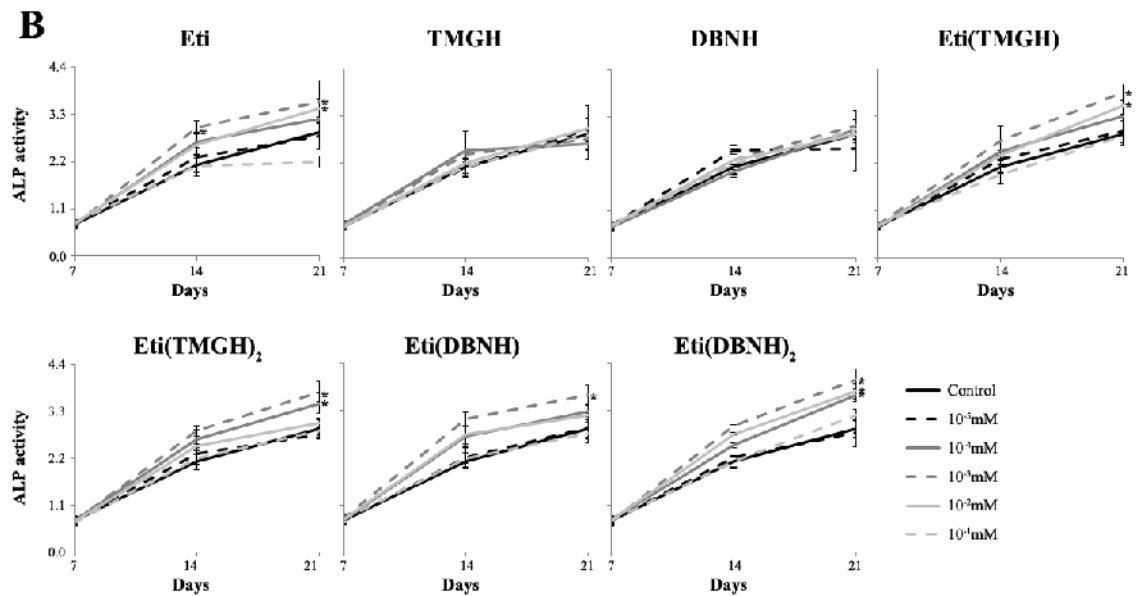
Figure 121 - Dose-response curves of HMSC cultures treated with Eti-ILs. B – ALP activity.
*Significantly different from the control.

HMSC cultures revealed an increase on total protein content over culture period. The presence of Eti, [TMGH][Eti] and [DBNH][Eti] at 10^{-3}mM caused a significant increase on cell response (~29-34%); in cultures supplemented with [TMGH]$_2$[Eti] and [DBNH]$_2$[Eti] the increase was also observed at 10^{-4}mM (~32-34%). [TMGH]Cl and [DBNH]Cl did not affect cell behavior. Regarding ALP activity, once again [TMGH]Cl and [DBNH]Cl did not elicit any significant effect. Supplementation with Eti and [TMGH][Eti] at 10^{-3}mM and 10^{-2}mM increased cell response (~22~33%). An increase in ALP activity was also observed in the presence of 10^{-3}mM [DBNH][Eti] (~27%) and 10^{-4}mM and 10^{-3}mM [TMGH]$_2$[Eti] and [DBNH]$_2$[Eti] (~21-39%).

After the characterization of the dose-dependent effects of the Eti-ILs on HMSC cultures, cell behavior was further analyzed regarding apoptosis (Fig. 122A), osteoblast-related gene expression (Fig. 122B) and modulation of several intracellular pathways involved in osteoblastogenesis (Fig. 122C). The following concentrations were used for these analyses: 10^{-3}mM for all the tested compounds, except for [TMGH]$_2$[Eti] and [DBNH]$_2$[Eti], which were used at 10^{-4}mM.
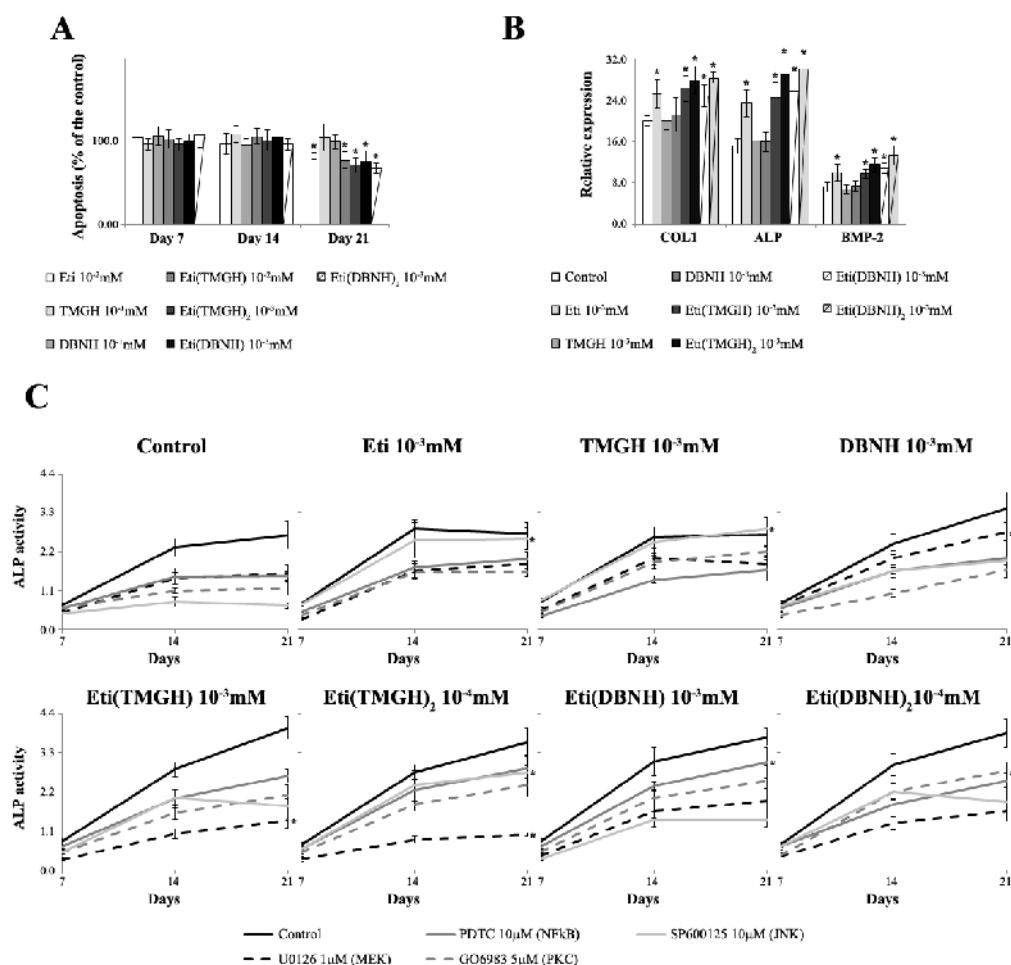
Figure 122 - Effects of Eti-ILs on HMSC cultures. A – Apoptosis. B – Expression of osteoblast-related genes. C – Modulation of MEK, NFkB, PKC and JNK signalling pathways. Cell response was evaluated by ALP activity. *Significantly different from the control.

All the tested compounds, except isolated [TMGH]Cl and [DBNH]Cl, promoted a significant decrease on apoptosis (~18-33%); this effect was only observed at day 21. Considering gene expression, the same set of tested compounds elicited a significant increase in all the analyzed genes, namely, COL1 (~24-42%), ALP (~56-93%) and BMP-2 (~35-84%). Both in apoptosis and in gene-expression evaluation, the highest effects were observed in the presence of [DBNH]$_2$[Eti], followed by [TMGH]$_2$[Eti]. Regarding the modulation of signaling pathways by the Eti-ILs, it was observed that in the absence of any compound, all the tested inhibitors elicited a decrease in ALP activity. The inhibitory profile of U0126 was potentiated by [TMGH][Eti] and [TMGH]$_2$[Eti], while an opposite behavior was observed in the presence of [DBNH]Cl. PDTC-induced decrease on ALP activity was lower in cell-cultures supplemented with [DBNH][Eti]; a similar situation was observed for GO6983 in the presence of [DBNH]$_2$[Eti]. Finally, the inhibitory effect of SP600125 was abolished by Eti and [TMGH]Cl, and significantly diminished by [TMGH]$_2$[Eti].

5.4 – Discussion

In the first half of the 40-year bisphosphonate life, there were important technical limitations that impaired a more accurate improvement in bisphosphonate composition and structure. Nowadays, this represents a very promising field, aiming to create new bisphosphonate molecules with better chemical and biological properties. The central carbon atom on P-C-P bisphosphonate core has been modified (either in one or in the two lateral chains, called R1 and R2) in the last decades, giving rise to different generations of Bisphosphonates (121). Small changes in those R groups are associated to profound differences in bisphosphonate physicochemical and biological characteristics. One of the most significant chemical modifications performed on bisphosphonates was the introduction of a lateral chain with at least one nitrogen atom, which was responsible for a dramatic increase in their inhibitory effects on bone resorption (119-121). Bisphosphonates with this kind of change acquired a new intracellular target, namely, the mevalonate pathway, which proved to be extremely important for their biological effects (120). It is undeniable that bisphosphonate utilization in clinical practice has a profound impact in bone disorders management, particularly those associated to a higher catabolic state, such as osteoporosis, Paget's disease and osteolytic metastases (121, 134, 135). Moreover, it is becoming now clear that at least theoretically, some of the developed drugs may also be effective in other clinical contexts, namely, in some types of cancer, immunomodulation and in many viral and protozoan infections, being associated to a decrease in overall mortality (136-142).

However, despite all the important findings and advances in the field, bisphosphonates are a class of drugs that still needs to be improved. The use of bisphosphonate-containing ILs may represent a very important way to overcome some of their present clinical limitations, such as their very low bioavailability and limited biological effects. Furthermore, since these molecules present a high affinity to bone tissue, their conjugation with ionic counterparts is a potentially unique opportunity to selectively deliver other compounds to bone. Thus, combining chemical with biological properties to create new and improved drugs may unravel new opportunities for drug design and development, aiming to improve therapeutic approaches and clinical outcomes.

Etidronate is a first generation bisphosphonate, presenting the simplest chemical composition among them. More precisely, it displays only a hydroxyl group attached to the central carbon atom (119). Due to its resemblance to inorganic pyrophosphate, it is incorporated into ATP molecules, leading to the formation of derivatives that impair osteoclast function (143). In the present work, the combination of etidronic acid with TMG and DBN in a straightforward fashion led to the formation of four new ionic liquids with

increased solubility in water and saline solution in comparison with the parent drug. Thus, the oral bioavailability of such compounds may be particularly enhanced, leading to a lower dose to be taken by the patients with particular decrease in side effects. In addition, both dianionic compounds are amorphous, i.e. do not tend to form polymorphic structures with various pharmacological activities during their shelf life.

Regarding the biological activity of the developed ILs, it was observed that etidronate revealed cytotoxicity against all the tested cell types, in the mM range, as described previously (144). However, some of the Eti-ILs displayed an increased cytotoxicity against human cancer cells, while maintaining a similar response in the fibroblast cell cultures. This behavior was particularly evident in the case of ILs containing DBNH. These observations may suggest some selectivity in the cytotoxicity of the ILs. Further studies are required in order to unravel the involved mechanisms. This work is underway.

Considering the effects on human bone cells, the present results point to specific effects of etidronate on osteoclastogenesis and osteoblastogenesis which are in line with previously published data. It was observed that Eti promoted a decrease on the functionality of mature osteoclasts isolated from rabbit bones, and an increase in apoptosis (145). In that study, the effects were observed for concentrations $100 \times 10^3 \mu M$, a value significantly higher than the minimum Eti concentration with biological effects observed in the present work (10μM). Besides the origin of the osteoclasts, also the fact that the starting point of that study were mature osteoclasts, and no observations were made regarding the osteoclastogenesic process, may account for the differences in the values between both studies. In another study, Eti at 1μM was able to decrease the differentiation and function or rat osteoclasts obtained in co-cultures with a rat osteoblastic cell line (146). The *in vivo* effects of Eti are also well-studied. It was demonstrated that Eti can prevent thyroid hormone induced-bone loss, regulating the development of both osteoclasts and osteoblasts (147). Eti was also able to promote osteoclastic degeneration in samples obtained from individuals with Paget's disease (148). In the present work, etidronate was used as a starting molecule to create different ILs. Globally, some the developed Eti-ILs seemed to affect cell density in wither PBMC or HMSC cultures. In the first case, cell density decreased over the culture time, as expected by the cellular fusion involved in the osteoclastogenic process (62, 127). The presence of Eti-ILs appeared to further decrease total protein content. In parallel, an increase in caspase-3 activity was observed, suggesting that the developed compounds may compromise cell survival by stimulating apoptosis. In HMSC cultures, it was observed an opposite behavior, that means, cell density increased over culture period, and treatment with Eti-ILs caused an additional increase. Once again, apoptosis appeared to be, at least partially, responsible

for these effects, since in this case caspase-3 activity was decreased by Eti-ILs. Considering cell differentiation, the Eti-ILs displayed increased anti-osteoclastogenic and pro-osteoblastogenic effects when compared to etidronic acid alone, particularly in the case of [TMGH]$_2$[Eti] and [DBNH]$_2$[Eti]. The results obtained with TMGH-ILs appeared to involve a downregulation of MEK pathway, while PKC appeared to lose relevance in the presence of ILs containing DBNH. Considering the results obtained with Eti, [TMGH]Cl and [DBNH]Cl alone, and the corresponding ILs, the observed effects of the latter group seemed to be caused by the overall combination of the cation and the anion, rather than a sum of their individual effects.

Taken together, the synthesis of ILs containing Eti allowed the creation of compounds with different characteristics, compared to the isolated base molecules. In more detail, some of the developed Eti-ILs appeared to be not only highly water soluble etidronic acid analogues with diminished or absent polymorphic structures, but also revealed better biological properties, with an apparent increase in cytotoxicity against cancer cells, an increase in osteoclast-inhibitory behavior and a stimulatory effect over osteoblasts. Since, at least in some cases, the developed ILs displayed better biological properties, those compounds may represent important starting points for the development of new drugs aiming to modulate bone metabolism, particularly in the case of increased bone resorption.

Chapter 6 - Discussion and Conclusion

6.1 - Discussion

The following discussion focuses essentially on the data presented in the previous chapters. In this thesis, each chapter is reported, as an accepted or submitted paper, which includes a comprehensive discussion and/or conclusion of the work presented.

The bone, like mentioned before, is a common site for the appearance of metastasis: between 65 to 75% in breast and prostate cancer, 60% in thyroid cancer and 40% in lung cancer (19). Bone metastasis may lead to many types of symptoms and complications like severe pain, pathological fractures, spinal cord and nerve compression, hypercalcemia of malignancy and bone marrow aplasia (1, 13, 19, 27, 58)

The elite choice of treatment for this kind of disorders is BPs, because of their ability to regulate bone metabolism. But since their bioavailability is very low, clinical applications are sill very limited. So the objective of this work was to chemically change the BPs, in order to make Ionic Liquidos (ILs) and/or molten salts, using BPs as cations or anions combined with appropriate biocompatible counter-ions. The developed compounds were expected to: present an enhanced solubility and permeability; avoid the problems of polymorphism; present improved biological proprieties, acting on human cancer cells and bone cells.

The counter-ions were selected to establish a stronger interaction with the bisphosphonates (BPs) scaffolds as well as to improve the original bioavailability of the BPs. In this context, it is considered that the organic superbases such as TMG and DBN can promote higher interaction with phosphonate groups while the other organic cations such as Choline, EMIM, CH_2OMIM, C_3OMIM can be relevant to improve the bioavailability behavior. In general, the organic cations such as choline and imidazolium structures showed a good biocompatibility and interesting recent applications in the pharmaceutical field; the choline has an important contribution in both proliferative growth and programmed cell death, while the imidazolium are one of the most common cations that are being applied as an antibacterial, antifungal and anti-tumor in ILs field (8, 149-151).

So, the present work was focused on the synthesis of ILs based on BPs belonging to the 1st, 2nd and 3rd generation, namely Etidronate, Alendronate and Zoledronate respectively; and their action on different types of human cells. All of them were analysed for their cytotoxicity on human cancer cells. The cancer cells lines selected for these studies were osteosarcoma cells (MG63) because their known ability to disturb bone metabolism and increase bone turnover (112, 113, 124), and breast cancer (T47D) and lung cancer cells (A549), because of their association with bone osteolytic metastasis (62, 103, 105).

The combination of an API, either as a cation or as an anion, with a suitable biocompatible counter-ion can increase the water solubility of the parent drug and even change its biological effect, so this suggests that the oral bioavailability of the new API-ILs may be particularly enhanced (60, 103, 112, 113). This is in accordance with the recently proposed idea that neutral ionic liquids can modulate the BCS system of an API and therefore enhance its membrane transport (6, 7). So based on this idea, it was possible to prepare and characterize twelve Zoledronate-based ILs or molten salts; eight Alendronate-based ILs or molten salts and 4 Etidronate-based ILs or molten salts.

The optimized methodology for the synthesis of these compounds was based on the direct protonation in the case of organic superbases (TMG and DBN based salts) or acid-base neutralization reactions in the case of choline and imidazolium based salts. In general, all prepared salts showed a significant improvement of water and saline solubility comparing to the starting ones. Some of the new compounds were not considered RTILs or ILs, but organic salts, because their melting temperatures (Tm) are higher than 100ºC. It is important to note the presence of amorphous structures for many of the prepared salts indicated by the detection of the characteristic glass transition temperature (Tg) and not tendency for crystallization (melting and crystallization temperatures not detected by calorimetric studies). It is particularly interest the case of [DBNH][Zol] which it showed a crystalline structure solved by Crystal X-Ray Diffraction analysis. It seems that the presence of the DBN as protic cation allowed the formation of the crystalline salt while in the case of larger organic cations such as choline or methylimidazolium structures the crystallization should be avoided. In parallel, [DBNH][ALN] was the unique example possessing a polymorphic behavior. These observations can proof that the suitable combination between API and counter-ions is relevant to modulate the physical-chemical as well as biological properties of the final salts.

All the products were completely characterized by NMR and FTIR spectroscopic techniques, as well as elemental analysis (C, H, N). ^{1}H-NMR spectra is an important technique in order to elucidate the final chemical structure of the salt as well as the presence of impurities (e.g. solvents or starting materials) and the cation:anion proportion. FTIR analysis is an additional characterization technique for the validation of specific functional groups (e.g. hydroxyl, carbonyl or phosphonate groups) or bonds in the cation or anion structures.   Elemental analysis (C, H, N) is a complementary analysis in order to proof the expected salt by simple comparison between theoretical and experimental percentages of C, H, N in the molecules. In the case of ILs and organic salts is considered that the difference between theoretical and experimental percentages should be lower than 0.5%.

Overall, it was possible to make almost all amorphous compounds and avoid the polymorphism, a great problem in the pharmaceutical industry with a real reduction of the therapeutical drug efficiency. Additionally, it was also possible to increase significantly their solubility in water, with a possible improvement on their bioavailability. The complementary permeability studies using octanol-water partition coefficients can elucidate the ability of the new salt to cross the membranes.

On a general way, the cytotoxic analysis demonstrated that some of the developed compounds presented better biological properties. More precisely, the monoanionic compounds presented lower cytotoxicity to the fibroblasts (non-neoplasic control) than the dianionic ones. It was also reported that the [Ch][Zol] and [C$_3$OMIM]$_2$[Zol] demonstrated the highest cytotoxicity against MG63 cells, the [EMIM]$_2$[Zol] evidenced some cytotoxicity against MG63 (lower than previous compounds) and average cytotoxicity against T47D cells. The [C$_2$OHMIM][ALN] showed the highest cytoxicity against A549 cells with a good response to MG63 cells and T47D cells in comparison with non-neoplasic control.

In addition to the analysis of cytotoxicity on human cancer cells, the Eti-ILs were also evaluated regarding their ability to modulate human osteoclastogenesis and osteoblastogenesis. For osteoclastogenesis, it was analysed: the total protein content, the TRAP activity and the caspase-3 activity. The TRAP (Tartrate-Resistant Acid Phosphatase) is an iron-containing enzyme, highly expressed in chondroclasts as well as osteoclasts and, therefore, used as a specific histochemical marker for these cells (152). Caspase-3 is an enzyme encoded by the *CASP3* gene, a member of the Caspase family (Cysteine-Aspartic cid Protease), which its sequential activation plays a central role in the execution-phase of cell apoptosis (153). Besides that, and in order to have a more detailed perspective about osteoclast differentiation, it was also evaluated the expression of several genes related to osteoclasts, namely the TRAP, cathepsin K (CATK) and Carbonic Anydrase 2 (CA2).

The results obtained consisted in a decrease of the protein content in the compounds that contained Eti with high concentrations; an inhibition of TRAP activity by [TMGH][Eti], [TMGH]$_2$[Eti] and [DBNH][Eti]; an increase on apoptosis quantificated through the activity of caspase-3 specially evidenced by [TMGH]$_2$[Eti] and [DBNH]$_2$[Eti]. The inhibitory effects on osteoclastogesis were also demonstrated by a decrease in the expression of the osteoclast-related genes. Moreover, the different ILs appears to modulate differentially some of the tested signaling pathways.

For osteoblastogenesis it was analysed: the total protein content, the ALP activity and the caspase-3 activity. The ALP is an enzyme, secreted by activated osteoblasts, when is needed to produce new bone tissue, for example, to regenerate a defect or a depleted bone matrix (154) Besides that, and in order to game some insights about

specific effects on osteoblastogenesis, the expression of genes related to osteoblasts was evaluated, namley the Collagen type 1 (COL1), ALP and Bone Morphogenetic Proteins 2 (BMP2).

The results obtained consisted in an increased of the protein content, an increased activity of the ALP enzyme and a decrease apoptosis especially evidenced by [DBNH]$_2$[Eti] and [TMGH]$_2$[Eti]. The results regarding the gene expression, demonstrated a significant increase in all the analyzed genes (COL1, ALP and BMP-2), whose highest effects were observed in the presence of [DBNH]$_2$[Eti] followed by [TMGH]$_2$[Eti]. The observed effects appeared to be caused, at least partially, by differential effects on some of the tested intracellular signaling pathways.

The results obtained both with osteoclast and osteoblast cell cultures suggested that some of the tested compounds may affect both cell types in an opposite way, decreasing osteoclastogeneis and increasing osteogenesis. That means, the results strongly suggest that those compounds may shift bone metabolism to an anabolic state, which may be very relevant in contexts where bone resorption may be elevated, such as, for example, bone osteolytic metastasis.

6.2 – Conclusion

In general, it was possible to make almost all amorphous compounds and avoid the original polymorphism, improve the solubility in water and biological fluids, with a possible enhancement of their bioavailability.

Taken together, the results obtained from the present work may be relevant because some of the new compounds synthesized were ILs or molten salts, which demonstrated average-to-high cytotoxicity against cancer cells lines from cancers that are known for their association with bone metastasis; comparatively, some of them revealed low cytotoxicity toward fibroblasts. Furthermore, some of the developed ILs containing Eti also appeared to directly modulate bone metabolism. More precisely, they seemed to promote bone anabolism, by inhibiting osteoclastogenesis and promoting osteoblastogenesis.

Therefore, the development of ILs or molten salts with a simultaneous potential inhibitory effect on bone resorption and a selective cytotoxicity towards types of cancer cells may represent an important strategy for the development of new pharmacological tools to be used in pathological conditions associated to high bone turnover rates, like for example bone metastasis. Since bone is a very common site for the appearance of

metastasis, it is extremely important to develop new drugs containing molecules that may selectively accumulate in bone tissue, as it happens with BPs, but without all of their adverse effects and with improved bioavailability and biological effects.

6.3 - Future Work

The developed work may be regarded as a starting point for many other experiments, in order to continue to investigate the properties and potential of BPs-containing ILs. For this, it would be interesting to proceed investigating further the cellular response of the other compounds in human bone cells, especially the Zoledronate-based ILs, like for example, the [Ch][Zol], the [C$_3$OMIM]$_2$[Zol] and the [EMIM]$_2$[Zol], which were the ones that revealed the more promising cytotoxic results against osteosarcoma and breast cancer cells.

And after this work, if the results continues to be promising, it woud be interesting to invest in the synthesis of ILs and/or RTILs based on BPs conjugated with antitumoral drugs, normally used in Breast Cancer, Prostate Cancer, Osteosarcoma or any other Cancer related with bone metastasis.

References

1.	M.T. Drake BLC, S. Khosla. Bisphosphonates: Mechanism of Action and Role in Clinical Practice. Mayo Clinic Proceedings. 2008;83(9):24.
2.	P.P. Lehenkari MK, J.P. Näpänkangas, K.V. Ylitalo, J. Mönkkönen, M.J. Rogers, A. Azhayev, H.K. Väänänen, I.E. Hassinen. Further Insight into Mechanism of Action of Clodronate: Inhibition of Mitochondrial ADP/ATP Translocase by a Nonhydrolyzable, Adenine-Containing Metabolite. Molecular Pharmacology. 2002;62(5):8.
3.	R.N. Bhatt SAH, C.F. Munns. The use of bisphosphonates in children: review of the literature and guidelines for dental management. Australian Dental Journal. 2014;59:11.
4.	A.J. Roelofs CAS, S. Sun, K.M. Błazewska, B.A. Kashemirov, C.E. McKenna, R.G.G. Russell, M.J. Rogers, M.W. Lundy, F.H. Ebetino, F.P. Coxon. Influence of Bone Affinity on the Skeletal Distribution of Fluorescently Labeled Bisphosphonates In Vivo. Journal of Bone and Mineral Research. 2012;27(4):13.
5.	Heidrun Karlic RT, Christopher Gerner, Thomas Grunt, Katharina Proestling, Florian Haider, Franz Varga. Inhibition of the mevalonate pathway affects epigenetic regulation in cancer cells. Cancer Genetics. 2015;208.
6.	Amidon RLaGL. Modern bioavailability, bioequivalence and biopharmaceutics classification system. New scientific approaches to international regulatory standards. European Journal of Pharmaceutics and Biopharmaceutics. 2000;50(1):10.
7.	Karunakar BBKRaA. Biopharmaceutics Classification System: A Regulatory Approach. Dissolution Technologies. 2011;18(1):7.
8.	R. Ferraz LCB, C. Prudencio, J.P. Noronha, Z. Petrovski. Ionic Liquids as Active Pharmaceutical Ingredients. ChemMedChem 2011;6(6):11.
9.	Fleisch H. Development of bisphosphonates. Breast Cancer Research. 2002;4:5.
10.	Papapoulos SE. Bisphosphonate actions: Physical chemistry revisited. Bone. 2006;38:4.
11.	L.F. Castro ATAS, M.C. Chung. Bifosfonatos (BFs) como transportadores osteotrópicos no planejamento de fármacos dirigidos. Quimica Nova. 2004;27(3):5.
12.	Russell RGG. Bisphosphonates: Mode of Action and Pharmacology. Pediatrics. 2007;119(S150):14.
13.	R.G.G. Russell NBW, F.H. Ebetino, M.J. Rogers. Mechanisms of action of bisphosphonates: similarities and differences and their potential influence on clinical efficacy. Osteoporosis International. 2008;19:27.
14.	M.J. Rogers SG, H.L. Benford, F.P. Coxon, S.P. Luckman, J. Mönkkönen, J.C. Frith. Cellular and Molecular Mechanisms of Action of Bisphosphonates. Cancer Supplement. 2000;88(12):18.
15.	G.H. Nancollas RT, R.J. Phipps, Z. Henneman, S. Gulde, W. Wu, A. Mangood, R.G.G. Russell, F.H. Ebetino. Novel insights into actions of bisphosphonates on bone: Differences in interactions with hydroxyapatite. Bone. 2006;38:11.
16.	H.L. Benford JCF, S. Auriola, J. Mönkkönen, M.J. Rogers. Farnesol and geranylgeraniol prevent activation of caspases by aminobisphosphonates: biochemical evidence for two distinct pharmacological classes of bisphosphonate drugs. Molecular Pharmacology. 1999;56:10.

17.　M.J. Rogers JCF, S.P. Luckman, F.P. Coxon, H.L. Benford, J. Mönkkönen, S. Auriola, K.M. Chilton, R.G. Russell. Molecular mechanisms of action of bisphosphonates. Bone. 1999;24:7.

18.　Martin NASTJ. Coupling the activities of bone formation and resorption: a multitude of signals within the basic multicellular unit. BMS BoneKEy Reports. 2014;3(481):10.

19.　M. Tolia AZ, J.R Kouvaris, C. Meristoudis, N. Margar, P. Karakitsos, I. Kokakis, D. Karkamakis, C. Papadimitriou, K. Mystakidou, N. Tsoukalas, G. Kyrgias, B. Armonis, D.K. Filippiadis, A.D. Kelekis, N. Kelekis, V, Kouloulias. The Key Role of Bisphosphonates in the Supportive Care of Cancer Patients. Anticancer Research. 2014;34:15.

20.　A. Fontana PDD. Markers of Bone Turnover in Bone Metastases. Skeletal Complications of Malignancy - Supplement to Cancer. 2000;88(12):9.

21.　H.K. Datta WFN, J.A. Walker, S.P. Tuck, S.S. Varanasi. The cell biology of bone metabolism. Journal of Clinical Pathology. 2008;61:12.

22.　S.C. Cremers GP, S.E. Papapoulos. Pharmacokinetics/pharmacodynamics of bisphosphonates: use for optimisation of intermittent therapy for osteoporosis. Clinical Pharmacokinetics. 2005;44:20.

23.　I. Fogelman LS, R. Mazess, M.A. Wilson, J.A. Bevan. Absorption of oral diphosphonate in normal subjects. Clinical Endocrinology (Oxf). 1986;24:6.

24.　M. Pazianas BA, S. Ferrari, R.G. Russell. Eliminating the need for fasting with oral administration of bisphosphonates. Therapeutics and Clinical Risk Management 2013;9:8.

25.　Russell RG. Bisphosphonates: the first 40 years. Bone. 2011;49:18.

26.　Mariotti A. Bisphosphonates and Osteonecrosis of the Jaws. Journal of Dental Education. 2008;72(8):11.

27.　Smith HS. Painful Osseous Metastases. Pain Physician. 2011;14:31.

28.　Vepsalainen JJ. Bisphosphonate prodrugs. Current Medicinal Chemistry. 2002;9:8.

29.　H. Mönkkönen SA, P. Lehenkari, M. Kellinsalmi, I.E. Hassinen, J. Vepsäläinen, J. Mönkkönen. A new endogenous ATP analog (ApppI) inhibits the mitochondrial adenine nucleotide translocase (ANT) and is responsible for the apoptosis induced by nitrogen-containing bisphosphonates. British Journal of Pharmacology. 2006;147:9.

30.　K. Thompson MJR, F.P. Coxon, J.C. Crockett. Cytosolic Entry of Bisphosphonate Drugs Requires Acidification of Vesicles after Fluid-Phase Endocytosis. Molecular Pharmacology. 2006;69(5):9.

31.　M.J. Rogers JCC, F.P. Coxon, J. Mönkkönen. Biochemical and molecular mechanisms of action of bisphosphonates. Bone. 2011;49:8.

32.　A.J. Roelofs KT, S. Gordon, M.J. Rogers. Molecular Mechanisms of Action of Bisphosphonates: Current Status. Clinical Cancer Research. 2006;12(20):10.

33.　Green JR. Bisphosphonates: Preclinical Review. The Oncologist. 2004;9(4):11.

34.　H.L. Benford NWAM, M.H. Helfrich, M.E. Nuttall, M.J. Rogers. Visualization of Bisphosphonate-induced Caspase-3 Activity in Apoptotic Osteoclasts In Vitro. Bone. 2001;28(5):9.

35.　P.G. Fournier VS, F.H. Ebetino, P. Clézardin. How Do Bisphosphonates Inhibit Bone Metastasis In Vivo? Neoplasia. 2010;12(7):8.

36.　L.A. Knight CMK, S. Glaysher, A. Fernando, R. Reichelt, S. Dexel, U. Reinhold, I.A. Cree. Activity of mevalonate pathway inhibitors against breast and

ovarian cancers in the ATP-based tumour chemosensitivity assay. BMC Cancer. 2009;9(38):10.

37. M. Marra DS, G. Tonini, G. Meo, S. Zappavigna, G. Facchini, A. Morabito, A. Abbruzzese, G. Cartenıì, A. Budillon, M. Caraglia. Molecular and preclinical models enhancing anti-tumour activity of zoledronic acid. European Journal of Cancer Suppements. 2008;6:7.

38. S.P. Jagdev REC, C.M. Shipman, A. Rostami-H, P.I. Croucher. The bisphosphonate, zoledronic acid, induces apoptosis of breast cancer cells: evidence for synergy with paclitaxel. British Journal of Cancer. 2001;84(8):9.

39. X.L. Xu WLG, A.Y. Wang, Y. Wang, Q.Y. Guo, Q.. Lu, S.B. Lu, J. Peng. Basic research and clinical applications of bisphosphonates in bone disease: what have we learned over the last 40 years? Journal of Translational Medicine. 2013;11:1.

40. Clezardin P. Bisphosphonates' antitumor activity: an unravelled side of a multifaceted drug class. Bone. 2011;48:9.

41. S.J. Koopmans LvdW-P, C.W. Lowik, S.E. Papapoulos. Use of a rat model for the simultaneous assessment of pharmacokinetic and pharmacodynamic aspects of bisphosphonate treatment: application to the study of intravenous 14C-labeled 1-hydroxy-3-(1-pyrrolidinyl)-propylidene-1,1-bisphosphonate. Journal of Bone and Mineral Research. 1994;9:6.

42. O. Israel DF, R. Hardoff, S. Ish-Shalom, J. Jerushalmi, G.M. Kolodny. In vivo SPECT quantitation of bone metabolism in hyperparathyroidism and thyrotoxicosis. Journal of Nuclear Medicine. 1991;32:5.

43. V. Carnevale FD, V. Frusciante, I. Chiodini, S. Minisola, A.J. Scillitani. Different patterns of global and regional skeletal uptake of 99mTc-methylene diphosphonate with age: relevance to the pathogenesis of bone loss. Journal of Nuclear Medicine. 2000;41:6.

44. A.G. Porras SDH, B.J. Gertz. Pharmacokinetics of alendronate. Clinical Pharmacokinetics. 1999;36:14.

45. A.L. Boskey RC. Aging and bone. Journal of Dental Research. 2010;89:16.

46. M. Sato WG, N. Endo, R. Akins, H. Simmons, D.D. Thompson, E. Golub, G.A. Rodan. Bisphosphonate action. Alendronate localization in rat bone and effects on osteoclast ultrastructure. The Journal of Clinical Investigation. 1991;88:11.

47. M.R. Allen DBB. Bisphosphonate effects on bone turnover, microdamage, and mechanical properties: What we think we know and what we know that we don't know. Bone. 2011;49:10.

48. L.I. Plotkin NB, T. Bellido. A bisphosphonate that does not affect osteoclasts prevents osteoblast and osteocyte apoptosis and the loss of bone strength induced by glucocorticoids in mice. Bone. 2011;49:6.

49. T. Bellido LIP. Novel actions of bisphosphonates in bone: Preservation of osteoblast and osteocyte viability. Bone. 2011;49:6.

50. R.L. Boland SM, G. Santillan, P. Scodelaro, A. Colicheo, A.R. de Boland, K. Vyas, L.I. Plotkin, T. Bellido. Connexin 43 Is Required for Bisphosphonate-Induced Survival of Osteoblastic Cells but not for Bisphosphonate Binding. Journal of Bone and Mineral Research. 2006;21:1.

51. Mandalunis NDEaPM. Influence of Bisphosphonate Treatment onMedullary Macrophages and Osteoclasts: An Experimental Study. BoneMarrow Research. 2012:8.

52.   M.M. Weivoda MJO. The Roles of Small GTPases in Osteoclast Biology. Orthopedic and Muscular System: Current Research. 2014;3:1.
53.   J. Zekri MM, S.M. Karim. The anti-tumour effects of zoledronic acid. Journal of Bone Oncology.3:10.
54.   S. Einav JSG. Prenylation inhibitors: a novel class of antiviral agents. Journal of Antimicrobial Chemotherapy. 2003;52:4.
55.   F.M. Jordão AYS, D.C. Miguel, V. de Jesus Peres, E.A. Kimura, A.M. Katzin. In vitro and in vivo antiplasmodial activities of risedronate and its interference with protein prenylation in Plasmodium falciparum. Antimicrobial Agents and Chemotherapy. 2011;55:6.
56.   A.J. Roelofs KT, F.H. Ebetino, M.J. Rogers, F.P. Coxon. Bisphosphonates: Molecular Mechanisms of Action and Effects on Bone Cells, Monocytes and Macrophages. Current Pharmaceutical Design. 2010;16:11.
57.   J.M. Sanders YS, J.M.W. Chan, Y. Zhang, S. Jennings, T. Kosztowski, S. Odeh, R. Flessner, C. Schwerdtfeger, E. Kotsikorou, G.A. Meints, A.O. Gómez, F. González-Pacanowska, A.M. Raker, H. Wang, E.R. van Beek, S.E. Papapoulos, C.T. Morita, E. Oldfield. Pyridinium-1-yl Bisphosphonates Are Potent Inhibitors of Farnesyl Diphosphate Synthase and Bone Resorption. Journal of Medicinal Chemistry. 2005;48:7.
58.   Jing Liu WH, Ruoyu Zhou, Shuting Jia, Wenru Tang, Ying Luo, and Jihong Zhang. Bisphosphonates in the Treatment of Patients With Metastatic Breast, Lung, and Prostate Cancer - A Meta-Analysis. Medicine. 2015;94 (46):5.
59.   Daniele Santini LS, Chiara Spoto, Loretta D'Onofrio, Francesco Pantano, Michele Iuliani, Marco fioramonti, Alice Zoccoli, Giulia Ribelli, Vladimir Virzì, Bruno Vincenzi and Giuseppe Tonini. Bisphosphonates as anticancer agents in early breast cancer: preclinical and clinical evidence. Breast Cancer Research 2015;17(121):7.
60.   J. Costa-Rodrigues KAM, M.R. Teixeira, M.H. Fernandes. Variability of the Paracrine-Induced Osteoclastogenesis by Human Breast Cancer Cell Lines. Journal of Cellular Biochemistry. 2012;113:11.
61.   J. Costa-Rodrigues AF, M.H. Fernandes. Reciprocal osteoblastic and osteoclastic modulation in co-cultured MG63 osteosar-coma cells and human osteoclast precursors. Journal of Cellular Biochemistry. 2011;112:10.
62.   J. Costa-Rodrigues CAT, M.H. Fernandes. Paracrine-mediated osteoclastogenesis by the osteosarcoma MG63 cell line: is RANKL/RANK signalling really important? Clinical & Experimental Metastasis. 2011;28:10.
63.   Guise TA. Molecular Mechanisms of Osteolytic Bone Metastases. Skeletal Complications of Malignancy - Supplement to Cancer. 2000;88(12):7.
64.   A. Mathew MP, A.M. Brufsky. The Use of Adjuvant Bisphosphonates in the Treatment of Early-Stage Breast Cancer. Clinical Advances in Hematology & Oncology. 2014;12(11):8.
65.   Paterson AHG. The Potential Role of Bisphosphonates as Adjuvant Therapy in the Prevention of Bone Metastases. Skeletal Complications of Malignancy - Supplement to Cancer. 2000;88(12):9.
66.   Mathew ABaA. Bisphosphonates, bone, and breast cancer recurrence. The Lancet. 2015;386:2.
67.   J. Wood KB, S. Ruetz, A. Bellahcène, L. Devy, J.M. Foidart, V. Castronovo, J.R. Green. Novel Antiangiogenic Effects of the Bisphosphonate Compound Zoledronic Acid. The Journal of Pharmacology and Experimental Therapeutics. 2002;302(3):7.

68.   S.G. Senaratne JLM, K.W. Colston. The bisphosphonate zoledronic acid impairs membrane localisation and induces cytochrome c release in breast cancer cells. British Journal of Cancer. 2002;86:8.

69.   J.P. Coxon GMO, R.S. Kirby, K.W. Colston. Zoledronic acid induces apoptosis and inhibits adhesion to mineralized matrix in prostate cancer cells via inhibition of protein prenylation. BJU International. 2004;94:7.

70.   P.G Dedes CHG, A.I. Tsonis, I. Kanakis, A.D. Theocharis, D. Kletsas, G.N. Tzanakakis, N.K. Karamanos. Expression of matrix macromolecules and functional properties of breast cancer cells are modulated by the bisphosphonate zoledronic acid. Biochimica et Biophysica Acta. 2012;1820:14.

71.   L. Insalaco FDG, M. Terrasi, V. Amodeo, S. Caruso, L.R. Corsini, D. Fanale, N. Margarese, D. Santini, V. Bazan, A. Russo. Analysis of molecular mechanisms and anti-tumoural effects of zoledronic acid in breast cancer cells. Journal of Cellular and Molecular Medicine. 2012;16:10.

72.   T. Yuen AS, J. Iqbal, M. Sgobba, Y. Gupta, P. Lu, G. Colaianni, Y. Ji, L. Zhu, S. Kim, J. Li, P. Liu, S. Izadmehr, J. Sangodkar, J. Bailey, Y. Latif, S. Mujtaba, S. Epstein, T.F. Davies, Z. Bian, A. Zallone, A.K. Aggarwal, S. Haider, M.I. New, L. Sun, G. Narla, M. Zaidi. Bisphosphonates inactivate human EGFRs to exert antitumor actions. Proceedings of the National Academy of Sciences (PNAS). 2014;111:6.

73.   H.J. Gober MK, L. Angman, P. Jenö, L. Mori, G. De Libero. Human T Cell Receptor Cells Recognize Endogenous Mevalonate Metabolites in Tumor Cells. Journal of Experimental Medicine. 2003;197(2):6.

74.   T.L. Rogers IH. Tumour macrophages as potential targets of bisphosphonates. . Journal of Translational Medicine. 2011;9:1.

75.   C. Rüegg AM. Vascular integrins: pleiotropic adhesion and signaling molecules in vascular homeostasis and angiogenesis. Cellular and Molecular Life Sciences. 2003;60:23.

76.   M. Bezzi MH, G. Bieler, O. Dormond, C. Rüegg. Zoledronate Sensitizes Endothelial Cells to Tumor Necrosis Factor-induced Programmed Cell Death. The Journal of Biological Chemistry. 2003;278(44):13.

77.   C. Scavelli GDP, T. Cirulli, M. Coluccia, A. Boccarelli, T. Giannini, G. Mangialardi, R. Bertieri, A.M.L. Coluccia, D. Ribatti, F. Dammacco, A. Vacca. Zoledronic acid affects over-angiogenic phenotype of endothelial cells in patients with multiple myeloma. Molecular Cancer Therapeutics. 2007;6:7.

78.   I. Pecheur OP, C.M, Serre, J. Guglielmi, C. Voland, F. Bourre, C. Margue, M. Cohen-Solal, A. Buffet, N. Kieffer, P. Clézardin. Integrin v 3 expression confers on tumor cells a greater propensity to metastasize to bone. The Federation of American Societies for Experimental Biology Journal. 2002:23.

79.   E. Terpos MK, M. Engelhardt, S. Zweegman, F. Gay, E. Kastritis, N.W. van de Donk, B. Bruno, O. Sezer, A. Broijl, S. Bringhen, M. Beksac, A. Larocca, R. Hajek, P. Musto, H.E. Johnsen, F. Morabito, H. Ludwig, M. Cavo, H. Einsele, P. Sonneveld, M.A. Dimopoulos, A. Palumbo. European Myeloma Network guidelines for the management of multiple myeloma-related complications. . Haematologica. 2015;100:13.

80.   Y. Qian DB, N. Kachru, R.K. Hernandez. Longitudinal patterns of bone-targeted agent use among patients with solid tumors and bone metastases in the United States. Supportive Care in Cancer. 2017;25:7.

81.   F.A. Trémollieres IC, H. Depypere, I. Lambrinoudaki, A. Mueck, F.R. Pérez-López, Y.T. van der Schouw, L.M. Senturk, T. Simoncini, J.C. Stevenson, P. Stute,

M. Rees. Osteoporosis management in patients with breast cancer: EMAS position statement. . Maturitas. 2017;95:71.

82. P.D. Miller SAJ, P. Evenepoel, R. Eastell, S. Boonen. Renal safety in patients treated with bisphosphonates for osteoporosis: a review. Journal of Bone and Mineral Research. 2013;28:11.

83. Y. Saita MI, K. Kaneko Atypical femoral fractures and bisphosphonate use: current evidence and clinical implications. Therapeutic Advances in Chronic Disease. 2015;6:9.

84. N.M. Maalouf HJH, C.V. Odvina, P.J. Kim, K. Sakhaee. Bisphosphonate-induced hypocalcemia: report of 3 cases and review of literature. Endocrine Practice. 2006;12:6.

85. D. Schuster CL, T. Langer. Why drugs fail – a study on side effects in new chemical entities. Current Pharmaceutical Design. 2005;11:5.

86. Stella VJ. Prodrugs: some thoughts and current issues. Journal of Pharmaceutical Sciences. 2010;99:11.

87. K. M. Huttunen HR, J. Rautio. Prodrugs--from serendipity to rational design. Pharmacological Reviews. 2011;63:22.

88. Serajuddin ATM. Salt formation to improve drug solubility. Advanced Drug Delivery Reviews. 2007;59:14.

89. J. Stoimenovski DRM, K. Bica, R.D. Rogers. Crystalline vs. Ionic Liquid Salt Forms of Active Pharmaceutical Ingredients: A Position Paper. Pharmaceutical Research 2010;27(4):5.

90. W.L. Hough MS, H. Rodriguez, R.P. Swatloski, S.K. Spear, D.T. Daly, J. Pernak, J.E. Grisel, R.D. Carliss, M.D. Soutullo, J.H. Davis, R.D. Rogers. The third evolution of ionic liquids: active pharmaceutical ingredients. New Journal of Chemistry. 2007;31:8.

91. K.S. Egorova EGG, V.P. Ananikov. Biological Activity of Ionic Liquids and Their Application in Pharmaceutics and Medicine. Chemical Reviews. 2017;117:58.

92. I.M. Marrucho LCB, L.P.N. Rebelo. Ionic Liquids in Pharmaceutical Applications. Annual Review of Chemical and Biomolecular Engineering. 2014;5:20.

93. O.A. Cojocaru KB, G. Gurau, A. Narita, P.D. McCrary, J.L. Shamshina, P.S. Barber, R.D. Rogers. Prodrug ionic liquids: functionalizing neutral active pharmaceutical ingredients to take advantage of the ionic liquid form. Medicinal Chemistry Communications. 2013;4(3):5.

94. K. Bica CR, M. Nieuwenhuyzen, R.D. Rogers. In search of pure liquid salt forms of aspirin: ionic liquid approaches with acetylsalicylic acid and salicylic acid. Physical Chemistry Chemical Physics. 2010;12(8):7.

95. J.L. Shamshina SPK, G. Gurau, R.D. Rogers. Chemistry: Develop ionic liquid drugs. Nature 2015;528:2.

96. P.M. Dean JT, M. Yoshizawa-Fujita, D.R. MacFarlane, J.L. Scott. Exploring an Anti-Crystal Engineering Approach to the Preparation of Pharmaceutically Active Ionic Liquids. Crystal Growth & Design. 2009;9(2):9.

97. C. Florindo AC, C. Matos, S.I. Nunes, A.N. Matias, C.M.M. Duarte, L.P.N. Rebelo, L.C. Branco, I.M. Marrucho. Novel organic salts based on fluoroquinolone drugs: Synthesis, bioavailability and toxicological profiles. . International Journal of Pharmaceutics 2014;469(1):11.

98.   J.M.M. Araujo CF, A.B. Pereiro, N.S.M. Vieira, A.A. Matias, C.M.M. Duarte, L.P.N. Rebelo, I.M. Marrucho. Cholinium-based ionic liquids with pharmaceutically active anions. . Royal Society of Chemistry. 2014;4(53):7.

99.   C. Florindo JMMA, F. Alves, C. Matos, R. Ferraz, C. Prudencio, J.P. Noronha, Z. Petrovski, L.C. Branco, L.P.N. Rebelo, I.M. Marrucho. Evaluation of solubility and partition properties of ampicillin-based ionic liquids. International Journal of Pharmaceutics 2013;456(2):7.

100.   S. Cherukuvada AN. Polymorphism in an API ionic liquid: ethambutol dibenzoate trimorphs. CrystEngComm. 2012;14(23):4.

101.   M. Smiglak JMP, X. Lu, L. Han, S. Zhang, H. Gao, D.R. MacFarlane, R.D. Rogers. Ionic liquids for energy, materials, and medicine. Chemical Communications 2014;50(66):23.

102.   R. Ferraz VT, D. Rodrigues, R. Fernandes, C. Prudencio, J.P. Noronha, Z. Petrovski, L.C. Branco. Antibacterial activity of Ionic Liquids based on ampicillin against resistant bacteria. Royal Society of Chemistry Advances. 2014;4(9):7.

103.   S. Avnet AL, M. Salerno, J. M. Halleen, F. Perut, D. Granchi, S. Ferrari, F. Bertoni, A. Giunti, N. Baldini. Increased osteoclast activity is associated with aggressiveness of osteosarcoma. International Journal of Oncology. 2008;33:8.

104.   R. Ruscica MB, M.Quintero, A. Martinez, D.R. Vega. Solid-State Forms of Zoledronic Acid: Polymorphism in Hydrates. Journal of Pharmaceutical Sciences. 2010;99:11.

105.   J. Costa-Rodrigues AF, M.H. Fernandes. Reciprocal Osteoblastic and Osteoclastic Modulation in Co-Cultured MG63 Osteosarcoma Cells and Human Osteoclast Precursors. Journal of Cellular Biochemistry. 2011;112:10.

106.   Ohta ISaY. New drugs—Reports of new drugs recently approved by the FDA: Alendronate. Bioorganic & Medicinal Chemistry. 1996;4:2.

107.   H.K. Hana HJS, D.H. Haa. Improved oral bioavailability of alendronate via the mucoadhesive liposomal delivery system. European Journal of Pharmaceutical Sciences. 2002;46:8.

108.   J. Iwamoto TT, Y. Sato. Efficacy and safety of alendronate and risedronate for postmenopausal osteoporosis. Current Medical Research and Opinion. 2006;22(5):10.

109.   R. Ferraz LCB, I. Marrucho, J. Araújo, M.N. da Ponte, C. Prudêncio, J.P. Noronha, Z. Petrovski. Development of Novel Ionic Liquids-APIs based on Ampicillin derivatives. Medicinal Chemistry Communications. 2012;3:4.

110.   Technology N-NIoSa. Chemistry Web Book.

111.   E. Afergan YN, D. Gutman, H. Epstein, O. Elmalak, G. Golomb. 31 P-NMR and Differential Scanning Calorimetry Studies for Determining Vesicle's Drug Physical State and Fraction in Alendronate Liposomes. Journal of Bioanalysis & Biomedicine. 2010:7.

112.   C. Kan GV, F. L. Pape, P. Clézardin. Cancer Cell Colonisation in the Bone Microenvironment. International Journal of Molecular Sciences 2016;17:1.

113.   C.S. Shemanko YC, A. Forsyth What Is Breast in the Bone? International Journal of Molecular Sciences. 2016;17:1.

114.   Katsimbri P. The biology of normal bone remodelling. European Journal of Cancer Care. 2017;26:5.

115.   B.Q. Le VN, S.M. Cool, C.A. van Blitterswijk, J. de Boer,V.L.S. LaPointe. The Components of Bone and What They Can Teach Us about Regeneration. Materials (Basel). 2017;11(14):16.

116. Y.E. Park DSM, D. Naot, J. Cornish. Cell-cell communication in bone development and whole-body homeostasis and pharmacological avenues for bone disorders. Current Opinion in Pharmacology. 2017;34:15.

117. T.R. Arnett IRO. Metabolic properties of the osteoclast. Bone. 2017.

118. M.T. Valenti LDC, M. Mottes. Osteogenic Differentiation in Healthy and Pathological Conditions. International Journal of Molecular Sciences 2017;18(41):9.

119. F.H. Ebetino AMH, S. Sun, M.K. Tsoumpra, X. Duan, J.T. Triffitt, A.A. Kwaasi, J.E. Dunford, B.L. Barnett, U. Oppermann, M.W. Lundy, A. Boyde, B.A. Kashemirov, C.E. McKenna, R.G. Russell. The relationship between the chemistry and biological activity of the bisphosphonates. Bone. 2011;49:14.

120. S. Teixeira LCB, M.H. Fernandes, J. Costa-Rodrigues. Bisphosphonates and cancer: a relationship beyond the antiresorptive effects. Mini-Reviews in Medicina Chemistry (in press). 2017.

121. L.J. Dominguez GDB, M. Belvedere, M. Barbagallo. Physiology of the aging bone and mechanisms of action of bisphosphonates. Biogerontology. 2011;12:7.

122. Lin JH. Bisphosphonates: a review of their pharmacokinetic properties. . Bone. 1996;18(2):11.

123. Costa-Rodrigues J, Martins EG, Fernandes MH. Induced osteoclastogenesis by fluoroquinolones in unstimulated and stimulated human osteoclast precursor cells. Bone. 2012;51(1):17-27.

124. C. Bessa Pereira PSG, J. Costa-Rodrigues, R. Almeida Palmas, L. Vieira, M.P. Ferraz, M.A. Lopes, M.H. Fernandes. Equisetum arvense hydromethanolic extracts in bone tissue regeneration: in vitro osteoblastic modulation and antibacterial activity. Cell Proliferation. 2012;45:11.

125. Bradford MM. A rapid and sensitive method for the quantitation of microgram quantities of protein utilizing the principle of protein-dye binding. Analytical Biochemistry 1976;72:7.

126. Zhao Q, Shao J, Chen W, Li YP. Osteoclast differentiation and gene regulation. Front Biosci. 2007;12:2519-29.

127. J. Costa-Rodrigues SC, I.P. Perpetuo, F.J. Monteiro, M.H. Fernandes. Osteoclastogenic differentiation of human precursor cells over micro- and nanostructured hydroxyapatite topography. Biochimica et Biophysica Acta. 2016;1860:11.

128. Costa-Rodrigues J, Teixeira CA, Fernandes MH. Paracrine-mediated osteoclastogenesis by the osteosarcoma MG63 cell line: is RANKL/RANK signalling really important? Clinical & experimental metastasis. 2011;28(6):505-14.

129. Lin JH. Bisphosphonates: a review of their pharmacokinetic properties. Bone. 1996;18(2):75-85.

130. Bessa Pereira C, Gomes PS, Costa-Rodrigues J, Almeida Palmas R, Vieira L, Ferraz MP, et al. Equisetum arvense hydromethanolic extracts in bone tissue regeneration: in vitro osteoblastic modulation and antibacterial activity. Cell proliferation. 2012;in press.

131. Bradford MM. A rapid and sensitive method for the quantitation of microgram quantities of protein utilizing the principle of protein-dye binding. Analytical biochemistry. 1976;72:248-54.

132. N.S. Soysa NA. Osteoclast function and bone-resorbing activity: An overview. Biochemical and Biophysical Research Communications. 2016;476:6.

133. J. Costa-Rodrigues SR, A. Castro, M.H. Fernandes. Bone Anabolic Effects of Soluble Si: In Vitro Studies with Human Mesenchymal Stem Cells and CD14+ Osteoclast Precursors. Stem Cells International. 2016;2016:12.

134. A. Qaseem VS, P. Shekelle, R. Hopkins Jr, M.A. Forciea, D.K. Owens. Pharmacologic treatment of low bone density or osteoporosis to prevent fractures: a clinical practice guideline from the American College of Physicians. Annals of Internal Medicine. 2008;149:7.

135. Silverman SL. Bisphosphonate use in conditions other than osteoporosis. Annals of the New York Academy of Sciences 2011;1218:5.

136. C.H. Huang SBG, E. Oldfield, L.M. Amzel. Binding of nitrogen-containing bisphosphonates (N-BPs) to the Trypanosoma cruzi farnesyl diphosphate synthase homodimer. Proteins 2010;78:7.

137. M. Machado LSC, G. Tannus, M. Fonseca. Efficacy of clodronate, pamidronate, and zoledronate in reducing morbidity and mortality in cancer patients with bone metastasis: a meta-analysis of randomized clinical trials. Clinical Therapeutics. 2009;31:18.

138. A. Guenther SG, M. Tiemann, R. Burger, F. Bakker, J.R. Green, W. Baum, A.J. Roelofs, M.J. Rogers, M. Gramatzki. The bisphosphonate zoledronic acid has antimyeloma activity in vivo by inhibition of protein prenylation. International Journal of Cancer 2010;126:8.

139. R.T. Chlebowski ZC, J.A. Cauley, G. Anderson, R.J. Rodabough, A. McTiernan, D.S. Lane, J.E. Manson, L. Snetselaar, S. Yasmeen, M.J. O'Sullivan, M. Safford, S.L. Hendrix, R.B. Wallace. Oral bisphosphonate use and breast cancer incidence in postmenopausal women. Journal of Clinical Oncology. 2010;28:9.

140. L.A. Beaupre DWM, D.A. Hanley, W.P. Maksymowych, N.R. Bell, A.G. Juby, S.R. Majumdar. Oral bisphosphonates are associated with reduced mortality after hip fracture. Osteoporosis International 2011;22:8.

141. J.R. Center DB, N.D. Nguyen, T.V. Nguyen, J.A. Eisman. Osteoporosis medication and reduced mortality risk in elderly women and men. The Journal of Clinical Endocrinology & Metabolism. 2011;96:9.

142. B. O'Carrigan B MHW, M.L. Willson, M.R. Stockler, N. Pavlakis, A. Goodwin. Bisphosphonates and other bone agents for breast cancer. The Cochrane Database of Systematic Reviews. 2017;10.

143. M.J. Rogers XJ, R.G. Russell, G.M. Blackburn, M.P Williamson MP, A.V. Bayless, F.H. Ebetino, D.J. Watts. Incorporation of bisphosphonates into adenine nucleotides by amoebae of the cellular slime mould Dictyostelium discoideum. Biochemical Journal. 1994;303:9.

144. Y. Zhou DB, R. Zhang, A. Kassa, E. Ashayeri, R. Sridhar. Cytotoxicity of etidronic acid to human breast cancer cells. Ethnicity & Disease. 2008;181(S2):6.

145. E. Hiroi-Furuya TK, K. Hiura, H. Mano, K. Miyazawa, Y. Nakamaru, M. Watanabe-Mano, N. Okuda, J. Shimada, Y. Yamamoto, Y. Hakeda, M. Kumegawa. Etidronate (EHDP) inhibits osteoclastic-bone resorption, promotes apoptosis and disrupts actin rings in isolate-mature osteoclasts. Calcified Tissue International. 1999;64:5.

146. M. Sahni HLG, H. Fleisch, P. Collin, TJ. Martin. Bisphosphonates act on rat bone resorption through the mediation of osteoblasts. The Journal of Clinical Investigation. 1993;91:8.

147. B. Ongphiphadhanakul LGJ, L.E. Braverman, S. Alex, G.S. Stein, J.B. Lian, D.T. Baran. Etidronate inhibits the thyroid hormone-induced bone loss in rats

assessed by bone mineral density and messenger ribonucleic acid markers of osteoblast and osteoclast function. Endocrinology 1993;133:6.

148.   M.F. Basle AR, J.C. Renier, M. Audran, R. Filmon, K. Malkani Bone tissue in Paget's disease treated by ethane-1, hydroxy-1, 1 diphosphonate (EHDP). Structure, ultrastructure, and immunocytology. Clinical Orthopaedics and Related Research. 1984(8).

149.   Ridgway ND. The role of phosphatidylcholine and choline metabolites to cell proliferation and survival. Critical Reviews in Biochemistry and Molecular Biology. 2013;48:19.

150.   D. Coleman MS, M.G. Teresa N. Gathergood. Antimicrobial toxicity studies of ionic liquids leading to a 'hit' MRSA selective antibacterial imidazolium salt. Green Chemistry. 2012;14:7.

151.   S.V. Malhotra VK. A profile of the in vitro anti-tumor activity of imidazolium-based ionic liquids. Bioorganic & Medicinal Chemistry Letters. 2010;20(5):581.

152.   M.J.F. Blumer BH, C. Schwarzer, A.R. Hayman, J. Stempel, H. Fritsch. Role of tartrate-resistant acid phosphatase (TRAP) in long bone development. Mechanisms of development. 2012;129:15.

153.   I.N. Lavrik AG, P.H. Krammer. Caspases: pharmacological manipulation of cell death. The Journal of Clinical Investigation. 2005;115(10):8.

154.   A. Rutkovskiy KOS, I.J. Vaage. Osteoblast Differentiation at a Glance. Medical Science Monitor Basic Research. 2016;22:12.